



**Transcriptional and posttranscriptional regulation of the  
c-di-GMP modulating phosphodiesterase NbdA of  
*Pseudomonas aeruginosa***

vom Fachbereich Biologie der Universität Kaiserslautern zur Verleihung  
des akademischen Grades „Doktor der Naturwissenschaften“  
genehmigte Dissertation

angefertigt im

**Fachbereich Biologie**

Abteilung Mikrobiologie

Wissenschaftliche Aussprache: Kaiserslautern, 03.12.2021

vorgelegt von

**Katrin Gerbracht**

**Referent:** Prof. Dr. Nicole Frankenberg-Dinkel  
**Korreferent:** Prof. Dr. Matthias Hahn  
**Vorsitz:** Prof. Dr. Michael Schroda

Kaiserslautern, 2021 - D 386

Für meine Familie.  
In Gedenken an meine Großmutter.

# Table of contents

<b>Table of contents .....</b>	<b>II</b>
<b>Danksagung .....</b>	<b>VII</b>
<b>Abbreviations .....</b>	<b>VIII</b>
<b>1. Introduction .....</b>	<b>1</b>
<b>1.1 The model organism <i>Pseudomonas aeruginosa</i> .....</b>	<b>1</b>
<b>1.2 The second messenger c-di-GMP .....</b>	<b>2</b>
1.2.1 Synthesis and degradation of c-di-GMP .....	2
1.2.2 Physiological role of c-di-GMP .....	3
1.2.3 Regulation of the c-di-GMP modulating protein network.....	3
1.2.4 c-di-GMP effector proteins .....	5
<b>1.3 Cellular appendages, motility and biofilm lifecycle .....</b>	<b>5</b>
1.3.1 Type IV pili .....	6
1.3.2 The polar flagellum of <i>P. aeruginosa</i> .....	7
1.3.3 The biofilm lifecycle.....	7
<b>1.4 Chemotaxis of <i>P. aeruginosa</i> .....</b>	<b>8</b>
<b>1.5 Physiological role of the diatomic gas nitric oxide .....</b>	<b>10</b>
1.5.1 Exogenous and endogenous sources of nitric oxide .....	10
1.5.2 Sensing and physiological role of NO within <i>P. aeruginosa</i> .....	12
<b>1.6 Transcriptional regulation in bacteria .....</b>	<b>13</b>
1.6.1 The alternative sigma-factor RpoS .....	13
1.6.2 The transcription factor AmrZ.....	14
<b>1.7 Post-transcriptional regulation mechanisms in bacteria.....</b>	<b>15</b>
1.7.1 RNA-thermometers .....	15
1.7.2 The RNA-binding proteins RsmA and RsmF in <i>P. aeruginosa</i> .....	16
<b>1.8 The membrane anchored protein NbdA .....</b>	<b>17</b>
1.8.1 The sensory MHYT domain .....	17
1.8.2 The putative role of NbdA within <i>P. aeruginosa</i> .....	18
<b>1.9 Objectives of this work .....</b>	<b>19</b>

---

<b>2</b>	<b>Material and Methods</b>	<b>20</b>
<b>2.1</b>	<b>Microbial strains, material and chemicals</b>	<b>20</b>
2.1.1	Microbial strains	20
2.1.2	Plasmids	23
2.1.3	Oligonucleotides	25
2.1.4	Chemicals	29
2.1.5	Sterilization	30
2.1.6	Culture media and supplements	30
2.1.7	Kits, enzymes and antibodies	31
2.1.8	Equipment and consumables	33
<b>2.2</b>	<b>Microbiological methods</b>	<b>35</b>
2.2.1	Cultivation of microorganisms	35
2.2.2	Storage of microorganisms	35
2.2.3	Determination of cell density	35
2.2.4	Analysis of aerobic and anaerobic growth	35
2.2.5	Preparation of chemically competent <i>E. coli</i> cells	35
2.2.6	Transformation of chemically competent <i>E. coli</i> cells	36
2.2.7	Preparation of electro-competent <i>P. aeruginosa</i> cells	36
2.2.8	Transformation of electro-competent <i>P. aeruginosa</i> cells	36
2.2.9	Conjugation of <i>P. aeruginosa</i> via biparental mating	36
2.2.10	Growth of colony biofilms	37
2.2.11	O <sub>2</sub> profiles within colony biofilms	37
<b>2.3</b>	<b>Molecular biological methods</b>	<b>37</b>
2.3.1	Preparation of genomic DNA from <i>P. aeruginosa</i>	37
2.3.2	Preparation of total RNA from <i>P. aeruginosa</i>	37
2.3.3	DNase digestion	38
2.3.4	cDNA synthesis	38
2.3.5	Preparation of plasmid DNA from <i>E. coli</i>	39
2.3.6	Determination of nucleic acid concentrations	40
2.3.7	Agarose gel electrophoresis	40
2.3.8	Polymerase chain reaction (PCR)	40
2.3.9	Purification of PCR products	42
2.3.10	Restriction digest of DNA	42
2.3.11	Extraction of DNA fragments from agarose gels	42
2.3.12	Ligation of DNA fragments	42
2.3.13	Splicing-by-overlap extension (SOE-) PCR	42

2.3.14	Colony PCR .....	43
2.3.15	Site-directed mutagenesis.....	44
2.3.16	Gibson Assembly® of DNA molecules .....	45
2.3.17	Construction of expression vectors encoding <i>nbda-mNeonGreen I-Venus</i> .....	46
2.3.18	Analysis of DNA sequences .....	46
2.3.19	Generation of <i>P. aeruginosa</i> mutants via two-step allelic exchange .....	47
2.3.20	Plasmid integration into phage attachment site of <i>P. aeruginosa</i> .....	48
2.3.21	5'-Rapid amplification of cDNA ends (RACE) PCR .....	49
2.3.22	Semiquantitative reverse transcriptase (RT) PCR.....	50
<b>2.4</b>	<b>Protein biochemical methods .....</b>	<b>50</b>
2.4.1	Homologous protein production in <i>P. aeruginosa</i> .....	50
2.4.2	SDS-polyacrylamide gel electrophoresis .....	51
2.4.3	Immuno-detection of immobilized 6x His fusion proteins (Western Blot) .....	52
<b>2.5</b>	<b>Transcriptional and translational regulation of <i>nbda</i> .....</b>	<b>53</b>
2.5.1	Construction of transcriptional <i>lacZ</i> -fusions.....	53
2.5.2	Construction of translational <i>bgaB</i> -fusions .....	54
2.5.3	$\beta$ -Galactosidase assay in <i>E. coli</i> .....	54
2.5.4	$\beta$ -Galactosidase assay in <i>P. aeruginosa</i> .....	55
<b>2.6</b>	<b>Confocal laser scanning microscopy .....</b>	<b>56</b>
2.6.1	Preparation of agarose pads for microscopy .....	56
2.6.2	Fluorescent proteins and dyes .....	56
2.6.3	Cellular localization of NbdA .....	57
2.6.4	Co-localization of NbdA and the polar flagellum .....	57
2.6.5	Co-localization of NbdA and CheA.....	58
2.6.6	Localization of NbdA in thin sections of colony biofilms.....	58
2.6.7	Localization of NbdA in single cells of colony biofilms .....	61
<b>2.7</b>	<b>Phenotypic analysis of <i>P. aeruginosa</i> strains over-producing NbdA variants .....</b>	<b>61</b>
2.7.1	Swimming motility .....	61
2.7.2	Twitching motility.....	61
2.7.3	Adhesion assay .....	62
2.7.4	Pellicle formation.....	62
2.7.5	Drop dilution assay .....	63
<b>3</b>	<b>Results .....</b>	<b>64</b>
3.1	Transcriptional regulation of <i>nbda</i> .....	64

3.1.1	Determination of transcriptional start site of <i>nbdA</i> reveals a regulatory region with RpoS and AmrZ binding sites .....	64
3.1.2	Impact of nitric oxide on the transcription of <i>nbdA</i> .....	66
<b>3.2</b>	<b>Translational regulation of <i>nbdA</i> .....</b>	<b>70</b>
3.2.1	Prediction and analysis of secondary structures of the <i>nbdA</i> 5'-UTR .....	70
3.2.2	Impact of temperature shifts and cellular c-di-GMP levels on <i>nbdA</i> translation in <i>E. coli</i> assays.....	71
3.2.3	Analysis of <i>nbdA</i> translation in <i>P. aeruginosa</i> .....	73
<b>3.3</b>	<b>Overproduction of different NbdA variants.....</b>	<b>77</b>
3.3.1	Impact of <i>nbdA</i> overexpression on cell motility and biofilm formation .....	79
<b>3.4</b>	<b>Localization studies of NbdA .....</b>	<b>84</b>
3.4.1	Cellular localization of NbdA .....	84
3.4.2	Co-localization studies of NbdA with the polar flagellum .....	89
3.4.3	Co-localization studies of NbdA with the chemotaxis protein CheA.....	94
3.4.4	Localization of NbdA in colony biofilms .....	97
<b>4</b>	<b>Discussion .....</b>	<b>101</b>
<b>4.1</b>	<b>Transcriptional regulation of <i>nbdA</i> in the context of the c-di-GMP network of <i>P. aeruginosa</i>.....</b>	<b>101</b>
4.1.1	Expression of <i>nbdA</i> is dependent on the alternative sigma-factor RpoS and the transcription factor AmrZ.....	101
4.1.2	Effects of endogenous or exogenous nitric oxide on <i>nbdA</i> expression .....	103
4.1.3	Effect of the nitrite reductase NirS on <i>nbdA</i> promoter activity.....	104
<b>4.2</b>	<b>Regulation of <i>nbdA</i> translation on the post-transcriptional level.....</b>	<b>105</b>
4.2.1	Does the <i>nbdA</i> 5'-UTR form a RNA thermometer?.....	105
4.2.2	Influence of c-di-GMP or NO on <i>nbdA</i> translation.....	106
4.2.3	Is the <i>nbdA</i> translation regulated by RsmA and RsmF? .....	107
<b>4.3</b>	<b>Overexpression of <i>nbdA</i> leads to various phenotypical changes .....</b>	<b>108</b>
<b>4.4</b>	<b>Localization studies reveal polar localization of NbdA.....</b>	<b>111</b>
<b>4.5</b>	<b>Putative function of the phosphodiesterase NbdA and outlook .....</b>	<b>113</b>
<b>5</b>	<b>Summary.....</b>	<b>117</b>
<b>6</b>	<b>Zusammenfassung .....</b>	<b>118</b>
<b>Appendix</b> .....		<b>119</b>

---

<b>References.....</b>	<b>120</b>
<b>Curriculum vitae.....</b>	<b>147</b>
<b>Eidesstattliche Erklärung .....</b>	<b>149</b>

---

# Danksagung

Zunächst möchte ich einen herzlichen Dank an meine Doktormutter Prof. Dr. Nicole Frankenberg-Dinkel aussprechen. Ich bedanke mich für die Vergabe dieses vielseitigen und spannenden Themas, das mich schon in meiner Bachelorarbeit gepackt und nicht mehr losgelassen hat. Ebenso möchte ich mich für die intensiven fachlichen Diskussionen und die zahlreichen Denkanstöße bedanken, die daraus hervorgingen.

Bei Prof. Dr. Matthias Hahn bedanke ich mich für die freundliche Übernahme des Korreferats. Außerdem danke ich Prof. Dr. Michael Schroda für die Bereitschaft der Übernahme des Vorsitzes der Prüfungskommission. Ein zusätzlicher Dank gilt zudem beiden für das Mitwirken in meinem Thesis Advisory Committee.

Weiterhin gilt mein Dank Prof. Dr. Kai Thormann von der Justus Liebig Universität Gießen für die Bereitstellung verschiedener Vektoren und die fachliche Unterstützung im Bereich der Mikroskopie.

Ich bedanke mich ebenfalls bei Prof. Dr. Lars Dietrich von der Columbia University in New York für die Möglichkeit in seinem Labor das Anfertigen von Koloniebiofilm-Dünnschnitten für die Mikroskopie zu erlernen und ich danke Hannah Dayton für die Betreuung dort.

Prof. Dr. Franz Narberhaus und Daniel Scheller von der Ruhr-Universität Bochum danke ich herzlich für die Zusammenarbeit zur Untersuchung der 5'-UTR von *nbpA* und die Bereitstellung der translationalen Fusionen.

Außerdem danke ich Prof. Dr. Simon Dove vom Boston Children's Hospital für die Bereitstellung der  $\Delta rsmA$  und  $\Delta rsmF$  Stämme sowie Plasmide.

Der Deutschen Forschungsgemeinschaft (DFG) danke ich für die finanzielle Förderung dieser Arbeit innerhalb des SPP 1879.

Mein besonderer Dank gilt zudem Dr. Susanne Zehner für unsere zahlreichen intensiven Gespräche und dabei neu generierten Ideen.

Ein großer Dank geht natürlich auch an die Pseudomonas Gruppe vor allem an Julia, Martina, Christina, Anna und Maike für unsere ausgiebigen Besprechungen und euren Input.

Ich danke den „alten“ Mibis Natascha, Loriana, Anne, Martina, Benni und Kerstin für die tolle Aufnahme in Kaiserslautern! Ihr habt es geschafft, dass ich mich auch auf der Arbeit ein Stück zu Hause gefühlt habe. Danke natürlich auch an Christina, Anna, Helen, Michelle und die neueren Doktoranden und Studenten für die tolle Arbeitsatmosphäre.

Mein größter Dank gilt natürlich meiner Familie, die immer an mich geglaubt und mich während meines Studiums und meiner Promotion stets unterstützt hat. Danke Mama, Papa, Oma, Tobi, Tina und Jonas! Danke auch an Anni, die trotz der Entfernung immer für mich da war.

Ein ganz besonderer Dank gilt außerdem meinem Freund Marco, der mir in den letzten Jahren eine sehr große Stütze war und auf den ich stets zählen konnte!



## Abbreviations

Abbreviations of the International System of Units (SI) are not listed separately. For amino acids and nucleic acids, the one letter code is used in this work.

5'-RACE	5' rapid amplification of cDNA ends
5'-UTR	5' untranslated region
AA	amino acid
A. dest.	<i>Aqua destillata</i>
Amp	Ampicillin
APS	ammonium persulfate
AmrZ	alginate and motility regulator Z
BCIP	5-bromo-4-chloro-3-indoxyl phosphate
BM2	basal medium 2
bp	base pairs
c-di-GMP	bis-(3'-5')-cyclic diguanosine monophosphate
CLSM	confocal laser scanning microscopy
CRP	cAMP receptor protein
CCW	counter clockwise
CW	clockwise
DGC	diguanylate cyclase
DMF	dimethylformamide
DMSO	dimethyl sulfoxide
DNA	desoxyribonucleic acid
EPS	extracellular polymeric substances
Fig	figure
FP	fluorescent protein
gDNA	genomic DNA
Gm	Gentamycin
GMP	guanosine monophosphate
GTP	guanosine triphosphate
IPTG	isopropyl $\beta$ -D-1-thiogalactopyranoside
LB	Luria Bertani
MCP	methyl-accepting chemotaxis protein

---

NBT	nitro blue tetrazolium chloride
NO	nitric oxide
OD <sub>x nm</sub>	optical density at x nm
ONC	over-night culture
ONPG	o-nitrophenyl- $\beta$ -D-1-galactopyranoside
ORF	open reading frame
PCR	polymerase chain reaction
PDE	phosphodiesterase
pGpG	5'-phosphoguanylyl-(3'-5')-guanosine
PVDF	Polyvinylidene fluoride
QS	quorum sensing
RBS	ribosome binding site
RNA	ribonucleic acid
RNAP	(DNA specific) RNA polymerase
RNAT	RNA thermometer
rpm	revolutions per minute
RT	room temperature
SDS	sodium dodecyl sulfate
SDS-PAGE	sodium dodecyl sulfate polyacrylamide gel electrophoresis
SNP	sodium nitroprusside
SOE-PCR	splicing-by-overlap-extension PCR
sRNA	small RNA
T4P	type IV pili
TEMED	N,N,N',N'-tetramethylethane-1,2-diamine
TF	transcription factor
Tet	Tetracycline
TLC	transmitted light channel
VC	vector control
v/v	volume per volume
w/o	without
WT	wild type
w/v	weight per volume

# 1. Introduction

## 1.1 The model organism *Pseudomonas aeruginosa*

*Pseudomonas aeruginosa* is one of the best characterized members of the genus *Pseudomonas* which belongs to the class of  $\gamma$ -proteobacteria. *P. aeruginosa* is a Gram<sup>-</sup>, monotrichous, rod-shaped bacterium with a length of  $\sim 2 \mu\text{m}$ . Two of the most common *P. aeruginosa* laboratory strains are the wound isolate PAO1 and the more virulent clinical isolate PA14. Their genomes are fully sequenced and have a size of 6.26 Mbp and 6.54 Mbp with 5,570 and 5,892 predicted open reading frames (ORFs), respectively (He *et al.*, 2004; Klockgether *et al.*, 2011; Stover *et al.*, 2000). As a ubiquitous bacterium and opportunistic pathogen of plant, animal and human hosts, *P. aeruginosa* is able to colonize various habitats. The high adaptability to varying environmental conditions, is based on its relatively large genome, encoding numerous transcriptional regulators and two-component regulatory systems (Klockgether *et al.*, 2011; Stover *et al.*, 2000). *P. aeruginosa* is able to metabolize diverse nutrient sources like aliphatic and aromatic amino acids, sugar derivatives and fatty acids (Stanier *et al.*, 1966). Under anaerobic conditions, the facultative anaerobe organism is furthermore able to use nitrate as alternative electron acceptor for denitrification or to utilize arginine and pyruvate for fermentation (Eschbach *et al.*, 2004; St John and Hollocher, 1977).

*P. aeruginosa* is one of the most common nosocomial pathogens and therefore of high clinical relevance. *P. aeruginosa* mainly infects immunosuppressed patients and causes various acute as well as chronic infections (Goodman *et al.*, 2004; Lyczak *et al.*, 2000). Most frequently, the respiratory or urinary tract, the skin, ears or eyes of human hosts are infected. In the lungs of Cystic Fibrosis patients, persistent *P. aeruginosa* infections are a severe problem and count as the main reason for mortality of affected patients (Courtney *et al.*, 2007). *P. aeruginosa* is able to form biofilms during infections and is thereby protected against the host immune system (Jensen *et al.*, 2010). Additionally, the organism is characterized by a broad natural antibiotic tolerance and a high frequency of emerging antibiotic resistances (Botelho *et al.*, 2019; Hancock and Speert, 2000). Therefore, *P. aeruginosa* infections are hard to eradicate. Moreover, *P. aeruginosa* colonization of pipes and drinking water systems have become a severe problem in the industry (Mattila-Sandholm and Wirtanen, 1992; Meliani and Bensoltane, 2015). Due to its high metabolic diversity and its clinical as well as industrial relevance, *P. aeruginosa* has become a model organism, especially for biofilm research.

## 1.2 The second messenger c-di-GMP

Second messengers are required in all organisms for the transduction of environmental or intracellular signals into a suitable cellular response (Pesavento and Hengge, 2009). In bacteria, many second messengers like cyclic adenosine monophosphate (cAMP), cyclic guanosine monophosphate (cGMP) or bis-(3'-5')-cyclic diguanosine monophosphate (c-di-GMP) are nucleotide-based. In 1987, c-di-GMP was initially discovered in *Gluconacetobacter xylinus* as the first cyclic dinucleotide second messenger and is now considered to be the most abundant second messenger in bacteria (Römling *et al.*, 2017; Ross *et al.*, 1987).

### 1.2.1 Synthesis and degradation of c-di-GMP

Cyclic di-GMP is built from two molecules of guanosine triphosphate (GTP) by diguanylate cyclases (DGCs) (Fig. 1.1), which possess a conserved GGDEF amino acid motif in their catalytical active A-site (Chan *et al.*, 2004). For DGC activity, formation of dimers is required with each DGC monomer binding one molecule of GTP (Wassmann *et al.*, 2007). The conserved amino acid motif RxxD of DGCs, called I-site, is able to bind c-di-GMP which then inactivates the DGC by product feedback inhibition (Wassmann *et al.*, 2007). Hydrolysis of c-di-GMP in *P. aeruginosa* is performed by two classes of phosphodiesterases (PDEs). PDEs with a conserved HD-GYP motif directly hydrolyze c-di-GMP into two molecules of guanosine monophosphate (GMP) (Stelitano *et al.*, 2013). The second class of PDEs contains a conserved EAL motif and mediates c-di-GMP linearization to 5'-phosphoguanylyl-(3'-5')-guanosine (pGpG) (Rao *et al.*, 2008; Tchigvintsev *et al.*, 2010). In *P. aeruginosa*, the enzyme Orn is able to further hydrolyze pGpG to GMP (Orr *et al.*, 2015).

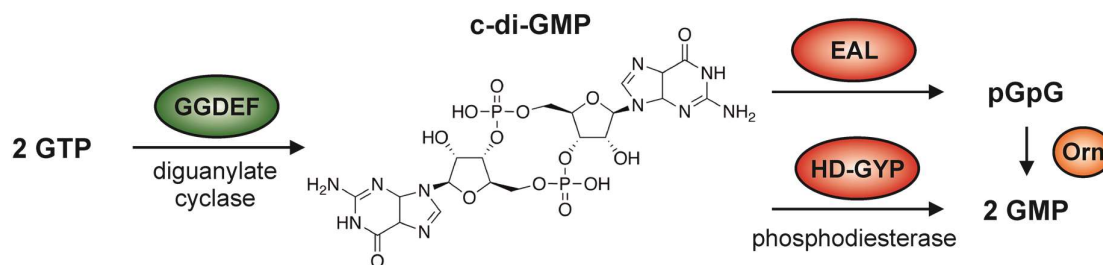


**Fig. 1.1: Synthesis and hydrolysis of c-di-GMP**

The second messenger c-di-GMP is synthesized from two molecules of GTP by diguanylate cyclases (DGCs; green) which possess a conserved GGDEF amino acid motif. Hydrolysis of c-di-GMP is mediated by phosphodiesterases (PDEs; red). PDEs with a conserved EAL motif hydrolyze c-di-GMP to pGpG which is further hydrolyzed by the enzyme Orn (orange) to two molecules of GMP. PDEs with a conserved HD-GYP motif directly convert c-di-GMP into two molecules of GMP.

## 1.2.2 Physiological role of c-di-GMP

In many bacteria, the second messenger c-di-GMP is described to be involved in various cellular processes like motility, biofilm formation, virulence or cell cycle progression and thereby influences the decision-making of each cell in response to environmental signals (Bobrov *et al.*, 2011; Cotter and Stibitz, 2007; Duerig *et al.*, 2009; Fang and Gomelsky, 2010; Petchiappan *et al.*, 2020). In *P. aeruginosa*, high intracellular levels of c-di-GMP promote the sessile lifestyle, including biofilm formation and the reduction of motility (Fig. 1.2; (Römling *et al.*, 2013; Valentini and Filloux, 2016)). In contrast, low concentrations of c-di-GMP lead to an increase of motility and virulence and induce biofilm dispersal (Römling *et al.*, 2013; Valentini and Filloux, 2016).

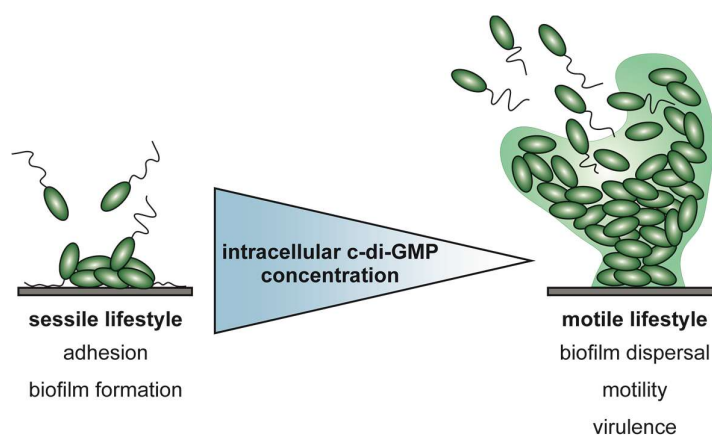


**Fig. 1.2: Influence of intracellular c-di-GMP concentrations on the *P. aeruginosa* lifestyle**

High intracellular concentrations of the second messenger c-di-GMP promote the sessile lifestyle of *P. aeruginosa*. Adhesive behavior and biofilm formation are increased. Low concentrations of c-di-GMP within the cells induce biofilm dispersal and motility and promote the motile lifestyle of the bacterium. Additionally the virulence of *P. aeruginosa* is increased.

## 1.2.3 Regulation of the c-di-GMP modulating protein network

Most bacteria encode a broad network of c-di-GMP modulating proteins, containing either single DGC or PDE domains or both domains (Hengge *et al.*, 2016; Römling *et al.*, 2013). In *P. aeruginosa* the c-di-GMP level is influenced by a regulatory network consisting of 40 proteins. From this network 16 proteins contain a DGC domain only, eight proteins only possess a PDE domain and 16 proteins are tandem proteins with both domains (Ha *et al.*, 2014; Kulasakara *et al.*, 2006). In order to avoid functional redundancies, not all c-di-GMP modulating proteins are present and active at the same time and in the same location in the cells. This sequestration of PDEs and DGCs is achieved by tight regulatory mechanisms (Hengge, 2009).

Temporal sequestration of redundant proteins is generated by the transcriptional regulation of the respective DGC and PDE encoding genes. In *E. coli*, 15 of the 28 encoded DGC/PDE genes are controlled by the alternative sigma-factor RpoS which is required for

general stress responses and gene expression in stationary growth phase (Sommerfeldt *et al.*, 2009). In *P. aeruginosa* and *P. fluorescens*, the transcription factor AmrZ is described to be involved in transcriptional regulation of DGC and PDE genes (Jones *et al.*, 2014; Muriel *et al.*, 2018). Additionally, expression levels of several DGC genes in *Vibrio cholerae* are increased at low temperatures compared to 37 °C, an effect that was also shown for some DGC/PDE encoding genes of *E. coli* (Sommerfeldt *et al.*, 2009; Townsley and Yildiz, 2015). Further regulatory mechanisms promote temporal sequestration of DGCs and PDEs on the post-transcriptional level. For example, the RNA-binding proteins CsrA and Hfq are involved in the post-transcriptional regulation of DGCs and PDEs in *Salmonella typhimurium* or *Yersinia pestis*, respectively (Bellows *et al.*, 2012; Jonas *et al.*, 2010). In *V. cholerae*, small RNA (sRNA)-dependent regulation of the DGC Vca0939 on the post-transcriptional level is described (Zhao *et al.*, 2013). On the post-translational level, sequestration can be generated by degradation of DGCs and PDEs under specific conditions. An example for this regulatory mechanism is the proteolysis of the *Y. pestis* DGC HmsT induced by shifts from low to high temperatures (Kirillina *et al.*, 2004).

DGC and PDE domains are often coupled to N-terminal sensory domains like PAS (Per-Arnt-Sim), GAF (present in cGMP-specific PDEs, Adenylyl cyclases and FhIA), CHASE (Cyclases/Histidine kinases Associated Sensory Extracellular), HAMP (present in Histidine kinases, Adenyl cyclases, Methyl-accepting proteins and Phosphatases) or MHYT (Hengge *et al.*, 2016). Perception of specific signals via these sensory domains are able to induce changes in the DGC or PDE activity of the c-di-GMP modulating proteins. Thereby the sensory domains prevent redundant DGCs and PDEs from being active at the same time. Binding of O<sub>2</sub> to the heme co-factor of the *E. coli* DosP, for example, is required for the protein's PDE activity (Tuckerman *et al.*, 2009). In the case of PA0575 of *P. aeruginosa*, binding of L-arginine to a sensory Venus flytrap (VFT) domain stimulates c-di-GMP degradation by the PDE domain (Paiardini *et al.*, 2018). Synthesis of c-di-GMP via the tandem protein MucR of *P. aeruginosa* is reduced in the presence of nitrate. The sensory domain of MucR was shown to be responsible for this effect, however, it remains unclear if nitrate was sensed directly or if an intermediate product of denitrification is the appropriate signal (Wang *et al.*, 2015). For additional spatial sequestration of DGCs and PDEs within a cell, the specific localization of these proteins is important (Hengge, 2009). For *E. coli*, localized c-di-GMP signaling is described in the so called "fountain" model. Under normal growth conditions, the cytoplasmic PDE PdeH (formerly YhjH), which is present in a high copy number per cell, acts as a drain for c-di-GMP and keeps the basal level of c-di-GMP low. This enables DGCs to produce local pools of c-di-GMP that specifically stimulate c-di-GMP effector proteins (Sarenko *et al.*, 2017).

### 1.2.4 c-di-GMP effector proteins

In bacteria, c-di-GMP mediated cellular processes are mainly regulated via c-di-GMP binding effector proteins. Binding of c-di-GMP induces a conformational change and thereby alters the function of the respective effector protein (Hengge, 2009; Sondermann *et al.*, 2012). The best studied class of c-di-GMP effectors are PilZ-domain containing proteins. This family was named after the *P. aeruginosa* type IV fimbrial biogenesis protein PilZ, which is involved in c-di-GMP dependent regulation of type IV pili synthesis (Alm *et al.*, 1996). Interestingly, the eponymous protein PilZ was later shown to be unable to bind c-di-GMP (Merighi *et al.*, 2007). Binding of c-di-GMP to PilZ-domains can either activate or repress the output function of effector proteins (Römling *et al.*, 2013). Other members of the PilZ-like regulator family in *P. aeruginosa* are the alginate biosynthesis protein Alg44, FlgZ which regulates swimming and swarming motility via interaction with the flagellar stator MotC and MapZ which is involved in chemotaxis (Bense *et al.*, 2019; Martínez-Granero *et al.*, 2014; Merighi *et al.*, 2007; Ramelot *et al.*, 2007; Xu *et al.*, 2016b). Catalytically inactive PDE domains or the I-site of inactive DGC domains are also able to serve as c-di-GMP binding sites of effector proteins (Hengge, 2009; Sondermann *et al.*, 2012). The protein FimX of *P. aeruginosa* possesses a GGDEF and an EAL motif, however neither DGC nor PDE function was described. Nevertheless, FimX is a high-affinity receptor of c-di-GMP that undergoes a conformational change upon c-di-GMP binding and is involved in type IV pili assembly and twitching motility (Jain *et al.*, 2017; Kazmierczak *et al.*, 2006; Navarro *et al.*, 2009; Qi *et al.*, 2011). In *P. aeruginosa*, expression of the polysaccharide Pel is regulated by the c-di-GMP effector protein PelD. Compared to DGCs, PelD has a degenerated A-site, but contains a conserved I-site which is able to bind c-di-GMP with high affinity and modulates PelD activity upon c-di-GMP binding (Lee *et al.*, 2007; Li *et al.*, 2012). The transcription factor FleQ of *P. aeruginosa* belongs to another class of c-di-GMP effector proteins. FleQ binds to the promoter region of the polysaccharide encoding *pel* cluster and inhibits transcription. Although the binding site of c-di-GMP is not identified yet, it was shown that c-di-GMP binding induces a conformational change of FleQ and alters binding of the transcriptional regulator to the *pel* promoter and thereby enables transcription (Hickman and Harwood, 2008; Matsuyama *et al.*, 2016).

## 1.3 Cellular appendages, motility and biofilm lifecycle

As already mentioned, motility and biofilm formation of *P. aeruginosa* are tightly regulated by the intracellular concentration of the second messenger c-di-GMP. Type IV pili as well as the polar flagellum of *P. aeruginosa* are involved in different forms of motility and are also required for the native biofilm lifecycle.

### 1.3.1 Type IV pili

Type IV pili (T4P) are flexible, filamentous surface appendages that are localized at the cell poles of *P. aeruginosa* (Alm *et al.*, 1996; DeLange *et al.*, 2007). T4P are composed of a retractable pilus, built from the pilin subunits PilA, a motor complex, an alignment subcomplex and a secretin pore (McCallum *et al.*, 2019). Formation of T4P is increased upon surface contact and cellular localization of the pili is mediated by the polar hub protein FimV in *P. aeruginosa* (Cowles and Gitai, 2010). T4P enable cellular movement on solid and semisolid surfaces, the twitching motility (Fig. 1.3; (Semmler *et al.*, 1999)). During this motility form of *P. aeruginosa*, the T4P extend, the adhesive tip attaches to the surface and forward motion is generated by subsequent retraction of the pili (Talà *et al.*, 2019). Twitching motility is also required for the formation of mature biofilm macrocolonies, as pili mutant strains form only flat biofilms compared to the wild type (Chiang and Burrows, 2003; Klausen *et al.*, 2003; O'Toole and Kolter, 1998). Together with the polar flagellum, T4P are additionally involved in swarming motility of *P. aeruginosa*, which is a coordinated form of movement on semisolid surfaces (Köhler *et al.*, 2000). During swarming motility, *P. aeruginosa* cells secrete anionic tensides, called rhamnolipids, in order to reduce surface tension and enable cellular movement (Fauvart *et al.*, 2012; Morris *et al.*, 2011). Furthermore, T4P contribute to the virulence of *P. aeruginosa* by facilitating initial surface contact to host cells during infections (Hahn, 1997) and surface contact of T4P induces the expression of virulence genes via the Chp chemotaxis system (Inclan *et al.*, 2016; Persat *et al.*, 2015).

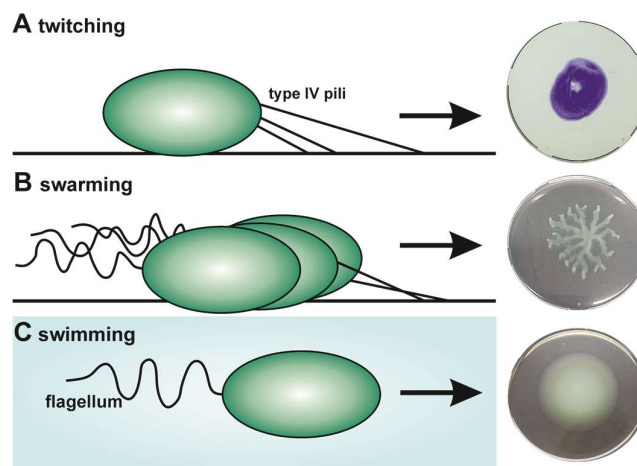


**Fig. 1.3: Different forms of *P. aeruginosa* motility**

*P. aeruginosa* is capable of twitching [A], swarming [B] and swimming [C] motility which are depicted as cartoons and on the respective assay plates. Twitching motility on solid surfaces is mediated by the attachment and retraction of type IV pili. Swarming motility is a highly coordinated motility form on semi-solid surfaces which is mediated by the flagellum in combination with type IV pili. Swarming motility on 0.5 % agar plates is characterized by the formation of so called dendrites by the cells. Swimming motility is mediated in liquid environments by rotation of the polar flagellum. The arrow indicates the movement direction of the cells.



### 1.3.2 The polar flagellum of *P. aeruginosa*

In aqueous environments, the polar flagellum of *P. aeruginosa* mediates swimming motility (Toutain *et al.*, 2005). In contrast to the peritrichously flagellated *E. coli* that performs a typical “run-and-tumble” swimming trajectory (Darnton *et al.*, 2007), *P. aeruginosa* shows a “run-reverse-turn” motility pattern (Qian *et al.*, 2013). This swimming trajectory is based on frequent switches between the counterclockwise (CCW) and clockwise (CW) flagellar rotation with short pauses in between, in which the cell is able to adjust its movement angle (Qian *et al.*, 2013). Directed movement towards attractant or away from repellent substances is facilitated by chemotaxis (see chapter 1.4). Besides swimming and swarming motility, the flagellum is involved in the initial surface attachment of cells which marks the first stage of biofilm formation (O'Toole and Kolter, 1998; Toutain *et al.*, 2007).

### 1.3.3 The biofilm lifecycle

*P. aeruginosa* is not only present in a motile lifestyle but is further able to switch into a sessile lifestyle by the formation of biofilms. A biofilm is defined as surface adherent multicellular bacterial population which is embedded in an extracellular matrix (Costerton *et al.*, 1995). Within biofilms, bacteria are well protected against environmental factors, the host immune system, or medical treatment. Therefore, biofilms are the preferred lifestyle of more than 90 % of all bacteria (Costerton *et al.*, 1987; Prakash *et al.*, 2003). Due to the high clinical and industrial relevance, *P. aeruginosa* biofilms have become a significant research topic over the last decades.

The biofilm lifecycle of *P. aeruginosa* can be divided into five stages (Fig. 1.4), beginning with the reversible attachment of motile cells to biotic or abiotic surfaces. The initial surface contact (1) is made by the polar flagellum, leading to polarly attached cells which are able to detach again (Sauer *et al.*, 2002). In the second step, the whole cell body makes contact to the surface and thereby cellular attachment becomes irreversible (2) (Bruzard *et al.*, 2015). Cell division together with the production and secretion of extracellular polymeric substances (EPS) lead to the formation of biofilm microcolonies (3) and later on to the maturation of the biofilm into mushroom-like macrocolonies (4). The structure providing biofilm matrix is composed of exopolysaccharides, extracellular DNA, proteins, and water (Sutherland, 2001). Within mature biofilms, a sharp oxygen gradient is present from the top of the colonies to the bottom layers (de Beer *et al.*, 1994; Werner *et al.*, 2004). To provide distribution of nutrients or oxygen within the biofilm and enable the removal of metabolic end products, the extracellular matrix is filled with void spaces that serve as channels for liquid flow (Davey *et al.*, 2003; Stewart and Franklin, 2008).

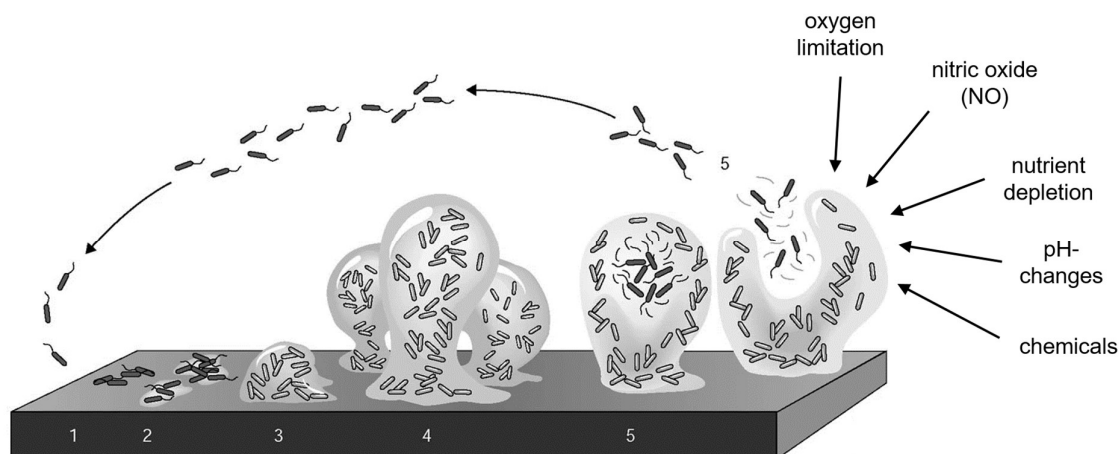


**Fig. 1.4: The biofilm lifecycle of *P. aeruginosa***

The biofilm lifecycle is divided into the following five stages: **1)** Reversible attachment of motile cells. **2)** Irreversible attachment. **3)** Formation of biofilm microcolonies. **4)** Biofilm maturation into macrocolonies. **5)** Biofilm dispersal by release of motile cells from biofilm colonies that are able to recolonize new habitats. Triggers of biofilm dispersal are indicated with arrows. Figure adapted from (Sauer, 2003).

During the last step of the biofilm lifecycle, a defined subpopulation of bacteria within the mature biofilm colony switches back to the planktonic lifestyle. Those cells undergo various transcriptional and translational changes and, for example, rebuild their polar flagellum (Guilhen *et al.*, 2017). Secreted enzymes degrade the biofilm matrix around this subpopulation (McDougald *et al.*, 2011). Motile cells are then released from the biofilm during the dispersal event (5) to enable colonization of new habitats or to cause a systemic spread of bacteria within the host (Fleming and Rumbaugh, 2018; Sauer, 2003). Biofilm dispersal can be triggered by various environmental cues like changes in the nutrient availability (Sauer *et al.*, 2004; Schleheck *et al.*, 2009), oxygen limitation (Schleheck *et al.*, 2009), the presence of specific chemicals (Kaplan, 2010) or non-lethal concentrations of the diatomic gas nitric oxide (NO) (Barraud *et al.*, 2006; Barraud *et al.*, 2009; Li *et al.*, 2013).

## 1.4 Chemotaxis of *P. aeruginosa*

Chemotaxis is defined as movement of organisms towards or away from a chemical (Adler, 1966). Desirable compounds like metabolizable nutrients or oxygen act as chemoattractants and induce movement of the bacteria in this direction (Hong *et al.*, 2004; Sampedro *et al.*, 2015; Taguchi *et al.*, 1997) while potentially harmful compounds like trichlorethylene act as chemorepellents and lead to motility in the opposite direction (Shitashiro *et al.*, 2003; Tso and Adler, 1974). Chemoattractants and chemorepellents are sensed by chemoreceptors, also referred to as methyl-accepting chemotaxis proteins (MCPs), which form complexes with other chemotaxis proteins in order to generate chemotactic responses.

In contrast to *P. aeruginosa*, *E. coli* possesses a comparatively simple chemotaxis machinery with only one chemotaxis pathway that includes five chemoreceptors. *P. aeruginosa* encodes for 26 MCPs which belong to four separated chemotaxis pathways (Porter *et al.*, 2011), namely Che (F6), Che2 (F7), Wsp (ACF) and Chp (TFP) pathway (Fig. 1.5; (Matilla *et al.*, 2021)).

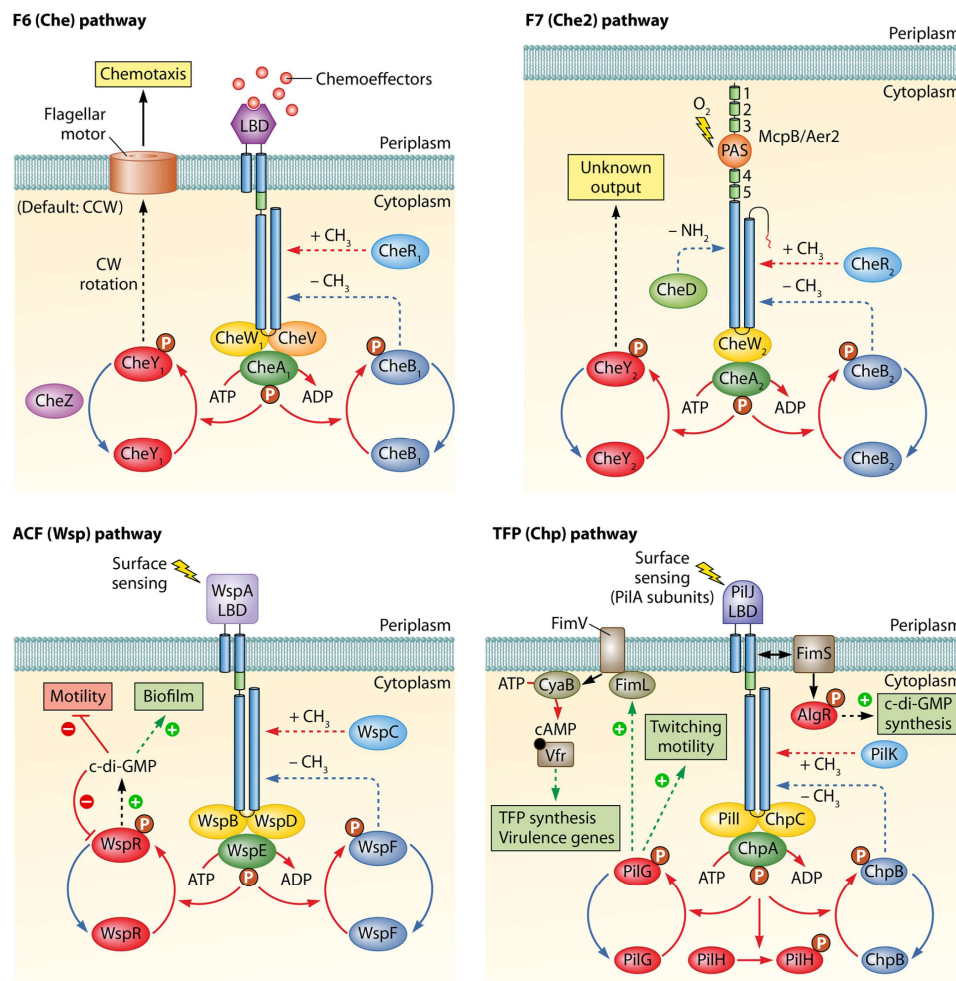


**Fig. 1.5: Overview of the four chemosensory pathways of *P. aeruginosa***

*P. aeruginosa* possesses four chemotaxis pathways, namely Che (F6), Che2 (F7), Wsp (ACF) and Chp (TFP). Cellular outputs of each pathway are marked in boxes. The chemotaxis compounds are colored as follows: histidine kinases: green; CheW-type coupling protein: yellow; CheV type coupling protein: orange; methyltransferase: light blue; methyl-erasure: dark blue; CheY-type response regulator: red; phosphatase: purple. (Matilla *et al.*, 2021)

While the exact function and cellular output of the Che2 pathway of *P. aeruginosa* is not fully understood yet, the remaining three pathways are quite well studied (Matilla *et al.*, 2021). The Wsp pathway includes the chemoreceptor WspA and was shown to influence motility and biofilm formation via modulation of intracellular c-di-GMP levels by the response regulator WspR upon surface sensing (Hickman *et al.*, 2005; O'Connor *et al.*, 2012). The Chp pathway is also activated by surface contact and regulates directed twitching motility and virulence of *P. aeruginosa* (Luo *et al.*, 2015; Matilla *et al.*, 2021; Persat *et al.*, 2015; Whitchurch *et al.*,

2004). However, chemotactic swimming motility and the resulting “run-reverse-turn” movement pattern are generated by the Che pathway of *P. aeruginosa* which integrates the highest number of MCPs of this organism (Matilla *et al.*, 2021; Qian *et al.*, 2013). Recognition of increasing chemoattractant concentrations by the MCPs inhibits the autophosphorylation activity of the histidine kinase CheA which is coupled to the MCP via CheW<sub>1</sub> and CheV (Bi and Sourjik, 2018; Sampedro *et al.*, 2015). This leads to a decreasing frequency of flagellar motor switches from CCW to CW rotation direction and therefore results in a “run” phenotype with directed swimming motility towards the chemoattractant (Sourjik and Wingreen, 2012). In contrast, decreasing attractant concentrations or an increase of chemorepellents induce autophosphorylation of CheA<sub>1</sub> (Bi and Sourjik, 2018; Sampedro *et al.*, 2015). The phosphoryl group can be transferred from CheA<sub>1</sub> to the response regulator CheY<sub>1</sub> which then transduces a signal to the flagellar motor which promotes a directional change of the flagellar rotation (Porter *et al.*, 2011; Sampedro *et al.*, 2015). Dephosphorylation of CheY<sub>1</sub> is performed by the phosphatase CheZ in order to reset the signal transduction pathway (Sampedro *et al.*, 2015; Silversmith *et al.*, 2003). Further modulation of the chemotactic response is generated by methylation of the MCPs by the methyl transferase CheR<sub>1</sub> (Schmidt *et al.*, 2011; Sheng *et al.*, 2019). Methylation of an MCP increases its ability to stimulate autophosphorylation activity of the coupled CheA<sub>1</sub> which induces, as described before, a directional change in the flagellar rotation (Borkovich *et al.*, 1992). Additionally, methylation of MCPs decreases the affinity of the receptor to chemoattractants (Vladimirov and Sourjik, 2009). Besides CheY<sub>1</sub>, the methylesterase CheB<sub>1</sub> can be target for the phosphotransfer from CheA<sub>1</sub>. Phosphorylated CheB<sub>1</sub> demethylates the MCPs and therefore resets the chemoreceptors for new signals (Wadhams and Armitage, 2004). Interestingly, the second messenger c-di-GMP seems to play a superior regulatory role within the Che chemotaxis pathway. Increasing levels of c-di-GMP are sensed by the PilZ-domain containing protein MapZ (Xu *et al.*, 2016b). Upon c-di-GMP binding, MapZ is able to directly interact with CheR<sub>1</sub> and thereby inhibits the CheR<sub>1</sub> mediated methylation of various MCPs (Sheng *et al.*, 2019). This lack of methylation results in a loss of flagellar motor switches and a “run” swimming pattern of *P. aeruginosa* (Sheng *et al.*, 2019; Xin *et al.*, 2019).

## 1.5 Physiological role of the diatomic gas nitric oxide

### 1.5.1 Exogenous and endogenous sources of nitric oxide

NO is a freely diffusible, colorless diatomic gas which is highly reactive due to an unpaired electron (Stamler *et al.*, 1992). In micromolar concentrations, NO is cytotoxic via direct and indirect antimicrobial activities like oxidation, nitration, S-nitrosylation, or DNA damage (Heinrich *et al.*, 2013; Schairer *et al.*, 2012; Stamler *et al.*, 1992). Therefore, a prevalent strategy for mammal host immune defense against pathogens is the production of high

amounts of NO by macrophages. Recognition of pathogens for example via lipopolysaccharides (LPS) induces the expression of NO-synthases in the macrophages, which then utilize L-arginine as substrate for NO production (MacMicking *et al.*, 1997). In addition to exogenous sources of NO, *P. aeruginosa* is able to form endogenous NO during denitrification (Fig. 1.6).

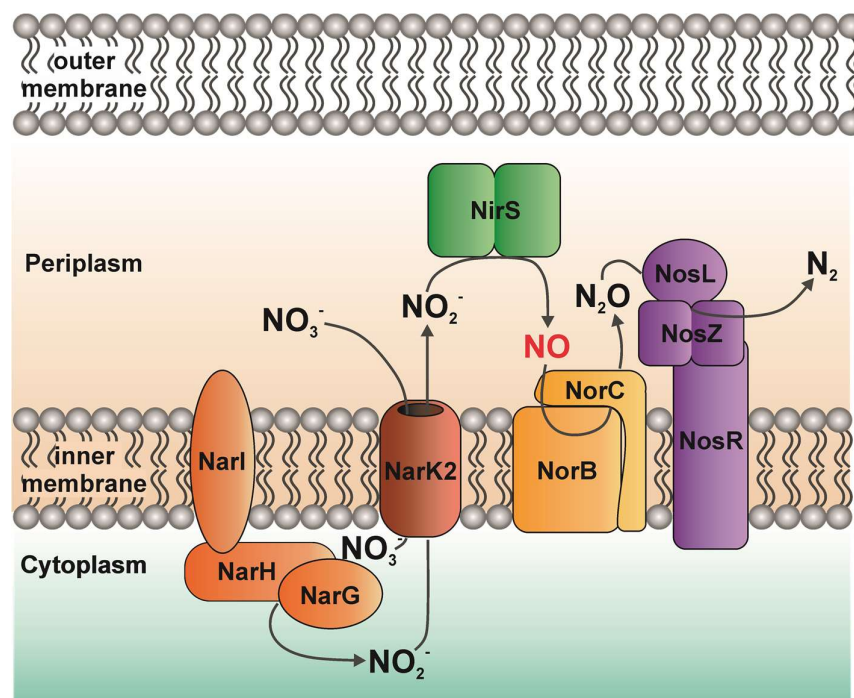


**Fig. 1.6: Schematic denitrification pathway of *P. aeruginosa***

The denitrification apparatus of *P. aeruginosa* is integrated in or associated with the cytoplasmic membrane. Under anaerobic conditions, nitrate ( $\text{NO}_3^-$ ) is utilized as alternative electron acceptor for anaerobic respiration. Periplasmic  $\text{NO}_3^-$  reaches the cytoplasm via the channel NarK2.  $\text{NO}_3^-$  is then reduced by the nitrate reductase (NAR, orange) to nitrite ( $\text{NO}_2^-$ ) which is channeled to the periplasm. The periplasmic nitrite reductase (NIR, green) reduces  $\text{NO}_2^-$  to nitric oxide (NO) which is further reduced by the nitric oxide reductase (NOR, yellow) to nitrous oxide ( $\text{N}_2\text{O}$ ).  $\text{N}_2\text{O}$  is reduced to molecular nitrogen ( $\text{N}_2$ ) by the nitrous oxide reductase (NOS, purple).

Under micro-aerobic and anaerobic conditions, the alternative electron acceptor nitrate can be utilized within the denitrification pathway. Nitrate is reduced to nitrite via the nitrate reductase (NAR). The periplasmic nitrite reductase (NIR, e.g. NirS) produces NO by reduction of nitrite. NO is further reduced to nitrous oxide and molecular nitrogen by the nitric oxide reductase (NOR, e.g. NorCB) and the nitrous oxide reductase (NOS), respectively. Deletion of *nirS* leads to a strain unable to form endogenous NO, while a deletion of *norCB* might lead to accumulation of NO during denitrification (Barraud *et al.*, 2006). NirS is a homo-dimeric protein with a heme *c* cofactor in the N-terminal domain and the essential catalytic cofactor heme *d*<sub>1</sub> in the C-terminal domain of each monomer (Nurizzo *et al.*, 1997). Currently, synthesis and incorporation of the heme *d*<sub>1</sub> cofactor is not fully understood. However, NirF and NirN are described to be essential for this process (Bali *et al.*, 2010; Nicke *et al.*, 2013). NirN catalyzes the last step of heme *d*<sub>1</sub> synthesis (Adamczack *et al.*, 2014; Klünemann *et al.*, 2019).

The function of NirF is not totally clarified so far, but it is predicted to form dihydro-heme  $d_1$ , the substrate of NirN (Bali *et al.*, 2010; Klünemann *et al.*, 2019). Therefore, deletion of *nirF* leads to a strain impaired in NO production during denitrifying conditions due to a catalytically inactive NirS (Nicke *et al.*, 2013).

### 1.5.2 Sensing and physiological role of NO within *P. aeruginosa*

In *P. aeruginosa*, the cellular response to NO is dependent on the concentration of the diatomic gas: High, toxic NO concentrations elicit a stress response and induce detoxification mechanisms via NorCB or flavohemoglobin (Arai *et al.*, 2005; Kakishima *et al.*, 2007). However, in nonlethal concentrations, NO acts as a signaling molecule regulating cellular behaviors of *P. aeruginosa* like biofilm dispersal by stimulation of c-di-GMP degrading PDEs (Barraud *et al.*, 2006; Barraud *et al.*, 2009). In many bacteria, like *Shewanella oneidensis* or *Legionella pneumophila*, heme-based sensory H-NOX domains are required for changes in bacterial behavior due to NO exposure (Nisbett and Boon, 2016; Plate and Marletta, 2013). Binding of NO or oxygen to the heme cofactor within the H-NOX domain leads to a conformational change and thereby stimulates activity of coupled DGC, PDE or histidine kinase domains (Carlson *et al.*, 2010; Plate and Marletta, 2012; Price *et al.*, 2007). *P. aeruginosa* does not possess any H-NOX proteins but is able to react to NO exposure for example by biofilm dispersal. The c-di-GMP modulating proteins RbdA, DipA, NbdA, and MucR and the chemotaxis transducer protein BdlA are described to be involved in NO-induced biofilm dispersal (Li *et al.*, 2013; Morgan *et al.*, 2006; Roy *et al.*, 2012). However, none of them could be proven to be the master regulator for this NO-response and direct NO binding was not shown for any of these proteins, until now (Cai *et al.*, 2020; Zemke *et al.*, 2020). In contrast, the recently discovered hemoprotein NosP binds NO directly and reduces the phosphorelay of the corresponding hybrid histidine kinase NahK which eventually leads to biofilm dispersal of *P. aeruginosa*, although the exact mechanism of this regulation remains unknown (Hossain and Boon, 2017). On the transcriptional level, two NO-responsive transcription factors (TF), e.g. the dissimilative nitrate respiration regulator (DNR) and FhpR, are described in *P. aeruginosa* (Arai *et al.*, 2005; Giardina *et al.*, 2009; Giardina *et al.*, 2008; Koskenkorva-Frank and Kallio, 2009). DNR, together with the O<sub>2</sub> sensing TF ANR, prevalently regulates the transcription of genes encoding the denitrification apparatus under micro-aerobic and anaerobic conditions (Trunk *et al.*, 2010). In contrast, FhpR regulates the expression of flavohemoglobin required for aerobic NO detoxification (Arai *et al.*, 2005).

## 1.6 Transcriptional regulation in bacteria

Gene expression in bacteria is driven by the DNA-dependent RNA polymerase (RNAP), which recognizes and binds to promoter regions within the genome and transcribes DNA into messenger RNA (mRNA). The core RNAP is composed of two  $\alpha$ -subunits and one  $\beta$ -,  $\beta'$ -, and  $\omega$ -subunit, each. Formation of the active holo-enzyme requires an additional  $\sigma$ -subunit, which is often the housekeeping sigma-factor  $\sigma^{70}$  (Browning and Busby, 2004; Vassylyev *et al.*, 2002). Typical bacterial  $\sigma^{70}$  promoters are characterized by the conserved consensus sequences 5'-TTGACA-3' and 5'-TATAAT-3' of the -35 and -10 region, respectively, which are located approximately 35 and 10 bp upstream of the transcriptional start site (Harley and Reynolds, 1987; Reznikoff *et al.*, 1985; Travers, 1984). Transcription is divided into three steps: Transcription initiation, elongation and termination. Most regulatory mechanisms of transcription affect the initiation, precisely interaction of the RNAP with the promoter region. As the number of free RNAP core enzymes and  $\sigma$ -subunits is limited within the cell, a competition between different promoters for the holo-RNAP exists (Browning and Busby, 2004). Changes in the DNA recognition sites can alter the binding efficiency of the RNAP and therefore contribute to the promoter activity. As  $\sigma$ -factors are required for binding of the RNAP to DNA promoter regions, these subunits regulate transcription initiation to a great extent. Bacteria utilize alternative sigma-factors with different recognition sites than  $\sigma^{70}$  to induce the transcription of specific genes for example during environmental stresses (Paget, 2015).

### 1.6.1 The alternative sigma-factor RpoS

*E. coli* encodes a pool of six alternative  $\sigma$  factors in addition to the housekeeping  $\sigma^{70}$  (Blattner *et al.*, 1997). One of them is the alternative sigma-factor RpoS ( $\sigma^S$ ) which directly or indirectly regulates approximately 10 % of the *E. coli* genome (Battesti *et al.*, 2011). Increased amounts of RpoS were observed when cells entered the stationary growth phase and under stressful conditions like starvation or unfavorable pH. Recognition of several stresses are linked to a rising intracellular concentration of the alarmone (p)ppGpp, which promotes *rpoS* transcription and translation and improves RpoS stability and activity through various mechanisms (Battesti *et al.*, 2011; Brown *et al.*, 2002; Lange *et al.*, 1995; Merrikh *et al.*, 2009). Therefore, RpoS is described to be a regulator of the general stress response in *E. coli*.

In *P. aeruginosa*, RpoS is described as alternative sigma-factor for gene regulation in stationary growth phase and in presence of various stresses (Potvin *et al.*, 2008). However, RpoS involvement during stress responses is not as pronounced as in *E. coli* (Venturi, 2003). In contrast to *E. coli*, *P. aeruginosa* possesses 24  $\sigma$ -factors, 19 of them with extracytoplasmic function (ECF) (Potvin *et al.*, 2008). RpoS controls, with ~800 directly or indirectly regulated genes, about 14 % of the whole genome (Schuster *et al.*, 2004). Transcription and translation of *rpoS* in *P. aeruginosa* is regulated by distinct regulatory mechanisms including

transcriptional activation at stationary growth phase, Hfq-mediated small RNAs (sRNAs) that affect *rpoS* translation under various conditions, and regulation of *rpoS* transcription by the cell-density dependent Las/Rhl quorum sensing (QS) system (Fujita *et al.*, 1994; Latifi *et al.*, 1996). Interestingly, 40 % of the QS regulated genes in *P. aeruginosa* also belong to the RpoS regulon, although not all of these genes possess consensus sequences for QS regulation in their promoter regions (Schuster *et al.*, 2004; Schuster *et al.*, 2003). Besides regulation of stationary phase genes and stress responses, RpoS is described to regulate the expression of virulence factors like exotoxin A and pyocyanin in *P. aeruginosa* (Dong and Schellhorn, 2010; Suh *et al.*, 1999).

### 1.6.2 The transcription factor AmrZ

The alginate and motility regulator *Z* (AmrZ; formerly AlgZ) of *P. aeruginosa* belongs to the ribbon-helix-helix class of TFs (Baynham *et al.*, 1999; Baynham and Wozniak, 1996). AmrZ can act as either transcriptional activator or repressor, however, DNA binding of AmrZ requires tetramerization via its C-terminus (Jones *et al.*, 2014; Xu *et al.*, 2016a). A global analysis revealed that the expression of over 300 genes was affected by AmrZ, nine of them were directly activated and 49 were directly repressed by AmrZ (Jones *et al.*, 2014). Most of the directly regulated genes are linked to *P. aeruginosa* motility and virulence. The production of alginate and resulting mucoidity is important for *P. aeruginosa* infections in CF lungs and is regulated by AmrZ via activation of the *algD* promoter. This promoter controls a large operon which is required for alginate synthesis (Baynham *et al.*, 1999; Baynham and Wozniak, 1996). Swimming motility is directly regulated by repression of the transcriptional regulator *fleQ*, while AmrZ is required for twitching motility and type IV pili biosynthesis (Baynham *et al.*, 2006; Tart *et al.*, 2006; Tart *et al.*, 2005). Biofilm formation is also affected via AmrZ-dependent transcriptional repression of the exopolysaccharide cluster *psl* and furthermore, AmrZ is involved in the c-di-GMP regulatory mechanisms of *P. fluorescens* and *P. aeruginosa* (Jones *et al.*, 2014; Jones *et al.*, 2013; Muriel *et al.*, 2018). AmrZ is known to directly repress its own expression by binding to the *amrZ* promoter region during an inhibitory feedback loop (Ramsey *et al.*, 2005). Additionally, transcription of *amrZ* is dependent on the alternative sigma-factor AlgU (formerly AlgT) which is required for the conversion from the non-mucoid phenotype to mucoidity (Baynham and Wozniak, 1996; Potvin *et al.*, 2008; Wozniak *et al.*, 2003). On the post transcriptional level, *amrZ* translation is promoted via binding of the sRNA ErsA, which is expressed together with stress-induced genes (Falcone *et al.*, 2018).



## 1.7 Post-transcriptional regulation mechanisms in bacteria

Translation of specific mRNAs is often regulated on the post-transcriptional level. Bacterial mRNAs are composed of 5'- and 3'- untranslated regions (UTRs) that flank the coding sequence of the gene of interest. The 5'-UTR frequently forms secondary structures and contains the ribosome binding site (RBS) and the translation start codon which is commonly AUG. For translation initiation, the RBS in the 5'-UTR needs to be accessible for binding of the 30S ribosomal subunit. Together with the three initiation factors (IF1, IF2 and IF3), the initiator tRNA and the 16S rRNA, the 70S initiation complex is formed and the elongation phase of translation can start (Duval *et al.*, 2015). Conformational changes of the secondary structure of the 5'-UTR can be induced by binding of sRNAs, RNA-binding proteins or, in the case of riboswitches, by direct binding of ligands to the mRNA structure (Balasubramanian and Vanderpool, 2013; Duval *et al.*, 2015; Meyer, 2017; Nudler and Mironov, 2004; Van Assche *et al.*, 2015). If the structural change of the mRNA leads to RBS accessibility, translation initiation is promoted. Otherwise, covering of the RBS inhibits translation and degradation of mRNA by ribonucleases can be increased (Belasco, 2010; Deana and Belasco, 2005).

### 1.7.1 RNA-thermometers

RNA-thermometers (RNATs) are temperature-sensing mRNA structures that are able to control translation in a temperature-dependent manner. Within an RNAT, the RBS is covered in the secondary structure of the mRNAs 5'-UTR. Sudden temperature increases or decreases lead to a zipper-like or switch-like conformational change in the 5'-UTR allowing the translation initiation complex to form and translation can start (Kortmann and Narberhaus, 2012). In bacteria, mainly heat-shock genes, cold-shock genes, and virulence genes are regulated by RNATs (Narberhaus *et al.*, 2006). The most common RNAT structure are the so-called ROSE (repression of heat shock gene expression) elements that control the translation of small heat shock genes (Kortmann and Narberhaus, 2012; Narberhaus *et al.*, 1998). Another well-studied RNAT family are the fourU elements. FourU thermometers are characterized by a pronounced hairpin structure of the 5'-UTR in which an eponymous stretch of four uridines pairs with the RBS to inhibit translation (Kortmann and Narberhaus, 2012; Waldminghaus *et al.*, 2007). The second characteristic of fourU elements, a single A-G mismatch besides the uridine stretch, is required for zipper-like opening of the hairpin structure at increasing temperatures and therefore for translation initiation (Rinnenthal *et al.*, 2011). So far, only few examples for temperature-dependent post-transcriptional regulation via RNATs are described for *Pseudomonads*. The heat shock gene *ibpA* and rhamnolipid production via the *rhlAB* operon are regulated by a short ROSE-like RNAT in *P. putida* and *P. aeruginosa* (Grosso-Becerra *et al.*, 2014; Krajewski *et al.*, 2013; Noll *et al.*, 2019). Another RNAT controls the expression of

the LasI encoding gene, which regulates QS-dependent production of virulence factors by synthesis of the QS autoinducer 3-oxo-dodecanoyl-homoserine lactone (3O-C12-HSL) in *P. aeruginosa* (Grosso-Becerra *et al.*, 2014).

### 1.7.2 The RNA-binding proteins RsmA and RsmF in *P. aeruginosa*

Regulation of translation initiation, mRNA stability and/or translation elongation by the CsrA-like family of RNA-binding proteins is a widespread form of post-transcriptional control in bacteria. The best studied candidate of these proteins is the carbon storage regulator protein CsrA from *E. coli*. It is described as a global regulator which, among other functions, represses expression of stationary growth phase genes while it is promoting expression of genes required for exponential growth (Potts *et al.*, 2017; Romeo *et al.*, 2013). CsrA-dimers specifically bind to GGA motifs which are presented in the loop of a secondary hairpin structure of the mRNA (Dubey *et al.*, 2005; Gutierrez *et al.*, 2005). In *P. aeruginosa*, two members of the CsrA family of RNA-binding proteins are described: RsmA (PA0905) and RsmF (PA5183.1), which is also known under the name RsmN (Marden *et al.*, 2013; Morris *et al.*, 2013; Pessi *et al.*, 2001). RsmA regulates the switch between acute and chronic infections of *P. aeruginosa* via repression of the type VI secretion system and exopolysaccharide production, while type III secretion and motility are promoted (Allsopp *et al.*, 2017; Brencic and Lory, 2009; Chihara *et al.*, 2021; Irie *et al.*, 2020; Irie *et al.*, 2010; Moscoso *et al.*, 2011). In general, RsmA is a global regulator in *P. aeruginosa* that influences over 500 targets by direct binding to the mRNA or indirectly by affecting transcriptional regulators like AmrZ, two-component systems or other RNA-binding proteins (Brencic and Lory, 2009; Gebhardt *et al.*, 2020). Abundance of the structurally different RsmF in *P. aeruginosa* is distinctly lower compared to RsmA, however RsmA and RsmF share a broad variety of mRNA targets (Chihara *et al.*, 2021; Marden *et al.*, 2013). RsmA and RsmF activity is regulated by sRNAs that are presenting several GGA binding motifs in their secondary structure and thereby sequester the RNA binding proteins from their target mRNAs. In *P. aeruginosa* four of these antagonistic sRNAs are described, namely RsmY, RsmZ, RsmV and RsmW. These regulatory sRNAs show different expression under various conditions and thereby seem to have distinct functions within the *P. aeruginosa* Rsm regulatory cascade (Brencic *et al.*, 2009; Janssen *et al.*, 2018; Miller *et al.*, 2016).

## 1.8 The membrane anchored protein NbdA

In *P. aeruginosa* PAO1 the gene PA3311 encodes for a protein called NO-induced biofilm dispersion locus A (NbdA). NbdA is a three domain protein, consisting of the membrane anchored MHYT domain, a diguanylate cyclase domain with degenerated GGDEF motif and a phosphodiesterase domain with conserved EAL motif (Fig. 1.7; (Li *et al.*, 2013)).

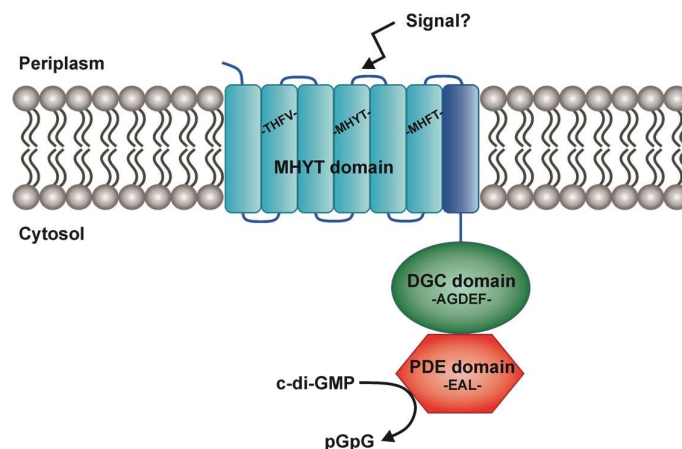


**Fig. 1.7: Domain structure of the phosphodiesterase NbdA**

The membrane-anchored phosphodiesterase NbdA of *P. aeruginosa* is composed of a membrane-spanning domain and two cytoplasmic domains. The predicted sensory MHYT-domain (light blue) possesses six transmembrane helices. The predicted sensory MHYT-domain (light blue) possesses six transmembrane helices. The conserved amino acid motifs which are predicted to coordinate a copper ion for NO, O<sub>2</sub> or CO sensing are facing the periplasmic side of the cytoplasmic membrane (Galperin *et al.*, 2001). The MHYT domain is connected to the cytoplasmic NbdA domains via an additional transmembrane helix (dark blue). In the cytoplasm, NbdA possesses a DGC domain (green) with degenerated GGDEF amino acid motif and a PDE domain (red) with EAL motif. Biochemical analyses have shown c-di-GMP degrading PDE activity of NbdA (Li *et al.*, 2013).

### 1.8.1 The sensory MHYT domain

The MHYT domain was first described in 2001 as putative sensory domain (Galperin *et al.*, 2001). It is predicted to possess six membrane-spanning helices connected via cytoplasmic and periplasmic loops that are rich of charged amino acids. Three of those transmembrane segments contain the eponymous MHYT amino acid motif or variants which are close to the periplasmic site of the cytoplasmic membrane (Fig. 1.7). The conserved histidine and methionine residues within the membrane segments of the MHYT domain are predicted to coordinate copper ions that might enable the protein to sense diatomic gases like oxygen (O<sub>2</sub>), carbon monoxide (CO) or nitric oxide (NO) (Galperin *et al.*, 2001). A search within the protein families database “Pfam” revealed occurrence with degenerated MHYT domains in 2,056 different species including  $\alpha$ -,  $\beta$ -, and  $\gamma$ -proteobacteria, Gram<sup>+</sup> bacteria, cyanobacteria and several fungi (Mistry *et al.*, 2021). However, the function of the MHYT domain remains uncertain. In *Oligotropha carboxidovorans* the proteins CoxC and CoxH, with a MHYT domain coupled to a DNA-binding helix-turn-helix domain, are encoded in the *cox* gene cluster, which is required for CO dehydrogenase synthesis (Galperin *et al.*, 2001; Paul *et al.*, 2011; Santiago *et al.*, 1999).

In *Burkholderia mallei* and *B. pseudomallei* the MHYT domain is part of a histidine kinase, further indicating a sensory function of this domain (Galperin *et al.*, 2001). However, coupling of the MHYT domain to DGC and PDE domains, occasionally combined with an additional sensory PAS domain, seems to be the predominant protein architecture within most organisms (Galperin *et al.*, 2001; Mistry *et al.*, 2021).

*P. aeruginosa* encodes two proteins, NbdA (PA3311) and MucR (PA1727), which share the domain architecture MHYT-GGDEF-EAL (Hay *et al.*, 2009; Li *et al.*, 2013). The N-terminus of both proteins is predicted to lie in the periplasm and the MHYT domain is connected to the cytoplasmic domains via an additional transmembrane helix. Interestingly, the annotated N-terminus of NbdA, with 80 amino acid residues in front of the MHYT-domain, is strikingly longer than in other MHYT-containing proteins (Galperin *et al.*, 2001). MucR is described to have both, DGC and PDE activity. However, NbdA was shown to only possess PDE activity but no DGC activity due to its degenerated GGDEF motif (Li *et al.*, 2013).

### 1.8.2 The putative role of NbdA within *P. aeruginosa*

In *P. aeruginosa*, MucR has been linked to nitrate dependent reduction of alginate production presumably via modulation of a local c-di-GMP pool (Hay *et al.*, 2009; Wang *et al.*, 2015). Both, the DGC and PDE domain of MucR are required for this function. Sensing of nitrate is dependent on the MHYT domain of MucR, but it is still unclear if nitrate is sensed directly or if MucR recognizes for example NO or changes in the redox potential of the cell (Wang *et al.*, 2015). In contrast, the role of NbdA in *P. aeruginosa* is still unsolved. In 2013, NbdA was described to be involved in NO-induced biofilm dispersal. A PAO1 *nbdA* deletion mutant was able to disperse biofilms in response to glutamate but not NO (Li *et al.*, 2013). This study also showed an activating effect of NO on *nbdA* transcription. However, in a recent study, a  $\Delta nbdA$  strain was still able to disperse biofilms after exposure to NO (Zemke *et al.*, 2020). The contradictory results might be due to different experimental conditions, but the finding of Zemke *et al.* agree with the results of a former PhD student of our lab who also found NO-induced biofilm dispersal in a newly generated, markerless *nbdA* deletion mutant (Rüger, 2019). Transposon mutants of *nbdA* in PA14 showed increased biofilm formation, reduced swimming, swarming and twitching motility and impaired virulence in a mouse model (Kulasakara *et al.*, 2006). However, the markerless PAO1 *nbdA* deletion strain possesses wt-like biofilm formation and motility behavior (Rüger, 2019). A recent publication revealed involvement of NbdA in a signaling network composed of three PDEs and the c-di-GMP binding effector MapZ that controls the chemotactic flagellar motor switching of *P. aeruginosa* (Xin *et al.*, 2019). Deletion of *nbdA* or inactivation of its PDE domain resulted in a loss of flagellar motor switching and therefore directional changes of swimming motility, indicating a link between NbdA and chemotaxis.

## 1.9 Objectives of this work

*Pseudomonas aeruginosa* possesses a large regulatory network of the second messenger c-di-GMP which is important for the control of cellular behavior and the cells “decision making”. On the first sight, the high number of c-di-GMP producing DGCs and c-di-GMP degrading PDEs in *P. aeruginosa* seem to cause redundancy in the cell. Nevertheless, a variety of studies demonstrated that strict regulation of transcription, translation and enzymatic activity together with the spatial separation of proteins with redundant functions leads to very specific roles of each DGC and PDE in *P. aeruginosa*.

The active PDE NbdA was long thought to induce biofilm dispersal of *P. aeruginosa* after sensing of the diatomic gas NO (Li *et al.*, 2013). However, a recently published study and a former PhD student of our group were both unable to reproduce this function of NbdA (Rüger, 2019; Zemke *et al.*, 2020). In general, published phenotypes for *nbdA* deletion mutants or overexpression strains are ambiguous and partly differ between *P. aeruginosa* PAO1 and PA14. We therefore decided to take a step back and have a closer look on regulation of *nbdA* on the transcriptional and post-transcriptional level to gain insights under which conditions NbdA is most likely active in *P. aeruginosa* PAO1. Investigation of *nbdA* regulation was performed utilizing transcriptional and translational *nbdA* reporter gene fusions (see chapters 3.1 and 3.2). Additional phenotypic assays with PAO1 strains overexpressing several variants of the NbdA domains were used to study the influence of the putative sensory MHYT domain, the DGC domain and the PDE domain on c-di-GMP dependent phenotypes (see chapter 3.3). Deletion of *nbdA* does not alter the global intracellular level of c-di-GMP (Rüger, 2019; Zemke *et al.*, 2020). Therefore, it was hypothesized that NbdA might only influence a small pool of c-di-GMP in the cells. Microscopic studies of the cellular NbdA localization were used to clarify whether NbdA is distributed through the whole cell or if it is only present at distinct locations in the cell (see chapter 3.4). Additionally, co-localization assays with the polar flagellum and the chemotaxis protein CheA were performed to reinforce the findings of Xin *et al.* who observed NbdA involvement in chemotaxis induced flagellar motor switching of *P. aeruginosa* (Xin *et al.*, 2019).

## 2 Material and Methods

### 2.1 Microbial strains, material and chemicals

#### 2.1.1 Microbial strains

**Table 2.1: Bacterial strains used in this study.**

Strain	Genotype	Reference
<b><i>Escherichia coli</i></b>		
DH5 $\alpha$	F <sup>-</sup> $\phi$ 80d <i>lacZ</i> $\Delta$ M15 $\Delta$ ( <i>lacZYA-argF</i> )U169 <i>endA1 hsdR17 deoR gyrA96 thi-1 relA1 supE44</i>	(Hanahan, 1983)
S17-I	<i>recA pro thi hsdR</i> M <sup>+</sup> T <sup>p</sup> Sm <sup>r</sup> ; RP4:2 Tc::Mu-Km::Tn7/ $\lambda$ pir	(de Lorenzo and Timmis, 1994)
MG1655	Derivate of <i>E. coli</i> K-12; F <sup>-</sup> ; $\lambda$ ; <i>rph</i> <sup>-</sup>	(Blattner <i>et al.</i> , 1997)
AB607	$\Delta$ <i>pdeH</i> ::Frt in MG1655 background	(Boehm <i>et al.</i> , 2010)
DH5 $\alpha$ pBAD2- <i>bgaB</i>	DH5 $\alpha$ with pBAD2- <i>bgaB</i> ; Amp <sup>R</sup>	This work
DH5 $\alpha$ pBAD2- <i>nbdA-bgaB</i>	DH5 $\alpha$ with pBAD2- <i>nbdA-bgaB</i> ; Amp <sup>R</sup>	This work
DH5 $\alpha$ pBAD2- <i>trxA-bgaB</i>	DH5 $\alpha$ with pBAD2- <i>trxA-bgaB</i> ; Amp <sup>R</sup>	This work
MG1655 pBAD2- <i>bgaB</i>	MG1655 with pBAD2- <i>bgaB</i> ; Amp <sup>R</sup>	This work
MG1655 pBAD2- <i>nbdA-bgaB</i>	MG1655 with pBAD2- <i>nbdA-bgaB</i> ; Amp <sup>R</sup>	This work
MG1655 pBAD2- <i>trxA-bgaB</i>	MG1655 with pBAD2- <i>trxA-bgaB</i> ; Amp <sup>R</sup>	This work
AB607 pBAD2- <i>bgaB</i>	AB607 with pBAD2- <i>bgaB</i> ; Amp <sup>R</sup>	This work
AB607 pBAD2- <i>nbdA-bgaB</i>	AB607 with pBAD2- <i>nbdA-bgaB</i> ; Amp <sup>R</sup>	This work
AB607 pBAD2- <i>trxA-bgaB</i>	AB607 with pBAD2- <i>trxA-bgaB</i> ; Amp <sup>R</sup>	This work
<b><i>Pseudomonas aeruginosa</i></b>		
PAO1	wild type (wt); DSM-22644	(Dunn and Holloway, 1971)
PAO1::mini-CTX1- <i>lacZ</i>	PAO1 with mini-CTX1- <i>lacZ</i> integrated at <i>attB</i> site	This work
PAO1::pKGE06	PAO1 with mini-CTX1- <i>pnbDA-lacZ</i> integrated at <i>attB</i> site	This work
PAO1:: $\Delta$ <i>rpoS</i>	<i>rpoS</i> deletion mutant in PAO1 background	This work
PAO1:: $\Delta$ <i>rpoS</i> ::pKGE06	$\Delta$ <i>rpoS</i> with mini-CTX1- <i>pnbDA-lacZ</i> integrated at <i>attB</i> site	This work

PAO1:: $\Delta amrZ$	<i>amrZ</i> deletion mutant in PAO1 background	This work
PAO1:: $\Delta amrZ$ ::pKGE06	$\Delta amrZ$ with mini-CTX1- <i>pnbDA-lacZ</i> integrated at <i>attB</i> site	This work
PAO1:: $\Delta nirS$	<i>nirS</i> deletion mutant in PAO1 background	This work
PAO1:: $\Delta nirS$ ::pKGE06	$\Delta nirS$ with mini-CTX1- <i>pnbDA-lacZ</i> integrated at <i>attB</i> site	This work
PAO1:: $\Delta nirF$	<i>nirF</i> deletion mutant in PAO1 background	This work
PAO1:: $\Delta nirF$ ::pKGE06	$\Delta nirF$ with mini-CTX1- <i>pnbDA-lacZ</i> integrated at <i>attB</i> site	This work
PAO1:: $\Delta norCB$	<i>norCB</i> deletion mutant in PAO1 background	This work
PAO1:: $\Delta norCB$ ::pKGE06	$\Delta norCB$ with mini-CTX1- <i>pnbDA-lacZ</i> integrated at <i>attB</i> site	This work
PAO1 BS	wt strain provided by Simon Dove (Boston Children's Hospital)	(Gebhardt <i>et al.</i> , 2020)
PAO1 BS:: $\Delta rsmA$	<i>rsmA</i> deletion mutant in Boston PAO1 background	(Gebhardt <i>et al.</i> , 2020)
PAO1 BS:: $\Delta rsmF$	<i>rsmF</i> deletion mutant in Boston PAO1 background	(Gebhardt <i>et al.</i> , 2020)
PAO1 BS:: $\Delta rsmA$ :: $\Delta rsmF$	<i>rsmA rsmF</i> double deletion mutant in Boston PAO1 background	(Gebhardt <i>et al.</i> , 2020)
PAO1 BS pJN105	Boston PAO1 wt with pJN105, Gm <sup>R</sup>	This work
PAO1 BS pKGE19	Boston PAO1 wt with pJN105- <i>nbdA-bgaB</i> , Gm <sup>R</sup>	This work
PAO1 BS pKGE18	Boston PAO1 wt with pJN105- <i>trxA-bgaB</i> , Gm <sup>R</sup>	This work
PAO1 BS:: $\Delta rsmA$ pJN105	$\Delta rsmA$ in Boston PAO1 background with pJN105, Gm <sup>R</sup>	This work
PAO1 BS:: $\Delta rsmA$ pKGE19	$\Delta rsmA$ in Boston PAO1 background with pJN105- <i>nbdA-bgaB</i> , Gm <sup>R</sup>	This work
PAO1 BS:: $\Delta rsmA$ pKGE18	$\Delta rsmA$ in Boston PAO1 background with pJN105- <i>trxA-bgaB</i> , Gm <sup>R</sup>	This work
PAO1 BS:: $\Delta rsmA$ :: $\Delta rsmF$ pJN105	$\Delta rsmA \Delta rsmF$ in Boston PAO1 background with pJN105, Gm <sup>R</sup>	This work
PAO1 BS:: $\Delta rsmA$ :: $\Delta rsmF$ pKGE19	$\Delta rsmA \Delta rsmF$ in Boston PAO1 background with pJN105- <i>nbdA-bgaB</i> , Gm <sup>R</sup>	This work
PAO1 BS:: $\Delta rsmA$ :: $\Delta rsmF$ pKGE18	$\Delta rsmA \Delta rsmF$ in Boston PAO1 background with pJN105- <i>trxA-bgaB</i> , Gm <sup>R</sup>	This work
PAO1:: <i>nbdA-mNeonGreen</i>	genomic integration of <i>nbdA-mNeonGreen</i> fusion with C-terminal 6x His-Tag into the original <i>nbdA</i> gene locus	This work

PAO1:: <i>nbda-Venus</i>	genomic integration of <i>nbda-Venus</i> fusion with C-terminal 6x His-Tag into the original <i>nbda</i> gene locus	This work
PAO1:: <i>nbda-mNeonGreen::pKGE16</i>	genomic integration of mini-CTX1- <i>mCherry</i> into the <i>attB</i> -site of <i>nbda-mNeonGreen</i> , Tet <sup>R</sup>	This work
PAO1:: <i>fliC(T394C)</i>	genomic integration of point mutation in <i>fliC</i> that causes AA exchange T394C	This work
PAO1:: <i>nbda-mNeonGreen::fliC(T394C)</i>	genomic integration of point mutation in <i>fliC</i> that causes AA exchange T394C in <i>nbda-mNeonGreen</i> background	This work
PAO1:: <i>nbda-Venus::fliC(T394C)</i>	genomic integration of point mutation in <i>fliC</i> that causes AA exchange T394C in <i>nbda-Venus</i> background	This work
PAO1:: <i>cheA-mCerulean</i>	genomic integration of <i>cheA-mCerulean</i> fusion into the original gene locus of <i>cheA</i>	This work
PAO1:: <i>cheA-tdTomato</i>	genomic integration of <i>cheA-tdTomato</i> fusion into the original gene locus of <i>cheA</i>	This work
PAO1:: <i>nbda-mNeonGreen::cheA-mCerulean</i>	genomic integration of <i>cheA-mCerulean</i> fusion into the original gene locus of <i>cheA</i> in <i>nbda-mNeonGreen</i> background	This work
PAO1:: <i>nbda-mNeonGreen::cheA-tdTomato</i>	genomic integration of <i>cheA-tdTomato</i> fusion into the original gene locus of <i>cheA</i> in <i>nbda-mNeonGreen</i> background	This work
PAO1 pKGE20	wt containing pME6032- <i>nbda-mNeonGreen</i> , Tet <sup>R</sup>	This work
PAO1 pKGE21	wt containing pME6032- <i>nbda-Venus</i> , Tet <sup>R</sup>	This work
PAO1:: <i>fliC(T394C)</i> pKGE20	<i>fliC(T394C)</i> containing pME6032- <i>nbda-mNeonGreen</i> , Tet <sup>R</sup>	This work
PAO1:: <i>fliC(T394C)</i> pKGE21	<i>fliC(T394C)</i> containing pME6032- <i>nbda-Venus</i> , Tet <sup>R</sup>	This work
PAO1:: $\Delta$ <i>nbda</i> pHERD26T	$\Delta$ <i>nbda</i> (markerless) containing pHERD26T, Tet <sup>R</sup>	(Rüger, 2019)
PAO1:: $\Delta$ <i>nbda</i> pMRP12	$\Delta$ <i>nbda</i> (markerless) containing pMRP12, Tet <sup>R</sup>	This work
PAO1:: $\Delta$ <i>nbda</i> pMRP14	$\Delta$ <i>nbda</i> (markerless) containing pMRP14, Tet <sup>R</sup>	(Rüger, 2019)
PAO1:: $\Delta$ <i>nbda</i> pASC04	$\Delta$ <i>nbda</i> (markerless) containing pASC04, Tet <sup>R</sup>	This work
PAO1:: $\Delta$ <i>nbda</i> pMKE02	$\Delta$ <i>nbda</i> (markerless) containing pKGE17, Tet <sup>R</sup>	This work
PAO1:: $\Delta$ <i>nbda</i> pJRE02	$\Delta$ <i>nbda</i> (markerless) containing pJRE02, Tet <sup>R</sup>	(Rehner, 2020)
PAO1:: $\Delta$ <i>nbda</i> pJRE01	$\Delta$ <i>nbda</i> (markerless) containing pJRE01, Tet <sup>R</sup>	(Rehner, 2020)



## 2.1.2 Plasmids

**Table 2.2: Plasmids used in this study.**

Plasmid	Relevant properties	Reference
pEXG2	Allelic exchange vector, Gm <sup>R</sup> , <i>mob</i> , <i>sacB</i>	(Rietsch <i>et al.</i> , 2005)
pASK-IBA3	Amp <sup>R</sup> , Strep-tag	IBA
mini-CTX1- <i>lacZ</i>	Tet <sup>R</sup> , <i>lacZ</i> , FRT site, attP site, <i>int</i>	(Becher and Schweizer, 2000)
pME6032	<i>Pseudomonas</i> / <i>E. coli</i> shuttle vector, Tet <sup>R</sup>	(Heeb <i>et al.</i> , 2002)
pJN105	Broad-host-range expression vector, <i>araC</i> -P <sub>BAD</sub> cassette, Gm <sup>R</sup>	(Newman and Fuqua, 1999)
pHERD26T	Broad-host-range expression vector, <i>araC</i> -P <sub>BAD</sub> cassette, Tet <sup>R</sup> ,	(Qiu <i>et al.</i> , 2008)
pNUT1239	Amp <sup>R</sup> , template for <i>mNeonGreen</i>	K. Drescher (JLU Giessen)
pXVENC-2	Kan <sup>R</sup> , template for <i>Venus</i>	(Thanbichler <i>et al.</i> , 2007)
pCR2.1- <i>mCherrySO</i>	Kan <sup>R</sup> , Amp <sup>R</sup> , template for <i>mCherry</i> (codon optimization for <i>Shewanella oneidensis</i> )	K. Drescher (JLU Giessen)
ptdTomato	Amp <sup>R</sup> , template for <i>tdTomato</i>	TaKaRa
mCerulean-C1	Kan <sup>r</sup> , template for <i>mCerulean</i>	Addgene

### Generation of markerless deletion mutants

pKGE01	pEXG2-derivate; truncated <i>rpoS</i> with 452 bp up- and 439 bp downstream	This work
pKGE02	pEXG2-derivate; truncated <i>amrZ</i> with 484 bp up- and 485 bp downstream	This work
pKGE03	pEXG2-derivate; truncated <i>nirS</i> with 448 bp up- and 512 bp downstream	This work
pKGE04	pEXG2-derivate; truncated <i>nirF</i> with 517 bp up- and 491 bp downstream	This work
pKGE05	pEXG2-derivate; truncated <i>norCB</i> with 452 bp- up and 439 bp downstream	This work
pKMC1161 (pEXG2- $\Delta$ <i>rsmA</i> )	pEXG2-derivate; truncated <i>rsmA</i>	(Gebhardt <i>et al.</i> , 2020)
pMJG243 (pEXG2- $\Delta$ <i>rsmF</i> )	pEXG2-derivate, truncated <i>rsmF</i>	(Gebhardt <i>et al.</i> , 2020)

**Analysis of transcriptional and translational regulation of *nbda***

pKGE06	mini-CTX1- <i>lacZ</i> -derivate; transcriptional fusion of <i>nbda</i> promoter (450 bp) to <i>lacZ</i>	This work
20ACJUUP_2876122_ <i>nbda</i> _5UTR30nt	synthetic DNA of <i>nbda</i> 5'-UTR with 30 nt of ORF	Thermo Fisher
pBAD2- <i>bgaB</i>	pBAD2-derivate encoding <i>bgaB</i> -His without RBS	(Klinkert <i>et al.</i> , 2012)
pBAD2- <i>trxA-bgaB</i>	pBAD2-derivate with translational fusion of <i>trxA</i> 5'-UTR and <i>bgaB</i> -His	D. Scheller (RUB)
pBAD2- <i>nbda-bgaB</i>	pBAD2-derivate with translational fusion of <i>nbda</i> 5'-UTR with 30 nt of ORF and <i>bgaB</i> -His	D. Scheller (RUB)
pKGE18	pJN105-derivate with translational fusion of <i>trxA</i> 5'-UTR and <i>bgaB</i> -His	This work
pKGE19	pJN105-derivate with translational fusion of <i>nbda</i> 5'-UTR and <i>bgaB</i> -His	This work

**Genomic integration of fluorescent protein tag**

pEXG2-PA3312	pEXG2-derivate, last 603 bp of PA3312	S. Zehner (TUK)
pKGE07	pASK-IBA3-derivate, coding region of <i>mNeonGreen</i> with 6x-His-tag	This work
pKGE08	pASK-IBA3-derivate, fusion of 508 bp of <i>nbda</i> to coding region of <i>mNeonGreen</i> with 6x-His-tag	This work
pKGE09	pEXG2-derivate, fusion of 508 bp of <i>nbda</i> to coding region of <i>mNeonGreen</i> with 6x-His-tag, last 603 bp of PA3312	This work
pKGE10	pASK-IBA3-derivate, coding region of <i>Venus</i> with 6x-His-tag	This work
pKGE11	pASK-IBA3-derivate, fusion of 508 bp of <i>nbda</i> to coding region of <i>Venus</i> with 6x-His-tag	This work
pKGE12	pEXG2-derivate, fusion of 508 bp of <i>nbda</i> to coding region of <i>Venus</i> with 6x-His-tag, last 603 bp of PA3312	This work
pKGE13	pEXG2-derivate, fusion of 588 bp of <i>cheA</i> to coding region of <i>tdTomato</i> , 629 bp of PA1459	This work
pKGE14	pEXG2-derivate, fusion of 588 bp of <i>cheA</i> to coding region of mCerulean, 629 bp of PA1459	This work

**Genomic integration of amino acid exchange**

pKGE15	pEXG2-derivate; 1133 bp of <i>fliC</i> with encoded AA exchange T394C and 450 bp downstream	This work
--------	---	-----------

pKGE25	pEXG2-derivate; full-length <i>kbdA</i> with encoded AA exchanges Q392S and K393E	This work
pKGE26	pEXG2-derivate; full-length <i>kbdA</i> with encoded AA exchanges Q392E and K393S	This work
<b>Genomic integration into phage attachment site</b>		
pKGE16	mini-CTX1- <i>lacZ</i> derivate, coding region of <i>mCherry</i> under control of constitutive PC promoter, <i>lacZ</i> truncated	This work
<b>Expression of <i>kbdA</i> variants</b>		
pMRP12	pHERD26T-derivate, full length coding region of <i>kbdA</i> with C-terminal Strep-tagII	(Rüger, 2019)
pMRP14	pHERD26T-derivate, full length coding region of <i>kbdA</i> with C-terminal Strep-tagII; EAL motif substituted to AAL	(Rüger, 2019)
pASC04	pHERD26T-derivate, coding regions of <i>kbdA</i> AGDEF and EAL domain with C-terminal Strep-tagII	A. Scherhag (TUK)
pMKE02	pHERD26T-derivate, coding regions of <i>kbdA</i> AGDEF and EAL domain with C-terminal Strep-tagII; EAL motif substituted to AAL	M. Karcher (TUK)
pJRE02	pHERD26T-derivate, coding regions of <i>kbdA</i> MHYT and AGDEF domain with C-terminal Strep-tagII	(Rehner, 2020)
pJRE01	pHERD26T-derivate, coding region of <i>kbdA</i> MHYT domain with C-terminal Strep-tagII	(Rehner, 2020)
pKGE20	pME6032-derivate, fusion of <i>kbdA</i> to <i>mNeonGreen</i> with C-terminal 6x-His-tag	This work
pKGE21	pME6032-derivate, fusion of <i>kbdA</i> to <i>Venus</i> with C-terminal 6x-His-tag	This work

### 2.1.3 Oligonucleotides

Custom DNA oligonucleotides used in this work have been purchased from Eurofins Genomics GmbH. For cDNA synthesis the Random Primer Mix of New England Biolabs was used. In Table 2.3, relevant endonuclease restriction sites are underlined. Positions of base exchanges for site-directed mutagenesis or construction of mutant alleles in pEXG2 are marked in blue. V stands for either A, C or G.

**Table 2.3: Oligonucleotides used in this study.**

Primer	Sequence (5'→3')
<b>Construction of mutant alleles by SOE-PCR and sequencing primers for the genes of interest</b>	
<i>rpoS</i> -Up-F	GCGCCTGCAGCAAGCTCCAGCATCTGGAGCGCTG
<i>rpoS</i> -Up-R	CTCCTGGAGCCC GGCCATCGCGCTGAAGCGCCTGCGG
<i>rpoS</i> -Down-F	GATGCCGGGCTCCAGGAGGAG
<i>rpoS</i> -Down-R	GCGCCTCGAGTCGGCCGTTTTGCCTCAAACGGAA
<i>rpoS</i> -seqF	CTAGAATCGCGCGCGCTTAGCCG
<i>rpoS</i> -seqR	TGCTCGGGGCCGTCGTCTGTTC
<i>amrZ</i> -Up-F	GCGCAAGCTTGATGCACCGATCAACGC
<i>amrZ</i> -Up-R	CTCCGCATCGTGTGCGGTAGGAGTTGCCTGTTTCA
<i>amrZ</i> -Down-F	GCACACGATGCGGAG
<i>amrZ</i> -Down-R	GCGCGAATTCTCAGGTTGACCAGCAGAAC
<i>amrZ</i> -seqF	ACCCAGCACGTGAT
<i>amrZ</i> -seqR	GGAATGACTCCGGGCT
<i>nirS</i> -Up-F	GCGCCTGCAGAAGAGGACAGGCGAACGTCAGCGC
<i>nirS</i> -Up-R	GGCACCTTGCTCGCCTCGCGGCTGATCACCCCGACCGGTAAG
<i>nirS</i> -Down-F	CGAGGCGAGCAAGGTGCCAC
<i>nirS</i> -Down-R	GCGCCTCGAGCCAGGTAGCAGATACCGCCTTCGCG
<i>nirS</i> -seqF	TGAGGAGAAGCGGCGGAGGGGA
<i>nirS</i> -seqR	GTAGTCGAAGCGCAACGCGACGAAACG
<i>nirF</i> -Up-F	GCGCCTGCAGCAGGTAGCGCAGGTGTTGCCG
<i>nirF</i> -Up-R	AGCCAGCAGCCGCCCTTGCCGAGCGGCATCTTCTTCAGCCAC
<i>nirF</i> -Down-F	CAAGGGCGGCTGCTGGCTACA
<i>nirF</i> -Down-R	GCGCCTCGAGCGCCGAAGCGGAACTCGCG
<i>nirF</i> -seqF	ATGGCCACATCGGCAGGCGAC
<i>nirF</i> -seqR	GCTCCCCCTACGAGGAACCGTG
<i>norCB</i> -Up-F	GCGCAAGCTTTGCTGGCGCCGGTGTATACGC
<i>norCB</i> -Up-R	TAGGCGACCAGGCCGATGAGCCCGCCGAAATAGATGTTCTTGCC
<i>norCB</i> -Down-F	CTCATCGGCCTGGTCGCCTACC
<i>norCB</i> -Down-R	GGGGAATTCATTTCCAGTTCGGCGTCTGCCGC
<i>norCB</i> -seqF	TCATCGGCGACGGCATGGACC
<i>norCB</i> -seqR	ATCGGTTGCAGCAGCACGTGG
<i>fliC</i> (T394C)-Up-F	GCAAGCTTGCAGAAAGAAGTCGCTGCGCAACAGGC

---

<i>fliC</i> (T394C)-Up-R	GCGTTCTGGGCGCCGTCGGC <u>GCAGGAGATATCGACGCT</u>
<i>fliC</i> (T394C)-Down-F	AGCGTCGATATCTCCT <u>TGCGCCGACGGCGCCAGAACGC</u>
<i>fliC</i> (T394C)-Down-R	<u>GCCTCGAGGGCAAGCACCATGCCAAGTCGTT</u>
<i>fliC</i> -seqF	GCAGAACCGCTTCAACGAGTGCAAG
<i>fliC</i> -seqR	CTCTTGAAGTGGCCAGGGCAGT
<i>rsmA</i> -seqF	CCAACATCGCCAAGGTTTC
<i>rsmA</i> -seqR	CTGAGCTATGAGTGCCTGTC
<i>rsmF</i> -seqF	TCCCTCCCGATTGAAACG
<i>rsmF</i> -seqR	GCAACTGTTGTTCTTCCCG

### ***P*<sub>*nbda*</sub>-*lacZ* fusion**

<i>P</i> <sub><i>nbda</i></sub> - <i>lacZ</i> -F	GCGCGAATTCATGCCTTTTCTCCCCGGGAAAATGC
<i>P</i> <sub><i>nbda</i></sub> - <i>lacZ</i> -R	GCGCGGATCCAGGTCGTAGCGCAGGGCGA

### **Construction of *nbda*-*mNeonGreen*/*Venus* fusions for genomic integration**

<i>nbda</i> - <i>EcoRI</i> -F	GATCGAATTC <u>CAATCTCGGCCGGGCCAGC</u>
<i>nbda</i> - <i>SacI</i> -R	GATGAGCTCGGCCTGGTTCAGGCTGCGC
<i>mNeonGreen</i> - <i>SacI</i> -F	GATCGAGCTCATGGTGAGCAAGGGC
<i>mNeonGreen</i> - <i>XhoI</i> -R	GATCTCGAGCTA <u>GTGATGATGGTGATGGTG</u> CCTTGACAGCTCGTCC
<i>Venus</i> - <i>SacI</i> -F	GATCGAGCTCATGGTGAGCAAGGGC
<i>Venus</i> - <i>XhoI</i> -R	GATCTCGAGCTA <u>GTGATGATGGTGATGGTG</u> CCTTGACAGCTCGTCC

### **5'-RACE PCR**

SP1_ <i>nbda</i>	ATGGCTGGTAGTACTGGGTGGC
SP3_ <i>BglII</i> _nbda	TAAGATCTGGCGAATAGGTGCAGTTCTG
Oligo (dt) anchor primer	GACCAGATCTATCGATGTCGACTTTTTTTTTTTTTTTTTT
anchor-1 primer	GACCAGATCTATCGATGTCGACT

### **RT-PCR**

<i>nbda</i> -RT1-F	TTCCTCGACCTCGATCACTT
<i>nbda</i> -RT1-R	TGGGTTCCATCATCTTCTGC
<i>recA</i> -RT1-F	GACCGAGGCGTAGAAGTTCA
<i>recA</i> -RT1-R	CAACTGCCTGGTCATCTTCA

### **Site-directed mutagenesis**

NbdA_QC_AAL_for	GTACACCAGTTGGCAGCATTGGTGCG
NbdA_QC_AAL_rev	CGCACCAATGCTGCCAACTGGTGTAC

**Gibson Assembly®**

PC-prom-G-F	CACCATCCAGTGCAGGAGCTTACGCGTAATTCTCGAATTG
PC-prom-G-R	TGGAAACCATCGTTGCTGCTCCATAACATC
<i>mCherry</i> -G-F	AGCAGCAACGATGGTTTCCAAAGGGGAAG
<i>mCherry</i> -G-R	CGAATTCCTGCAGCCCGGGGAATTCGCCCTTTAACTCG
<i>cheA</i> -G-F	CAAGCTTCTGCAGGTGCTACTAACCTGATTTTCGCCCCG
<i>cheA</i> -G-F	TGCTCACCATGATGCGCCGTGCGTAACG
<i>tom/cer</i> -G-F	ACGGCGCATCATGGTGAGCAAGGGCGAG
<i>tdTomato</i> -G-R	ATACGCGGCGCTTGTACAGCTCGTCCATGC
<i>cerulean</i> -G-R	ATACGCGGCGTTATCTAGATCCGGTGGATCCC
PA1459- <i>tom</i> -G-F	GCTGTACAAGCGCCGCGTATGGGTTTCC
PA1459- <i>cer</i> -G-F	ATCTAGATAACGCCGCGTATGGGTTTCC
PA1459-G-R	AGCTCGAGCCCGGGGATCCTAAGTTGGCCGGCAACTGG
<i>nbDA-bgaB</i> -G-R	GCCCGGGGATCCACTAGTTAGCAAGCACAATGCCACC
<i>nbDA-bgaB</i> -G-R	CCACCGCGGTGGCGGCCGCTCTAGTGGTGATGGTGATGATG
<i>trxA-bgaB</i> -G-F	GCCCGGGGATCCACTAGTTATCCTACTGTTGGTTAATG
<i>trxA-bgaB</i> -G-R	CCACCGCGGTGGCGGCCGCTCTAGTGGTGATGGTGATG
<i>mNeonGreen</i> -G-F	TGCCATGGTACCCGGGAGCTCTAGTGATGATGGTGATGGTG
<i>mNeonGreen</i> -G-R	GAACCAGGCCATGGTGAGCAAGGGCGAG
<i>nbDA</i> (FL)-FP-G-F	TGCTCACCATGGCCTGGTTCAGGCTGCG
<i>nbDA</i> (FL)-FP-G-R	CAGGAAACAGAATTCGAGCTATGGATTGGCAAGGCCTGC

**Additional sequencing primers**

pEXG2-seqF	CGACCTCATTCTATTAGACTCTCGTTTGGATTGC
pEXG2-seqR	GTTTCGCTCGCGTATCGGTGATTCATTCTG
pASKseqfwd	GAGTTATTTTACCACTCCCT
pASKseqrev	CGCAGTAGCGGTAAACG
<i>lacZ</i> -rev	GGATTTTCTTACGCGAAATACGGG
<i>lacZ</i> 2	AAGCGCCATTCGCCATTTCAG
seq3miniCTX/ <i>lacZ</i>	ATCCACCGGCGCGCGTAATACG
ptac_seq	GAGCGGATAACAATTTACACAG
pME6032-seqF	CAGTTGCAAACCCTCACTGA
pBADfwd	ATGCCATAGCATTTTTATCC
T7_fwd	TAATACGACTCACTATAGGG
<i>bgaB</i> -seqR	TGTGGTTTGGAACTTAGTTC

---

PA3311fwd1EcoRI	GCGAATTCTCGGGGCGTAGGTGGAATAG
PA3311rev4BamHI	GCGGATCCGAAAGCGGCAGCCTGGCGATC
PA3311fwd4	CAGGAACTGCAGATGGAGGA
RT PA3311 fwd	CACGGCATTCAACGAAGTGT

---

## 2.1.4 Chemicals

All chemicals used in this work were ACS grade or higher and were purchased from AppliChem (Darmstadt), Becton Dickinson (Heidelberg), Carl Roth (Karlsruhe), Merck (Darmstadt) and Sigma-Aldrich (Munich) as not stated otherwise.

**Table 2.4: Chemicals**

---

<b>Chemical</b>	<b>Manufacturer</b>
β-Mercaptoethanol	Sigma-Aldrich
Agarose	Axon
Albumin fraction V	Carl Roth
Ammonium persulfate (APS)	Carl Roth
Ampicillin sodium salt	AppliChem
Blue Prestained Protein Standard, broad range	New England Biolabs
5-Bromo-4-chloro-3-indoxyl phosphate (BCIP)	Sigma-Aldrich
Casamino acids (CAA)	Becton Dickinson
Crystal violet	Riedel-de-Haen
D(+)-glucose	Merck
D(+)-sucrose	Carl Roth
Difco™ agar technical	Becton Dickinson
Dimethylsulfoxide (DMSO)	AppliChem
DNA-loading dye (6x)	Thermo Fisher Scientific
Ethidium bromide (5 mg/ml)	Carl Roth
Formaldehyde, 37 % aqueous (Formalin)	Ricca Chemical
GeneRuler™ DNA Ladder Mix	Thermo Fisher Scientific
Gentamicin sulfate	Carl Roth
Histo-Clear® II	National Diagnostics
Isopropyl-β-D-galactopyranoside (IPTG)	BioChemika
L(+)-arabinose	Carl Roth
Nitro blue tetrazolium chloride (NBT)	Sigma-Aldrich
Pseudomonas Isolation Agar	Becton Dickinson
Rotiphorese Gel 30	Carl Roth

---

Sodium dodecyl sulfate (SDS)	Carl Roth
Sodium nitroprusside (SNP)	Merck
Tetramethylethylenediamin (TEMED)	Carl Roth
Tetracycline hydrochloride	Sigma-Aldrich
Tryptone	Becton Dickinson

---

### 2.1.5 Sterilization

All media and supplements used for microbiological techniques were sterilized prior to use. If applicable solutions were autoclaved at 120 °C and 1 bar for 20 min. Heat sensitive solutions were filter sterilized using a pore size of 0.2 µm. Reaction tubes were autoclaved as describes above and glass ware was sterilized for 3 h by dry heat at 180 °C.

### 2.1.6 Culture media and supplements

As not stated otherwise in the protocol, liquid cultures of *P. aeruginosa* or *E. coli* strains were routinely grown in lysogeny broth (LB) with the appropriate antibiotics or supplements. For the preparation of solid media, 1.5 % (w/v) agar were added to the medium prior to sterilization. All media used for phenotypic *P. aeruginosa* assays were prepared with LB (Lennox) and technical Difco™ agar from Becton Dickinson (BD).

#### LB-medium (Lennox)

Tryptone	10 g/L
Yeast extract	5 g/L
NaCl	5 g/L

#### Basal medium 2 (BM2)

BM2-solution	1x
Glucose	0.4 % (w/v)
MgSO <sub>4</sub>	2 mM
FeSO <sub>4</sub>	0.01 mM

#### BM2-solution (10x)

(NH <sub>4</sub> ) <sub>2</sub> SO <sub>4</sub>	0.07 M
K <sub>2</sub> HPO <sub>4</sub>	0.4 M
KH <sub>2</sub> PO <sub>4</sub>	0.22 M
→ adjust to pH 7	

#### Biofilm medium

BM2-solution	1x
Glucose	0.4 % (w/v)
MgSO <sub>4</sub>	2 mM
FeSO <sub>4</sub>	0.01 mM
CAA	0.1 % (w/v)

#### Adhesion medium

BM2-solution	1x
Glucose	0.4 % (w/v)
MgSO <sub>4</sub>	2 mM
FeSO <sub>4</sub>	0.01 mM
CAA	0.5 % (w/v)



<u>Swimming-agar</u>		<u>Twitching-agar</u>	
LB Lennox (BD)	20 g/L	LB Lennox (BD)	20 g/L
Difco™ agar (BD)	0.3 % (w/v)	Difco™ agar (BD)	1 % (w/v)
<u>Tryptone medium (liquid)</u>		<u>Tryptone-agar</u>	
Tryptone	10 g/L	Tryptone	10 g/L
LB Lennox (BD)	20 g/L	Difco™ agar (BD)	1 % (w/v)

**Table 2.5: Antibiotics**

Antibiotic	Stock concentration	Solvent	Final conc.	Final conc.
			<i>E. coli</i>	<i>P. aeruginosa</i>
Ampicillin (Amp)	100 mg/ml	H <sub>2</sub> O	100 µg/ml	–
Gentamicin (Gm)	10 mg/ml 300 mg/ml	H <sub>2</sub> O	10 µg/ml	75-300 µg/ml
Kanamycin (Kan)	50 mg/ml	H <sub>2</sub> O	50 µg/ml	–
Tetracycline (Tet)	5 mg/ml 50 mg/ml	70 % (v/v) ethanol	5 µg/ml	50-100 µg/ml

**Table 2.6: Media supplements**

Supplement	Stock concentration	Final concentration
Casamino acids (CAA)	5 % (w/v)	0.1 / 0.5 % (w/v)
Isopropyl-β-D-galactopyranoside (IPTG)	100 mM	100 µM
KNO <sub>3</sub>	1 M	40 mM/ 50 mM
L(+)-Arabinose	10 % (w/v)	0.1 % (w/v)

### 2.1.7 Kits, enzymes and antibodies

All enzymes and kits were used according to the manufacturer's protocol or as stated in the method description.

**Table 2.7: Enzymes and Kits**

Product	Name	Manufacturer
Alkaline phosphatase	Shrimp Alkaline Phosphatase (rSAP)	New England Biolabs
DNase I	DNase I (RNase-free)	New England Biolabs

DNA ligase	Taq DNA-Ligase	Biozym Scientific
	T4 DNA Ligase	New England Biolabs
DNA polymerase	DreamTaq Green PCR Master Mix (2x)	Thermo Fisher Scientific
	Pfu DNA polymerase	TU Kaiserslautern (N. Münden)
	Phusion™ High-Fidelity DNA Polymerase	Thermo Fisher Scientific
	Q5® Hot Start High-Fidelity 2x Master Mix	New England Biolabs
gDNA extraction kit	NucleoSpin® Microbial DNA Kit	Macherey-Nagel
Lysozyme	Lysozyme (lyophilized)	Roth
PCR clean-up kit	NucleoSpin™ Gel and PCR Clean-up Kit	Macherey-Nagel
Plasmid DNA miniprep kit	NucleoSpin™ Plasmid EasyPure Mini Kit	Macherey-Nagel
Proteinase K		
Reaction clean-up kit	MinElute Reaction Cleanup Kit	Qiagen
Restriction endonucleases	Restriction endonucleases or high fidelity endonucleases (HF®-line)	New England Biolabs
Reverse transcriptase	M-MLV Reverse Transcriptase	Promega
	ProtoScript® II Reverse Transcriptase	New England Biolabs
RNA extraction kit	Quick-RNA Miniprep Kit	Zymo Research
	RNeasy Plus Mini Kit	Qiagen
RNase inhibitor	RNase Inhibitor (Human Placenta)	New England Biolabs
T5-exonuclease	T5 Exonuclease	New England Biolabs

**Table 2.8: Antibodies**

Antibody	Dilution	Antigen	Manufacturer
6x-His Tag Monoclonal Antibody (HIS.H8)	1:2,000 in TBS-T	His-tag	Thermo Fisher Scientific
Goat anti-mouse IgG-alkaline phosphatase	1:10,000 in TBS-T	Mouse IgG	Sigma-Aldrich
Strep-Tactin® AP conjugate	1:4,000 in TBS-T	Strep II-tag	IBA Lifesciences GmbH

## 2.1.8 Equipment and consumables

**Table 2.9: Equipment and consumables**

<b>Instrument / Consumable</b>	<b>Name</b>	<b>Manufacturer</b>
Agarose gel electrophoresis chamber	EasyPhor Mini	Biozym
	Big electrophoresis chamber	built at TU Kaiserslautern
Aspirator	Buchner Aspirator	
Autoclave	VX 150	Systec
Blotting system	Semidry Blot Trans-Blot® SD	BioRad
Centrifuges	5415 D	Eppendorf
	5418 R	Eppendorf
	5810 R	Eppendorf
Cuvettes	Cuvettes, single use (semi micro)	Hartenstein
	MicroPulser Electroporation cuvettes (2 mm gap)	BioRad
Electroporator	MicroPulser™	BioRad
Embedding cassette	Histosette™ II	Thermo Fisher Scientific
Gel documentation	Gel iX20 Imager	Intas
Incubator	Kelvitron® t	Heraeus Instruments
Incubator shaker	Incubator hood TH 30 with shaker SM 30 Control	Edmund Buehler
	Innova 2300 Platform Shaker (in 37 °C room)	New Brunswick Scientific
	Innova 44 Incubator Shaker Series	New Brunswick Scientific
Microscope	LSM 700 confocal microscope	Zeiss
	LSM 880 confocal microscope	Zeiss
	Eclipse E600 fluorescence microscope	Nikon
Microsensor	Calibration chamber CAL300	Unisense
	Micromanipulator MM33	Unisense
	Multimeter	Unisense
	O <sub>2</sub> microsensor OX-25	Unisense
Microtiter plate	Nunc™ 96-well Polystyrene Round Bottom Microwell Plates (sterile)	Nunc

---

Microtome	Microm HM 355S	Thermo Fisher Scientific
Mounting medium	Fluoro-Gel Mounting Medium with Tris Buffer	Electron Microscopy Sciences
Paraffin wax	Leica Paraplast® X-tra	McCormick Scientific
Paraffin embedding mold	3D printed by Dietrich Lab	Columbia University
pH meter	Basic pH Meter p-11	Sartorius
Plate reader	Infinite® F200 PRO	Tecan
Power supply	EPS 301	Amersham pharmacia biotech
	EPS 601	GE Healthcare
	Power Pac HC	BioRad
PVDF membrane	Roti® PVDF membrane	Carl Roth
Scales	PB4000-2	Gottlieb KERN & Sohn
	R 300 S	Sartorius
SDS-PAGE chamber	Mini-PROTEAN® Tetra Vertical Electrophoresis Cell	BioRad
Slide warmer	Small Slide Warmer (24 slides)	Ted Pella
Spectrometer	NanoDrop™ Lite	Thermo Fisher Scientific
	Ultrospec 500 <i>pro</i>	Amersham Biosciences
Syringe filters	ROTILABO® Mini-Tip PVDF (0.2 µm)	Carl Roth
Thermo block	Thermocell CHB-202	Bioer
	Thermomixer compact	Eppendorf
Thermocycler	Peqstar 2	Peqlab
	T1 Thermocycler	Biometra
	TGradient	Biometra
Tissue embedding system	EG1150 H	Leica
	EG1150 C	Leica
Tissue flotation water bath	Lighted Tissue Floating Bath XH-1003	Premiere
Tissue processor	STP 120 Spin Tissue Processor	Thermo Fisher Scientific
Ultra-pure water system	MilliQ® Integral Water Purification System	Merck

---

---

Vacuum pump	Laboport®	KNF Neuberger
Vortexer	REAX top	Heidolph

---

## 2.2 Microbiological methods

### 2.2.1 Cultivation of microorganisms

Bacterial strains from cryo-stocks (chapter 2.2.2) were initially cultivated on LB-agar plates, containing the appropriate antibiotic (Tab. 2.5), performing the triple streaking technique with a sterile inoculation loop. The plates were then incubated at 37 °C over night. Pre-cultures (ONCs) were prepared with LB-medium or the appropriate assay medium with the required antibiotics in either test tubes for volumes from 2-5 ml or Erlenmeyer flasks for volumes above 5 ml. The medium was inoculated with a single colony and incubated over night at 37 °C with constant shaking at 160 rpm (Innova 2300).

### 2.2.2 Storage of microorganisms

For long term storage, *P. aeruginosa* strains were conserved in media containing 7.5 % (v/v) DMSO and *E. coli* strains in media containing 20 % (v/v) glycerol. Strains were then stored at -80 °C.

### 2.2.3 Determination of cell density

Cell density of liquid cultures has been determined photometrically as optical density (OD) at 600 nm with the according growth medium as reference.

### 2.2.4 Analysis of aerobic and anaerobic growth

For the analysis of growth behavior, *P. aeruginosa* strains were cultivated at 37 °C with 160 rpm (Innova 2300). Optical density was monitored during the desired time period at 600 nm. LB pre-cultures were diluted to an OD<sub>600 nm</sub> of 0.05 in 50 ml LB for aerobic growth curves. For anaerobic growth analysis, pre-cultures were diluted to an OD<sub>600 nm</sub> of 0.1 in 90 ml LB supplemented with 50 mM KNO<sub>3</sub> in 100 ml threaded laboratory glass bottles (Schott Duran®). Bottles were closed with septum lids and the gas phase was exchanged with nitrogen for 2 min in order to replace remaining oxygen.

### 2.2.5 Preparation of chemically competent *E. coli* cells

For the preparation of chemically competent *E. coli* cells, a pre-culture of the corresponding strain was diluted 1:100 in 100 ml LB medium and grown at 37 °C with 160 rpm to an OD<sub>600 nm</sub> of ~ 0.5. Cells were collected by centrifugation at 4,000 rpm and 4 °C (Centrifuge 5810 R, Eppendorf) in 50 ml tubes. The cell pellets were resuspended in 50 ml ice-cold 50 mM CaCl<sub>2</sub>

and incubated on ice for 1 h. After a second incubation step (4,000 rpm, 4 °C), cell pellets were resuspended in 2.5 ml ice-cold 50 mM CaCl<sub>2</sub> with 15 % (v/v) glycerol, each. Aliquots of 200 µl competent cells were stored at - 80 °C.

### **2.2.6 Transformation of chemically competent *E. coli* cells**

Prior to transformation, chemically competent cells were thawed on ice. 0.75-1 µl of plasmid DNA or 10 µl of ligation or Gibson assembly reaction were added to the cells and the mixture was incubated on ice for 30 min. Cells were heat shocked at 42 °C for 2 min, followed by a 2 min recovery time on ice. 700 µl LB medium were added and cells were incubated at 37 °C and 160 rpm for 1 h (Innova 2300). The transformed cells were then plated on selective LB-agar and incubated at 37 °C over night.

### **2.2.7 Preparation of electro-competent *P. aeruginosa* cells**

Electro-competent *P. aeruginosa* cells were prepared freshly prior to electroporation. The overnight culture was grown in 8 ml LB medium at 37 °C and 160 rpm (Innova 2300). A total of 3 ml ONC was centrifuged at 8,000 rpm and 4 °C for 2 min (Centrifuge 5810 R, Eppendorf). Pelleted cells were kept on ice and washed twice with ice-cold 0.3 M sucrose solution. After each washing step, cells were collected by centrifugation for 2 min at 8,000 rpm and 4 °C. The cell pellet was then resuspended in 200 µl ice-cold 0.3 M sucrose solution and stored on ice until transformation.

### **2.2.8 Transformation of electro-competent *P. aeruginosa* cells**

For transformation of electro-competent *P. aeruginosa* cells, electroporation cuvettes with a 2 mm gap were required. Cuvettes were cooled down on ice prior to transformation and either LB or SOC-medium was pre-heated to 37 °C. 500 ng-1 µg of plasmid DNA was added to the competent cells and the mixture was transferred into the electroporation cuvette. After the electrostatic shock (program Ec2: 2.5 kV, 200 Ω, 25 µF), 1 ml of preheated medium was added and the cells were transferred to a fresh 1.5 ml tube. After an incubation time of 1-2 h at 37 °C and 160 rpm (Innova 2300) cells were plated on selective agar plates and incubated over night at 37 °C.

### **2.2.9 Conjugation of *P. aeruginosa* via biparental mating**

Conjugation of *P. aeruginosa* was performed via biparental mating with the *E. coli* strain S17.1 as donor. Pre-cultures of *P. aeruginosa* and *E. coli* S17.1, harboring the desired plasmid, were prepared in 5 ml LB medium supplemented with antibiotics if required. Cells were grown over night at 37 °C and 160 rpm. For the biparental mating ONCs of donor and recipient were mixed in a 9:1 ratio in 2 ml total volume and the mix was incubated at room temperature for 30 min.

Cells were pelleted by centrifugation at 4,000 rpm for 7 min (Eppendorf 5415 D), resuspended in 100  $\mu$ l fresh LB medium and spotted on a LB-agar plate. The mating plate was incubated upright at 37 °C for 24 h. After incubation the cells were harvested with a sterile inoculation loop and resuspended in 2 ml 0.9 % (w/v) NaCl solution. A serial dilution in 0.9 % (w/v) NaCl was prepared and 100  $\mu$ l of each dilution step was plated on Pseudomonas Isolation agar containing the corresponding antibiotic. Plates were incubated over night at 37 °C.

### **2.2.10 Growth of colony biofilms**

*P. aeruginosa* colony biofilms were grown on tryptone-agar plates. The plates were poured and incubated with closed lids at room temperature until solidified. Condensed water was removed from the lid with a clean paper towel. Precultures were prepared in 5 ml tryptone medium and grown over night at 37 °C and 160 rpm. The preculture was then diluted 1:100 in fresh tryptone medium and grown at 37 °C to an OD<sub>600 nm</sub> of ~ 0.5. Then, 5  $\mu$ l of culture were spotted on the agar surface and incubated at room temperature until dry. Plates were then incubated in the dark at 25 °C for 3 or 4 days. A moist surrounding was created by placing a bowl with water in the incubator.

### **2.2.11 O<sub>2</sub> profiles within colony biofilms**

The measurement of oxygen profiles was performed in colony biofilms grown on tryptone-agar or on plates supplemented with 40 mM KNO<sub>3</sub> as described in chapter 2.2.10. For O<sub>2</sub> probing an oxygen microsensor with 25  $\mu$ m tip size (Unisense) was utilized. The microsensor was previously calibrated with a two-step calibration method. Within the calibration chamber, the sensor was first calibrated in water continuously bubbled with air (atmospheric oxygen) and afterwards the zero point was set in water bubbled with N<sub>2</sub> for 30 min. The oxygen profile was measured by moving the microsensor in 5  $\mu$ m steps from the top to the bottom of the biofilm colony using a micromanipulator (Unisense). Each O<sub>2</sub> concentration measurement took 3 s and was performed 5 s after the microsensor movement.

## **2.3 Molecular biological methods**

### **2.3.1 Preparation of genomic DNA from *P. aeruginosa***

Genomic DNA of *P. aeruginosa* strains was obtained with the NucleoSpin® Microbial DNA kit (Macherey Nagel) according to the manufacturer's protocol. Concentration of the gDNA samples was measured photometrically (chapter 2.2.5).

### **2.3.2 Preparation of total RNA from *P. aeruginosa***

For the extraction of total *P. aeruginosa* RNA, a combination of the protocol 4 (Enzymatic lysis and proteinase K digestion of bacteria) of the QIAGEN RNA-protect handbook and the

QIAGEN RNeasy Plus Mini kit protocol was used as follows. Cells of an equivalent of  $OD_{600\text{ nm}} = 1$  in 1 ml were mixed with 100  $\mu\text{l}$  of RNA-stop solution to prevent RNA degradation. Cells were then harvested by centrifugation at 5,000 rpm and 4 °C for 5 min (Eppendorf 5418 R). Cell pellets were stored at - 80 °C or used directly for RNA extraction. Prior to RNA extraction, 10  $\mu\text{l}$   $\beta$ -mercapthoethanol were added per 1 ml of the kits RLT-buffer and 15 mg/ml lysozyme in TE-buffer was prepared in the required amounts. 15  $\mu\text{l}$  proteinase K were added to 200  $\mu\text{l}$  TE-buffer with 15 mg/ml lysozyme and cell pellets were carefully resuspend in this mixture. Samples were incubated for 10 min at room temperature and vortexed every 2 min for 10 s. 700  $\mu\text{l}$  RLT buffer were added and the sample was vortexed vigorously for 30 s. After this step, the manufacturer's protocol of the RNeasy Plus Mini kit (Qiagen) was followed without any further changes. RNA concentration was determined photometrically (chapter 2.3.6) and samples were checked for gDNA contamination via PCR (chapter 2.3.8). If the RNA sample contained remaining gDNA, DNase digestion (chapter 2.3.3) followed by another RNA purification was performed.

#### RNA-stop solution

5 % (v/v) phenol in ethanol

### **2.3.3 DNase digestion**

gDNA contaminations in RNA samples were removed by DNase I digestion (New England Biolabs) according to the manufacturer's protocol. RNA samples were cleaned from reaction components using the *Quick*-RNA Miniprep kit (Zymo Research) and checked for residual DNA by PCR.

### **2.3.4 cDNA synthesis**

Total RNA was reverse transcribed into cDNA using the ProtoScript® II Reverse Transcriptase (New England Biolabs) in combination with random hexamer primers.

#### Mix in an RNase-free 1.5 ml reaction tube:

total RNA	1 $\mu\text{g}$ (x $\mu\text{l}$ )
random primer mix	2 $\mu\text{l}$
10 mM dNTPs	1 $\mu\text{l}$
nuclease-free H <sub>2</sub> O	ad 10 $\mu\text{l}$

In order to improve primer annealing by destroying secondary structures of the RNA, the mixture was incubated for 5 min at 65 °C. Samples were centrifuged briefly and chilled on ice. Then, 10  $\mu\text{l}$  of following master mix were added to each RNA sample and mixed carefully.



**Table 2.10: RT-master mix (per sample)**

Component	Volume
5x ProtoScript® II buffer	4 µl
DTT (0.1 M)	2 µl
ProtoScript® II Reverse Transcriptase (200 U/µl)	1 µl
RNase inhibitor (40 U/µl)	0.2 µl
Nuclease-free H <sub>2</sub> O	ad 10 µl

Samples were first incubated for 5 min at room temperature and afterwards for 1 h at 42 °C. The reverse transcriptase was heat inactivated at 65 °C for 20 min and remaining RNA was hydrolyzed. Therefore 16 µl of 1 M NaOH were added and the sample was incubated another 30 min at 65 °C. For neutralization of the NaOH, 16 µl of 1 M HCl were added. cDNA was then purified using the NucleoSpin® Gel and PCR Clean-up kit (Macherey Nagel) according to the manufacturer's protocol.

### 2.3.5 Preparation of plasmid DNA from *E. coli*

Plasmid DNA was isolated from *E. coli* DH5α cells. 5 ml of LB containing the appropriate antibiotic were inoculated with a single colony from a transformation plate and cells were grown over night at 37 °C and 160 rpm (Innova 2300). Plasmid DNA was isolated from the ONC by using the NucleoSpin® Plasmid Easy Pure kit (Macherey Nagel) following the manufacturer's protocol with the included A1 buffer diluted 1:2 with 1 % (w/v) SDS solution for better sample quality. Otherwise, plasmid DNA was obtained by alkaline lysis (Sambrook *et al.*, 1989). Cells of 2 ml ONC were harvested by centrifugation at full speed for 30 s. The cell pellet was resuspended in 100 µl mix I supplemented with RNase and the suspension was incubated at room temperature for 5 min. 200 µl mix II was added and the reaction tube was inverted 5 times. After the addition of 150 µl ice-cold mix III, the tube was inverted several times and the sample was incubated on ice for 5 min. Cell debris was removed by centrifugation at full speed for 5 min and the supernatant was then transferred to a fresh 1.5 ml tube. One volume of isopropanol was added, the sample was vortexed and incubated at room temperature for 2 min and the precipitated plasmid DNA was collected by a 5 min centrifugation step at full speed. The DNA pellet was washed with 1 ml ice cold 70 % (v/v) ethanol, followed by centrifugation at full speed for 2 min. The ethanol was removed completely and the DNA pellet was dried at 37 °C. The isolated plasmid DNA was then resuspended in 50 µl of H<sub>2</sub>O or TE-buffer, which were preheated to ~70 °C, and stored at -20 °C.

<u>Mix I</u>		<u>Mix II</u>	
Tris-HCl pH 8	50 mM	SDS	1 % (w/v)
EDTA	10 mM	NaOH	0.2 M

Mix III

Potassium acetate	3 M
Formic acid	1.8 M

→ adjust the pH to 5.2 with formic acid

### 2.3.6 Determination of nucleic acid concentrations

DNA and RNA concentrations in aqueous solutions were determined by measuring the absorbance at 260 nm using a NanoDrop™ Lite photometer (Thermo Fisher). Purity of the samples was represented by the ratio of the absorbance at 260 nm ( $A_{260}$ ) and 280 nm ( $A_{280}$ ). An  $A_{260}/A_{280}$  ratio of ~ 1.8 for double stranded DNA and of ~ 2.0 for RNA was accepted as sufficiently pure.

### 2.3.7 Agarose gel electrophoresis

Agarose gel electrophoresis of nucleic acids was used to separate DNA and RNA molecules within an electrical field according to their size (Aaij and Borst, 1972). Agarose gels were prepared by dissolving 0.8-1 % (w/v) of agarose in 1x TAE buffer and boiling the solution until the agarose was melted completely. The solution was then poured into prepared gel chambers and the gel polymerized at room temperature. DNA and RNA samples were prepared with 6x DNA loading dye (Thermo Fisher) before loading on the gel. As a reference for fragment sizes and DNA-amount, the GeneRuler™ DNA Ladder mix (Thermo Fisher) was used. Gel electrophoresis was performed in 1x TAE buffer at a constant current of 90-120 V. The gel was then stained in an ethidium bromide bath (0.5 µg/ml) for 20 min. To visualize the nucleic acids, fluorescence of the DNA/RNA-ethidium bromide complex was excited with UV light at 312 nm. Agarose gel electrophoresis with RNA samples was performed as described above using RNase-free buffers and gel chambers.

50x TAE buffer

Tris/acetate pH 8.0	40 mM
EDTA	1 mM

### 2.3.8 Polymerase chain reaction (PCR)

Amplification of specific DNA fragments was performed by polymerase chain reaction (PCR) (Mullis and Faloona, 1987). For cloning procedures, DNA-polymerases (Tab. 2.7) with 3'-5' exonuclease proofreading activity were utilized to avoid the integration of mutations. However,

colony PCRs (chapter 2.3.14) were performed using the faster Taq DNA polymerase. All PCR procedures were conducted according to the manufacturer's protocol in either 50  $\mu$ l or 25  $\mu$ l reaction volume. The self-produced Pfu DNA polymerase of the laboratory was used as follows:

**Table 2.11: Generic PCR reaction mix for Pfu DNA polymerase**

Component	Final concentration
Pfu DNA polymerase	1 U
5x Pfu buffer	1x
dNTPs	200 $\mu$ M each
DMSO	5 % (v/v)
Forward primer	0.5 $\mu$ M
Reverse primer	0.5 $\mu$ M
Template DNA	5-10 ng
H <sub>2</sub> O	ad 50 $\mu$ l

**Table 2.12: PCR thermocycler program**

Reaction step	Temperature	Time	
Initial denaturation	98 °C	2 min	
Denaturation	98 °C	10 s	} 30-35 cycles
Annealing	T <sub>m</sub> - 5 °C	30 s	
Elongation	72 °C	1 min/kb	
Final elongation	72 °C	7 min	

**5x Pfu buffer**

Tris-HCl pH 8.2	200 mM
KCl	100 mM
(NH <sub>4</sub> ) <sub>2</sub> SO <sub>4</sub>	100 mM
MgSO <sub>4</sub>	20 mM
Triton X-100	1 % (v/v)
nuclease-free BSA	1 mg/ml

### 2.3.9 Purification of PCR products

PCR products were purified for cloning reactions using the NucleoSpin® Gel and PCR Clean-up kit (Macherey Nagel) according to the manufacturer's protocol.

### 2.3.10 Restriction digest of DNA

Restriction digest of DNA was performed using restriction endonucleases in CutSmart™ buffer (New England Biolabs) according to the manufacturer's instructions. After digestion, enzymes were thermally inactivated at the required temperatures. For double digest reactions, the digestion was performed stepwise with thermal inactivation of the first enzyme before addition of the second. Digestion performance was verified via agarose gel electrophoresis (chapter 2.3.7).

### 2.3.11 Extraction of DNA fragments from agarose gels

For the extraction of DNA fragments from agarose gels, low melting point (LMP) agarose was used. 1.2 % (w/v) LMP-agarose was dissolved in 1x TAE buffer and a gel with broad pockets was cast. Gel electrophoresis was performed at 90 V for 60-90 min and the gel was stained as stated in chapter 2.3.7. The desired DNA fragment was cut out of the gel and purified using the NucleoSpin® Gel and PCR Clean-up kit (Macherey Nagel) according to the manufacturer's protocol.

### 2.3.12 Ligation of DNA fragments

Ligation of DNA fragments was performed using the T4 DNA Ligase (New England Biolabs). For a ligation reaction, vector DNA and insert DNA were mixed in a molar ratio of 1:3. The ligation reaction was incubated at room temperature for 1 h or at 16 °C over night. The T4 DNA ligase was thermally inactivated at 65 °C for 10 min prior to transformation of the ligation product into *E. coli* DH5α (chapter 2.2.5).

### 2.3.13 Splicing-by-overlap extension (SOE-) PCR

The splicing-by-overlap extension PCR has been utilized to generate in-frame mutant alleles for *P. aeruginosa* which are not interrupted by antibiotic resistance cassettes (Hmelo *et al.*, 2015). SOE-PCR was used to construct deletion mutants as well as alleles with single nucleotide polymorphisms (SNPs). For the deletion of open reading frames (ORFs), the flanking up- and downstream regions of the gene of interest were amplified in two separated PCR reactions. PCR reactions were set up using gDNA of *P. aeruginosa* PAO1 as template and the gene specific primer pairs Up-F and Up-R or Down-F and Down-R (Tab. 2.3) for up- and downstream fragment, respectively. To generate an in-frame deletion, it is crucial that the up- and downstream fragments contain the start and stop-codon of the target gene and an

additional number of nucleotides from the ORF that is a multiple of 3. The primers Up-F and Down-R contain restriction sites that are suitable for the multiple cloning site of the target vector pEXG2, whereas the end of the primer Up-R is homologous to the primer Down-F. The amplified up- and downstream fragments were checked via agarose gel-electrophoresis and cleaned up using the NucleoSpin® Gel and PCR Clean-up kit (Macherey Nagel). In the next PCR step up- and downstream fragments were used as template in equal amounts. In this reaction only the Up-F and Down-R primers were added. During the PCR the homologous regions between up- and downstream fragment align and the fused fragment is amplified (Fig. 2.1). The generation of alleles containing SNPs was performed likewise with the difference that the Up-R and Down-F primers are homologous to each other and both contain the desired point mutation.

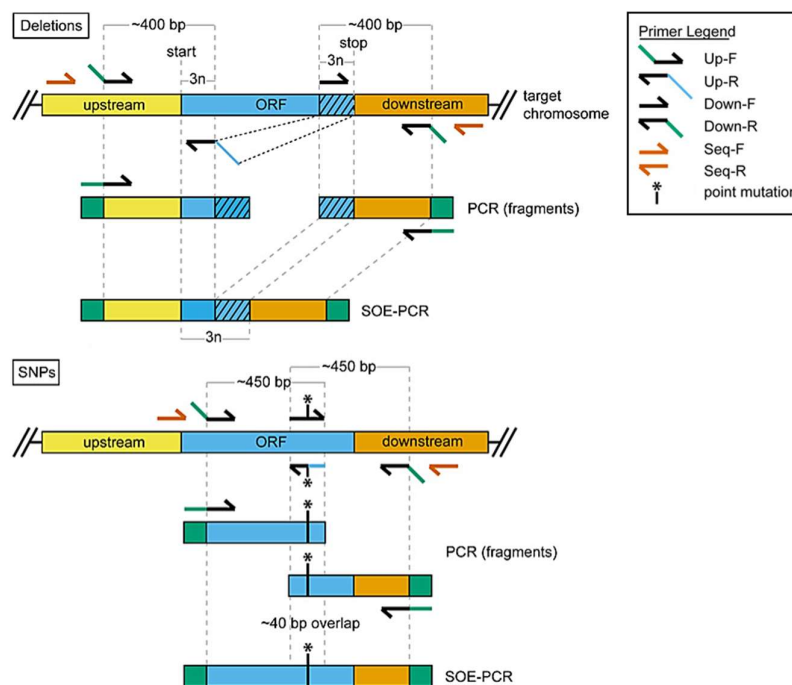


**Fig. 2.1: Principle of splicing-by-overlap extension PCR**

Alleles for either deletion mutant alleles or alleles containing SNPs, a two-step PCR procedure was performed. In the first step the up- and downstream fragment were amplified. Those fragments are then used as template for a second PCR to generate a fusion DNA-fragment with the desired mutation allele. Primers are designed with specific modifications: restriction sites (green), homologous region to downstream fragment (blue), and point mutations (\*). Sequencing primers (orange) bind within the *P. aeruginosa* genome up and downstream of the modified genomic region. Figure modified from (Hmelo *et al.*, 2015).

### 2.3.14 Colony PCR

Colony PCR was frequently used to screen *P. aeruginosa* and *E. coli* colonies for the uptake of desired plasmid DNA after conjugation or transformation events. Additionally, this method was used to check for the genomic integration of mutant alleles in *P. aeruginosa*. Single colonies of *E. coli* were picked from transformation plates, preserved by streaking on a fresh

LB-agar plate with the appropriate antibiotic and resuspended in 10  $\mu\text{l}$   $\text{H}_2\text{O}$ . Then, 1  $\mu\text{l}$  of this suspension was used directly as PCR template. The PCR reaction was set up as described in chapter 2.3.8. except the extension of the first denaturation step to 10 min and the second denaturation step to 30 s. *P. aeruginosa* colonies were preserved similarly but resuspended in 100  $\mu\text{l}$   $\text{H}_2\text{O}$  and boiled afterwards for 10 min at 95 °C. The boiled suspension was vortexed briefly and 1  $\mu\text{l}$  was used as PCR template. In the case of *P. aeruginosa* colony PCR, the first denaturation step was extended to 5 min and the second one to 30 s. In order to screen a large number of colonies, up to 5 colonies were pooled in one sample. If the pooled sample gave a positive PCR result, the included colonies were tested individually using cell material from the preservation plate.

### 2.3.15 Site-directed mutagenesis

NbdA variants were generated via site-directed mutagenesis (Wang and Malcolm, 1999). For the substitution of target bases of *nbdA* that result in the generation of protein variants, specific primers for site-directed mutagenesis were created (see tab. 2.3; the site of mutation is underlined). The target plasmids were used in a dual-step PCR procedure utilizing the Phusion® High-Fidelity DNA Polymerase (Thermo Fisher) and the corresponding primer pair. Two separate PCR reactions (A and B) containing only one primer, were set up in the first step to prevent dimerization of the oligonucleotides and increase the number of mutated single-stranded plasmid copies. In the second step, the two reactions were combined to generate double stranded plasmids with introduced mutation sites. The methylated parental plasmid DNA was degraded afterwards via *DpnI* (New England Biolabs) digestion and 10  $\mu\text{l}$  of the generated plasmid was transformed into chemically competent *E. coli* DH5 $\alpha$  cells (chapter 2.2.6).

**Table 2.13: PCR reaction setups of first step**

Component	A	B
5x HF Phusion® buffer	10 $\mu\text{l}$	10 $\mu\text{l}$
Plasmid DNA-template (30 ng/ $\mu\text{l}$ )	1 $\mu\text{l}$	1 $\mu\text{l}$
Forward primer (10 nM)	2.5 $\mu\text{l}$	–
Reverse primer (10 nM)	–	2.5 $\mu\text{l}$
dNTPs (200 $\mu\text{M}$ each)	1 $\mu\text{l}$	1 $\mu\text{l}$
Phusion® High-Fidelity DNA polymerase (2 U/ $\mu\text{l}$ )	0.5 $\mu\text{l}$	0.5 $\mu\text{l}$
$\text{H}_2\text{O}$	ad 50 $\mu\text{l}$	ad 50 $\mu\text{l}$

**Table 2.14: PCR thermocycler program of first step**

Reaction step	Temperature	Time	
Initial denaturation	98 °C	30 s	
Denaturation	98 °C	15 s	} 8 cycles
Annealing	55 °C	30 s	
Elongation	72 °C	6 min	

**Table 2.15: PCR reaction setup of second step**

Component	Volume
PCR mix A	25 µl
PCR mix B	25 µl
Phusion® High-Fidelity DNA polymerase (2 U/µl)	0.5 µl

**Table 2.16: PCR thermocycler program of second step**

Reaction step	Temperature	Time	
Initial denaturation	98 °C	30 s	
Denaturation	98 °C	15 s	} 18 cycles
Annealing	55 °C	30 s	
Elongation	72 °C	6 min	
Final Elongation	72 °C	10 min	

### 2.3.16 Gibson Assembly® of DNA molecules

Gibson Assembly® was used to assemble several DNA fragments within a single isothermal reaction (Gibson *et al.*, 2009). Gibson primers containing a 20-40 bp homologous region to the adjacent fragment or the vector backbone were generated using the NEBuilder® assembly tool of New England Biolabs (Tab. 2.7). Required DNA fragments were amplified via PCR (chapter 2.3.8) and the vector backbone was nicked by restriction enzyme digest (chapter 2.3.10). Then, 50-100 ng of vector DNA and a 2-fold molar excess of each fragment were adjusted with H<sub>2</sub>O to a volume of 5 µl and added to 25 µl Gibson assembly master mix. The reaction mix was incubated for 1 h at 50 °C. All contained enzymes are active at 50 °C and do not inhibit each other's activity. The homologous 5'-ends of the DNA double-strands are digested by the T5-exonuclease (New England Biolabs) to generate sticky ends and enable annealing of the DNA fragments. The Phusion® High-Fidelity DNA polymerase (New England Biolabs) closes the gaps between the fragments and nicks are sealed by the Taq DNA ligase (Biozym Scientific).

Then, 10  $\mu$ l of the Gibson reaction mix were directly transformed into competent *E. coli* DH5 $\alpha$  cells (chapter 2.2.6).

#### 5x isothermal Gibson assembly reaction buffer

PEG 8000	25 % (w/v)
Tris-HCl pH 7.5	500 mM
MgCl <sub>2</sub>	50 mM
DTT	50 mM
dNTPs	1 mM each

#### Gibson assembly master mix

5x isothermal Gibson assembly reaction buffer	320 $\mu$ l
T5-exonuclease (10 U/ $\mu$ l)	0.64 $\mu$ l
Phusion <sup>®</sup> High-Fidelity DNA polymerase (2 U/ $\mu$ l)	20 $\mu$ l
Taq DNA ligase (40 U/ $\mu$ l)	160 $\mu$ l
H <sub>2</sub> O	ad 1200 $\mu$ l

### **2.3.17 Construction of expression vectors encoding *kbdA-mNeonGreen* /-Venus**

For the expression of NbdA-mNeonGreen or Venus fusion proteins, the medium copy-number vector pME6032 was utilized. The construction of the expression vectors was performed by Gibson Assembly<sup>®</sup> (chapter 2.3.16) using the corresponding Gibson primers shown in table 2.3. Therefore, the full length *kbdA* gene without stop-codon was amplified by PCR using the Q5<sup>®</sup> Hot Start High-Fidelity 2x Master Mix (New England Biolabs). For the amplification of *mNeonGreen* and *Venus* the plasmids pASK-IBA3-*mNeonGreen* and pASK-IBA3-*Venus*, which encode for the fusion of the fluorescent protein to a 6x-His tag, were used respectively. The same primer pair (*mNG-G-F/R*) was used for both genes as the amplified sequences possess similar beginnings and endings. The target vector pME6032 was linearized by *SacI* restriction digest prior to Gibson Assembly<sup>®</sup>. The assembled plasmids were transformed into *E. coli* DH5 $\alpha$  and plated on selective LB-agar plates. Transformants were validated for the correct insert size by colony PCR and plasmids with the correct size were prepared from liquid cultures and sent for sequencing.

### **2.3.18 Analysis of DNA sequences**

PCR fragments or plasmid DNA were analyzed via the Sanger sequencing services of Eurofins Genomics or SeqIT. Samples were prepared according to the sequencing companies' instructions.



### 2.3.19 Generation of *P. aeruginosa* mutants via two-step allelic exchange

Two-step allelic exchange is a method to generate unmarked mutations within the *P. aeruginosa* genome (Hmelo *et al.*, 2015). It is suitable to introduce deletion mutants, integration mutants as well as point mutations within the gene of interest via homologous recombination. Therefore, the required DNA sequence was integrated into the suicide-vector pEXG2 using SOE-PCR (chapter 2.3.13) and conventional cloning (chapter 2.3.10-2.3.12) or Gibson Assembly® (chapter 2.3.16).

**Table 2.17: Utilized pEXG2-variants for desired kind of mutation**

Deletion mutant	Integration mutant	Point mutation
pEXG2- $\Delta$ <i>amrZ</i>	pEXG2_3312_ <i>nbdA-mNeonGreen</i>	pEXG2_ <i>fliC</i> T394C
pEXG2- $\Delta$ <i>nirF</i>	pEXG2_3312_ <i>nbdA-Venus</i>	
pEXG2- $\Delta$ <i>nirS</i>	pEXG2_ <i>cheA-mCerulean</i>	
pEXG2- $\Delta$ <i>norCB</i>	pEXG2_ <i>cheA-tdTomato</i>	
pEXG2- $\Delta$ <i>rpoS</i>		
pEXG2- $\Delta$ <i>rsmA</i>		
pEXG2- $\Delta$ <i>rsmF</i>		

The pEXG2-derivates were introduced into *P. aeruginosa* by biparental mating (chapter 2.2.9). Genomic integration of the plasmid via homologous recombination was verified by growth on Pseudomonas isolation agar containing gentamicin, as the pEXG2 is a non-replicative vector in *P. aeruginosa*. 10 single colonies were picked, streaked on LB-agar plates and incubated at 37 °C over night. Single colonies were then streaked on LB-agar plates containing 15 % (w/v) sucrose and incubated at 37 °C over night. This step was repeated with single colonies from the sucrose agar plates. On pEXG2 the gene *sacB* encodes for a levransucrase which uses sucrose as substrate for the synthesis of toxic levans. For that reason, growth on sucrose-containing medium forces a second homologous recombination event in which the plasmid backbone is excised from the *P. aeruginosa* genome as only these bacteria are able to survive. Colonies were then picked on LB-agar, LB-agar with 15 % (w/v) sucrose and LB-agar with gentamicin and incubated over night at 37 °C. Desired strains should be sucrose resistant and gentamicin sensitive. Integration of the desired mutant allele was additionally verified by colony PCR (chapter 2.3.14) since a return to the wt allele was also possible (Fig. 2.2).

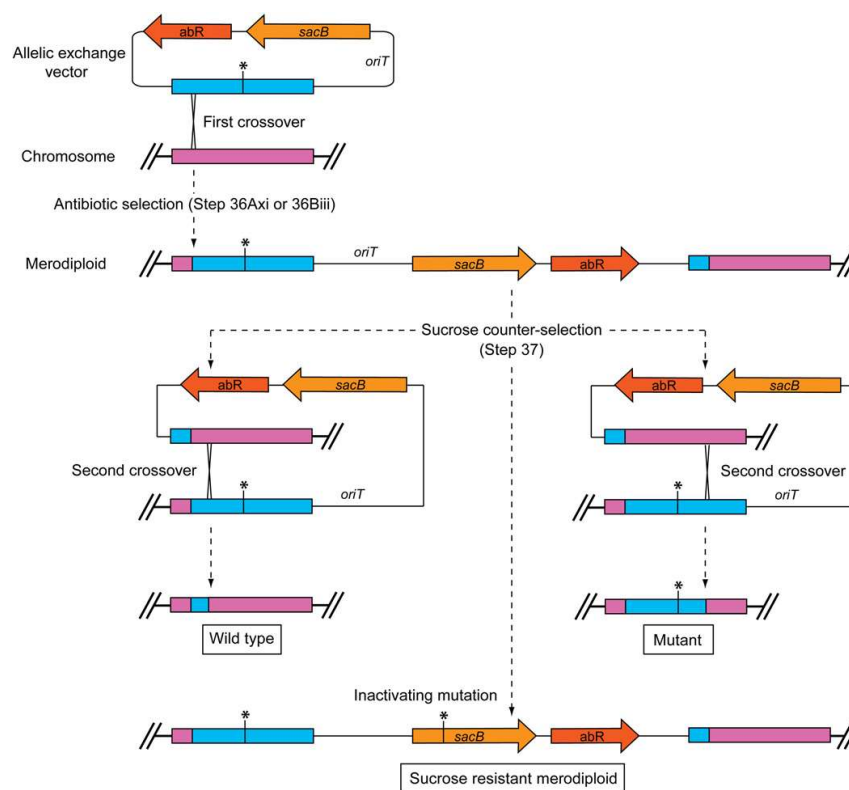


**Fig. 2.2: Two-step allelic exchange**

Two-step allelic exchange was performed using the suicide vector pEXG2 which contains the gene *sacB* and a gentamicin resistance gene. In the first crossover event, the whole vector is integrated into the *P. aeruginosa* genome by homologous recombination, generating gentamicin resistant bacteria. Sucrose counter selection forces a second crossover event in which the pEXG2 vector backbone is excised from the genome. This results in gentamicin sensitive, sucrose resistant bacteria containing either the desired mutation or the wt allele. In very rare cases a mutation in the *sacB* gene can cause strains that harbor both, wt and mutant allele at the same time. Figure taken from (Hmelo *et al.*, 2015).

### 2.3.20 Plasmid integration into phage attachment site of *P. aeruginosa*

Genomic integration of plasmids into the phage attachment site of *P. aeruginosa* was performed with mini-CTX1-*lacZ* derivatives. Those plasmids contain a  $\phi$ CTX attachment site (*attP*) and encode for the cognate integrase (*int*) (Becher and Schweizer, 2000; Hoang *et al.*, 2000). Plasmid DNA was conjugated into the *P. aeruginosa* strain of interest via biparental mating (chapter 2.2.9). The encoded integrase mediates incorporation of the plasmid at the *P. aeruginosa attB* site (Fig. 2.3). As mini-CTX derivatives are non-replicative within *P. aeruginosa*, only bacteria with integrated plasmid DNA are able to survive on selective medium. These tetracycline resistant strains were ready to employ for e.g.,  $\beta$ -galactosidase assays.

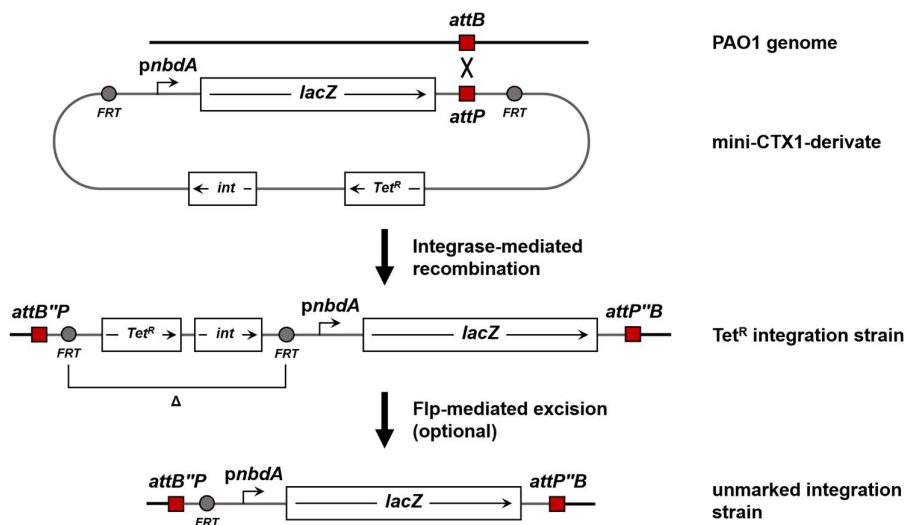


**Fig. 2.3: Genomic integration of mini-CTX1-*lacZ* derivatives**

The mini-CTX1-*lacZ* derivate was introduced into the *P. aeruginosa* genome at the *attB*-site by integrase-mediated recombination. This results in tetracycline resistant strains containing the desired integration. Via flippase (Flp)-mediated excision, the vector backbone can be excised from the *P. aeruginosa* genome in between the *FRT*-sites. Figure based on (Becher and Schweizer, 2000).

A flippase mediated excision of the vector backbone in between the *FRT* sites could be utilized afterwards in order to generate unmarked integration strains (Hoang *et al.*, 2000). As this work would not benefit from this procedure, flippase-mediated excision was not performed for the generated integration strains.

### 2.3.21 5'-Rapid amplification of cDNA ends (RACE) PCR

5'-Rapid amplification of cDNA ends (RACE) PCR is a method to analyze the length or start site of RNA transcripts in the cell. It was performed by Dr. Susanne Zehner (TU Kaiserslautern) in order to identify the transcriptional start site of the *nbdA* gene of *P. aeruginosa* PAO1 according to the following protocol. *P. aeruginosa* cells were inoculated 1:100 from an overnight culture in LB medium and incubated 5 h at 37 °C with vigorous shaking. Primers used for 5'-RACE are listed in table 2.3. Total RNA isolation was performed as previously described (Hauser *et al.*, 2007). Then, cDNA was synthesized at 42 °C for 60 min with M-MLV Reverse Transcriptase (Promega) using the gene-specific primer SP1\_nbdA. The cDNA was treated with NaOH and HCl to remove remaining RNA and subsequently purified with MinElute kit (Qiagen). The cDNA solution was treated with shrimp alkaline phosphatase (New England Biolabs). A deoxyadenosine tail was added to the 3' end of the cDNA using terminal transferase (Thermo Fisher Scientific). Second-strand synthesis was performed with an oligo (dT) anchor primer. The obtained double-stranded DNA was amplified with the anchor-1 primer and the nested gene-specific primer SP3\_BgIII\_nbdA. The resulting PCR product was purified (MinElute kit, Qiagen) and cloned in pDrive using the Qiagen PCR cloning kit (Qiagen). For the determination of the transcriptional start site 10 individual clones were sequenced.

### 2.3.22 Semiquantitative reverse transcriptase (RT) PCR

Semiquantitative reverse transcriptase PCR was used to detect and compare the *nbda* transcript under different growth conditions and in different *P. aeruginosa* backgrounds. PAO1 wt and  $\Delta nirS$  were grown to exponential (4 h) and early stationary (7 h) phase. Total RNA was extracted and reverse transcribed into cDNA (see chapters 2.3.2-2.3.4). For the PCR reaction, 2.5 ng of cDNA were used as template together with the *nbda*-RT1 or the *recA*-RT1 primer pair (Tab. 2.3) and a Taq DNA-polymerase. The resulting PCR fragments were analyzed on agarose gels after ethidium bromide staining. An image was taken from the stained agarose gel and band intensities thereon were calculated using the ImageJ software.

**Table 2.18: RT-PCR reaction mix**

Component	Final concentration
2x DreamTaq Green PCR Master Mix	1x
DMSO	2 % (v/v)
Forward primer	0.2 $\mu$ M
Reverse primer	0.2 $\mu$ M
Template cDNA	2.5 ng
H <sub>2</sub> O	ad 25 $\mu$ l

**Table 2.19: RT-PCR thermocycler program**

Reaction step	Temperature	Time	
Initial denaturation	95 °C	3 min	
Denaturation	95 °C	30 s	} 28 cycles
Annealing	60 °C	30 s	
Elongation	72 °C	20 s	

## 2.4 Protein biochemical methods

### 2.4.1 Homologous protein production in *P. aeruginosa*

For homologous gene expression in *P. aeruginosa* either pHERD26T- or pME6032-derivates were utilized with the gene of interest under the control of a pBAD or *tac* promoter, respectively. The high-copy number plasmid pHERD26T was used for overexpression experiments with various NbdA-variants, which are described further in chapter 2.7. Expression of *nbda* fusions to either *mNeonGreen* or *Venus*, both encoding fluorescent proteins, was performed using the medium copy-number plasmid pME6032. Therefore, precultures were prepared in 10 ml LB

medium supplemented with tetracycline (50 µg/ml) and grown over night at 37 °C and 160 rpm. The ONCs were diluted 1:100 in 10 ml of fresh LB medium containing tetracycline and grown at 37 °C and 160 rpm to an OD<sub>600 nm</sub> of 0.2-0.5. In order to evaluate the best conditions for protein production a test expression experiment was performed first. Therefore, gene expression was induced by the addition of either 100 µM or 500 µM IPTG and the cultures were incubated further at 37 °C. Cells of an equivalent of OD<sub>600 nm</sub> = 0.5 in 1 ml were harvested prior to induction and 1 h, 2 h, and 3 h after induction and prepared for western blot analysis (chapter 2.4.3). For CLSM analysis (chapter 2.6), protein expression was induced with 100 µM IPTG and cells were incubated for 2 h prior to microscopy.

## 2.4.2 SDS-polyacrylamide gel electrophoresis

For further analysis, proteins were separated under reducing conditions according to their molecular weight during SDS-polyacrylamide gel electrophoresis (SDS-PAGE). A discontinuous system consisting of a stacking gel with an acrylamide concentration of 5.25 % (pH 6.8) and a separation gel with an acrylamide concentration of 12.5 % (pH 8.8) was used (Laemmli, 1970). Sodium dodecyl sulfate (SDS) is a denaturing agent that is able to bind to proteins and mask their native charge with a negative charge, which allows the proteins to migrate through the gel following the electric field. Smaller proteins move faster through the polyacrylamide gel than large proteins. Thereby a separation according to the molecular weight is achieved. Cell pellets were resuspended in 30 µl 1x PBS buffer and 10 µl 4x SDS loading dye and boiled for 15 min at 95 °C. Prior to load, samples were centrifuged for 10 min at 13,000 rpm (Eppendorf 5415 D). 15 or 10 µl sample were loaded onto gels with 10 or 15 pockets, respectively and 5 µl broad range protein standard were loaded for size comparison. Electrophoresis was performed at 200 V for ~ 45 min. Afterwards, the separated proteins were visualized by staining with Coomassie Brilliant Blue G250. Therefore, the gel was incubated for 10 min under continuous shaking in staining solution and discolored until the desired contrast in destaining solution. Alternatively, the unstained gel was used for western blot analysis.

### 4x Stacking gel buffer

Tris/HCl pH 6.8	0.5 M
SDS	0.4 % (w/v)

### 4x Separation gel buffer

Tris/HCl pH 8.8	1.5 M
SDS	0.4 % (w/v)

<u>4x SDS loading dye</u>		<u>10x SDS-PAGE running buffer</u>	
Tris	100 mM	Tris/HCl pH 8.8	250 $\mu$ M
SDS	8 % (w/v)	Glycine	1.92 M
Glycerol	40 % (v/v)	SDS	1 % (w/v)
$\beta$ -Mercaptoethanol	10 % (v/v)		
Bromphenol blue	1 % (w/v)		
<u>Stacking gel 5.25 % (4 mini gels)</u>		<u>Separating gel 12.5 % (4 mini gels)</u>	
Rotiphorese Gel 30*	1.4 ml	Rotiphorese Gel 30*	6.7 ml
4x Stacking gel buffer	2 ml	4x Separation gel buffer	4 ml
H <sub>2</sub> O	4.6 ml	H <sub>2</sub> O	5.3 ml
APS (10 % w/v)	30 $\mu$ l	APS (10 % w/v)	80 $\mu$ l
TEMED	20 $\mu$ l	TEMED	8 $\mu$ l

\* 30 % acrylamide, 0.8 % bis-acrylamide

<u>Staining solution</u>		<u>Destaining solution</u>	
Acetic acid	10 % (v/v)	Acetic acid	10 % (v/v)
Ethanol	30 % (v/v)	Ethanol	30 % (v/v)
Coomassie Brilliant Blue G250	0.25 % (w/v)		

### 2.4.3 Immuno-detection of immobilized 6x His fusion proteins (Western Blot)

Western Blot analysis was utilized to transfer proteins from polyacrylamide gels onto PVDF membranes and detect 6x His fusion proteins using specific antibodies (Towbin *et al.*, 1979). Protein samples were separated by SDS-PAGE (chapter 2.4.2) and then transferred to a PVDF membrane using a semi-dry technique. Therefore, the PVDF membrane had to be activated in 100 % methanol for 1 min, washed with water thoroughly and equilibrated in Towbin buffer. The gel and two sheets of Whatman paper (3 mm) were also equilibrated for 10 min in Towbin buffer. For the protein transfer, a sandwich of the equilibrated membrane and polyacrylamide gel in between of two Whatman papers was built and placed between anode and cathode of the semi-dry blot system. The electroblotting was performed for 20 min at 15 V. The membrane was then incubated under constant shaking in blocking solution for 1 h at room temperature or 4 °C over night to saturate unspecific binding sites. The saturated membrane was washed three times in TBS-T buffer for 5 min each. Afterwards, the membrane was incubated at room temperature for 1 h with the primary anti 6x His antibody (Tab. 2.8) in TBS-T buffer under constant shaking. The antibody solution was removed and the membrane was washed three times for 5 min with TBS-T buffer to remove unbound primary antibody. For detection of His-

tagged proteins a secondary antibody conjugated to an alkaline phosphatase was required. The membrane was incubated for 1 h under constant shaking in TBS-T buffer containing 1:10,000 diluted secondary antibody (Tab. 2.8). Subsequently, the membrane was washed three times in TBS-T buffer and twice in PBS buffer for 5 min each. The detection of the His-fusion proteins was accomplished by incubation of the membrane in an NBT/BCIP detection solution in AP buffer. The alkaline phosphatase catalyzes a chromogenic reaction of BCIP with NBT which results in an insoluble purple-blue precipitate that marks the position of the His-tagged proteins on the blot. The reaction was stopped at the desired point of coloration by washing the membrane with water.

Towbin transfer buffer

Tris-base	25 mM
Glycine	192 mM

10x TBS buffer

Tris-HCl	50 mM
NaCl	140 mM
→ adjust to pH 7.4	

TBS-T buffer

TBS buffer	1x
Tween-20	0.1 % (v/v)

Blocking solution

PBS-T buffer	1x
Albumin fraction V	5 % (w/v)

AP buffer

Tris/HCl pH 9.5	100 mM
NaCl	100 mM
MgCl <sub>2</sub>	5 mM

NBT solution

NBT	10 % (w/v)
DMF	70 % (v/v)

BCIP solution

BCIP	5 % (w/v)
DMF	100 % (v/v)

## 2.5 Transcriptional and translational regulation of *nbdA*

### 2.5.1 Construction of transcriptional *lacZ*-fusions

The transcriptional fusion of the *nbdA* promoter to the reporter gene *lacZ* was constructed in the vector mini-CTX1-*lacZ*. Therefore, the *nbdA* promoter region and 276 bp of the *nbdA* coding region were amplified by PCR and integrated into the *EcoRI* and *BamHI* restriction sites of the vectors multiple cloning site. The resulting plasmid pKGE06 was integrated into the *P. aeruginosa* genome as described in chapter 2.3.20 and integration was confirmed via colony PCR (chapter 2.3.14).

## 2.5.2 Construction of translational *bgaB*-fusions

Translational *bgaB*-fusions to the 5' untranslated region (5'-UTR) of *kbdA* were utilized to analyze *kbdA* translation under different conditions in order to identify possible post-transcriptional regulation mechanisms. Therefore, synthetic DNA of the native *kbdA* 5'-UTR plus 30 nucleotides of the open reading frame (ORF) was purchased from Thermo Fisher Scientific. The 111 bp long DNA sequence was integrated into the vector pBAD2 to generate a fusion with the  $\beta$ -galactosidase encoding reporter gene *bgaB* (Klinkert *et al.*, 2012). A fusion of the predicted RNA-thermometer 5'-UTR of the *E. coli* gene *trxA* to *bgaB* was used as control. Design and purchase of synthetic DNA as well as pBAD2-derivate construction was done by Daniel Scheller of the Microbiology department at the Ruhr-Universität Bochum (cooperation with Prof. Dr. F. Narberhaus). As the pBAD2-derivates are only suitable for *E. coli* the translational *bgaB*-fusions were introduced into the broad-host vector pJN105 by Gibson Assembly® (chapter 2.3.16) for use in *P. aeruginosa*. The resulted plasmids are listed in table 2.2.

## 2.5.3 $\beta$ -Galactosidase assay in *E. coli*

Translation of *kbdA* was analyzed by the performance of  $\beta$ -galactosidase assays in *E. coli* DH5 $\alpha$  using the previously constructed translational *bgaB*-fusions (chapter 2.5.2). The temperature-dependent translation was investigated after a temperature shift as follows (Gaubig *et al.*, 2011; Klinkert *et al.*, 2012). Precultures were prepared in 10 ml LB medium supplemented with ampicillin and grown over night at 30 °C and 160 rpm. ONCs were diluted to an OD<sub>600 nm</sub> of 0.1 in 30 ml fresh LB medium containing ampicillin and grown at 30 °C and 160 rpm to an OD<sub>600 nm</sub> of ~ 0.5. Subsequently, transcription of the *bgaB*-fusion was induced by the addition of 0.1 % (w/v) L-arabinose. The cultures were separated immediately into 3 flasks prewarmed to 30 °C, 37 °C and 42 °C and incubated at the respective temperature for 30 min. Aliquots of 35  $\mu$ l Mix I per 1.5 ml reaction tube were prepared in duplicates for each strain and stored on ice. After incubation, 400  $\mu$ l culture were added to the Mix I aliquots, vortexed for 10 s and incubated at 55 °C in a thermo block for 15 min. Enzymatic reaction was started by the addition of 400  $\mu$ l freshly prepared Mix II. Samples were incubated at 55 °C until a color change to yellow indicated the production of ortho nitrophenol. The reaction was immediately stopped by the addition of 400  $\mu$ l 1 M Na<sub>2</sub>NO<sub>3</sub> and short vortexing. Cell debris was pelleted by centrifugation at 13,000 rpm for 15 min and the OD<sub>420 nm</sub> of the supernatant was measured. A 1:1:1 mixture of LB medium, Mix II and Na<sub>2</sub>NO<sub>3</sub> served as blank. The  $\beta$ -galactosidase activity in Miller units was calculated as follows:

$$\text{Miller units (MU)} = \frac{OD_{420 \text{ nm}}}{OD_{600 \text{ nm}} \times \text{sample volume [ml]} \times \text{time [min]}} \times 1000$$



For the analysis of *nbdA* translation after a shift to lower temperatures, pre- and main cultures were grown at 37 °C. After the addition of 0.1 % L-arabinose, the culture was split into a 37 °C, 25 °C and 20 °C warm flask and incubated at the respective temperatures. The  $\beta$ -galactosidase assay was then performed as described above. Additionally, the influence of high intracellular c-di-GMP levels on the *nbdA* translation was investigated. Therefore, the *E. coli* strains MG1655 and AB607 were employed (Boehm *et al.*, 2010). The strain AB607 lacks the master phosphodiesterase PdeH and therefore accumulates c-di-GMP, whereas MG1655 is the appropriate wt background. Both strains were cultivated at 37 °C and the main culture was prepared in 10 ml LB medium only. Again, the  $\beta$ -galactosidase assay was performed in order to measure the translational level via the enzyme's activity.

#### 10x Z-buffer

Na <sub>2</sub> HPO <sub>4</sub> x 2H <sub>2</sub> O	600 mM
NaH <sub>2</sub> PO <sub>4</sub> x 2H <sub>2</sub> O	400 mM
KCl	100 mM
MgSO <sub>4</sub> x 7H <sub>2</sub> O	10 mM

#### Mix I (per sample)

4x Z-buffer	25 $\mu$ l
$\beta$ -Mercaptoethanol	0.35 $\mu$ l
Lysozyme (20 mg/ml)	10 $\mu$ l

#### Mix II (per sample)

1x Z-buffer	399 $\mu$ l
$\beta$ -Mercaptoethanol	1.08 $\mu$ l
ONPG	0.8 mg

### **2.5.4 $\beta$ -Galactosidase assay in *P. aeruginosa***

In *P. aeruginosa*,  $\beta$ -galactosidase assays were used to investigate both, transcription and translation of *nbdA*. For the measurement of the *nbdA* promoter activity transcriptional *lacZ*-fusions were utilized (chapter 2.5.1) and the  $\beta$ -galactosidase assay protocol of Miller (Miller, 1972) has been modified as follows. Overnight cultures containing the promoter-*lacZ* fusion were diluted to an OD<sub>600 nm</sub> of 0.01 in 20 ml LB with respective antibiotics and incubated at 37 °C and 160 rpm. In exponential (4 h) and early stationary growth phase (7 h) OD<sub>600 nm</sub> was measured and cells of 100  $\mu$ l culture were harvested by centrifugation (Eppendorf 5415 D). Cells were resuspended in 800  $\mu$ l Z-buffer. For cell lysis, 25  $\mu$ l of 0.1 % (w/v) sodium-dodecyl sulfate (SDS) and 25  $\mu$ l chloroform were added, samples were vortexed for 5 s and incubated at room temperature for 5 min. Enzymatic reaction was started by the addition of 200  $\mu$ l of 4 mg/ml ortho-nitrophenyl- $\beta$ -D-galactosid (ONPG) and samples were incubated at 37 °C. When  $\beta$ -galactosidase activity was indicated by a color change due to the formation of the yellow-colored product ortho nitrophenol, the reaction was stopped by the addition of 500  $\mu$ l 1 M Na<sub>2</sub>CO<sub>3</sub>. Cell debris was precipitated by centrifugation at 13,000 rpm (Eppendorf 5415 D)

for 15 min and product formation was measured in the supernatant at OD<sub>420 nm</sub>. The activity of  $\beta$ -galactosidase was calculated as described in chapter 2.5.3.

Translation of *nbdA* was analyzed using translational *bgaB*-fusions (chapter 2.5.2) in PAO1 wt and *rsmA* and *rsmF* deletion mutant strains. Main cultures were prepared and incubated as described above. Transcription of the *bgaB* fusion was induced by the addition of 0.1 % (w/v) L-arabinose at either OD<sub>600 nm</sub> ~ 0.5 or at desired time points (after 3.5 h growth for exponential and after 6.5 h for early stationary growth phase). For the analysis of NO-involvement in *nbdA* translation, additionally 500  $\mu$ M SNP was added to the culture. The mock control was supplemented with the same volume of H<sub>2</sub>O instead. After incubation at 37 °C for 30 min, cells of 200  $\mu$ l culture were harvested and treated as described previously. However, the assay temperature was increased to 55 °C to activate the thermostable  $\beta$ -galactosidase BgaB.

#### Z-buffer

Na <sub>2</sub> HPO <sub>4</sub> x 7H <sub>2</sub> O	60 mM
NaH <sub>2</sub> PO <sub>4</sub> x H <sub>2</sub> O	40 mM
KCl	10 mM
MgSO <sub>4</sub> x 7H <sub>2</sub> O	1 mM
$\beta$ -Mercaptoethanol	50 mM

## 2.6 Confocal laser scanning microscopy

### 2.6.1 Preparation of agarose pads for microscopy

For confocal laser scanning microscopy of liquid *P. aeruginosa* cultures, cells were immobilized on agarose pads. 1.2 % (w/v) agarose was solubilized in 1x PBS buffer. The pads were cast in an SDS-gel casting stand with 1 mm spacer plates.

### 2.6.2 Fluorescent proteins and dyes

For investigation of the cellular localization of NbdA and co-localization experiments, several fluorescent proteins and fluorescent dyes were used in this work. The properties of these proteins and dyes, as well as the used laser lines for detection are listed in table 2.20.

**Table 2.20: Properties of used fluorescent proteins and dyes**

Fluorescent protein / dye	Ex $\lambda$ (nm)	Em $\lambda$ (nm)	QY	Brightness	Laser line (Zeiss LSM 880)
Alexa Fluor™ 594	588	612			HeNe 594 nm
mCerulean	433	475	0.49	16.17	Argon 458 nm
mCherry	587	610	0.22	15.84	HeNe 594 nm
mNeonGreen	506	517	0.8	92.8	Argon 488 nm
tdTomato	554	581	0.69	95.22	HeNe 543 nm
Venus	514	528	0.57	52.55	Argon 514 nm

### 2.6.3 Cellular localization of NbdA

The cellular localization of NbdA was investigated in *P. aeruginosa* cells containing genomically integrated or plasmid encoded fusions of NbdA to the fluorescent proteins (FPs) mNeonGreen or Venus. For protein detection, a C-terminal 6x His tag was attached to the fusions. Cultures of strains with a genomically encoded *nbdA*-FP fusion were prepared in 20 ml LB medium and grown at 37 °C and 160 rpm over night. The culture was diluted 1:4 with fresh LB medium and used for microscopy immediately. Cultures of strains containing pME6032-*nbdA-mNeonGreen* or -*Venus* were prepared as described in chapter 2.4.1. For CLSM 3  $\mu$ l of the respective culture were spotted on a cover slip and covered with an agarose pad (chapter 2.6.1) and a second cover slip. NbdA-FP was detected using the more sensitive detector ChS1 and the required laser lines (Tab. 2.20).

### 2.6.4 Co-localization of NbdA and the polar flagellum

For co-localization assays of NbdA-FP with the polar flagellum of *P. aeruginosa*, the flagellar subunit FliC was modified by an amino acid exchange at the position 394 from threonine to cysteine. The introduction of a cysteine residue into FliC allows flagellar staining with the red fluorescent dye Alexa Fluor™ 594 C5 Maleimide (Thermo Fisher Scientific) by formation of thiol bonds between the cysteine and the maleimide group of the dye. The staining protocol of Zhu *et al.* was modified as follows (Zhu *et al.*, 2019). Cultures were grown over night at 37 °C and 160 rpm in flasks containing 10 ml LB medium. Cells of an equivalent of  $OD_{600\text{ nm}} = 0.5$  in 1 ml were spun down at 3,000 rpm for 5 min. The cell pellet was carefully resuspended in 50  $\mu$ l PBS buffer containing 50  $\mu$ g/ml Alexa Fluor™ dye and incubated for 15 min in the dark. Cells were collected by a 5 min centrifugation step at 3,000 rpm and washed carefully in 300  $\mu$ l 1x PBS buffer. Cells were centrifuged again for 5 min at 3,000 rpm and then resuspended in 30  $\mu$ l 1x PBS buffer for microscopy. 3  $\mu$ l of stained cells were pipetted on a cover slip and

covered with an agarose pad and another cover slip. Detection of NbdA-FP was performed using the more sensitive detector ChS1 and images of the different fluorophores were taken in separated frames. Required laser lines for CLSM are listed in table 2.20.

### 2.6.5 Co-localization of NbdA and CheA

The histidine kinase component CheA of the chemotaxis machinery of *P. aeruginosa* locates to the flagellated cell pole and is present in nearly all cells (Kulasekara *et al.*, 2013). Therefore, CheA was used in co-localization studies with NbdA to mark the flagellated pole. Fusions of *cheA* to either *tdTomato* or *mCerulean*, encoding for a red or cyan fluorescent protein respectively, were genomically integrated into the original gene locus (chapter 2.3.19). Likewise, the *nbdA-mNeonGreen* fusion was integrated into the original *nbdA* locus and expression was under the control of its native promoter. Cultures were prepared in 20 ml LB medium and incubated at 37 °C and 160 rpm (Innova 2300) over night. The ONCs were diluted 1:4 in fresh LB medium and prepared directly for CLSM as stated in part 2.6.2. Laser lines were chosen according the fluorescent proteins' requirements (Tab. 2.20) and emission of each FP was captured in a separated track. For NbdA detection, the more sensitive ChS1 detector was used.

### 2.6.6 Localization of NbdA in thin sections of colony biofilms

The distribution of NbdA within *P. aeruginosa* biofilm colonies was investigated by confocal laser scanning microscopy. Therefore, biofilm thin sections of the strain PAO1 *nbdA-mNeonGreen* mini-CTX1-*mCherry* were produced. Thin sectioning of colony biofilms was performed at the Columbia University (New York City, NY, USA) in the working group of Prof. Dr. Lars Dietrich according to the following protocol (Cornell *et al.*, 2018). Tryptone agar bilayer plates were prepared one day prior to biofilm inoculation. Therefore, the agar was cooled down to ~ 60 °C and 45 ml of the agar was poured into a 10 cm x 10 cm square petri dish. To eradicate air bubbles, the agar surface was flamed with a Bunsen burner immediately. After solidification with closed lid for 20 min, the first layer was covered by another 15 ml tryptone agar and flamed again. The bilayer plates were dried with closed lid at room temperature and condensed water was removed from the lid. Plates were then stored next to each other at 25 °C over night. For anaerobic biofilms, the tryptone-agar was supplemented with 40 mM KNO<sub>3</sub>. Pre cultures were prepared in 2 ml of LB medium and incubated over night at 37 °C and 160 rpm. ONCs were diluted 1:100 in 3 ml fresh LB medium and grown at 37 °C and 160 rpm to an OD<sub>600 nm</sub> of ~ 0.5. Each bilayer plate was inoculated with 4 technical replicates by spotting 5 µl of the subculture onto the agar. The liquid was allowed to dry at room temperature and plates were than stacked and incubated upside down in a 25 °C incubator for 3 or 4 days. A moist environment was created by setting up a bowl of water in the incubator. Anaerobically

grown biofilms were brought into an anaerobic cabinet and incubated 3 or 4 days at room temperature. It is noteworthy, that biofilms grown for longer than 4 days were very smooth and got destroyed during the following process. After incubation, the biofilm colonies were covered with 15 ml 1 % agar in H<sub>2</sub>O. To protect the biofilm structure, the agar was not poured directly onto the colonies. After solidification of the agar, squares around the biofilm colonies were cut out using a razor blade. With a wet spatula the “agar sandwich” containing a biofilm colony was carefully lifted from the bottom agar layer and transferred into an embedding cassette. The samples were then placed into a glass container with previously prepared fixative (4 % formaldehyde (v/v) in 1x PBS buffer). The lid was sealed with parafilm and the samples were incubated for 24 h in the dark at 25 °C. The samples were transferred into the metal basket of the tissue processor and were washed twice in 1 l 1x PBS buffer for 1 h each. Long air contact of the samples was to be avoided. After buffer wash, the tissue processor was prepared with 1 l of each solution listed in table 2.21. During sample processing, increasing ethanol concentrations dehydrated the sample. Afterwards, HistoClear was used to clear the samples from the alcohol which were then infiltrated by paraffin wax. In order to save chemicals, in some cases solutions were reused.

**Table 2.21: Sample processing steps in spin tissue processor**

Step	Duration	Solution (1 l each)
1	1 h	25 % (v/v) ethanol in 1x PBS buffer
2	1 h	50 % (v/v) ethanol in 1x PBS buffer
3	1 h	70 % (v/v) ethanol in 1x PBS buffer
4	1 h	95 % (v/v) ethanol in 1x PBS buffer
5	1 h	100 % ethanol (used)
6	1 h	100 % ethanol (50 % used, 50 % fresh)
7	1 h	100 % ethanol (fresh)
8	1 h	HistoClear (used)
9	1 h	HistoClear (50 % used, 50 % fresh)
10	1 h	HistoClear (fresh)
11	3 h	Paraffin wax
12	3 h	Paraffin wax

After the sample processing procedure, the biofilm samples were embedded in paraffin wax blocks. Therefore, the 3D-printed embedding molds were assembled and sealed with melted wax. The molds were then placed on a cold plate to let the wax solidify. Afterwards, the molds were filled with melted paraffin wax and each infiltrated biofilm sample was carefully transferred

with a prewarmed, flat spatula from the histological cassette into the smaller side of the embedding mold. The sample should rest parallel to the bottom of the mold to allow even thin sections. The paraffin wax solidified over night at 4 °C.

On the next day, the wax blocks were taken out of the embedding molds and excess wax was trimmed with a razor blade, leaving an extending wax part for clamping into the microtome. It is important, that the wax is trimmed parallel to the embedded sample to ensure even thin sections. The wax surrounding the sample was additionally smoothed with the razor blade. A tissue floating water bath was filled to the top and heated to 42 °C. Bubbles were removed from the bottom of the water bath using a brush. The embedded biofilm sample was clamped into the microtome for thin sectioning. The sample was trimmed in 50 µm intervals first, until the middle of the biofilm colony was reached and residual wax shavings were removed from the sample and the microtome blade. A ribbon of 4-5 thin sections of 10 µm thickness were created using the "Feed" function of the microtome (settings: Feed: 10 µm; Velocity: 70 rpm). The ribbon was carefully removed from the microtome blade with a wet brush. It was then transferred to the surface of the prewarmed water bath using a water drop on a pasteur pipette avoiding to trap air bubbles under the sections. A microscope slide was inserted into the water bath and positioned below the ribbon in a ~ 45 ° angle. When the top of the ribbon touched the slide and adhered to the glass surface, the microscope slide was pulled out of the water bath allowing the section to lie flat on the glass. The thin sections were allowed to dry in the dark for 1-2 days at room temperature.

Afterwards, the thin sections were placed on a hot plate at 45 °C for 30-60 min to heat fix the samples. The microscope slides were then placed on a cool surface to allow the molten wax to solidify again. For microscopy, the thin sections had to be rehydrated again. Therefore, the microscope slides were placed into a glass slide mailer and washed four times with HistoClear to remove the wax. After each 5 min wash, the solution was removed using a Büchner aspirator. The samples were then washed three times for 1 min in 100 % ethanol. Rehydration was performed by incubation of the slides in PBS buffer with decreasing ethanol concentrations (95 %, 70 %, 50 %, and 25 % (v/v)) for 1 min each. The samples were then washed twice in 1x PBS buffer for 1 min. The rehydrated biofilm thin sections were mounted immediately with Tris-buffered mounting medium and the coverslip was carefully attached, avoiding introduction of air bubbles. The mounting medium was allowed to polymerize over night at room temperature and the cover slip was then sealed by application of clear nail polish. CLSM of the biofilm thin sections was performed using the Zeiss LSM 700 with airy scan. NbdA-mNeonGreen was excited using the 488 nm argon laser and mCherry was excited with the 594 nm laser.

### 2.6.7 Localization of NbdA in single cells of colony biofilms

Investigation of cellular NbdA distribution was performed in 3- and 4-day-old biofilm colonies. Biofilms of PAO1 *nbdA-mNeonGreen* mini-CTX1-*mCherry* were grown as described in chapter 2.2.10. At the desired time points, a smear of the biofilm cells was taken using a sterile inoculation loop and applied to a microscope slide. The sample was covered with a cover slip which was sealed with color-less nail polish. CLSM was performed using the appropriate laser lines of the Zeiss LSM 880 (Tab. 2.20). The remaining cells from the biofilm colonies were frozen in liquid nitrogen for western blot analysis (chapter 2.4.3).

## 2.7 Phenotypic analysis of *P. aeruginosa* strains over-producing NbdA variants

### 2.7.1 Swimming motility

Precultures of *P. aeruginosa* strains harboring pHERD26T-derivates were prepared in 8 ml LB medium supplemented with tetracycline and grown over night at 37 °C and 160 rpm. ONCs were then diluted 1:20 in 8 ml of LB medium with tetracycline. Cultures were grown at 37 °C and 160 rpm to an OD<sub>600 nm</sub> of ~ 0.5. Gene expression was induced by the addition of 0.1 % (w/v) L-arabinose and cultures were incubated at 22 °C and 160 rpm for 5 h. Swimming agar was supplemented with tetracycline and 0.1 % (w/v) L-arabinose and plates were poured with 20 ml medium each. The swimming plates were dried for 20 min with closed lid and afterwards another 10 min with open lid. The cell density of the cultures was adjusted to an OD<sub>600 nm</sub> = 1.5. 1 µl culture was spotted carefully onto the swimming-agar, each plate containing the vector control as comparison. Swimming plates were then incubated upright at 30 °C for 18 h. Images of the swimming plates were taken and swimming zone areas were calculated using the ImageJ software.

### 2.7.2 Twitching motility

Precultures of *P. aeruginosa* strains harboring pHERD26T-derivates were prepared in 8 ml LB medium supplemented with tetracycline and grown over night at 37 °C and 160 rpm. ONCs were then diluted 1:20 in 8 ml of LB medium with tetracycline. Cultures were grown at 37 °C and 160 rpm to an OD<sub>600 nm</sub> of ~ 0.5. Gene expression was induced by the addition of 0.1 % (w/v) L-arabinose and cultures were incubated at 22 °C and 160 rpm for 5 h. Twitching-agar was supplemented with tetracycline and 0.1 % (w/v) L-arabinose and plates were poured with 20 ml medium each. The twitching plates were dried for 20 min with closed lid and afterwards another 10 min with open lid. The cell density of the cultures was adjusted to an OD<sub>600 nm</sub> = 1.5. The agar was then pierced with a pipette tip and 1 µl culture was spotted onto the bottom of the petri dish. Each twitching plate contained the vector control as comparison.

Plates were incubated for 40 h at 37 °C. After incubation, the agar was carefully removed and the twitching zones were stained with 0.05 % (w/v) crystal violet for 20 min. The petri dishes were then carefully washed with water to remove excessive stain and dried at room temperature. Images of stained twitching zones were taken and measured using the ImageJ software.

### 2.7.3 Adhesion assay

Precultures of *P. aeruginosa* strains harboring pHERD26T-derivates were prepared in 8 ml BM2 supplemented with tetracycline and grown over night at 37 °C and 160 rpm. ONCs were then diluted 1:20 in 8 ml of BM2 with tetracycline. Cultures were grown at 37 °C and 160 rpm to an OD<sub>600 nm</sub> of ~ 0.5. Gene expression was induced by the addition of 0.1 % (w/v) L-arabinose and cultures were incubated at 22 °C and 160 rpm for 5 h. Cell density was adjusted to an OD<sub>600 nm</sub> of 1.5 in adhesion medium containing tetracycline and 0.1 % (w/v) L-arabinose. A round bottom 96-well plate was inoculated with 100 µl culture per well, however the outer ring of wells was filled with 100 µl adhesion medium. The microtiter dish was incubated for 1 h at 37 °C in a moist chamber. After incubation, cells were discarded and each well was washed with 300 µl H<sub>2</sub>O. To stain the attached biomass, 125 µl of a 0.1 % (w/v) crystal violet solution was added into each well and incubated for 15 min. The stain was discarded and the plate was tapped several times on paper towels to remove excessive crystal violet. Wells were then washed twice with 150 µl H<sub>2</sub>O, tapped on paper towels and dried for 5 min at room temperature. The bound crystal violet was resuspended by the addition of 200 µl 95 % (v/v) ethanol to each well and incubation for 15 min (closed lid). In order to equally distribute the crystal violet, the solution was mixed by pipetting. The OD at 595 nm was measured in the TECAN plate reader in order to evaluate attached biomass.

### 2.7.4 Pellicle formation

Pellicle formation of *P. aeruginosa* strains overexpressing NbdA variants was investigated in LB medium or basal medium 2. Precultures were prepared in 8 ml of the respective medium, supplemented with tetracycline, and grown over night at 37 °C and 160 rpm. ONCs were diluted 1:20 in fresh medium with tetracycline. Cultures were grown at 37 °C and 160 rpm to an OD<sub>600 nm</sub> of ~ 0.5. Gene expression was induced by the addition of 0.1 % (w/v) L-arabinose and cultures were incubated at 22 °C and 160 rpm for 5 h. The OD<sub>600 nm</sub> was adjusted to 0.03 in LB or BM2 biofilm medium containing tetracycline and 0.1 % (w/v) L-arabinose. Each test tube was inoculated with 4 ml of culture and incubated at 22 °C for 48 h. The cultures were then checked for pellicle formation at the air-liquid junction. As a control, cultures were inoculated as described before, however incubated at 22 °C and 160 rpm for 48 h.



### **2.7.5 Drop dilution assay**

The drop dilution assay was utilized for the identification of vital cells after the pellicle formation assay or to analyze growth of *P. aeruginosa* cells overexpressing NbdA variants on solid medium. Therefore, 1.5 % LB-agar plates supplemented with 150 µg/ml tetracycline were prepared in square petri dishes. Half of the plates additionally contained 0.1 % (w/v) L-arabinose as inductor. Cultures were vortexed briefly and OD<sub>600 nm</sub> was adjusted to 0.1 in fresh medium. A dilution series from 10<sup>0</sup> to 10<sup>-4</sup> was prepared and 1 µl of each dilution was spotted onto the agar. Plates were incubated over night at 37 °C and cell growth was evaluated for each strain.

## 3 Results

### 3.1 Transcriptional regulation of *nbda*

#### 3.1.1 Determination of transcriptional start site of *nbda* reveals a regulatory region with RpoS and AmrZ binding sites

Automated annotation of the genome sequence of PAO1 predicted the open reading frame (ORF) for *nbda* to code for 783 amino acid residues. Sequence alignments of the translated sequence with proteins containing N-terminal MHYT-domains revealed a long N-terminal extended region for NbdA. This incited us to analyze the gene region in more detail. In close proximity to the annotated start codon no ribosomal binding site (RBS) could be detected. A 5'-RACE PCR experiment, performed by Dr. Susanne Zehner, revealed the transcriptional start site of *nbda* 103 nucleotides downstream of the computationally annotated translation start (Fig. 3.1). The nearest potential translational start site is 170 nucleotides downstream of the previously annotated translation start and possesses a bona fide ribosome binding site. This results in a shorter ORF coding for a 726 amino acid protein whose N-terminus aligns well with the N-termini of other MHYT-domain proteins. With the new defined transcriptional start, the *nbda* promoter region was analyzed. Conserved binding sites for the alternative sigma-factor RpoS ( $\sigma^S$ ) and the transcription factor AmrZ were identified (Jones *et al.*, 2014; Schulz *et al.*, 2015).



**Fig. 3.1: Reannotation of the promoter region of *nbda* with the experimentally determined transcriptional start site**

5'-RACE PCR experiments revealed transcriptional start site of the *nbda* gene with a C (+1), 171 nucleotides downstream from the previously annotated ORF start site (*Pseudomonas* database (Winsor *et al.*, 2016)). The promoter region of *nbda* was reanalyzed and reveals deduced binding sequences for the alternative  $\sigma$ -factor RpoS and the transcriptional regulator AmrZ. Pale green = annotated translational start site (TLS); grey = old *nbda* ORF annotation; underlined = -10 and -35 promoter region; arrow = transcriptional start site revealed by 5'-RACE (+1); blue = putative RpoS binding site; red = putative AmrZ binding site; bold grey = putative RBS; green = putative TLS; bold black = shorter *nbda* ORF.

The binding motif for RpoS lies in the -10 region of the *nbdA* promoter. The predicted AmrZ binding sequence covers the transcriptional start site of *nbdA* indicating a repressor function. In order to investigate the role of the alternative sigma-factor RpoS and the transcription factor AmrZ on *nbdA* expression, the promoter region of *nbdA* was transcriptionally fused to the reporter gene *lacZ* and integrated in the  $\phi$ CTX attachment site of PAO1 wt,  $\Delta rpoS$  and  $\Delta amrZ$ . Activity of the  $\beta$ -galactosidase in the respective strains was determined in exponential (4 h) and early stationary (7 h) growth phase. In the wt strain, a 4-fold increase in *nbdA* transcription was observed when cells entered the early stationary phase, suggesting transcriptional activation by RpoS. Deletion of *rpoS* resulted in a loss of *nbdA* promoter activity in both, exponential and stationary growth phase (Fig. 3.2), confirming the role of RpoS as transcriptional activator of *nbdA*. In the  $\Delta amrZ$  strain a strong increase of *nbdA* promoter activity was observed in both, exponential and early stationary growth phase (Fig. 3.2). AmrZ is therefore likely acting as a transcriptional repressor for *nbdA*.

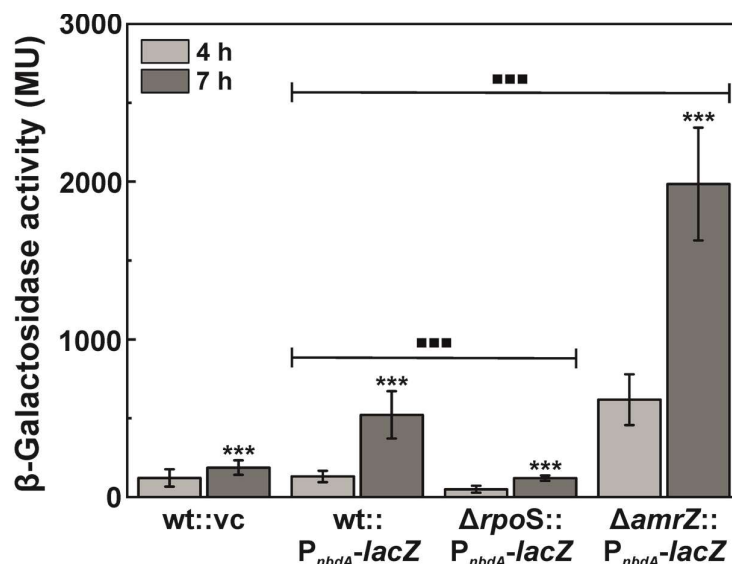


**Fig. 3.2: Transcription of *nbdA* is activated by RpoS and repressed by AmrZ**

Promoter activity was determined with integrated  $P_{nbdA}$ -lacZ fusions in late exponential (4 h) and early stationary (7 h) growth phase in wild type (wt) and deletion mutants  $\Delta rpoS$  and  $\Delta amrZ$ . Additionally, the wt with integrated vector control (vc) was tested for background  $\beta$ -galactosidase activity. The assay was performed in triplicates. Significant changes in *nbdA* expression levels between deletion mutant strains and the corresponding wt sample are marked with ■ (\*\*\*) ( $P < 0.001$ , determined by Student's T-test).

As there is a sharp oxygen gradient present in biofilm macrocolonies (James *et al.*, 2016),  $O_2$  might also have an impact on the expression of genes active in biofilms. Although there is no hint for an FNR-like, ANR, or DNR regulator binding site in the promoter region, we tested *nbdA* promoter activity also under anaerobic conditions. Induction of the *nbdA* promoter was observed when cultures reached stationary phase in all tested strains, similarly to the aerobic growth conditions (Fig. 3.3). Overall, the values for promoter activity under oxygen limitation were significantly lower than in aerobic conditions. The *nbdA* promoter activity in the *amrZ*

deletion strain was significantly increased compared to the wild-type background. Therefore, AmrZ seems to repress *nbda* transcription similarly in aerobic and anaerobic growth conditions.

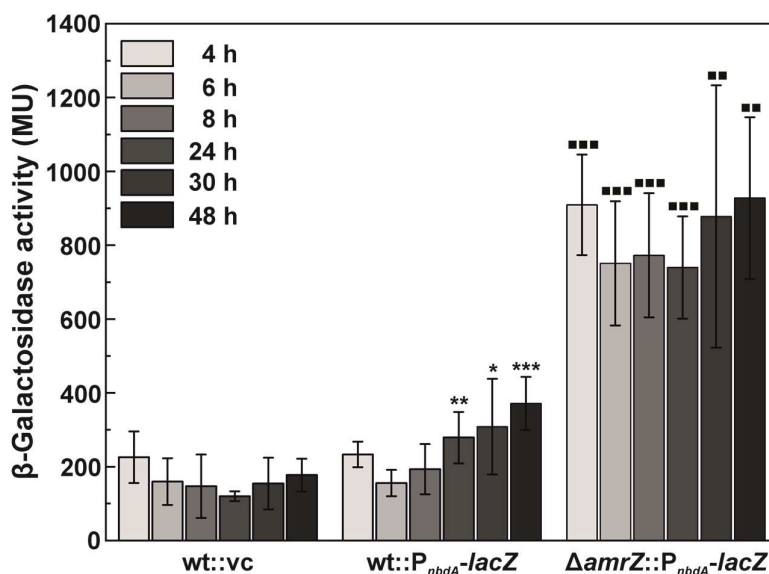


**Fig. 3.3: Under oxygen limitation, transcription levels of *nbda* are introduced in stationary growth phase**

PAO1 wt and  $\Delta amrZ$  containing an integrated  $P_{nbda}$ -lacZ fusion and the vector control (vc) were grown anaerobically for 48 h in LB medium with 50 mM NaNO<sub>3</sub>. Inoculation of cultures was performed aerobically therefore the first hours of growth were required to consume remaining oxygen. Expression levels were determined by  $\beta$ -galactosidase assays in triplicates. Significant changes in *nbda* transcription levels of wt samples to the 6 h sample are marked with \*. Significant changes in *nbda* transcription level of  $\Delta amrZ$  samples to corresponding wt levels are marked with ■. (\* P < 0.05; \*\* P < 0.01; \*\*\* P < 0.001, determined by Student's T-test).

### 3.1.2 Impact of nitric oxide on the transcription of *nbda*

We previously reported increased amounts of *nbda* transcript in dispersed cells after NO-induced biofilm dispersal compared to untreated planktonic cells and suggested a NO-dependent transcriptional regulation of *nbda* (Li *et al.*, 2013). In the light of divergent results on the role of *nbda* in NO-induced biofilm dispersion (Li *et al.*, 2013; Zemke *et al.*, 2020) we wanted to clarify the regulation of *nbda* in response to endogenous and exogenous NO. During infections, host macrophages release exogenous NO in order to eradicate bacteria (Denis, 1994). However, under anaerobic conditions, *P. aeruginosa* is able to form endogenous NO during denitrification. Within the denitrification process, nitrite is reduced by the nitrite reductase NirS into NO, which is then further reduced to nitrous oxide by NorCB (Cutruzzola and Frankenberg-Dinkel, 2016; Ye *et al.*, 1994). For its enzymatic activity, NirS requires the incorporation of a heme *d*<sub>1</sub> cofactor which is synthesized by NirF (Nicke *et al.*, 2013). Interruption of the denitrification pathway by deletion of the *norCB* gene leads to the accumulation of intrinsic NO under denitrifying conditions (Barraud *et al.*, 2006). A  $\Delta norCB$  strain containing the *nbda* promoter lacZ-fusion was used to analyze the effect of endogenous

---

NO on *nbdA* transcription. Deletion mutants of *nirS* and *nirF*, both unable to form endogenous NO, served as negative controls. The denitrification deficient strains showed normal growth under aerobic conditions in LB medium complemented with KNO<sub>3</sub> (Fig. 3.4A). In contrast, under anaerobic denitrifying conditions the growth of PAO1  $\Delta$ *nirS* and  $\Delta$ *nirF* was reduced compared to the wt PAO1 (Fig. 3.4B). The  $\Delta$ *norCB* strain was no longer able to grow. For the analysis of *nbdA* transcription, the strains containing the *nbdA* promoter *lacZ*-fusion were grown under aerobic/microaerobic conditions and  $\beta$ -galactosidase assays were performed with samples of the exponential (4 h) and early stationary growth phase (7 h) (Fig. 3.4C). Compared to the wt, the *nirS* deletion had a severe activating effect on *nbdA* expression in both, exponential and early stationary growth phase. Surprisingly, *nbdA* transcription in the  $\Delta$ *nirF* strain, which produces an enzymatically inactive NirS, was not as high as in the  $\Delta$ *nirS* strain but comparable to the level of transcription in the wt background. The transcription of *nbdA* in the  $\Delta$ *norCB* strain is slightly decreased compared to the wt background. Due to the impaired growth in anaerobic conditions of  $\Delta$ *norCB* strain, we could not test for the effect of accumulation of endogenous NO on *nbdA* transcription. In order to confirm the findings for the  $\Delta$ *nirS* strain, a semi quantitative RT-PCR experiment was performed with cDNA of wt and deletion mutant in both tested growth phases (Fig. 3.4D). While the control PCR with *recA* primers showed equally strong bands for all samples, *nbdA* expression in the wt in exponential growth phase was weaker than in early stationary growth phase (Fig. 3.4E). In the *nirS* deletion strain, there was more transcript of *nbdA* detectable than in wt, which is consistent to the findings of the  $\beta$ -galactosidase assay.

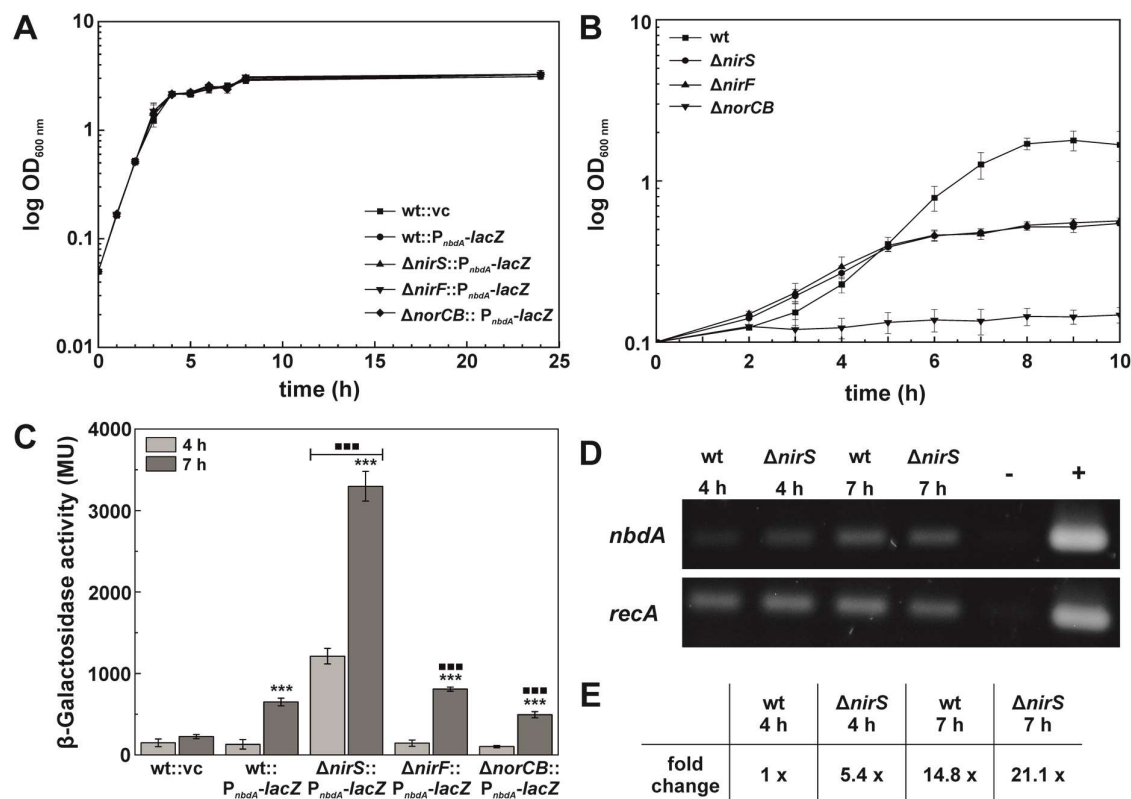


**Fig. 3.4: Impact of denitrification mutants on *nbdA* transcription**

*P. aeruginosa* wild type (wt),  $\Delta nirS$ ,  $\Delta nirF$ , and  $\Delta norCB$  strains harboring a transcriptional  $P_{nbdA}$ -*lacZ*-fusion and the wt containing the vector control (vc) were grown in LB supplemented with 50 mM  $KNO_3$ . **[A]** Growth in glass culture flasks was monitored during 24 h in three biological replicates. **[B]** Anaerobic growth in LB medium supplemented with 50 mM  $KNO_3$  of the wt and deletion mutants was analyzed in sealed bottles for 10 h in biological triplicates. **[C]**  $\beta$ -galactosidase activity was determined from cells aerobically/ microaerobically grown to exponential (4 h) and early stationary phase (7 h). All assays were performed in triplicates. Significant changes between 4 and 7 h samples are marked with \*. Significant changes in *nbdA* expression levels between deletion mutant strains and the corresponding wt sample are marked with ■. (\*\*\*)  $P < 0.001$ , determined by Student's T-test). **[D]** Semi quantitative RT-PCR for *nbdA* transcript and the control *recA* was performed. RNA was extracted from wt and  $\Delta nirS$  strains after 4 and 7 h growth in LB medium. - : negative control without transcript; + : positive control performed with gDNA of PAO1. **[E]** Quantification of semi quantitative RT-PCR band intensities on ethidium bromide stained agarose gel using ImageJ software. Intensities were normalized to the intensities of the internal control *recA* and the fold change was calculated in relation to the value of the wt strain after 4 h of growth.

In addition to the influence of intrinsic nitric oxide on *nbdA* transcription, the effect of exogenous NO was investigated. Therefore, the PAO1 wt harboring the *nbdA*-*lacZ* fusion was grown with increasing amounts of the NO donor sodium nitroprusside (SNP) and *nbdA* promoter activity was determined by  $\beta$ -galactosidase activity (Fig. 3.5A). Low concentration of added SNP to the growth medium had no effect on *nbdA* promoter activity, whereas the addition of 500  $\mu$ M SNP led to a decrease of *nbdA* transcription. This effect is comparable to the observed decrease of *nbdA* transcription in the NO-accumulating strain  $\Delta norCB$ . As *P. aeruginosa* is able to detoxify nitric oxide via flavohemoglobin (Arai *et al.*, 2005; Forrester and Foster, 2012) under aerobic conditions, the influence of short-term NO stress on *nbdA* transcription was analyzed. Therefore, PAO1 wt *nbdA*-*lacZ* was grown to stationary phase in LB and then

stressed for 30 min by the addition of 500  $\mu$ M SNP. Compared to the untreated control, no changes in the *nbdA* promoter activity were observed (data not shown).

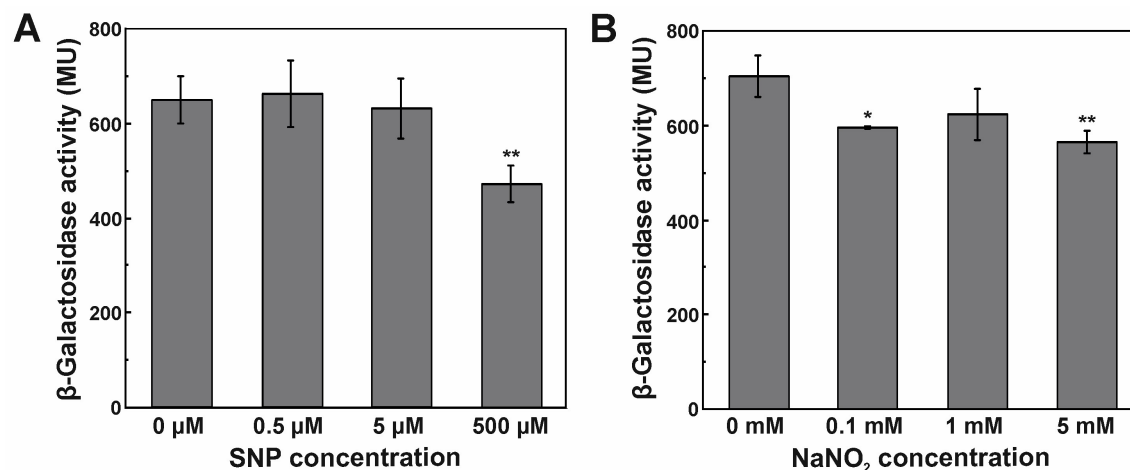


**Fig. 3.5: Analysis of transcriptional activity of *nbdA* promoter in response to exogenic NO and NO<sub>2</sub> sources**

Reporter strain PAO1 wt::*nbdA-lacZ* was grown to early stationary phase (7 h) in medium containing increasing amounts of the NO-releasing compound sodium nitroprusside (SNP) [A] or NaNO<sub>2</sub> [B].  $\beta$ -Galactosidase activity was measured in triplicates (\* P < 0.05; \*\* P < 0.01, determined by Student's T-test).

In order to figure out whether the strong increase of *nbdA* expression in the  $\Delta$ *nirS* strain was based on nitrite accumulation due to interrupted denitrification (Barraud *et al.*, 2006),  $\beta$ -galactosidase assays were performed with different amounts of nitrite in the growth medium (Fig. 3.5B). None of the tested nitrite concentrations had a comparable effect on the *nbdA* promoter as the deletion of *nirS*. The addition of nitrite to the medium rather decreased expression of *nbdA* slightly, probably due to bacteriostatic effect of nitrite.

## 3.2 Translational regulation of *nbdA*

For the *Pseudomonas aeruginosa* strain PA14, *nbdA* deletion mutants are described to show strong changes in motility and biofilm formation (Ha *et al.*, 2014; Kulasakara *et al.*, 2006). However, analyses of motility and biofilm formation of PAO1  $\Delta nbdA$  did not result in comparable phenotypes (Rüger, 2019). Furthermore, the previously described involvement of NbdA in NO-induced biofilm dispersal could not be reproduced with the newly generated markerless *nbdA* deletion mutant (Li *et al.*, 2013; Rüger, 2019). A screening of *P. aeruginosa* proteome data revealed only one publication in which NbdA was detected in stationary growth phase. Nevertheless, for the NbdA detection by LC-MS/MS, a previous enrichment of c-di-GMP binding proteins via affinity pull-down was required (Düvel *et al.*, 2012). The non-distinct phenotypic changes of the *nbdA* knock-out mutant and the lack of proteome data for NbdA arose the question whether translation of *nbdA* might be further regulated on the post-transcriptional level.

### 3.2.1 Prediction and analysis of secondary structures of the *nbdA* 5'-UTR

In the context of the new annotation of the *nbdA* transcriptional start site also the 5'-untranslated region (5'-UTR) of the *nbdA* mRNA was re-defined. For the investigation of possible regulatory mechanisms on the post-transcriptional level, secondary structures of the *nbdA* 5'-UTR were predicted using the mFold web tool (Zuker, 2003). Two possible structures were predicted by the program (Fig 3.6), with structure 1 ( $\Delta G = -20.3$ ) slightly more stable than structure 2 ( $\Delta G = -19.7$ ).



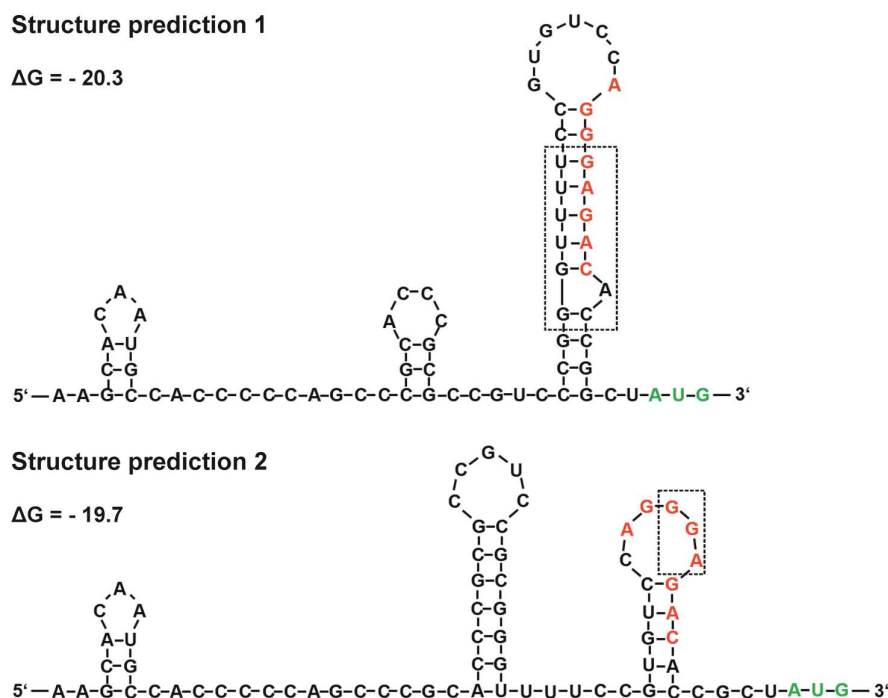


**Fig. 3.6: Secondary structure predictions of the 5'-UTR of *nbdA* with mFold**

Analysis via the mFold web tool revealed two possible secondary structures for the 5'-UTR of *nbdA* with different thermodynamical stabilities ( $\Delta G$ ). The predicted ribosome binding site is marked with red letters. The putative *nbdA* translational start codon is depicted in green. The third hairpin of structure 1 resembles a fourU-type RNA thermometer structure while the third hairpin of structure 2 presents the binding motif GGA of the RNA-binding proteins RsmA and RsmF. Important structures of the mRNA are marked by the dotted rectangles.

In both predicted secondary structures, the ribosome binding site (RBS) is located within a hairpin structure. Therefore, the RBS is most likely not accessible for the ribosome, indicating post-transcriptional regulation of translation initiation. Structure 1 strongly resembles a fourU-type RNA thermometer which is characterized by a hairpin structure in which the shine-dalgarno sequence is paired with a stretch of four uracil residues (Waldminghaus *et al.*, 2007). Additionally, the RBS is often flanked by an unpaired adenine residue, required for opening up the hairpin structure (Rinnenthal *et al.*, 2011). In the second predicted structure, the RBS is integrated into a smaller hairpin which presents a GGA motif in its loop. This GGA motif might be target for the RNA-binding proteins RsmA or RsmF which stabilize the mRNA secondary structure and thereby inhibit translation initiation (Schulmeyer *et al.*, 2016).

### 3.2.2 Impact of temperature shifts and cellular c-di-GMP levels on *nbdA* translation in *E. coli* assays

A possible RNA-thermometer function of the *nbdA* 5'-UTR was investigated utilizing translational reporter gene fusions in *E. coli* DH5 $\alpha$ . Therefore, fusions of the *nbdA* 5'-UTR to the gene *bgaB*, encoding the thermostable  $\beta$ -galactosidase of *Bacillus stearothermophilus*,

were generated in cooperation with the group of Prof. Dr. Franz Narberhaus from the Ruhr-University Bochum. The 5'-UTR of the *E. coli* gene *trxA*, which was shown to be an RNA-thermometer (unpublished data), served as positive control for the experiments. *E. coli* cells containing the translational *bgaB* fusions or the vector control (vc) were grown at 30 °C and transcription was induced by the addition of arabinose to the growth medium. One third of the culture remained at 30 °C and one part each was rapidly shifted to either 37 °C or 42 °C. Translation of the *bgaB* mRNA was investigated by the  $\beta$ -galactosidase activity. The temperature shift to either 37 °C or 42 °C led to a significant increase of the  $\beta$ -galactosidase activity for the *trxA-bgaB* fusion containing strain (Fig. 3.7A). However,  $\beta$ -galactosidase activity of *E. coli* cells containing the *nbdA-bgaB* fusion did not increase after the heat shock. In general, translation of *bgaB* in these cells appeared to be very low, as the measured  $\beta$ -galactosidase activity was comparable to the vector control. In parallel, c-di-GMP dependent phenotypes of *P. aeruginosa* PAO1 wt in comparison to the *nbdA* deletion mutant were investigated at respective assay temperatures (see chapter 2.7) and at 42 °C. No changes between the wt and the mutant strain were observed for swimming and twitching motility, 24 h biofilm formation under static conditions in 96-well microtiter plates or for pellicle formation (data not shown).

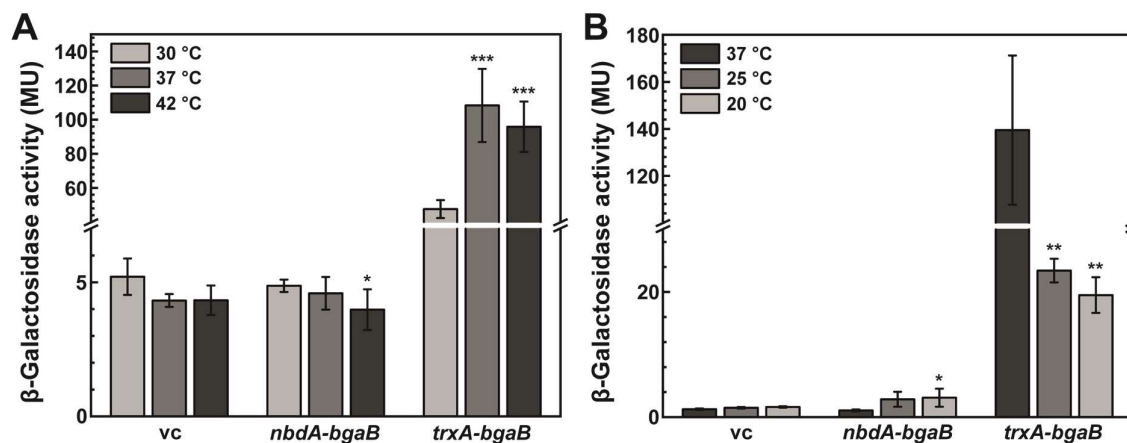


**Fig. 3.7: Regulation of *nbdA* translation by temperature shifts**

Analysis of translational levels was performed utilizing translational fusions of the 5'-UTRs of *nbdA* or the *E. coli* gene *trxA* to the reporter gene *bgaB* in *E. coli* DH5 $\alpha$ . Translational fusions were under the control of an arabinose promoter on the vector pBAD2. Transcription was induced by the addition of 0.1 % (w/v) L-arabinose and translation was measured indirectly by the  $\beta$ -galactosidase activity of BgaB.  $\beta$ -Galactosidase assays were performed after 30 min shifts to either (A) increased temperatures or (B) decreased temperatures. Experiments were performed in 3 biological replicates with 2 technical replicates each. Error bars represent the standard deviation. Significant changes between samples of the initial temperature and samples after temperature shift are marked with \* (\* P < 0.05; \*\* P < 0.01; \*\*\* P < 0.001, determined by Student's T-test). vc = vector control.

RNA-thermometer not always open up when temperatures increases. In some cases, the thermometer works in the opposite direction and the RBS is revealed when the temperature rapidly decreases (Giuliodori *et al.*, 2010). To consider this possibility, a similar experiment was performed by shifting *E. coli* cultures containing the translational *bgaB* fusions from 37 °C

to 25 °C and 20 °C, respectively. Cells containing the *trxA* control showed high *bgaB* translation at 37 °C, which decreased when cultures were shifted to lower temperatures (Fig. 3.7B).  $\beta$ -Galactosidase activity in the cells containing the *nbdA-bgaB* fusion again was comparable to the vector control when grown at 37 °C. However, temperature shifts to 25 °C or 20 °C led to a 3-fold increase of the *bgaB* translation.

Considering the role of *nbdA* as a phosphodiesterase, it might be beneficial for *P. aeruginosa* to regulate translation of *nbdA* by high intracellular levels of its substrate c-di-GMP. To investigate involvement of c-di-GMP in *nbdA* translation *E. coli* strains AB607 and its corresponding wt MG1655 were used (Boehm *et al.*, 2010). AB607 lacks the *E. coli* master PDE PdeH and therefore intracellular c-di-GMP levels are elevated. The translational *bgaB* fusions were introduced into these *E. coli* strains and translation was analyzed by  $\beta$ -galactosidase assay as described previously (Fig. 3.8).

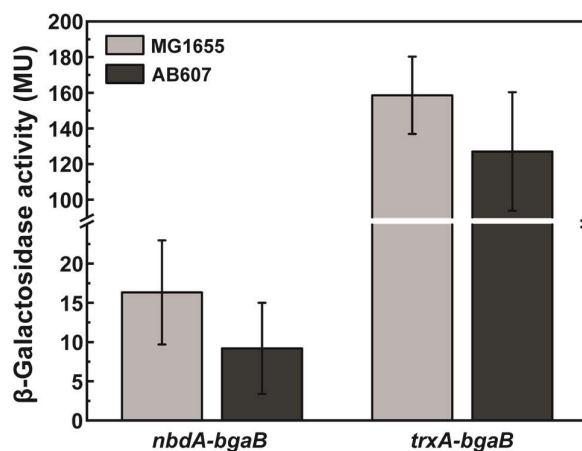


**Fig. 3.8: Influence of c-di-GMP on *nbdA* translation**

Influence of c-di-GMP on the *nbdA* translation was tested using translational fusions of the 5'-UTRs of *nbdA* or the *E. coli* gene *trxA* to the reporter gene *bgaB* in the *E. coli* strain MG1655 and the corresponding deletion mutant strain AB607 ( $\Delta pdeH$ ). Translational fusions were under the control of an arabinose promoter on the vector pBAD2. Transcription was induced by the addition of 0.1 % (w/v) L-arabinose and  $\beta$ -galactosidase activity of BgaB was tested after 30 min of incubation at 37 °C. Background  $\beta$ -galactosidase activity of the vector control was subtracted from each value. The experiment was performed in 3 biological replicates with 2 technical replicates each. Error bars represent the standard deviation.

Compared to the  $\beta$ -galactosidase activity of strains containing the *trxA-bgaB* fusion, measured Miller Units of strains containing the *nbdA-bgaB* fusion was very low. For both translational fusions a non-significant decrease of  $\beta$ -galactosidase activity in the AB607 strain was observed in comparison to the wt background.

### 3.2.3 Analysis of *nbdA* translation in *P. aeruginosa*

Since in *E. coli* almost no *nbdA* translation was observable under the tested conditions, a *Pseudomonas* specific regulatory mechanism was considered. Indicated by the second predicted secondary structure of the *nbdA* 5'-UTR (Fig. 3.6), inhibition of translation by the RNA-binding proteins RsmA or RsmF might be possible. In this case, the homologous protein

of *E. coli*, CsrA, would be able to recognize the GGA motif within the 5'-UTR and inhibit *nbda* translation via the same mechanism in the *E. coli* assays. For the investigation of an influence of RsmA and RsmF on *nbda* translation, PAO1 wt, *rsmA* deletion mutant and *rsmA rsmF* double mutant strains were received from the group of Prof. Dr. Simon Dove from the Harvard Medical School Boston (Gebhardt *et al.*, 2020). The translational *bgaB*-fusions were transferred into a vector suitable for replication and expression in *P. aeruginosa* and introduced into the respective strains. As *nbda* transcription is growth phase dependent, translational regulation in the stationary growth phase was also investigated. Therefore, *P. aeruginosa* strains containing the translational fusions or pJN105 as vector control were grown at 37 °C for 3.5 h or 6.5 h respectively before induction of transcription by addition of arabinose to the growth medium. Translation was analyzed in exponential (4 h) and early stationary (7 h) growth phase by the  $\beta$ -galactosidase activity of BgaB (Fig. 3.9A). Background levels of the vector control of each strain were subtracted from the obtained Miller Units. Additionally, samples for Western Blot analysis were taken (Fig. 3.9B).

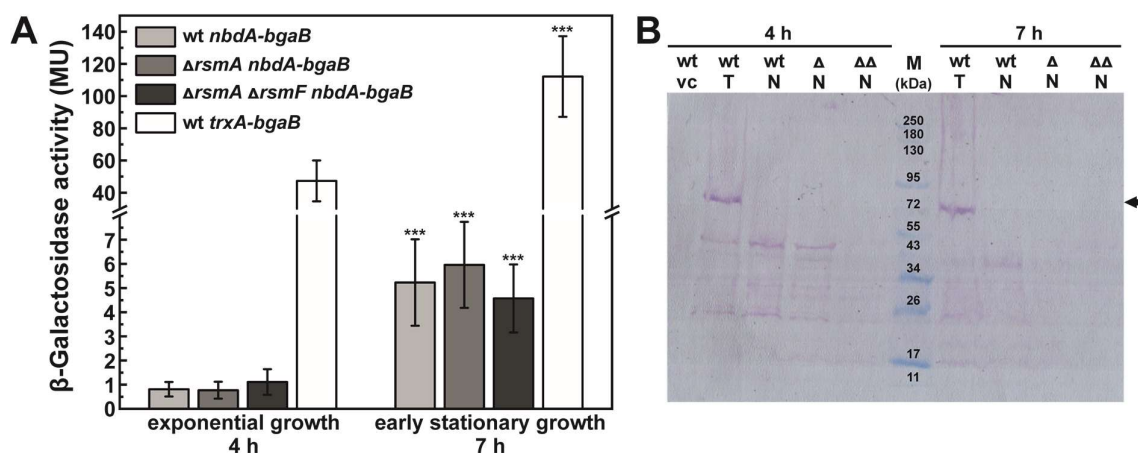


**Fig. 3.9: Dependency of *nbda* translation on growth phase and the RNA-binding proteins RsmA and RsmF**

Analysis of translational levels was performed utilizing translational fusions of the 5'-UTRs of *nbda* or the *E. coli* gene *trxA* to the reporter gene *bgaB* in *P. aeruginosa* PAO1 wt,  $\Delta$ *rsmA* or  $\Delta$ *rsmA*  $\Delta$ *rsmF* obtained from Simon Dove. Translational fusions were under the control of an arabinose promoter on the vector pJN105. Transcription was induced after 3.5 h and 6.5 h of growth at 37 °C by the addition of 0.1 % (w/v) L-arabinose and 4 h and 7 h samples were taken after 30 min of incubation, each. (A) Translation was measured indirectly via  $\beta$ -galactosidase activity of BgaB. Background  $\beta$ -galactosidase activity of the vector control was subtracted from each value. The experiment was performed in three biological replicates with two technical replicates each. Error bars represent the standard deviation. Significant changes of the 7 h samples to the 4 h sample of each tested strain are marked with \* (\*\*\*)  $P < 0.001$ , determined by Student's T-test). (B) Production of his-tagged BgaB protein was determined via Western Blot analysis (anti 6x-His antibody). The arrow indicates the expected position of BgaB on the Western Blot.  $\Delta$  =  $\Delta$ *rsmA*,  $\Delta\Delta$  =  $\Delta$ *rsmA*  $\Delta$ *rsmF*, vc = vector control, T = *trxA-bgaB* fusion, N = *nbda-bgaB* fusion, M = protein ladder (Blue Prestained Protein Standard, Broad Range; NEB).

Compared to the positive control *trxA*,  $\beta$ -galactosidase activity in strains containing the translational *nbda-bgaB* fusion were low in exponential as well as early stationary growth phase. However, translation levels of *nbda* and *trxA* significantly increased in stationary growth phase compared to exponential phase. No significant differences in *nbda* translation were

observable between the wt background and the  $\Delta rsmA$  and  $\Delta rsmA \Delta rsmF$  mutant strains. Detection of a protein band in the western blot corresponding with the size of the His-tagged BgaB protein (~78 kDa) was possible for the strain containing the *trxA* 5'-UTR fusion to *bgaB*. In *P. aeruginosa* strains containing the *nbdA-bgaB* fusion only protein bands below the expected band were detected which could also be observed in the positive control.

Formerly, nitric oxide was assumed to be sensed by the MHYT-domain of NbdA, activating its PDE domain to induce biofilm dispersal (Cutruzzola and Frankenberg-Dinkel, 2016; Li *et al.*, 2013). However, Zemke *et al.* recently questioned involvement of NbdA in NO-induced biofilm dispersal and also the work of the previous PhD student Martina Ruger also could not reveal an NO-dependent phenotype for PAO1  $\Delta nbdA$  (Ruger, 2019; Zemke *et al.*, 2020). In this work, NO-dependent transcriptional regulation of *nbdA* already was disproved, but for the sake of completeness, involvement of NO on *nbdA* translation was investigated. Therefore, PAO1 strains containing the translational *bgaB* fusions were grown at 37 °C until an OD<sub>600 nm</sub> of ~0.5. Transcription was induced by the addition of arabinose and the cultures were then divided into two parts, one part treated with 500 μM of the NO-releasing compound SNP and the other one with an equivalent volume of H<sub>2</sub>O. Translation of *nbdA* was investigated via β-galactosidase activity of BgaB (Fig. 3.10A) and western blot analysis was performed in order to detect the His-tagged BgaB-His (Fig. 3.10B).

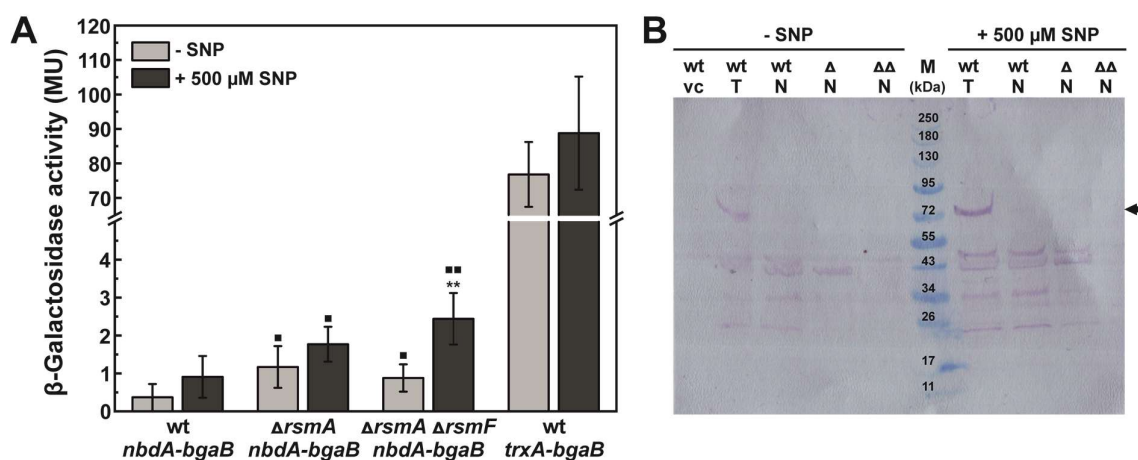


**Fig. 3.10: Impact of exogenous NO on *nbdA* translation**

Analysis of the impact of NO on translational levels was performed utilizing translational fusions of the 5'-UTRs of *nbdA* or the *E. coli* gene *trxA* to the reporter gene *bgaB* in *P. aeruginosa* PAO1 wt,  $\Delta rsmA$  or  $\Delta rsmA \Delta rsmF$ . Translational fusions were under the control of an arabinose promoter on the vector pJN105. Transcription was induced by the addition of 0.1 % (w/v) L-arabinose and either 500 μM SNP or an equivalent volume of H<sub>2</sub>O was added to the culture. Samples were taken after 30 min of incubation. (A) Translation was measured indirectly via β-galactosidase activity of BgaB. Background β-galactosidase activity of the vector control was subtracted from each value. The experiment was performed in 3 biological replicates with 2 technical replicates each. Error bars represent the standard deviation. Significant changes of the NO-treated samples to the H<sub>2</sub>O controls are marked with \*. Significant changes between the deletion mutant background and the wt background are marked with ■ (\*\*\*) P < 0.001, determined by Student's T-test). (B) Production of the BgaB protein was determined via Western Blot analysis (anti 6x-His antibody). The arrow indicates the expected position of BgaB on the Western Blot. Δ =  $\Delta rsmA$ , ΔΔ =  $\Delta rsmA \Delta rsmF$ , vc = vector control, T = *trxA-bgaB* fusion, N = *nbdA-bgaB* fusion, M = protein ladder (Blue Prestained Protein Standard, Broad Range; NEB).

---

In all tested strains,  $\beta$ -galactosidase activity was increased after treatment with the NO-releasing compound SNP. The double mutant strain  $\Delta rsmA \Delta rsmF$  showed a significant 3-fold increase of *nbdA* translation. Interestingly, in this assay *nbdA* translation in the  $\Delta rsmA$  or the double deletion strain was significantly increased compared to the corresponding wt background. Again, the positive control containing the translational *trxA* fusion showed higher  $\beta$ -galactosidase activity than the *nbdA-bgaB* fusion containing strains. This observation is also reflected in the detection of the His-tagged BgaB protein via western blot, as only the strain containing the *trxA-bgaB* fusion revealed a protein band at the expected position (~78 kDa).

### 3.3 Overproduction of different NbdA variants

The investigation of *nbdA* translation revealed extremely low translational levels under the tested conditions. This might be the reason why in previous works no phenotypes for an *nbdA* deletion mutant were observed. To gain more insights about the role of NbdA within c-di-GMP dependent motility and biofilm formation of *P. aeruginosa*, full length *nbdA* and truncated gene variants were overexpressed in PAO1  $\Delta nbdA$ . In order to inactivate the PDE function of NbdA, the conserved EAL motif was changed to AAL by site-directed mutagenesis. Additionally, truncated versions lacking either the membrane anchored MHYT-domain, one, or both cytosolic domains (e.g. AGDEF and/or EAL) of NbdA were generated in order to evaluate the influence of the particular domains on the role of NbdA within *P. aeruginosa*. For a global analysis of the NbdA function, former data of the PhD thesis of Martina Ruger and the master thesis of Jacqueline Rehner were incorporated into the analyses (Rehner, 2020; Ruger, 2019). For the production of C-terminally Strep-tagged NbdA protein variants, the expression vector pHERD26T was utilized (Tab. 3.1).

**Table 3.1: Overproduced NbdA-variants**

All overproduced NbdA-variants possess a C-terminal StrepII-tag. NbdA domains are colored as follows: membrane anchored MHYT domain = black, DGC-domain (AGDEF) = green, active PDE-domain (EAL) = red, inactive PDE-domain (AAL) = pale red.

Strain	produced NbdA domains (following name)	calculated molecular mass (kDa)
PAO1 $\Delta nbdA$ pHERD26T	vector control (vc)	none
PAO1 $\Delta nbdA$ pMRP12	MHYT-AGDEF-EAL	81.62
PAO1 $\Delta nbdA$ pMRP14	MHYT-AGDEF-AAL	81.62
PAO1 $\Delta nbdA$ pASC04	AGDEF-EAL	53.25
PAO1 $\Delta nbdA$ pMKE02	AGDEF-AAL	53.25
PAO1 $\Delta nbdA$ pJRE03	MHYT-AGDEF	52.04
PAO1 $\Delta nbdA$ pJRE02	MHYT	32.03

Strains were grown in either LB or BM2 medium at 37 °C until an OD<sub>600 nm</sub> of ~0.5. Gene expression was then induced by the addition of L-arabinose and cells were incubated for 5 h at 22 °C prior to the respective assay. Protein production of each variant was verified on a Western Blot using an antibody against the C-terminal StrepII-tag (Fig. 3.11).

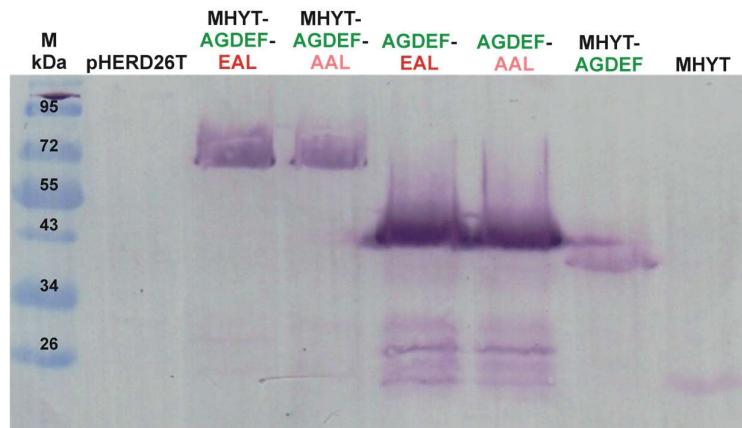


**Fig. 3.11: Overproduction of the NbdA-variants**

NbdA protein variants were overproduced in PAO1  $\Delta nbdA$  cells containing various pHERD26T derivatives. Strains were grown in LB medium supplemented with 150  $\mu\text{g}/\mu\text{L}$  tetracycline and gene expression was induced by the addition of 0.1 % (w/v) L-arabinose. Samples for Western Blot analysis were taken after 5 h of incubation at 22 °C. Cell pellets were resuspended in SDS sample buffer and boiled for 15 min at 95 °C. 20  $\mu\text{L}$  sample volume per pocket was loaded on a 12.5 % SDS gel. Protein production was determined by Western Blot analysis (Strep-Tactin® AP conjugate) after transfer onto a PVDF membrane. M = protein ladder (Blue Prestained Protein Standard, Broad Range; NEB).

The protein variants were calculated to have a molecular mass of ~82 kDa for the full length NbdA, ~53 kDa for the cytosolic variants, ~52 kDa for the MHYT-AGDEF variant, and ~32 kDa for the MHYT domain only (see Tab. 3.1). All protein variants were detected on a western blot. However, the different NbdA variants showed varying band intensities on the blot. According to the molecular mass weight standard, the protein bands of all overproduced NbdA variants showed a lower molecular weight than predicted.

Microscopy of cells overproducing the NbdA variants revealed striking changes in their cell morphology (Fig. 3.12). Before induction of gene expression, cells of all tested strains were ~2  $\mu\text{m}$  long and rod shaped. Cell morphology remained unchanged after induction for the vector control and for the  $\Delta nbdA$  strains overproducing the cytosolic NbdA domains (e.g. AGDEF-EAL and AGDEF-AAL) in both LB and BM2 medium.



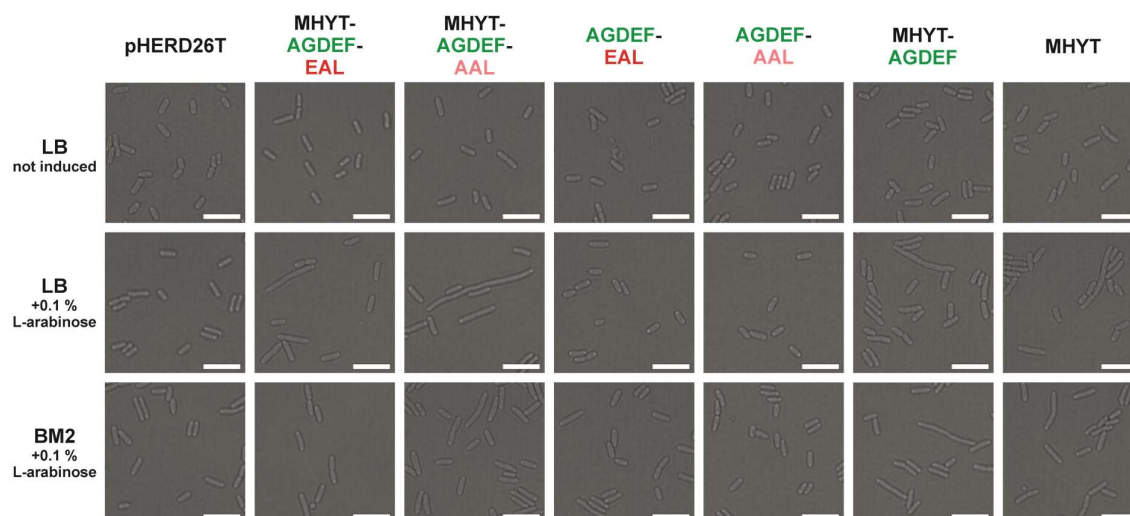


**Fig. 3.12: Morphology of cells overproducing NbdA variants**

Cell morphology of PAO1  $\Delta nbdA$  cells containing different pHERD26T derivatives for the overproduction of NbdA protein variants was analyzed by microscopy before and after protein production. Cells were grown in either LB or BM2 medium supplemented with 150  $\mu\text{g}/\mu\text{L}$  tetracycline. Gene expression was induced by the addition of 0.1 % (w/v) L-arabinose and cells were incubated for 5 h at 22 °C. For microscopy, cells were immobilized using agarose pads (1.5 % w/v in PBS-buffer). Images were taken with the Zeiss LSM 880. Scale bar = 5  $\mu\text{m}$ .

However, all strains overproducing NbdA variants including the membrane anchored MHYT domain showed cells with an elongated morphology up to a maximum cell length of  $\sim 15$   $\mu\text{m}$ . Cell elongation was observable in both tested media, but more pronounced in the complex LB medium than the minimal medium BM2. Interestingly, the cultures contained a heterologous mixture of cells with the expected length of  $\sim 2$   $\mu\text{m}$  and elongated cells of various enlargements.

### 3.3.1 Impact of *nbdA* overexpression on cell motility and biofilm formation

The second messenger c-di-GMP is known to regulate the switch between the planktonic and sessile lifestyle of *P. aeruginosa*. In general, low intracellular c-di-GMP concentrations promote cellular motility, whereas high intracellular levels of c-di-GMP induce biofilm formation (Valentini and Filloux, 2016). When overproducing a functional PDE, a decrease in c-di-GMP levels is expected. This effect was shown in the PhD thesis of Martina Ruger for PAO1 wt overexpressing the full length *nbdA* (Ruger, 2019). The influence of the overproduction of several NbdA protein variants on the flagellar-based swimming motility (Fig. 3.13) and type-IV-pili dependent twitching motility (Fig. 3.14) was analyzed. Additionally, the ability to adhere to solid surfaces (Fig. 3.15A) and the formation of pellicles at the air liquid interface (Fig. 3.15B) were investigated.

For swimming and twitching assays, L-arabinose containing swimming or twitching-agar plates were inoculated and incubated for 18 or 40 h, respectively. Evaluation of motility was performed by comparison of swimming or twitching zones of the vector control (vc) and the respective overexpression strains. The  $\Delta nbdA$  strains overproducing the full-length NbdA

variants both showed significantly decreased swimming motility (Fig. 3.13). Production of the active full-length NbdA reduced swimming motility by ~20 %, while the strain overproducing the inactive protein variant showed a ~60 % decrease in swimming motility. Both strains overproducing the cytosolic domains of NbdA did not show significant changes in their swimming behavior.

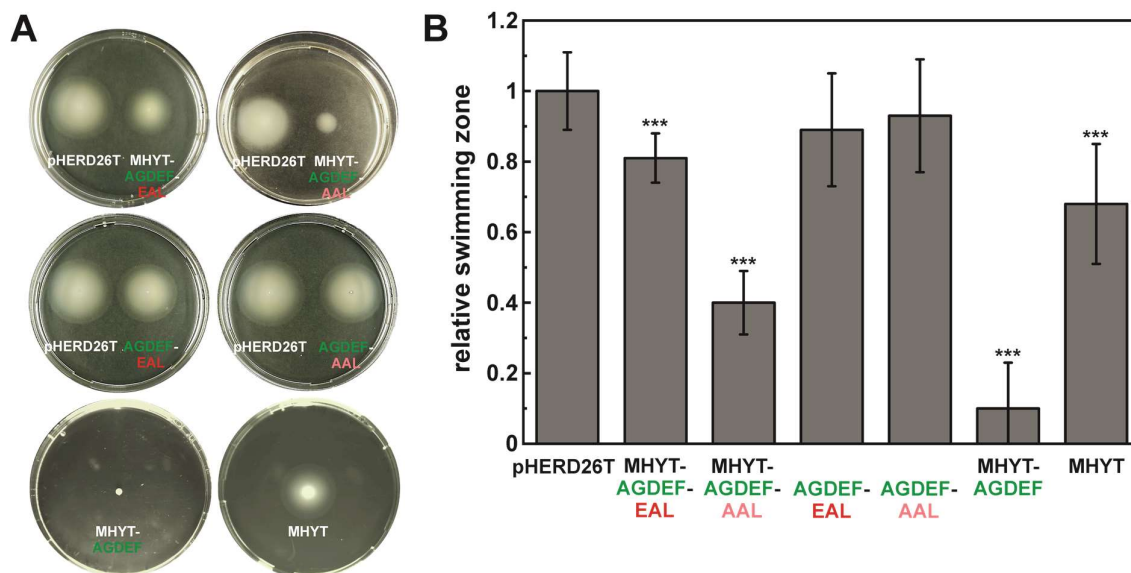


**Fig. 3.13: Swimming motility of cells overproducing NbdA variants**

For the analysis of swimming motility, PAO1  $\Delta nbdA$  containing different pHERD26T derivatives for the overproduction of NbdA protein variants was grown in LB medium supplemented with 150  $\mu\text{g}/\mu\text{L}$  tetracycline. Gene expression was induced by the addition of 0.1 % (w/v) L-arabinose and cultures were incubated for 5 h at 22 °C.  $\text{OD}_{600 \text{ nm}}$  of the cultures was adjusted to 1.5. LB swimming-agar plates (0.3 % w/v) supplemented with tetracycline and 0.1 % (w/v) L-arabinose were inoculated with 1  $\mu\text{L}$  culture per strain. Plates were incubated upright at 30 °C for 18 h and the radius of the swimming zone was measured. **(A)** Pictures of swimming plates after incubation. **(B)** Evaluation of swimming zones in relation to the vector control. The experiment was performed at a minimum of three biological replicates for each tested strain. Error bars represent the standard deviation. Significant changes between the tested strains and the vector control are marked with \* (\*\*\*)  $P < 0.001$ , determined by Student's T-test). Data of M. Ruger, J. Rehner, and K. Gerbracht were combined (Rehner, 2020; Ruger, 2019).

When overproducing the MHYT domain only, swimming motility was significantly reduced by ~30 %. The most distinct impact on swimming motility with a decrease of ~90 % showed the  $\Delta nbdA$  strain overproducing the MHYT-AGDEF domains of NbdA.

While swimming motility was only decreased, twitching motility was completely abolished when overproducing either the active or inactive full length variant of NbdA (Fig. 3.14). Strains overproducing the cytosolic domains of NbdA both showed impaired twitching motility compared to the vector control. Overproduction of the MHYT domain or MHYT-AGDEF domains both revealed almost no twitching motility. In summary, the overproduction of NbdA variants containing the membrane-anchored MHYT domain seems to impair motility of *P. aeruginosa*. An effect which is more pronounced in the T4P-dependent twitching motility than in the flagellum-dependent swimming motility.

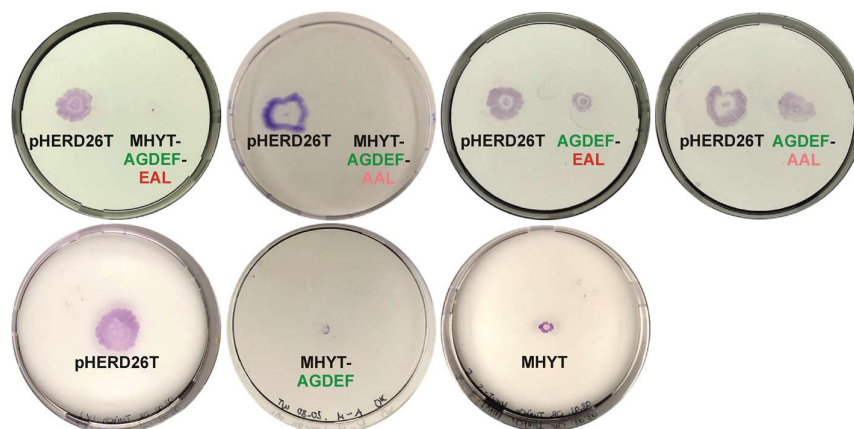


**Fig. 3.14: Twitching motility of cells overproducing NbdA variants**

For the analysis of twitching motility, PAO1  $\Delta nbdA$  strains containing different pHERD26T derivatives for the overproduction of NbdA protein variants were grown in LB medium supplemented with 150  $\mu\text{g}/\mu\text{L}$  tetracycline. Gene expression was induced by the addition of 0.1 % (w/v) L-arabinose and cultures were incubated for 5 h at 22 °C.  $\text{OD}_{600 \text{ nm}}$  of the cultures was adjusted to 1.5 and LB twitching-agar plates (1 % w/v) supplemented with tetracycline and 0.1 % (w/v) L-arabinose were inoculated below the agar with 1  $\mu\text{L}$  culture per strain. Plates were incubated upright at 37 °C for 40 h and the twitching zones were stained with 0.05 % (w/v) crystal violet. Pictures of twitching zones were taken and compared to the vector control. The experiment was performed at a minimum of three biological replicates for each tested strain. Data of M. Ruger, J. Rehner, and K. Gerbracht were combined (Rehner, 2020; Ruger, 2019).

The ability to adhere to solid surfaces is required for biofilm formation and therefore gives a hint on the possible biofilm phenotype of the examined overexpression strains. Therefore, 96-well plates were inoculated with strains overproducing NbdA variants and adhered biomass was investigated after 1 h incubation at 37 °C (Fig. 3.15A). Compared to the vector control, the  $\Delta nbdA$  strains overproducing the full length and cytosolic variants of NbdA showed significantly decreased attachment. Overproduction of the active full-length variant of NbdA decreased the attachment by ~80 % while overproduction of the inactive full-length NbdA, active or inactive cytosolic NbdA domains led to a decrease by ~45 %, ~40 % or ~35 %, respectively.

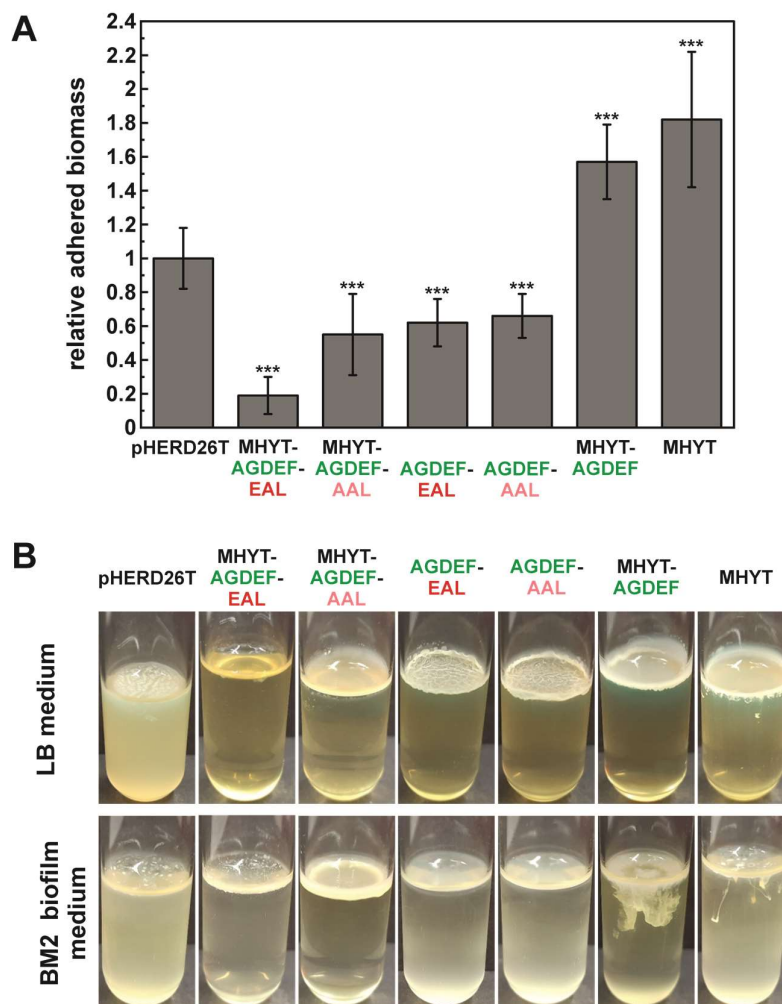


**Fig. 3.15: Adhesion and pellicle formation of cells overproducing NbdA variants**

For the adhesion and pellicle formation assays, PAO1  $\Delta nbdA$  strains containing different pHERD26T derivatives for the overproduction of NbdA protein variants were grown in LB or BM2 medium supplemented with 150  $\mu\text{g}/\mu\text{L}$  tetracycline. Gene expression was induced by the addition of 0.1 % (w/v) L-arabinose and cultures were incubated for 5 h at 22 °C. **(A)** Adhesion to solid surfaces was tested in 96-well plates.  $\text{OD}_{600 \text{ nm}}$  of the BM2 cultures was adjusted to 1.5 in adhesion medium supplemented with tetracycline and L-arabinose. Each well was inoculated with 100  $\mu\text{L}$  culture and the plate was incubated for 1 h at 37 °C in a moist chamber. Adhered biomass was measured indirectly after crystal violet staining via the  $\text{OD}_{595 \text{ nm}}$  of the bound dye and evaluated in relation to the vector control. The experiment was performed at a minimum of three biological replicates for each tested strain. Error bars represent the standard deviation. Significant changes between the tested strains and the vector control are marked with \* (\*\*\*)  $P < 0.001$ , determined by Student's T-test). Data of M. Ruger, J. Rehner, and K. Gerbracht were combined (Rehner, 2020; Ruger, 2019). **(B)** Pellicle formation was tested in either LB or biofilm medium supplemented with tetracycline and L-arabinose.  $\text{OD}_{600 \text{ nm}}$  of the cultures was adjusted to 0.03 in the respective medium and reaction tubes were inoculated with 4 mL each. Tubes were incubated statically at 22 °C for 2 d.

Pellicle formation at the air-liquid interface is another biofilm-specific phenotype which is controlled by c-di-GMP (Friedman and Kolter, 2004). Reaction tubes were inoculated with strains overproducing NbdA variants and incubated statically at 22 °C for 2 d. After incubation, the formation of pellicles of each strain was compared to the vector control (Fig. 3.15B). The strain overproducing the active full-length variant of NbdA was unable to form a pellicle in both LB and BM2 biofilm medium. Additionally, the growth medium was only slightly turbid compared to the vector control strain. In contrast, when grown under constant shaking

conditions at 22 °C, growth of the *nbdA* overexpression strain was comparable to the vector control strain. A drop dilution assay with samples taken out of the, only slightly, turbid pellicle assay culture revealed that contained cells were still vital and able to form colonies on LB-agar (data not shown). All other tested strains formed pellicles in either LB or BM2 biofilm medium. Pellicles of strains grown in LB medium appeared to be thicker and more robust than in BM2 biofilm medium. Pellicles formed by the strains overproducing either the active or inactive form of the cytosolic NbdA domains showed a wrinkly morphology when grown in LB medium.

Growth on solid medium was tested after the 2 d shaking incubation for all strains utilizing the drop dilution assay. Therefore, OD<sub>600 nm</sub> was adjusted to 0.1 and a dilution series from 10<sup>0</sup> to 10<sup>-4</sup> was prepared and spotted on LB-agar (1.5 %) with tetracycline. Growth behavior of strains overproducing the NbdA variants was investigated on agar supplemented with 0.1 % L-arabinose (Fig. 3.16).

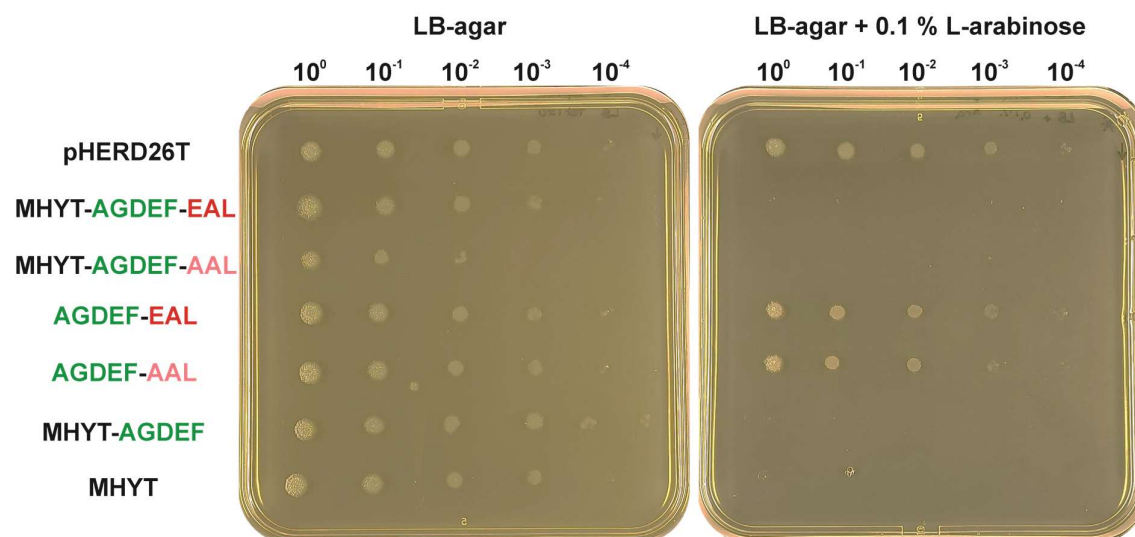


**Fig. 3.16: Growth on solid surfaces tested by drop dilution assay**

The ability to grow on solid surfaces was tested on LB-agar (1.5 % w/v) plates supplemented with 150 µg/µL tetracycline. PAO1  $\Delta nbdA$  containing pHERD26T derivatives for overproduction of NbdA protein variants was grown in LB medium supplemented with tetracycline. Gene expression was induced by the addition of 0.1 % (w/v) L-arabinose and cultures were incubated at 22 °C for 5 h. Cultures were adjusted to an OD<sub>600 nm</sub> of 0.03 in LB medium containing tetracycline and L-arabinose. Strains were incubated shaking at 22 °C for 2 d. OD<sub>600 nm</sub> was then adjusted to 0.1 and a dilution series from 10<sup>0</sup> to 10<sup>-4</sup> was prepared in fresh LB medium. 1 µL of each dilution per strain was spotted on LB-agar with or without 0.1 % (w/v) L-arabinose and plates were incubated over night at 37 °C. Growth was identified by the ability to form colonies on the agar.

All tested strains formed colonies on LB-agar at least up to the 10<sup>-2</sup> dilution. Interestingly, when spotted on LB-agar supplemented with the inducer L-arabinose, all strains overproducing an NbdA variant containing the membrane domain MHYT, were unable to grow.

## 3.4 Localization studies of NbdA

### 3.4.1 Cellular localization of NbdA

To analyze the function of a specific protein it can be beneficial to identify its cellular localization by microscopy. Therefore, NbdA was tagged with the green fluorescent protein (FP) mNeonGreen or the yellow fluorescent protein Venus. In order to avoid cellular dysfunction by a strong overproduction of the c-di-GMP degrading NbdA, *nbdA*-FP fusions were integrated into the original gene locus under the control of the native promoter. As *nbdA* translational levels appeared to be very low under normal growth conditions (see chapter 3.2.3), the *nbdA*-FP fusions were additionally integrated into an expression vector. A strong overproduction of the full length NbdA from pHERD26T led to elongated cells (see Fig. 3.12). In order to avoid this effect, the low copy number vector pME6032 was used instead for microscopic analysis. PAO1::*nbdA*-mNeonGreen or PAO1::*nbdA*-Venus were grown in LB medium over night at 37 °C to late stationary phase. Cultures were diluted in fresh medium and immobilized on agarose pads prior to microscopy. Cellular localization of NbdA was then examined by confocal laser scanning microscopy (CLSM) using the excitation wavelengths 488 nm and 514 nm for the mNeonGreen and Venus fusion, respectively. CLSM revealed that NbdA was not distributed equally in all examined cells. Fluorescence signal of NbdA-mNeonGreen or -Venus emerged either diffuse in the cells or accumulated to one or two distinct foci in the cell membrane, which were located lateral or at one or both cell poles (Fig. 3.17). Although detectable during CLSM by their fluorescence, the NbdA-FP fusions could not be detected on a Western Blot via their C-terminal His-tag (data not shown). Nevertheless, formation of the observed fluorescent foci is dependent on NbdA-localization as cells expressing plasmid encoded mNeonGreen or Venus showed equal distribution of fluorescence across the whole cytoplasm (data from Maike Karcher).

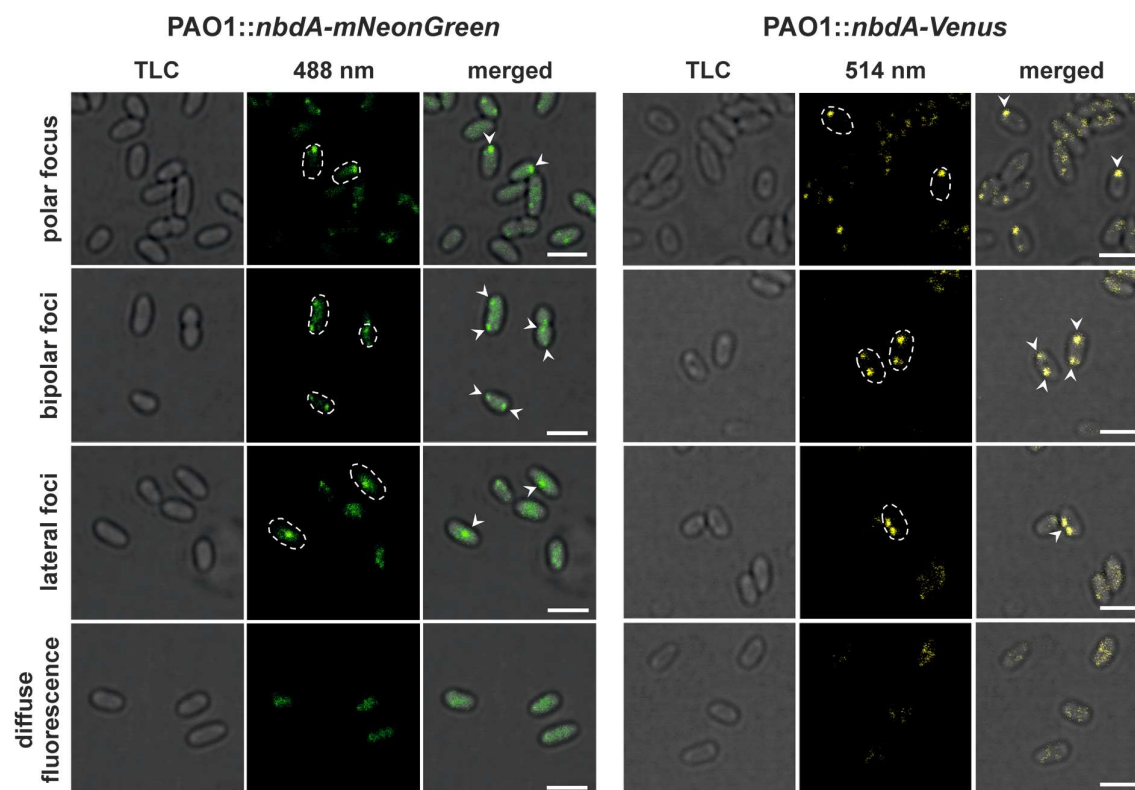


**Fig. 3.17: Observation of NbdA localization in PAO1::nbdA-mNeonGreen and PAO1::nbdA-Venus by CLSM**

PAO1::nbdA-mNeonGreen and PAO1::nbdA-Venus strains were grown over night in LB medium at 37 °C. Cultures were diluted 1:4 in fresh medium prior to microscopy and cells were immobilized using 1.5 % (w/v) agarose pads. Single cells were detected by transmitted light microscopy. NbdA-mNeonGreen was excited using the 488 nm laser line, NbdA-Venus was excited with the 514 nm laser line. Images were taken with the Zeiss LSM 880. Outlines of designated cells are marked with dotted lines. White arrow heads mark NbdA-mNeonGreen/-Venus localization. TLC = transmitted light channel. Scale bar = 2  $\mu$ m.

For further analysis, the percentage of total cells exhibiting the four different NbdA localizations was calculated (Fig. 3.18). In PAO1::nbdA-mNeonGreen 50 % of all examined cells showed diffuse fluorescent signal. For PAO1::nbdA-Venus it was a fraction of 36 % of the cells. The other cells showed distinct fluorescent foci with the majority of 32 % for the mNeonGreen- and 38 % for the Venus-fusion possessing one polar focus. 8 % or 13 % of the examined cells exhibited bipolar foci and 10 % or 13 % of the cells showed lateral fluorescent foci for NbdA-mNeonGreen or -Venus, respectively.

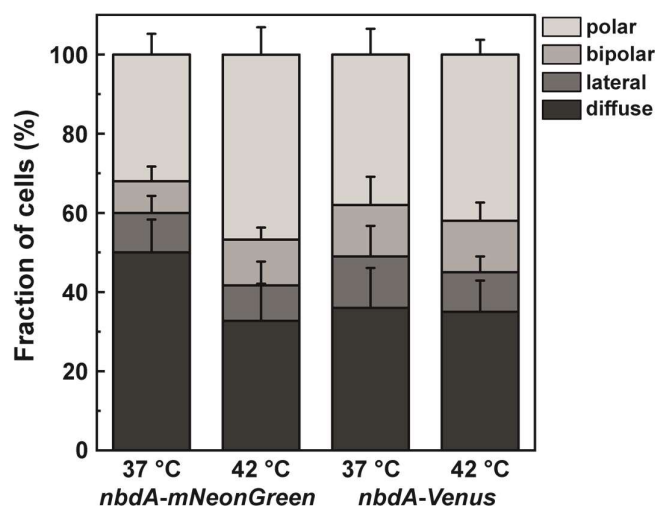


**Fig. 3.18: Evaluation of cellular NbdA localization at 37 °C or after heat shock at 42 °C in PAO1::*nbdA-mNeonGreen* and PAO1::*nbdA-Venus***

PAO1::*nbdA-mNeonGreen* and PAO1::*nbdA-Venus* strains were grown over night in LB medium at 37 °C. Cultures were diluted 1:4 in fresh medium and used directly for CLSM or after a 15 min heat shock at 42 °C. Cells exhibiting polar, bipolar, lateral or diffuse fluorescent signals were counted and the fraction of total cells was evaluated for each NbdA localization. Total cell counts: NbdA-mNeonGreen 37 °C = 1101, 42 °C = 1773; NbdA-Venus 37 °C = 488, 42 °C = 676. Error bars represent the standard deviation.

Cells heat stressed for 15 min at 42 °C revealed a comparable cellular distribution of NbdA (Fig. 3.18). The amount of cells with diffuse fluorescent signal (33 %) and lateral foci (9 %) decreased in PAO1::*nbdA-mNeonGreen* while the amount of cells possessing polar (47 %) or bipolar (12 %) fluorescent foci increased. For PAO1::*nbdA-Venus* the fraction of cells with only one polar signal increased (42 %) whereas the lateral (10 %) and diffuse (10 %) signals decreased slightly. The amount of cells with bipolar signal remained unchanged.

PAO1 cells harboring the plasmids pME6032-*nbdA-mNeonGreen* or pME6032-*nbdA-Venus* were grown to an  $OD_{600\text{ nm}}$  of 0.2-0.5 in LB medium and gene expression was induced by the addition of either 100  $\mu\text{M}$  or 500  $\mu\text{M}$  IPTG. Samples of both cultures were taken before induction (b.i.) and 1 h, 2 h, and 3 h after induction and the His-tagged fusion proteins were detected in whole cells via Western Blot analysis (Fig. 3.19). The fusion proteins NbdA-mNeonGreen and NbdA-Venus with the calculated molecular weight of ~108 kDa were detectable 2 h after induction with 100  $\mu\text{M}$  IPTG or 1 h after induction with 500  $\mu\text{M}$  IPTG.



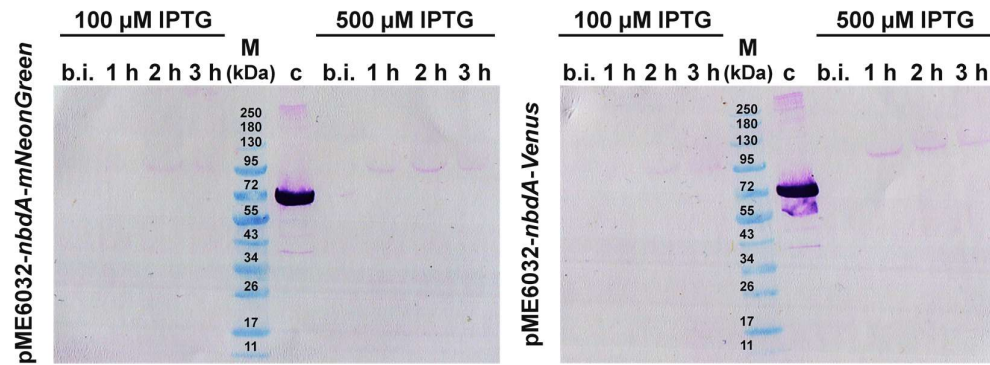


**Fig. 3.19: Detection of plasmid-encoded His-tagged fusion proteins NbdA-mNeonGreen and NbdA-Venus via Western Blot analysis.**

PAO1 pME6032-*nbdA-mNeonGreen* and PAO1 pME6032-*nbdA-Venus* strains were grown in LB medium to an  $OD_{600\text{ nm}}$  of  $\sim 0.5$ . Gene expression was induced by the addition of 100  $\mu\text{M}$  or 500  $\mu\text{M}$  IPTG and cells were incubated at 37  $^{\circ}\text{C}$ . Samples for Western Blot analysis were taken before induction (b.i.) or 1 h, 2 h, and 3 h after induction. Cell pellets were resuspended in SDS sample buffer and boiled for 15 min at 95  $^{\circ}\text{C}$  prior to SDS-PAGE. Protein production was determined by Western Blot analysis (anti 6x-His antibody) after transfer onto a PVDF membrane. M = protein ladder (Blue Prestained Protein Standard, Broad Range; NEB). C = positive control ArnC-His ( $\sim 79$  kDa).

Proceeding from the test-expression results, for localization experiments 100  $\mu\text{M}$  IPTG was used for induction of gene expression and cells were examined 2 h after induction by CLSM as described previously. Cells expressing the plasmid-encoded *nbdA-mNeonGreen* and -*Venus* fusions showed only three possible localizations of NbdA: polar foci, bipolar foci or diffuse fluorescence (Fig. 3.20A).

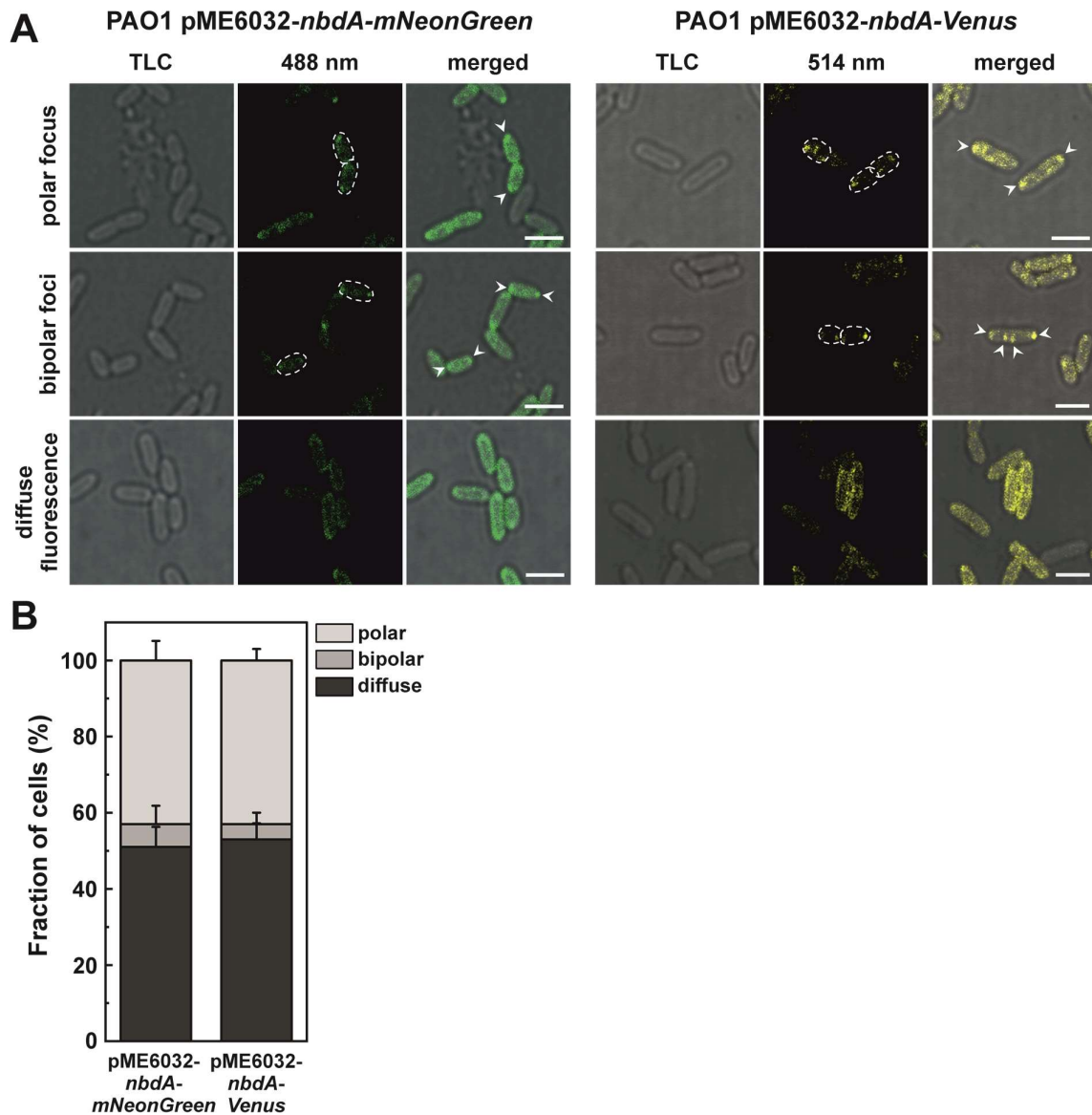


**Fig. 3.20: Cellular localization of plasmid-encoded *nbdA-mNeonGreen* and *nbdA-Venus***

PAO1 pME6032-*nbdA-mNeonGreen* and PAO1 pME6032-*nbdA-Venus* strains were grown to an  $OD_{600\text{ nm}}$  of  $\sim 0.5$  and gene expression was induced by the addition of  $100\ \mu\text{M}$  IPTG. Cultures were incubated for 2 h prior to microscopy and cells were immobilized using 1.5 % (w/v) agarose pads. Single cells were detected by transmitted light microscopy. NbdA-mNeonGreen was excited using the 488 nm laser line, NbdA-Venus was excited with the 514 nm laser line. Images were taken with the Zeiss LSM 880. Outlines of designated cells are marked with dotted lines. White arrow heads mark NbdA-mNeonGreen/-Venus localization. TLC = transmitted light channel. Scale bar =  $2\ \mu\text{m}$ . (B) Fractions of cells exhibiting polar, bipolar or diffuse NbdA localization was evaluated from CLSM images of PAO1 pME6032-*nbdA-mNeonGreen* and PAO1 pME6032-*nbdA-Venus* after 2 h protein production ( $100\ \mu\text{M}$  IPTG). Total cell count NbdA-mNeonGreen = 1395; NbdA-Venus = 943. Error bars represent the standard deviation.

Cells with diffuse fluorescence of NbdA-FP revealed higher intensity of fluorescence across the cell membrane than in the cytoplasm. Approximately 50 % of the total cells showed this NbdA distribution for both NbdA fusions (Fig. 3.20B). Only a small amount of cells contained bipolar fluorescent foci for NbdA-mNeonGreen (6 %) or NbdA-Venus (4 %), whereas 43 % of cells showed polar localization of NbdA.

### 3.4.2 Co-localization studies of NbdA with the polar flagellum

A recent publication linked the three PDEs NbdA, DipA, and RbdA with the control of flagellar motor switching (Xin *et al.*, 2019). As demonstrated before, NbdA is often localized at one cell pole (Fig. 3.17; 3.20), but the NbdA localization in relation to the polar flagellum remained unclear. Here, the flagellated cell pole was identified by flagellar staining and co-localization of NbdA-FP with the flagellum was investigated. Therefore, the flagellar subunit FliC was modified by the amino acid exchange T394C. This amino acid exchange allows fluorescent labeling of the flagellum with maleimide dyes which are able to form a disulfide bond with the introduced cysteine residue (Zhu *et al.*, 2019). To avoid interference of the flagella staining with the green and yellow fluorescent tags of NbdA, the red fluorescent dye Alexa Fluor™ 594 C5 Maleimide was used in the co-localization assays. PAO1::*nbdA-mNeonGreen::fliC(T394C)* and PAO1::*nbdA-Venus::fliC(T394C)* were grown over night, diluted and stained with the red fluorescent dye. Fluorescence of the tagged NbdA and the stained flagella were captured in different frames during CLSM (Fig. 3.21; 3.22).

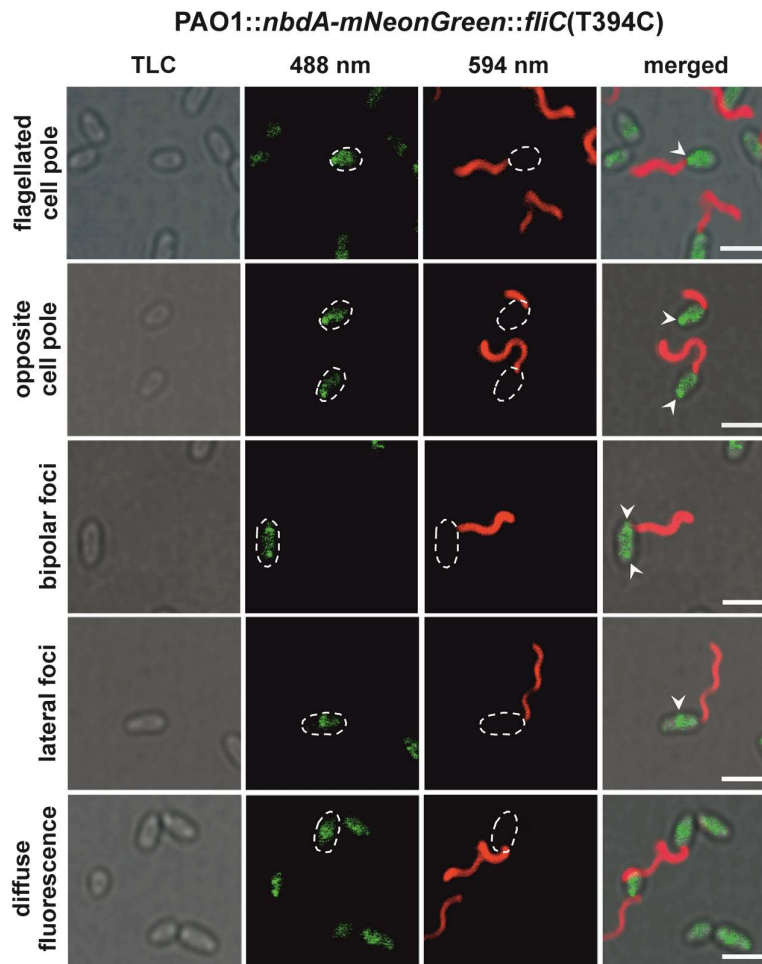


**Fig. 3.21: Co-localization of genomically encoded NbdA-mNeonGreen with the polar flagellum**

PAO1::*nbdA-mNeonGreen::fliC(T394C)* was grown in LB medium at 37 °C over night. Flagella were stained with the fluorescent dye Alexa Fluor™ 594 C5 Maleimide. Cells were immobilized for CLSM using 1.5 % (w/v) agarose pads. Single cells were detected by transmitted light microscopy. NbdA-mNeonGreen was excited using the 488 nm laser line, Alexa Fluor™ 594 was excited using the 594 nm laser line. Images were taken in separate frames with the Zeiss LSM 880. Outlines of designated cells are marked with dotted lines. White arrow heads mark NbdA-mNeonGreen localization. TLC = transmitted light channel. Scale bar = 2 µm.

Cells containing the fusion proteins NbdA-mNeonGreen (Fig. 3.21) or -Venus (Fig. 3.22) again showed either diffuse fluorescence or distinct fluorescent foci within the cell membrane. These foci were located either at the flagellated or opposite cell pole, bipolar or lateral in the cell.

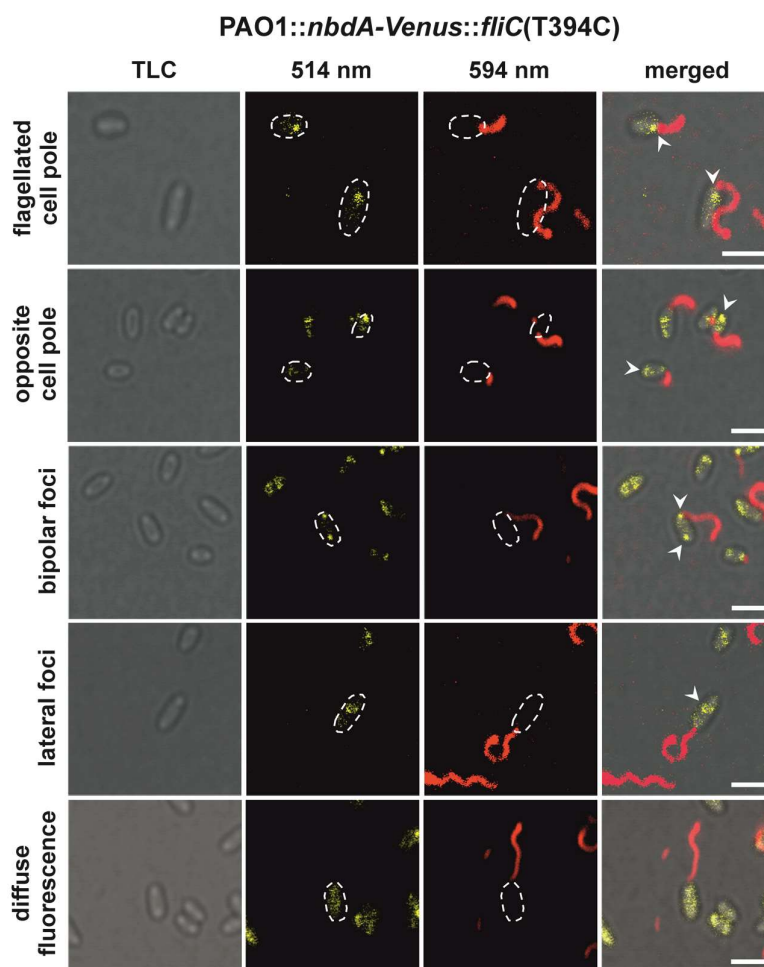


**Fig. 3.22: Co-localization of genomically encoded NbdA-Venus with the polar flagellum**

PAO1::*nbdA-Venus::fliC(T394C)* was grown in LB medium at 37 °C over night. Flagella were stained with the fluorescent dye Alexa Fluor™ 594 C5 Maleimide. Cells were immobilized for CLSM using 1.5 % (w/v) agarose pads. Single cells were detected by transmitted light microscopy. NbdA-Venus was excited using the 514 nm laser line, Alexa Fluor™ 594 was excited using the 594 nm laser line. Images were taken in separate frames with the Zeiss LSM 880. Outlines of designated cells are marked with dotted lines. White arrow heads mark NbdA-Venus localization. TLC = transmitted light channel. Scale bar = 2 µm.

PAO1::*fliC(T394C)* containing the pME6032-variants for NbdA-FP production were grown to an  $OD_{600\text{ nm}}$  of 0.2-0.5 in LB medium. Gene expression was then induced by the addition of 100 µM IPTG and cells were incubated for 2 h prior to flagellar staining. As described previously, fluorescence of the different fluorophores was captured in separate frames during CLSM. Localization of NbdA-mNeonGreen (Fig. 3.23) and -Venus (Fig. 3.24) was analyzed in relation to the polar flagellum.

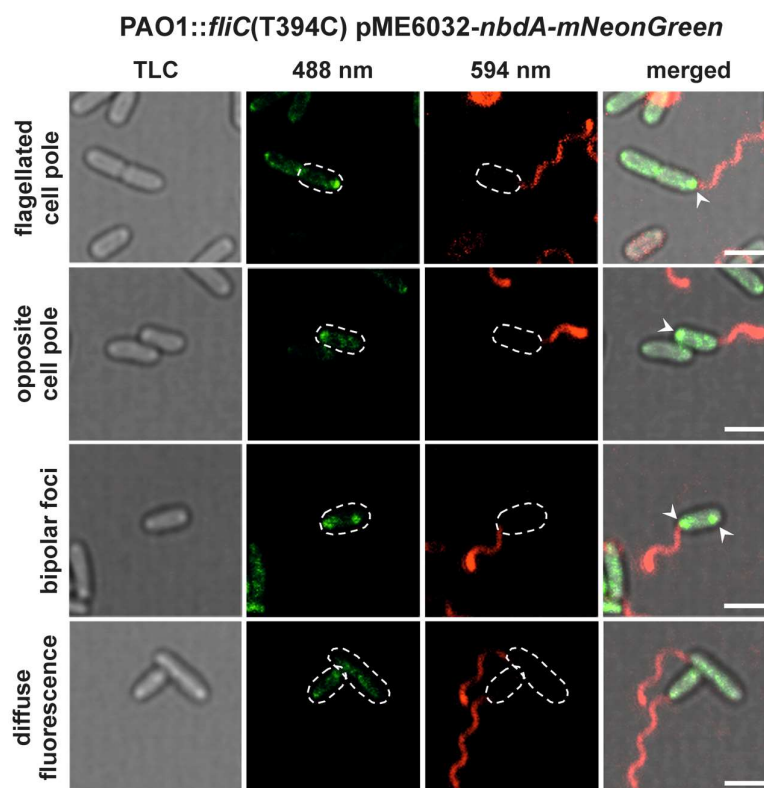


**Fig. 3.23: Co-localization of plasmid encoded NbdA-mNeonGreen with the polar flagellum**

PAO1::*fliC*(T394C) pME6032-*nbdA*-mNeonGreen was grown in LB medium at 37 °C to an OD<sub>600 nm</sub> of ~0.5. Gene expression was induced by the addition of 100 µM IPTG and cells were incubated for 2 h at 37 °C. Flagella were stained with the fluorescent dye Alexa Fluor™ 594 C5 Maleimide. Cells were immobilized for CLSM using 1.5 % (w/v) agarose pads. Single cells were detected by transmitted light microscopy. NbdA-mNeonGreen was excited using the 488 nm laser line, Alexa Fluor™ 594 was excited using the 594 nm laser line. Images were taken in separate frames with the Zeiss LSM 880. Outlines of designated cells are marked with dotted lines. White arrow heads mark NbdA-mNeonGreen localization. TLC = transmitted light channel. Scale bar = 2 µm.

As observed before, when expressed from the pME6032 plasmid, NbdA-FP did not form lateral fluorescent foci in the cells. Though, diffuse fluorescence, bipolar or polar foci were observed for both, NbdA-mNeonGreen and -Venus. The polar foci were either located at the flagellated cell pole or the opposite pole.

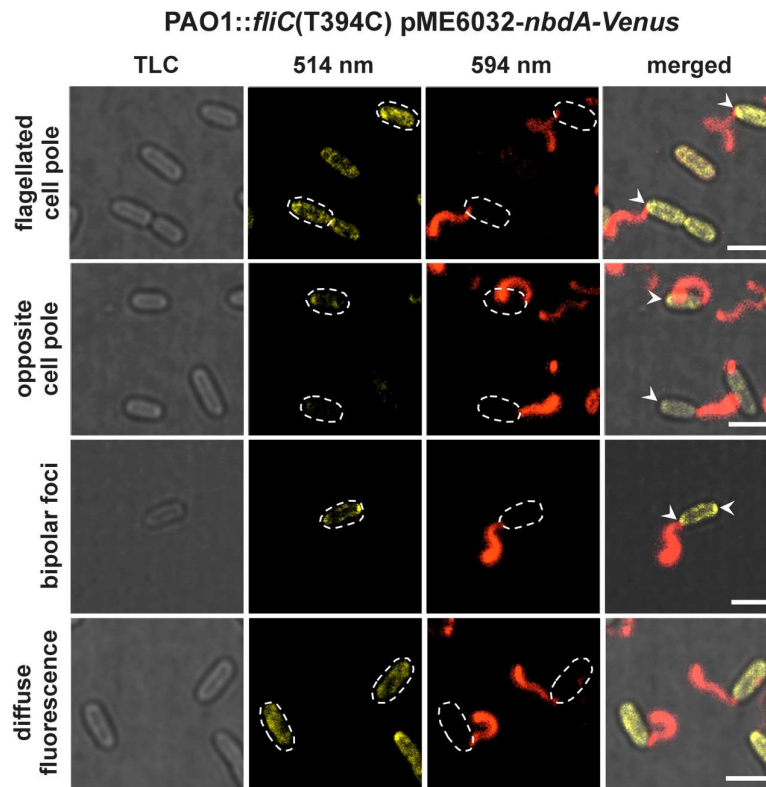


**Fig. 3.24: Co-localization of plasmid encoded NbdA-Venus with the polar flagellum**

PAO1::*fliC*(T394C) pME6032-*nbdA*-Venus was grown in LB medium at 37 °C to an OD<sub>600 nm</sub> of ~0.5. Gene expression was induced by the addition of 100 µM IPTG and cells were incubated for 2 h at 37 °C. Flagella were stained with the fluorescent dye Alexa Fluor™ 594 C5 Maleimide. Cells were immobilized for CLSM using 1.5 % (w/v) agarose pads. Single cells were detected by transmitted light microscopy. NbdA-Venus was excited using the 514 nm laser line, Alexa Fluor™ 594 was excited using the 594 nm laser line. Images were taken in separate frames with the Zeiss LSM 880. Outlines of designated cells are marked with dotted lines. White arrow heads mark NbdA-Venus localization. TLC = transmitted light channel. Scale bar = 2 µm.

Localization of NbdA-FP was evaluated in relation to the polar flagellum of PAO1::*fliC*(T394C) by calculating the fraction of cells showing one of the previously described NbdA-distributions (Fig. 3.25). Only cells with clearly assigned flagellum were considered for this evaluation.

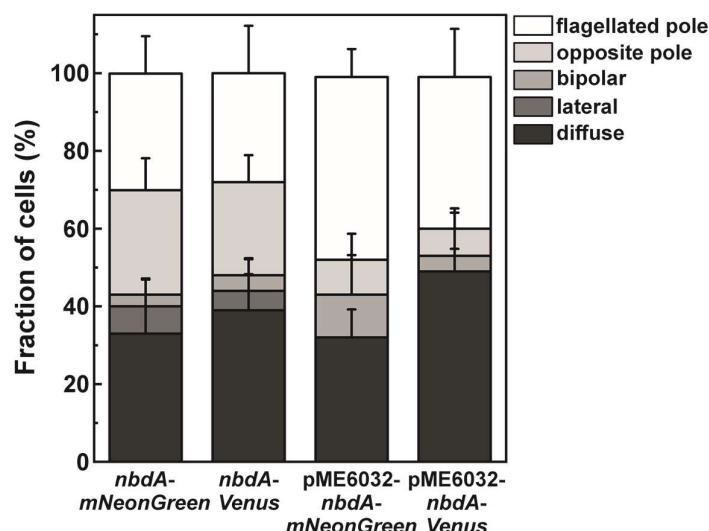


**Fig. 3.25: Evaluation of the co-localization of NbdA-FP and polar flagellum**

PAO1::*fliC*(T394C) strains with genomically or plasmid encoded *nbdA-mNeonGreen/-Venus* were used for co-localization assays with the polar flagellum after flagella stain at stationary growth phase or after protein production, respectively. Cells exhibiting NbdA localization at the flagellated pole, the opposite pole, bipolar, lateral, or diffuse were counted and the fraction of total cells was evaluated for each NbdA localization. Only cells with clearly assigned flagellum were considered. Cell counts: NbdA-mNeonGreen genomic = 310, pME6032 = 293; NbdA-Venus genomic = 370, pME6032 = 182. Error bars represent the standard deviation.

Cells expressing the genomically integrated versions of *nbdA-mNeonGreen* or *-Venus* showed diffuse fluorescence in ~33 % or ~39 % of the cases, respectively. Only a small amount of cells showed bipolar (3 %; 4 %) or lateral (7 %; 5 %) fluorescent NbdA-foci. The majority of cells with 57 % for NbdA-mNeonGreen and 52 % for NbdA-Venus, displayed only one polar fluorescent focus. In approximately half of these cases NbdA co-localized with the polar flagellum, in the other half it was located at the opposite cell pole.

When expressed from the plasmid pME6032, ~32 % of the cells showed diffuse fluorescence across the cell membrane for NbdA-mNeonGreen. All other cells exhibited distinct foci with 11 % of the total cells showing bipolar fluorescent foci, ~47 % of the cells showing co-localization of NbdA-mNeonGreen with the flagellum and 9 % showing a NbdA focus at the opposite cell pole. For cells harboring pME6032-*nbdA-Venus* the fraction of cells showing diffuse fluorescent signal was 49 %. In contrast, 4 % of cells showed bipolar fluorescent foci, 7 % of the NbdA foci were located at the opposite cell pole and 39 % of the cells revealed co-localization of NbdA and the flagellum.

### 3.4.3 Co-localization studies of NbdA with the chemotaxis protein CheA

In *P. aeruginosa*, CheA is described to be localized at the flagellated cell pole and to be present in almost every cell (Kulasekara *et al.*, 2013). Therefore, CheA is a suitable candidate for co-localization studies as it allows a certain identification of the flagellated cell pole of PAO1. For co-localization studies with the genomically integrated *nbdA-mNeonGreen* fusion, CheA was chromosomally tagged with either the red fluorescent protein tdTomato or the cyan fluorescent



protein mCerulean. PAO1::*nbdA-mNeonGreen::cheA-tdTomato* and PAO1::*nbdA-mNeonGreen::cheA-mCerulean* were grown in LB medium over night. Cultures were diluted in fresh medium and used directly for CLSM. Fluorescent signals of NbdA-FP and CheA-FP were captured in separated frames.

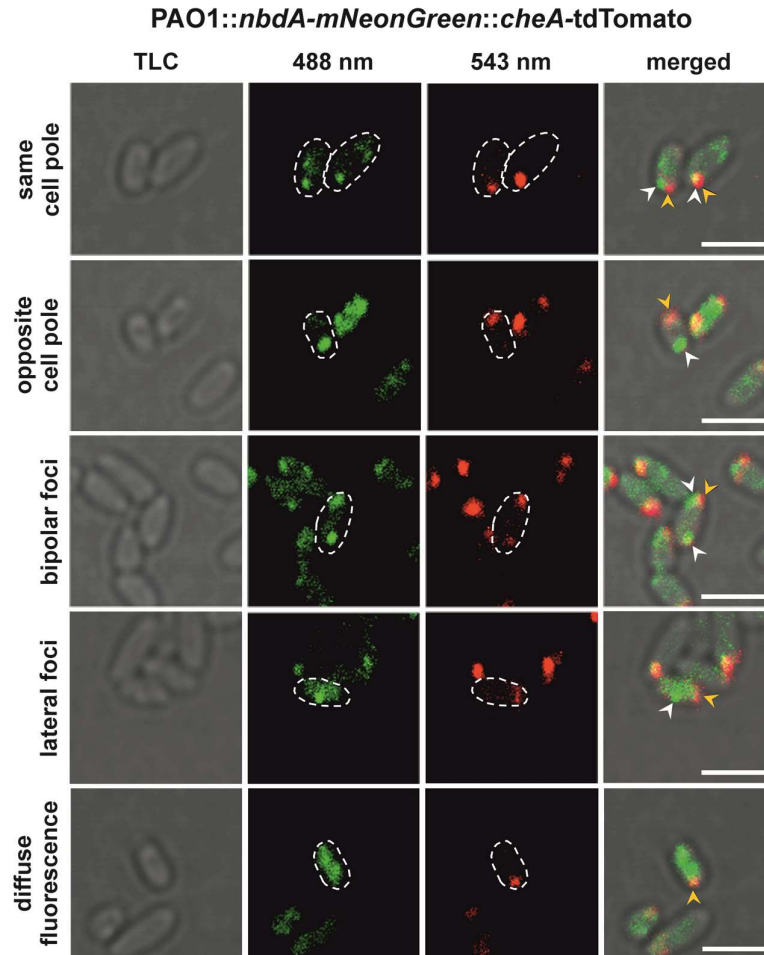


**Fig. 3.26: Co-localization of NbdA-mNeonGreen and CheA-tdTomato**

PAO1::*nbdA-mNeonGreen::cheA-tdTomato* was grown in LB medium at 37 °C over night. The culture was diluted 1:4 prior to microscopy and cells were immobilized using 1.5 % (w/v) agarose pads. Single cells were detected by transmitted light microscopy. NbdA-mNeonGreen was excited using the 488 nm laser line, CheA-tdTomato was excited using the 543 nm laser line. Images were taken in separate frames with the Zeiss LSM 880. Outlines of designated cells are marked with dotted lines. White arrow heads mark NbdA-mNeonGreen localization. Yellow arrow heads mark CheA-tdTomato localization. TLC = transmitted light channel. Scale bar = 2 µm.

In almost all examined cells, CheA-tdTomato (Fig. 3.26) and CheA-mCerulean (Fig. 3.27) showed polar localization. NbdA-mNeonGreen showed the same distribution pattern as observed before. Cells displayed either diffuse fluorescence of mNeonGreen or harbored one or several fluorescent foci. These foci appeared lateral in the cell, bipolar or at the same or opposite cell pole as CheA-FP.

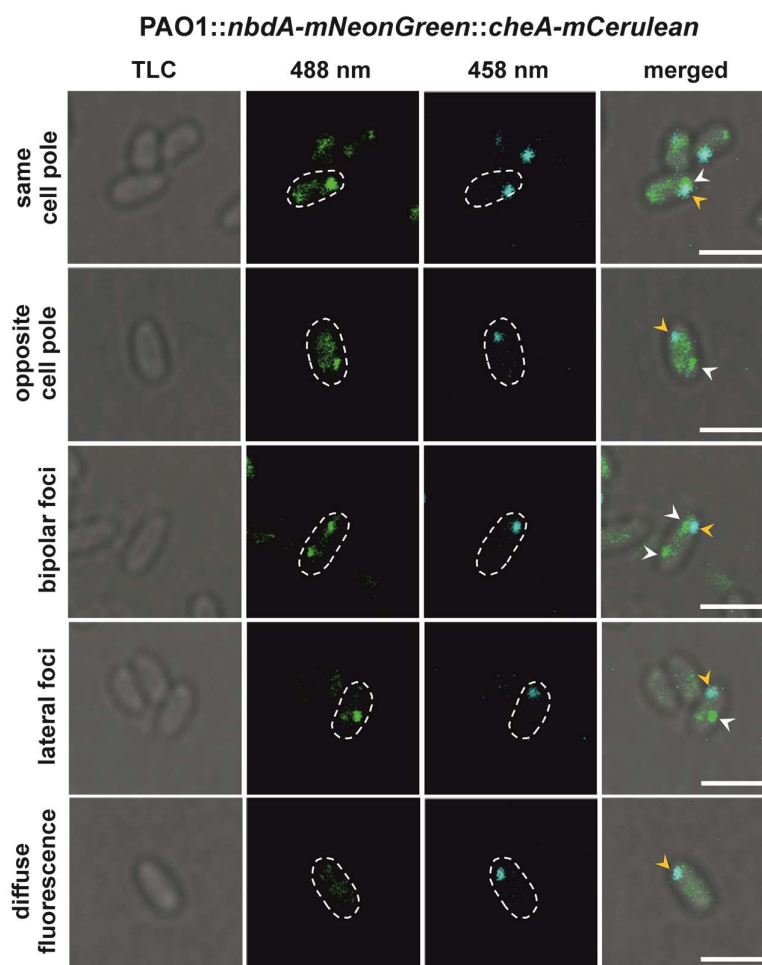


**Fig. 3.27: Co-localization of NbdA-mNeonGreen and CheA-mCerulean**

PAO1::*nbda-mNeonGreen*::*cheA-mCerulean* was grown in LB medium at 37 °C over night. The culture was diluted 1:4 prior to microscopy and cells were immobilized using 1.5 % (w/v) agarose pads. Single cells were detected by transmitted light microscopy. NbdA-mNeonGreen was excited using the 488 nm laser line, CheA-mCerulean was excited using the 458 nm laser line. Images were taken in separate frames with the Zeiss LSM 880. Outlines of designated cells are marked with dotted lines. White arrow heads mark NbdA-mNeonGreen localization. Yellow arrow heads mark CheA-mCerulean localization. TLC = transmitted light channel. Scale bar = 2 µm.

Evaluation of the co-localization experiments of NbdA-mNeonGreen with CheA revealed varying results for CheA-tdTomato and CheA-mCerulean (Fig. 3.28). With a fraction of ~43 % of the total count, the amount of cells exhibiting co-localization of CheA-tdTomato and NbdA at the same cell pole is twice as high as of CheA-mCerulean and NbdA (~20 %). Additionally, co-localization studies of CheA-tdTomato and NbdA-mNeonGreen revealed 40 % cells with diffuse NbdA signal, 2 % cells with lateral fluorescent foci of NbdA, 4 % cells with bipolar NbdA distribution and 11 % with an NbdA signal at the opposite cell pole of CheA.

For CheA-mCerulean co-localization studies, NbdA localization was evaluated as follows: 49 % of the cells showed diffuse mNeonGreen fluorescence, 6 % of the cells revealed lateral or bipolar NbdA localization, each, and 19 % of the cells showed localization of NbdA and CheA at opposite cell poles.

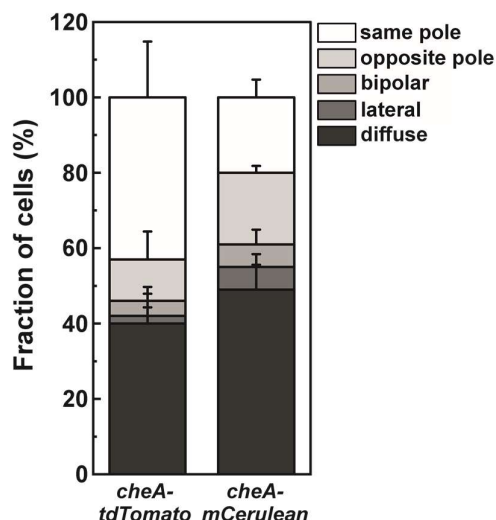


**Fig. 3.28: Evaluation of the co-localization of NbdA-mNeonGreen and CheA-FP**

Over night cultures of PAO1::*nbdA-mNeonGreen::cheA-tdTomato* and PAO1::*nbdA-mNeonGreen::cheA-mCerulean* were used for co-localization studies of NbdA with CheA. Cells exhibiting NbdA foci at the same or opposite pole than CheA, bipolar foci, lateral foci or diffuse fluorescence were counted. Fractions of total cells were evaluated for each NbdA localization. Only cells showing clear CheA fluorescent signal were considered for the evaluation. Cell counts CheA-tdTomato = 683; CheA-mCerulean = 856. Error bars represent the standard deviation.

### 3.4.4 Localization of NbdA in colony biofilms

NbdA has been previously described to be involved in biofilm dispersal of *P. aeruginosa* (Li *et al.*, 2013). This arose the question, if the NbdA localization in biofilm grown cells differs from the observed localization within planktonic cells. Therefore, PAO1::*nbdA-mNeonGreen* cells were fluorescently labeled by the genomic integration of a constitutively expressed *mCherry* gene which encodes for the cytosolic, red fluorescent protein mCherry. Biofilm colonies were grown on tryptone-agar at 25 °C for 3 or 4 days, respectively. Cells were taken from the biofilm colonies using a sterile inoculation loop and prepared for CLSM. Fluorescence of mNeonGreen and mCherry was captured in two separate frames (Fig. 3.29).

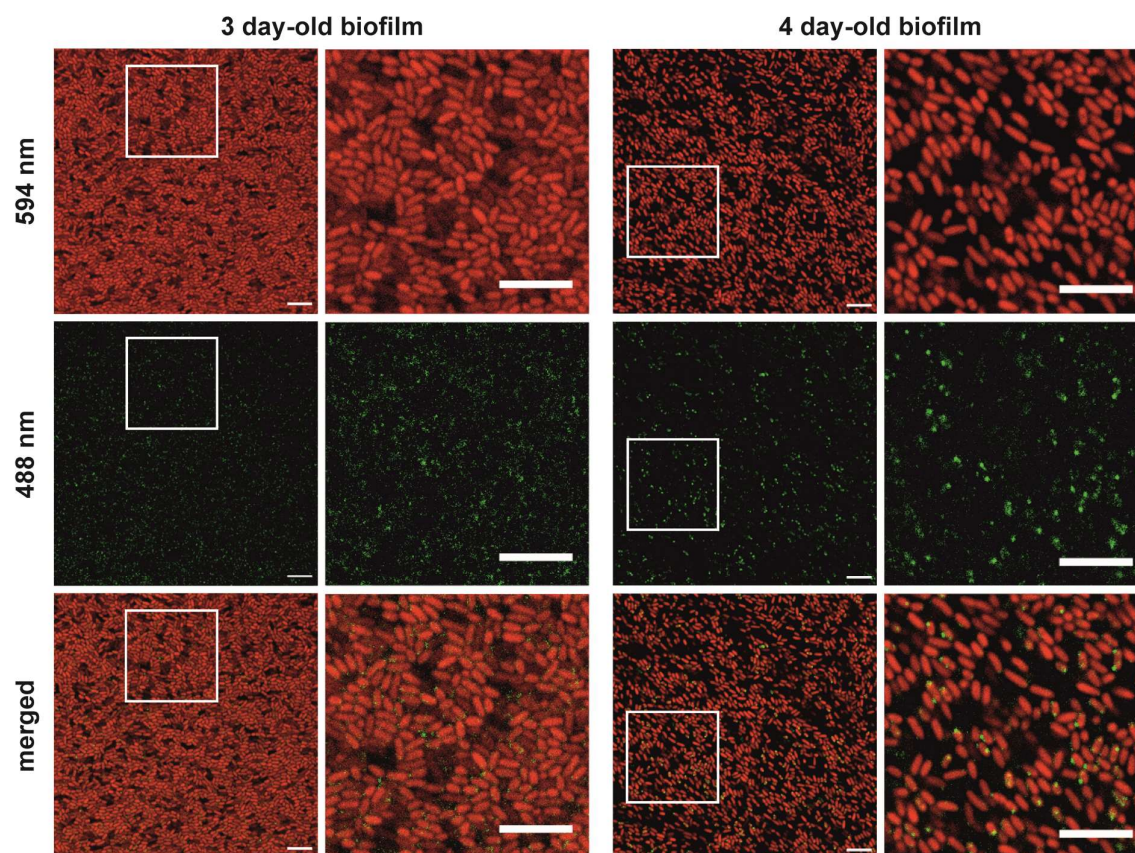


**Fig. 3.29: Cellular localization of NbdA-mNeonGreen within cells from 3 or 4 day-old biofilm colonies**

Biofilm colonies of PAO1::*nbdA-mNeonGreen::mini-CTX1-mCherry* were grown on tryptone-agar for 3 or 4 days at 25 °C. Cells from the biofilm colony were streaked onto a microscope slide prior to CLSM. Single cells in the biomass were detected by the fluorescence of mCherry, excited with the 594 nm laser line. NbdA-mNeonGreen was excited with the 488 nm laser line. Images were captured in separate frames with the Zeiss LSM 880. White squares mark the cutout shown in the detailed image. Scale bar = 10  $\mu$ m.

The identification of single cells in the biomass was possible via the red fluorescence of mCherry in the cytosol. Approximately half of the cells additionally contained distinct fluorescent signal of NbdA-mNeonGreen, mainly located to distinct polar foci in the membrane. Compared to the 3 day-old biofilm sample, intensities of these foci were increased in 4 day-old biofilm colonies.

The distribution of NbdA through a biofilm colony was investigated in collaboration with the group of Prof. Dr. Lars Dietrich at the Columbia University in New York City, USA. As previously described (see chapter 3.1), activation of *nbdA* transcription is dependent on the alternative  $\sigma$ -factor RpoS. In *P. aeruginosa*, RpoS is described to have a higher abundance in the upper layers of biofilms (Folsom *et al.*, 2010). Additionally, a sharp oxygen gradient from the top to the bottom layers of biofilm colonies is present (James *et al.*, 2016). Therefore, in the lower, anoxic biofilm layers, the DNR and ANR regulated denitrification apparatus of *P. aeruginosa* is expected to show higher expression. The presence of the nitrite reductase NirS seems to reduce *nbdA* transcription (see chapter 3.1.2). Due to this and the activating

effect of RpoS on *nbdA* expression, accumulation of the NbdA protein in the top layers of the biofilm colonies was hypothesized. In order to confirm this hypothesis, biofilm colonies of PAO1::*nbdA-mNeonGreen::mini-CTX1-mCherry* were grown on tryptone-agar with or without the addition of KNO<sub>3</sub> as alternative electron acceptor for denitrification. Growth of the biofilms was performed either aerobically or anaerobically at 25 °C for 3 or 4 days. To evaluate oxygen levels within an aerobically grown biofilm colony, O<sub>2</sub>-profiles were measured using a microsensor after 3 days of growth (Fig. 3.30).

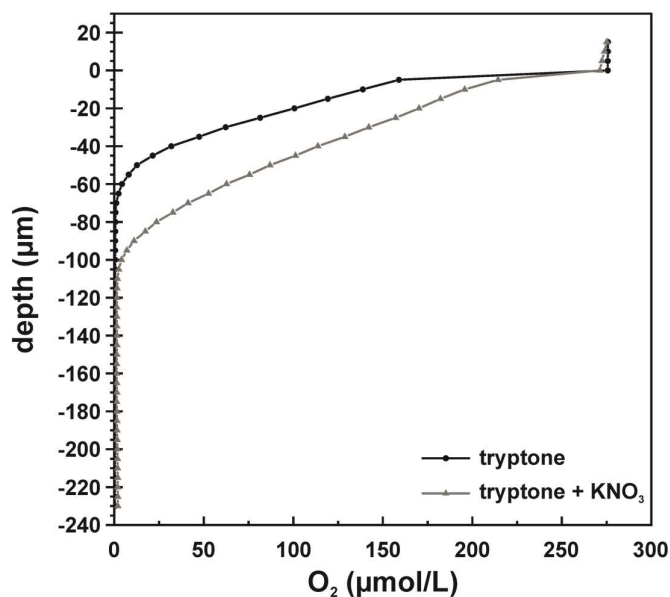


**Fig. 3.30: Oxygen profiles of biofilm colonies grown on tryptone-agar with or without nitrate supplementation**

Biofilm colonies of PAO1::*nbdA-mNeonGreen::mini-CTX1-mCherry* were grown for 3 days on tryptone-agar with or without addition of 40 mM KNO<sub>3</sub>. Oxygen profiles of the biofilm colonies were measured using the O<sub>2</sub> microsensor OX-25 (Unisense). The microsensor was moved in 5 µm steps from the top of the biofilm colony to the bottom and O<sub>2</sub> levels were measured for 3 s at each depth. The experiment was performed with 3 biological replicates each.

Above the biofilm colonies ~275 µmol/L O<sub>2</sub> were detected. The oxygen level distinctly dropped, when the microsensor tip entered the biofilm colony. When grown on tryptone-agar without additional nitrate, oxygen levels within the biofilm colony continuously decreased from the top of the colony to the bottom layers, until a depth of ~70 µm where no more oxygen was present. In comparison, oxygen levels in biofilm colonies grown on tryptone with additional nitrate were higher for each evaluated depth until at a depth of ~110 µm where all present O<sub>2</sub> was consumed.

After 3 and 4 days of aerobic or anaerobic growth, biofilm colonies were prepared for confocal microscopy by thin sectioning. Biomass of the whole biofilm was detected by transmitted light microscopy. Single cells within the biofilm were marked by the red fluorescent, constitutively produced, mCherry which was excited with the 594 nm laser. NbdA-mNeonGreen within the cells was excited with the 488 nm laser line. Emission of both

fluorescent proteins was captured in separate frames and better resolution was achieved using the Zeiss Airyscan mode. Fluorescence of mCherry was lost during the thin sectioning process and therefore no images of the biofilms excited at 594 nm are shown in Fig. 3.31.

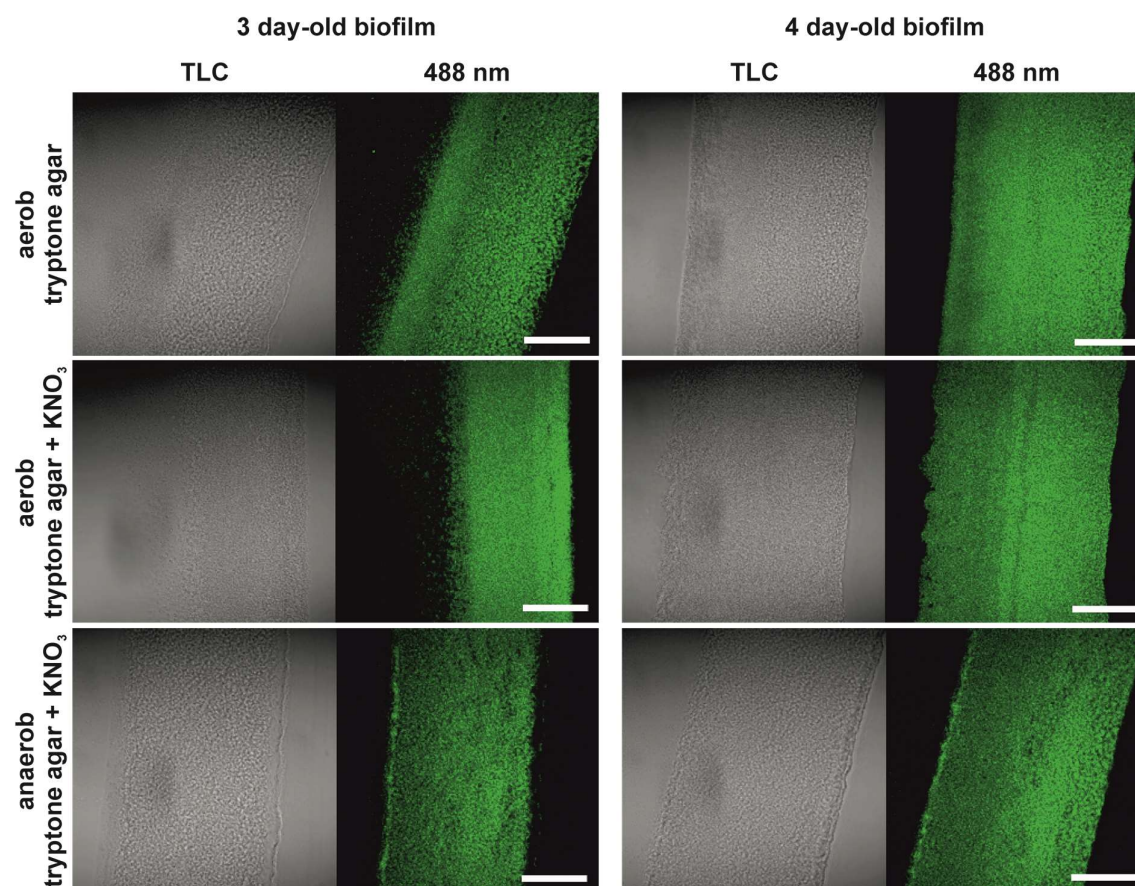


**Fig. 3.31: Distribution of NbdA-mNeonGreen within biofilm colony thin sections**

Biofilm colonies of PAO1::*nbdA-mNeonGreen::mini-CTX1-mCherry* were grown on tryptone-agar with or without addition of 40 mM  $\text{KNO}_3$ . Biofilms were grown either aerobically or anaerobically for for 3 or 4 days. For CLSM thin sections of 10  $\mu\text{m}$  thickness of each biofilm colony were produced. Biomass was detected by transmitted light microscopy. NbdA-mNeonGreen was excited using the 488 nm laser line. Images were taken with the Zeiss LSM 700 using the Airyscan mode. TLC = transmitted light channel. Scale bar = 100  $\mu\text{m}$ .

3 day-old biofilm colonies grew to a height of 150-200 nm, while biofilm colonies after 4 days were thicker and reached a height of ~250 nm. All tested biofilm colonies displayed green fluorescence after excitation with the 488 nm laser line. Compared to aerobically grown biofilms, fluorescence intensity was lower in biofilm colonies grown under anaerobic, denitrifying conditions. These biofilms displayed a thin layer of high fluorescence on top of the colony. When grown on tryptone-agar supplemented with  $\text{KNO}_3$ , intensity of fluorescence appeared to be increased in the bottom layers of the colony. No clear NbdA distribution pattern was observed in this experiment.

## 4 Discussion

In this study, the regulation and function of the phosphodiesterase NbdA was investigated on different levels in order to be able to incorporate it into the complex network of c-di-GMP modulating proteins of *P. aeruginosa* PAO1. Analysis of the transcriptional and post-transcriptional regulation of *nbdA* were performed to identify the conditions under which NbdA is present in the cells. Additionally, phenotypic assays with PAO1 strains overexpressing several variants of NbdA revealed a number of putative functions for NbdA. Further insights into the possible NbdA function were provided by microscopic studies of the cellular NbdA localization.

### 4.1 Transcriptional regulation of *nbdA* in the context of the c-di-GMP network of *P. aeruginosa*

Determination of the transcription initiation site of *nbdA* by 5'-RACE revealed an erroneous annotation of the ORF in the databases. A new promoter region was identified, containing putative binding sites for RpoS and AmrZ. Gene expression of *nbdA* was shown to be activated in stationary growth phase by the alternative sigma-factor RpoS ( $\sigma^S$ ). A further level of regulation is introduced through the repression by the ribbon-helix-helix transcription factor AmrZ. Oxygen limitation, supplementation with nitrite, and endogenous or exogenous nitric oxide did not affect the transcription of *nbdA*. Surprisingly, deletion of the nitrite reductase NirS showed a strong activating effect on *nbdA* transcription, while a strain with an enzymatically inactive NirS ( $\Delta nirF$ ) showed no transcriptional changes.

#### 4.1.1 Expression of *nbdA* is dependent on the alternative sigma-factor RpoS and the transcription factor AmrZ

The sigma-factor RpoS is known as the master regulator of gene expression during stationary growth phase. Furthermore, it is responsible for the activation of genes in response to different stresses, e.g. starvation, heat, oxygen or osmotic stress (Fujita *et al.*, 1994; Jorgensen *et al.*, 1999; Landini *et al.*, 2014). In some proteobacteria, RpoS is additionally involved in regulation of virulence genes, quorum sensing and motility (Dong and Schellhorn, 2010; Guan *et al.*, 2015; Tian *et al.*, 2008; Yildiz and Schoolnik, 1998). In *E. coli*, RpoS has been shown to play an important role in biofilm maturation, architecture and density (Adams and McLean, 1999; Ito *et al.*, 2008; Mika and Hengge, 2014). This link is partly due to the involvement of RpoS in the c-di-GMP regulatory network of *E. coli*. In the *E. coli* K12 strains MC4100 and W3110 a great subset of GGDEF/EAL-domain encoding genes was identified to be under control of RpoS (Sommerfeldt *et al.*, 2009; Weber *et al.*, 2006). Similarly, in *Pseudomonas* sp. several genes related to biofilm formation, maturation and architecture were shown to be regulated by

RpoS (Heydorn *et al.*, 2002; Whiteley *et al.*, 2001). A global analysis of *P. aeruginosa* PA14 revealed that 30 out of 40 genes encoding for c-di-GMP modulating enzymes, are either transcriptionally activated or repressed by RpoS (Tab. 4.1 and references therein). Thus, similar to *E. coli*, RpoS-dependent regulation significantly affects the c-di-GMP network of *P. aeruginosa*. RpoS regulated genes are often subject to further regulatory mechanisms. Activator or repressor proteins might be involved, as well as post-transcriptional regulation. The *psl* operon coding for matrix polysaccharide biosynthesis genes in *P. aeruginosa* is controlled transcriptionally by RpoS and post-transcriptionally by RsmA (Irie *et al.*, 2010). In *P. putida* KT2440 the exopolysaccharide cluster *pea* is activated by RpoS and repressed by AmrZ (Liu *et al.*, 2019). Actually, when we evaluated and compared the data of the PA14 RpoS regulon (Schulz *et al.*, 2015) and the PAO1 AmrZ regulon (Jones *et al.*, 2014) we found 18 out of 40 genes encoding for c-di-GMP modulating enzymes in *P. aeruginosa* presumably regulated by both proteins, RpoS and AmrZ (Tab. 4.1, (Jones *et al.*, 2014; Schulz *et al.*, 2015)).

**Table 4.1: Genes coding for c-di-GMP modulating proteins in PAO1 and PA14 and their association to RpoS or AmrZ regulon. Data extracted from Schulz 2015, and Jones 2014.**

RpoS regulon was analyzed in *P. aeruginosa* PA14 via mRNA profiling of  $\Delta rpoS$  vs. wt (Schulz *et al.*, 2015). AmrZ regulon was measured via RNA-Seq experiments in a PAO1 *amrZ* complementation strain vs.  $\Delta amrZ$  (Jones *et al.*, 2014). GGDEF: diguanylate cyclase domain, EAL: phosphodiesterase domain, GGDEF-EAL: tandem diguanylate cyclase – phosphodiesterase domain, HD-GYP: phosphodiesterase domain. +: activation; -: repression; none: is not part of the indicated regulon.

PAO1 gene locus	PA14 gene locus	name	domain(s)	RpoS regulation	AmrZ regulation
PA0169	PA14_02110	<i>siaD</i>	GGDEF	-	-
PA0285	PA14_03720		GGDEF-EAL	none	-
PA0290	PA14_03790		GGDEF	none	none
PA0338	PA14_04420		GGDEF	-	-
PA0575	PA14_07500	<i>rmcA</i>	GGDEF-EAL	+	none
PA0847	PA14_53310		GGDEF	+	none
PA0861	PA14_53140	<i>rbdA</i>	GGDEF-EAL	+	none
PA1107	PA14_50060	<i>roeA</i>	GGDEF	+	-
PA1120	PA14_49890	<i>tpbB</i>	GGDEF	+	none
PA1181	PA14_49160		GGDEF-EAL	+	+
PA1433	PA14_45930		GGDEF-EAL	+	none
PA1727	PA14_42220	<i>mucR</i>	GGDEF-EAL	+	-
PA1851	PA14_40570		GGDEF	+	none
PA2072	PA14_37690		GGDEF-EAL	+	+
PA2133	PA14_36990		EAL	+	none
PA2200	PA14_36260		EAL	+	none
PA2567	PA14_31330		GGDEF-EAL	none	-
PA2572	PA14_30830		HD-GYP	+	+
PA2870	PA14_26970		GGDEF	+	+
PA3177	PA14_23130		GGDEF	none	+
PA3258	PA14_21870		GGDEF-EAL	none	none
<b>PA3311</b>	<b>PA14_21190</b>	<b><i>nbdA</i></b>	<b>GGDEF-EAL</b>	<b>+</b>	<b>-</b>
PA3343	PA14_20820	<i>hsbD</i>	GGDEF	+	-
PA3702	PA14_16500	<i>wspR</i>	GGDEF	+	+
PA3825	PA14_14530		EAL	+	+
PA3947	PA14_12810	<i>rocR</i>	EAL	+	none
PA4108	PA14_10820		HD-GYP	+	none
PA4332	PA14_56280	<i>sadC</i>	GGDEF	none	-
PA4367	PA14_56790	<i>bifA</i>	GGDEF-EAL	+	-



PA4396	PA14_57140		GGDEF	none	none
PA4601	PA14_60870	<i>morA</i>	GGDEF-EAL	+	-
PA4781	PA14_63210		HD-GYP	+	+
PA4843	PA14_64050	<i>gcbA</i>	GGDEF	none	+
PA4929	PA14_65090		GGDEF	+	-
PA4959	PA14_65540	<i>fimX</i>	GGDEF-EAL	+	+
PA5017	PA14_66320	<i>dipA</i>	GGDEF-EAL	none	-
PA5295	PA14_69900	<i>proE</i>	GGDEF-EAL	+	none
PA5442	PA14_71850		GGDEF-EAL	-	-
PA5487	PA14_72420	<i>dgch</i>	GGDEF	+	none
*	PA14_59790	<i>pvrR</i>	EAL	none	none

\* gene not present in PAO1

The transcriptional regulator AmrZ controls a large regulon containing 398 gene regions in PAO1. Transcription of *amrZ* itself is in a great extent dependent on the alternative sigma-factor AlgT ( $\sigma^{22}$ ) which is known to regulate conversion to mucoidity and stress responses in *P. aeruginosa* (Baynham and Wozniak, 1996; Wozniak et al., 2003). AmrZ was shown to regulate genes important for *P. aeruginosa* virulence, including type IV pili, extracellular polysaccharides, and the flagellum (Jones et al., 2014). It particularly influences genes required for alginate production and twitching-motility (Baynham et al., 1999; Baynham et al., 2006; Jones et al., 2014; Xu et al., 2021). Within the c-di-GMP network of *P. aeruginosa*, AmrZ activates transcription of 14 genes and represses 10 genes encoding GGDEF/EAL-domain proteins ((Jones et al., 2014), Tab. 4.1). With these numbers, AmrZ appears to be one of the major regulators for genes coding for c-di-GMP modulating enzymes in *P. aeruginosa*, possibly affecting the cellular c-di-GMP level. This role for AmrZ was previously also observed in *P. fluorescens* F113, where the cellular c-di-GMP level was affected by AmrZ through the regulation of a complex network of genes encoding DGCs and PDEs (Muriel et al., 2018). From our work we conclude that *nbdA* transcription is repressed by AmrZ during aerobic as well as anaerobic planktonic growth while a condition in which the *nbdA* promoter is de-repressed remains uncertain. Repression through AmrZ is described to be dependent on the C-terminus mediated tetramerization of the protein (Xu et al., 2016a). In some cases, e.g. *pilA* repression, the expression level of AmrZ plays an important role for its function, as binding efficiency of AmrZ to different promoter regions differs (Xu et al., 2021). Additionally, a competition of the activator RpoS and the repressor AmrZ upon binding to the *nbdA* promoter might be possible.

#### 4.1.2 Effects of endogenous or exogenous nitric oxide on *nbdA* expression

In our previous study we observed elevated transcription levels of *nbdA* in cells dispersed from biofilms after NO-treatment when compared to planktonically grown cells in RT-qPCR experiments (Li et al., 2013). Therefore, we suggested transcriptional regulation of *nbdA* by NO in this biofilm model. For *P. aeruginosa* two NO-responsive transcriptional regulators, FhpR and DNR are described. DNR is a heme-containing CRP/FNR type regulator that specifically activates denitrification genes under anaerobic conditions (Arai et al., 1995; Trunk

*et al.*, 2010). Transcription of the second NO responsive regulator in *P. aeruginosa*, FhpR, is  $\sigma^{54}$ -dependent and activates flavohemoglobin expression under aerobic conditions for the detoxification of NO in the cell (Arai *et al.*, 2005; Forrester and Foster, 2012). When analyzing the reannotated *nbdA* gene and promoter region, no similarity with either the FhpR or DNR consensus binding site was detected (Rodionov *et al.*, 2005). Therefore, a direct influence of NO on *nbdA* transcription was unlikely. These findings in addition to the contradictory results in the literature concerning the involvement of NbdA in NO-induced biofilm dispersal of *P. aeruginosa* (Li *et al.*, 2013; Zemke *et al.*, 2020) led to the reevaluation of the transcriptional regulation of *nbdA* by NO. In this study, no direct stimulation of *nbdA* promoter activity by NO, neither by addition of exogenous NO nor by accumulation of intrinsic NO in planktonically grown cells was observed. The previously observed induction of *nbdA* expression in our qRT-PCR experiments (Li *et al.*, 2013) might be due to more complex regulatory processes during biofilm formation and dispersal. From the present data, we conclude that *nbdA* expression in planktonic cells is not directly induced by NO at the transcriptional level.

#### 4.1.3 Effect of the nitrite reductase NirS on *nbdA* promoter activity

In this study, we observed a strong increase in the *nbdA* transcription level when the nitrite reductase NirS was deleted. At first, we assumed that the upregulation of *nbdA* expression might be due to accumulation of intrinsic nitrite from interrupted denitrification. However, addition of nitrite to the growth medium did not change *nbdA* promoter activity. Further, the  $\Delta$ *nirF* strain producing an enzymatically inactive NirS protein (Nicke *et al.*, 2013) did not enhance *nbdA* transcription. Therefore, we suggest that the presence of the periplasmic protein NirS affects *nbdA* transcription independently of its enzymatic activity. The moonlighting role of NirS was previously described for the type III secretion system in *P. aeruginosa* (Van Alst *et al.*, 2009). Additionally, NirS was shown to affect flagellum biogenesis by the formation of a complex with the flagellar subunit FliC and the chaperone DnaK (Barraud *et al.*, 2006; Borrero-de Acuna *et al.*, 2015; Borrero-de Acuna *et al.*, 2017). Suggesting this complex role for NirS besides denitrification in *P. aeruginosa*, the increase of *nbdA* promoter activity in the  $\Delta$ *nirS* strain is probably derived from a global regulatory change in the cell.

All in all, we were able to reannotate the *nbdA* gene and revealed consensus sequences for the alternative sigma-factor RpoS and the transcription factor AmrZ within the *nbdA* promoter region. Our data confirmed RpoS as activator and AmrZ as repressor for *nbdA* transcription, however, no transcriptional regulation by endogenous or exogenous NO or nitrite was observed in planktonically grown cells.

## 4.2 Regulation of *nbdA* translation on the post-transcriptional level

Due to the reannotation of the *nbdA* promoter region, the annotated translational start site of *nbdA* became obsolete. Additional sequence analysis of the *nbdA* gene revealed a putative RBS with the sequence -AGGGAGAC- followed by a 6 bp spacer and an AUG codon, which is commonly used as translational start site in bacteria (Hecht *et al.*, 2017). This newly defined 5'-UTR region was fused, together with 30 bp of the *nbdA* coding sequence, to the reporter gene *bgaB*, encoding the thermostable  $\beta$ -galactosidase of *B. stearothermophilus*. This translational fusion was then utilized for the investigation of translational levels of *nbdA* in *E. coli* and *P. aeruginosa*. Predictions of the secondary structures of the 5'-UTR of *nbdA* by the online tool mFold (Zuker, 2003) highly resembled either a fourU-type RNA thermometer or a structure which is likely bound by the RNA-binding proteins RsmA and RsmF of *P. aeruginosa* (Schulmeyer *et al.*, 2016). These structures strongly indicate regulation of *nbdA* translation on the post-transcriptional level.

### 4.2.1 Does the *nbdA* 5'-UTR form a RNA thermometer?

The first predicted structure of the *nbdA* 5'-UTR (see Fig. 3.6) resembles the fourU-type RNAT which was first discovered in *Salmonella enterica* (Waldminghaus *et al.*, 2007). FourU thermometer structures are characterized by a stretch of four uridines that cover the RBS of an mRNA within a hairpin secondary structure. Increasing temperatures lead to a zipper-like opening of this secondary structure and enable ribosome binding to the mRNA. A mismatch in base pairing next to the uridine stretch, which is also present in the predicted secondary structure of the 5'-UTR of *nbdA*, can further promote this process (Rinnenthal *et al.*, 2011). In bacteria, three gene classes are often under the control of RNATs and thereby regulated on the post-transcriptional level by temperature changes: heat shock genes, cold shock genes and virulence genes (Kortmann and Narberhaus, 2012). Only a few genes of *P. aeruginosa* were shown to be under the control of an RNAT so far. The small heat shock protein IbpA is controlled by a small ROSE-like RNAT and its translation is induced at 42 °C in *P. aeruginosa* and *P. putida* (Krajewski *et al.*, 2013). Additionally, thermoregulation of quorum-sensing dependent virulence factor production has been shown for *P. aeruginosa* (Grosso-Becerra *et al.*, 2014). In fact, the *lasI* gene, encoding for the 3-oxo-dodecanoyl-homoserine lactone producing enzyme LasI, is under the control of a ROSE-like RNAT and translation is induced at 37 °C. This autoinducer activates the transcriptional regulator LasR which then induces the transcription of several virulence factors (Grosso-Becerra *et al.*, 2014; Williams and Cámara, 2009). Furthermore, the operon *rhlABR* is controlled by an RNAT that opens up at 37 °C. This increases rhamnolipid production and the expression of the QS transcriptional regulator RhIR, which controls further virulence genes in *P. aeruginosa* (Grosso-Becerra *et al.*, 2014).

During the host's immune response, NO is released from macrophages to eradicate pathogens (MacMicking *et al.*, 1997). Whilst the immune response, the body temperature of the host often rises above 37 °C when it is developing a fever (Jampel *et al.*, 1983). Therefore, it might be beneficial for *P. aeruginosa* to induce its own defense strategy against the host's immune system with increasing temperatures. *NbdA* transcript would possibly accumulate in the upper layers of biofilm macrocolonies, due to high abundancies of the alternative sigma-factor RpoS which induces *nbdA* transcription (Folsom *et al.*, 2010). Considering the putative role of NbdA in NO-induced biofilm dispersal (Li *et al.*, 2013), NbdA might only be required during active host immune response. Therefore, activation of *nbdA* translation at increased temperatures due to RNAT control could be a way of *P. aeruginosa* to avoid the host's immune response and to prevent NO-induced biofilm dispersal to endogenously produced NO by NbdA under normal growth conditions. Additionally, NbdA was shown to promote virulence of *P. aeruginosa* PA14 (Kulasakara *et al.*, 2006). Although the role of NbdA during infections remains unclear, the PDE might only be required after a switch of the ambient temperature to 37 °C which is present in host organisms like humans or mice. This would strengthen the theory of a temperature-dependent regulation of *nbdA* translation by a fourU-like RNA thermometer. However, no effect of temperature shifts from 30 °C to 37 °C or 42 °C could be observed using the translational reporter gene fusion of the *nbdA* 5'-UTR. Additionally, no changes in the c-di-GMP dependent swimming motility, twitching motility, pellicle formation and biofilm formation could be recognized at 42 °C when comparing the phenotypes of PAO1 wt and  $\Delta nbdA$ . Shifts from 37 °C to lower temperatures, which were shown to be optimal for biofilm formation of *P. aeruginosa* (Kim *et al.*, 2020) also had no influence on the translational level of *nbdA*.

#### 4.2.2 Influence of c-di-GMP or NO on *nbdA* translation

Riboswitches that are able to respond to the second messenger c-di-GMP are widespread in bacteria (Römling *et al.*, 2013), however no c-di-GMP recognizing riboswitch has been demonstrated so far in *P. aeruginosa*. Nevertheless, dependency of *nbdA* translation has been analyzed in an *E. coli* strain lacking the master PDE PdeH and therefore having increased global c-di-GMP levels. The presence of c-di-GMP alone seems not to modulate *nbdA* translation as no significant difference in  $\beta$ -galactosidase activity was detected in the wt background and the  $\Delta pdeH$  strain. Therefore, the 5'-UTR of *nbdA* is most likely no c-di-GMP riboswitch. However, c-di-GMP might induce activity of other proteins of *P. aeruginosa* that could be involved in the regulation of *nbdA* translation. To examine this possibility, translational assays should be repeated in a *P. aeruginosa* strain with artificially elevated intracellular c-di-GMP. Besides c-di-GMP, influence of exogenously added NO on *nbdA* translation was investigated. During translational studies within *P. aeruginosa*, no effect of NO on the

translational level of *nbdA* could be observed. Therefore, NO most likely does not trigger any cellular response that influences *nbdA* on the post-transcriptional level.

#### 4.2.3 Is the *nbdA* translation regulated by RsmA and RsmF?

In the second predicted structure of the 5'-UTR of *nbdA* (see Fig. 3.6), the putative RBS is integrated into a small hairpin structure, presenting the GGA motif of the RBS within the loop. In *P. aeruginosa*, this motif is often recognized by the RNA binding protein RsmA or its homolog RsmF (Schulmeyer *et al.*, 2016) and in *E. coli* the same structure is bound by the protein CsrA (Dubey *et al.*, 2005). Post-transcriptional regulation by RsmA and RsmF has been shown to control the switch between acute and chronic infections of *P. aeruginosa* (Brencic and Lory, 2009; Mulcahy *et al.*, 2008; Romero *et al.*, 2018). Motility and type III secretion, which are required for acute infections, are positively influenced by the Rsm regulatory system (Brencic and Lory, 2009). In contrast, exopolysaccharide production and type VI secretion, which are essential for biofilm formation and chronic virulence, are repressed by direct binding of RsmA and RsmF to the respective mRNA targets (Allsopp *et al.*, 2017; Irie *et al.*, 2020; Irie *et al.*, 2010; Romero *et al.*, 2018). In addition to their direct targets, RsmA and RsmF influence many pathways indirectly by modulating the abundancies of other global regulators. For example, translation of the transcription factor AmrZ is directly repressed by RsmA (Gebhardt *et al.*, 2020). In *P. aeruginosa*, AmrZ acts as a transcriptional regulator of all three type VI secretion system (T6SS) gene clusters by activating the clusters H1 and H3-T6SS and repressing the H2-T6SS cluster (Allsopp *et al.*, 2017). Therefore, direct repression of the *amrZ* translation by RsmA has an indirect effect on the translation of the T6SS gene clusters. However, many mRNAs of T6SS genes are additionally direct targets of RsmA (Allsopp *et al.*, 2017). In several bacteria, CsrA or homologs are described to influence the intracellular c-di-GMP level by direct or indirect regulation of DGC or PDE domain containing proteins. CsrA was shown to directly bind to and change the mRNA levels of the DGCs YcdT and YdeH in *E. coli* (Jonas *et al.*, 2008). Furthermore, regulation of five more c-di-GMP modulating DGCs and PDEs by CsrA was demonstrated in this study. A similar picture was shown for CsrA in *S. typhimurium* where it controls the expression of five DGCs and PDEs directly and three others indirectly (Jonas *et al.*, 2010). The diguanylate cyclase CfcR which is able to influence the global c-di-GMP level of *P. putida* KT2440 is regulated by the three CsrA homologs RsmA, RsmE and RsmI on two levels. Translation of *cfcR* is repressed directly by binding of the Rsm proteins to the mRNA and *cfcR* transcription is influenced indirectly by modulation of RpoS by the Rsm regulatory pathway (Huertas-Rosales *et al.*, 2017).

For *P. aeruginosa* no specific analysis of the regulatory effect of the Rsm system on c-di-GMP modulating proteins exist. However, it is known that the c-di-GMP dependent switch between the motile and the sessile lifestyle of *P. aeruginosa* and the switch between acute and chronic infections are linked on several levels (Coggan and Wolfgang, 2012). Therefore, a

post-transcriptional regulation of the PDE NbdA would make sense. Unfortunately, all global studies for the identification of direct RsmA and RsmF mRNA targets in *P. aeruginosa* were performed in the exponential growth phase so far (Chihara *et al.*, 2021; Gebhardt *et al.*, 2020; Romero *et al.*, 2018). As *nbdA* expression is induced in the stationary growth phase by RpoS, these studies would be unable to identify *nbdA* as a target for Rsm regulation. Analysis of *nbdA* translation utilizing the translational fusion of the *nbdA* 5'-UTR to the reporter gene *bgaB* in PAO1 wt compared to  $\Delta rsmA$  and  $\Delta rsmA \Delta rsmF$  did not reveal a strong regulation by the Rsm proteins. Translation levels in the *rsmA* deletion mutant were slightly elevated in comparison to the wt. However, production of the BgaB protein was not detectable on the Western Blot. Therefore, regulation of *nbdA* translation by RsmA and RsmF has to be further verified using another reporter system or analysis method like a translational fusion to a reporter gene encoding a strongly fluorescent protein. Additionally it has to be considered that translation rates of membrane proteins are relatively low, compared to cytosolic proteins (Wagner *et al.*, 2006) which might be the reason why NbdA translation has to be analyzed with a more sensitive method.

### 4.3 Overexpression of *nbdA* leads to various phenotypical changes

In order to gain further insights into the role of NbdA within *P. aeruginosa* PAO1, six different variants of NbdA were overproduced in a *nbdA* mutant strain and several c-di-GMP dependent phenotypes were analyzed (Tab. 4.2). Previous work of Martina Ruger revealed that deletion of *nbdA* did not affect the global c-di-GMP level of PAO1. In contrast, overexpression of the full length *nbdA* in PAO1  $\Delta nbdA$  drastically reduced the global c-di-GMP level compared to the vector control, confirming PDE activity of NbdA (Ruger, 2019). However, not all observed phenotypes for the *nbdA* overexpression strain fit to the expectations for a PDE overexpression in *P. aeruginosa*. Thinking in terms of c-di-GMP regulations, cells with low intracellular concentrations of c-di-GMP would be expected to show no or decreased biofilm formation and an increase in motility (Kulasakara *et al.*, 2006; Valentini and Filloux, 2016). Formation of a pellicle at the air-liquid interface is one of the major biofilm types *P. aeruginosa* is capable of (Friedman and Kolter, 2004). Pellicle formation requires the polysaccharide pel, whose production is stimulated by high c-di-GMP levels that are sensed through PelD (Lee *et al.*, 2007). In accordance to that, reduction of the intracellular c-di-GMP level by the overproduction of the active full-length NbdA leads to a strain incapable of pellicle formation. Overproduction of the cytosolic domains AGDEF-EAL should inhibit pellicle formation likewise. However, this strain produces an even thicker pellicle with wrinkly structure. It is noteworthy, that the PAO1  $\Delta nbdA$  strain overexpressing the cytosolic domains without the Strep-tag does not form a pellicle (data not shown). This might indicate an inhibition of the PDE function by the C-terminal

Strep-tag in this NbdA variant. In accordance to the c-di-GMP dependency of pellicle formation in *P. aeruginosa*, strains overproducing NbdA variants without or with inactive PDE domain were capable of pellicle formation. Overproduction of the inactive cytosolic AGDEF-AAL domains again led to the formation of a robust, wrinkly pellicle.

**Table 4.2: Summarized phenotypes of PAO1  $\Delta nbdA$  overproducing different NbdA variants**

Data were combined from this work and results of M. Ruger and J. Rehner (Rehner, 2020; Ruger, 2019). NbdA domains are colored as follows: membrane anchored MHYT domain = black, DGC-domain (AGDEF) = green, active PDE-domain (EAL) = red, inactive PDE-domain (AAL) = pale red. (↓) = statistically significant reduction, (↑) = statistically significant increase, (w) = wrinkly morphology in LB medium.

	Vector control	MHYT-AGDEF-EAL	MHYT-AGDEF-AAL	AGDEF-EAL	AGDEF-AAL	MHYT-AGDEF	MHYT
cell length	~ 2 nm	elongated	elongated	~ 2 nm	~ 2 nm	elongated	elongated
swimming	100 %	82 % (↓)	40 % (↓)	89 %	93 %	10 % (↓)	68 % (↓)
twitching	yes	no	no	reduced	yes	no	no
adhesion	100 %	19 % (↓)	55 % (↓)	62 % (↓)	66 % (↓)	157 % (↑)	182 % (↑)
pellicle formation	yes	no	yes	yes (w)	yes (w)	yes	yes
growth on solid agar	yes	no	no	yes	yes	no	no

In general, rising intracellular c-di-GMP levels promote formation of biofilms. As attachment to surfaces is the initial step of biofilm formation, PAO1  $\Delta nbdA$  strains overproducing NbdA variants were tested for adherence of cells to the polystyrene surface of a 96-well plate after 1 h of incubation. For the strain overexpressing the full length *nbdA* with active PDE domain, a strong decrease in adhesion was observed which is most likely based on the low global c-di-GMP concentration. In relation to the vector control, inactivation of the PDE domain of NbdA still decreased adhesion efficiency by 45 %, indicating an additional effect of the *nbdA* overexpression besides the PDE activity. Overproduction of the cytosolic domains of NbdA also reduced adhesion, independent of the PDE-domain functionality. Interestingly, in this case the overexpression of Strep-tagged and untagged variants again differ from each other. While the strain overproducing the inactive, untagged cytosolic domains of NbdA showed attachment levels similar to the vector control, the strain overproducing the active, untagged variant showed adhesion similar to the overexpression strain of the full length *nbdA* (data not shown). This indicates either that the untagged protein variants are not produced in the tested strains

or an effect of the Strep-tag on the activity of the produced NbdA. Interestingly, overproduction of the MHYT domain alone or MHYT-AGDEF led to a significant increase in adhesion compared to the vector control which needs to be further characterized.

In contrast to the biofilm phenotypes which can be explained by the PDE activity of NbdA, swimming motility seems to be affected independently of the c-di-GMP level in the cells. For the overproduction of a PDE which results in low global c-di-GMP concentration, an increase of *P. aeruginosa* motility would be expected (Kulasakara *et al.*, 2006; Valentini and Filloux, 2016). However, overproduction of the active full-length or cytosolic variants of NbdA led to only a slight decrease of swimming motility. In general, all strains overproducing a variant of NbdA showed decreased swimming motility compared to the vector control. This effect was the strongest for the MHYT-AGDEF-AAL and the MHYT-AGDEF overproduction with a reduction of swimming motility of 60 % and 90 %, respectively. This observation might indicate a DGC activity of the AGDEF domain of NbdA. As the strain overproducing the cytosolic AGDEF-AAL domains shows swimming motility comparable to the vector control, DGC activity of NbdA might require the presence of the MHYT domain and inactivity or absence of the PDE domain.

Growth on solid agar plates and movement on solid surfaces via twitching motility were correlated in all tested overexpression strains. When the overproduced NbdA variant included the MHYT domain, cells lost ability to twitch and to grow on LB-agar. Additionally, cell morphology was altered in these strains, as some cells were elongated up to 7.5-fold after induction compared to the vector control strain. This effect is most likely caused by the integration of too many copies of the MHYT domain of NbdA into the inner membrane of *P. aeruginosa* which alters the native membrane equilibrium. In *E. coli* cells overproducing membrane anchored proteins (e.g. *yidC*, *yedZ* and *lepl*), a reduction of native membrane proteins and protein complexes was observed (Wagner *et al.*, 2007). Assuming similar consequences caused by an overproduction of the MHYT domain in *P. aeruginosa*, surface-sensing via membrane proteins and assembly of type IV-pili might be altered, impairing surface attached growth and twitching motility. Additionally, distinct elongation of cells overproducing membrane proteins was also observed in *E. coli* (Gubellini *et al.*, 2011; Wagner *et al.*, 2007). This phenomenon was speculated to be caused by either altered cell division (Wagner *et al.*, 2007) or a blockage of the entry into stationary growth phase (Gubellini *et al.*, 2011) during overexpression. Similar effects might be true for *P. aeruginosa* cells overexpressing the membrane protein encoding *nbdA*. Therefore, it is unclear if the observed phenotypic changes of the strains overproducing NbdA variants that contain the membrane anchored MHYT domain are really based on NbdA function or caused by an altered membrane protein equilibrium. Nevertheless, it should be kept in mind that the putative sensory MHYT domain might be crucial for correct NbdA function and therefore production of only the cytosolic NbdA



domains can distort the observation. A putative blockage of the transcriptional program of the stationary growth phase during overexpression experiments (Gubellini *et al.*, 2011) might additionally prevent the formation of important NbdA interaction partners that could influence NbdA function.

#### 4.4 Localization studies reveal polar localization of NbdA

As described previously, the PDE activity of NbdA does not influence the global c-di-GMP level in *P. aeruginosa* (Kulasakara *et al.*, 2006; Ruger, 2019), indicating that NbdA rather influences a local c-di-GMP pool in the cell. In order to support this hypothesis, localization studies with fluorescently tagged NbdA were performed in *P. aeruginosa* PAO1. As the regulation of *nbdA* translation remained unclear so far, not only genomic integrations of *nbdA-mNeonGreen* and *-Venus* into the native *nbdA* locus were generated, but also plasmid driven variants were used for these studies. Both, the plasmid encoded and the genomically encoded NbdA-mNeonGreen and NbdA-Venus were detectable during confocal microscopy and revealed comparable NbdA localization. In approximately 50 % of the analyzed cells, fluorescence was distributed through the whole cell. However, when expressed from the inducible promoter on the plasmid pME6032, it became more visible that NbdA is localized in the cell membrane. In the other half of the analyzed cells, NbdA formed distinct fluorescent foci in the membrane, which were mainly localized at one or both cell poles. This distribution pattern of NbdA was observed for both the genomically integrated variants during stationary growth phase and the plasmid driven variants in exponential phase. Therefore, polar localization of NbdA seems to be independent of protein interaction partners that are only present in stationary phase. Co-localization studies with the polar flagellum or the chemotaxis protein CheA, which localizes to the flagellated cell pole of *P. aeruginosa* (Kulasekara *et al.*, 2013), were performed in order to identify the cell pole, where NbdA is mainly localized to. Regarding the observations from the co-localization studies with the fluorescently labeled flagellum or the CheA-mCerulean fusion, NbdA localizes with approximately equal frequency to the flagellated and the opposite cell pole. However, in co-localization studies with CheA-tdTomato, NbdA appeared to often co-localize with CheA. The discrepancy of results during co-localization studies of NbdA-mNeonGreen and either CheA-mCerulean or CheA-tdTomato indicates a crosstalk between the fluorescent proteins in one of the cases. The excitation spectrum of tdTomato is very broad, ranging from ~425 nm to ~590 nm with the excitation maximum at 554 nm (Shaner *et al.*, 2004). Therefore, the excitation laser wavelength 488 nm, used for mNeonGreen, as well as the emitted wavelengths of mNeonGreen from ~490 nm to ~590 nm (Shaner *et al.*, 2013) would be able to excite tdTomato (see appendix). For this reason, co-localization between NbdA-mNeonGreen and CheA-tdTomato is most likely incorrect and the results of the co-localization assay with CheA-mCerulean is more reasonable.

Xin *et al.* demonstrated that the PDEs DipA, RbdA and NbdA are involved in chemotaxis mediated flagellar motor switching by degrading c-di-GMP, sensed by MapZ (Xin *et al.*, 2019). In contrast to NbdA, the PDE DipA was demonstrated to interact with the chemotaxis protein CheA and therefore be located at the flagellated cell pole (Kulasekara *et al.*, 2013). In this work, it was shown, that NbdA does not co-localize with CheA, but is at least occasionally located at the same cell pole. However, MapZ has been shown to locate to both cell poles of *P. aeruginosa* (Xu *et al.*, 2016b) and therefore an interaction with the c-di-GMP pool controlled by the polar localized NbdA would be possible. This study demonstrates, that NbdA is not localized at the flagellated cell pole, in contrast the observed cellular distribution pattern of NbdA resembles the distribution of type IV pili of *P. aeruginosa* cells during surface contact (Tab. 4.3; (Cowles and Gitai, 2010)).

**Table 4.3: Comparison of cellular location of NbdA and type IV pili**

NbdA localization was studied by CLSM on agarose pads with PAO1::*nbdA-mNeonGreen* and PAO1::*nbdA-Venus* in stationary growth phase. Type IV pili distribution was analyzed by transmission electron microscopy of PAO1 cells grown on agar plates (Cowles and Gitai, 2010).

<b>NbdA distribution</b>	<b>NbdA-mNeonGreen</b>	<b>NbdA-Venus</b>	<b>type IV pili</b>	<b>type IV pili distribution</b>
diffuse fluorescence	50 %	36 %	38 %	not piliated
unipolar	32 %	38 %	41 %	unipolar
bipolar	8 %	13 %	15 %	bipolar
nonpolar	10 %	13 %	7 %	nonpolar

Localization of the type IV pili of *P. aeruginosa* is mediated by the polar hub protein FimV (Wehbi *et al.*, 2011) which is also known to polarly localize the DGC PA14\_72420 (GgcP) of *P. aeruginosa* PA14 by interacting with its GGDEF domain (Nicastro *et al.*, 2020). In *Shewanella putrefaciens*, the dual domain PDE PdeB localizes to the cell pole by a similar interaction of the polar landmark protein HubP, a homolog of FimV, with the proteins GGDEF domain (Rossmann *et al.*, 2019). The group of Kai Thormann, identified an amino acid motif within the GGDEF domain of PdeB which is required for the polar localization (unpublished data). Analysis of the DGC domain of NbdA revealed a similar motif, indicating a putative function of FimV for the cellular localization of NbdA (personal communication with Kai Thormann, Justus-Liebig-University of Gießen). Cloning of allelic exchange vectors (pEXG2-variants), containing site-directed mutagenesis variants of the respective amino acid motif at the positions 392 and 393 (based on the new *nbdA* annotation) was already performed during this work (Tab. 2.2). However, localization studies with fluorescently tagged NbdA variants Q392S/K393E and Q392E/K393S still have to be done. Another approach to analyze FimV-dependent localization of NbdA, would be to delete *fimV* in PAO1::*nbdA-mNeonGreen*

or *-Venus* and examine the cellular localization of NbdA in the  $\Delta fimV$  background. However, this approach only shows whether NbdA localization requires FimV but is not suitable to prove if FimV directly interacts with NbdA in order to provide its polar localization. If NbdA localization is lost in the  $\Delta fimV$  background, it might also be due to interaction of NbdA with another polar protein which is directly localized by FimV. Possible candidates might be the DGC SadC or the PDE DipA. SadC was described to interact with the NbdA homolog of *P. fluorescens* (Dahlstrom *et al.*, 2018) and interaction of both proteins with the PAO1 NbdA in bacterial two hybrid assays could be shown in our group (Beganovic, 2018; Schultheiß, 2020). Both proteins possess a GGDEF domain which might be required for FimV interaction and are described to either localize at the cell pole of *P. aeruginosa* (DipA (Kulasekara *et al.*, 2013)) or to directly interact with the motor stator protein MotC at the polar flagellum (SadC (Baker *et al.*, 2019)).

## 4.5 Putative function of the phosphodiesterase NbdA and outlook

Considering the published data concerning NbdA and combining these information with the findings of our working group, we might need to rethink our current working hypothesis. NbdA was postulated to be involved in NO-induced biofilm dispersal by degrading c-di-GMP upon stimulation of the PDE domain by the diatomic gas NO, sensed by the MHYT domain, and binding of GTP to the non-functional DGC domain (Cutruzzola and Frankenberg-Dinkel, 2016; Li *et al.*, 2013). In contrast, NO-induced biofilm dispersal was still observed for the newly generated, markerless *nbdA* deletion mutant in our group (Rüger, 2019) and for the *nbdA* mutant in the work of Zemke *et al.* (Zemke *et al.*, 2020), however the experimental conditions differed in all three studies. The intracellular c-di-GMP concentration of *P. aeruginosa* PAO1 overexpressing *nbdA* was significantly decreased compared to the vector control, indicating PDE activity of NbdA without NO as a signal (Rüger, 2019). *In vivo* PDE activity of NbdA was additionally shown in *E. coli* assays where heterologously expressed *nbdA* was able to complement the swimming defect caused by the deletion of the master PDE *pdeH* (Rüger, 2019). Xin *et al.* observed inactivation of c-di-GMP dependent flagellar motor switching for both, an *nbdA* deletion mutant and a PAO1 strain expressing an NbdA variant with inactive PDE domain (Xin *et al.*, 2019). Therefore, NbdA seems to be some kind of “always-on” PDE. It might also be possible, that the required signal for PDE activity is oxygen, as all these assays were performed under aerobic conditions and the MHYT domain of NbdA was predicted to sense either NO, CO or O<sub>2</sub> (Galperin *et al.*, 2001). In contrast to the current hypothesis, sensing of a, yet to be identified, signal might inactivate the PDE domain of NbdA and thereby lead to an increase of c-di-GMP in a local pool at the cell pole of *P. aeruginosa*. Under these conditions, the PilZ protein MapZ would bind c-di-GMP and inhibit methylation of several MCPs by interacting with the chemotaxis protein CheR1 (Sheng *et al.*, 2019; Xin *et al.*, 2019). This

eventually inhibits flagellar motor switching from CCW to CW or vice versa and therefore changes the usual “run-reverse-turn” swimming pattern of *P. aeruginosa* into a straight “run” swimming motility (Xin *et al.*, 2019). Interruption of this chemotactic pathway by deletion of *mapZ* leads to impaired virulence of *P. aeruginosa* PAO1 in *C. elegans* and mouse infection studies (Sheng *et al.*, 2019). Interestingly, NbdA was also shown to be involved in virulence of *P. aeruginosa* PA14 in mouse infection models (Kulasakara *et al.*, 2006). This might indicate, that the c-di-GMP mediated chemotactic response of impaired flagellar motor switching and effective virulence of *P. aeruginosa* are connected. Correlation of virulence and flagellar motor switching was already demonstrated for *Salmonella typhimurium* and *S. enterica*. Chemotaxis mutants of *S. typhimurium* with straight swimming motility instead of the regular “run and tumble” swimming pattern were shown to invade tissue cells more efficiently (Jones *et al.*, 1992). Likewise, *S. enterica* cells with “run” swimming pattern, due to inactivation of flagellar motor switches, were able to infect host macrophages more efficiently (Achouri *et al.*, 2015). A similar role of the chemotactic stimulation of the “run” swimming pattern of *P. aeruginosa* is possible and would be an explanation for the published involvement of NbdA in virulence. It is also noteworthy, that the identified interaction partners of NbdA, DipA and SadC, both regulate virulence of PA14 to the same extent as NbdA (Kulasakara *et al.*, 2006). Additionally, DipA was demonstrated to regulate flagellar motor switching in PAO1 (Xin *et al.*, 2019). Taken together, NbdA might sense a specific signal during infection that leads to inactivation of the PDE domain, putatively by a conformational change of the protein, causing increasing c-di-GMP concentrations within a specific intracellular c-di-GMP pool. Elevated c-di-GMP levels then might stimulate the MapZ mediated inactivation of flagellar motor switching which eventually enhances virulence of *P. aeruginosa* (Fig. 4.1).

Either CO or NO could be promising candidates as signal for the inactivation of the NbdA PDE domain. According to the predictions of Galperin, the MHYT domain of NbdA might be able to sense both of the diatomic gases (Galperin *et al.*, 2001) which are released within the host’s immune response during a bacterial infection. On the one hand, recognition of pathogens stimulates the activity of NO-synthases in the host’s macrophages (MacMicking *et al.*, 1997). On the other hand, the stress responsive heme oxygenase-1 (HO-1) is upregulated in macrophages upon infection and generates CO by degrading heme (Wegiel *et al.*, 2014). Sensing of these signals by NbdA might be part of a defense strategy of *P. aeruginosa* against the host’s immune response. Increasing c-di-GMP levels due to NbdA inactivation might enable more efficient targeting and infection of macrophages and additionally might stimulate the biosynthesis of type IV pili, which are also involved in effective virulence of *P. aeruginosa* (Burrows, 2012; Jain *et al.*, 2017; Persat *et al.*, 2015).

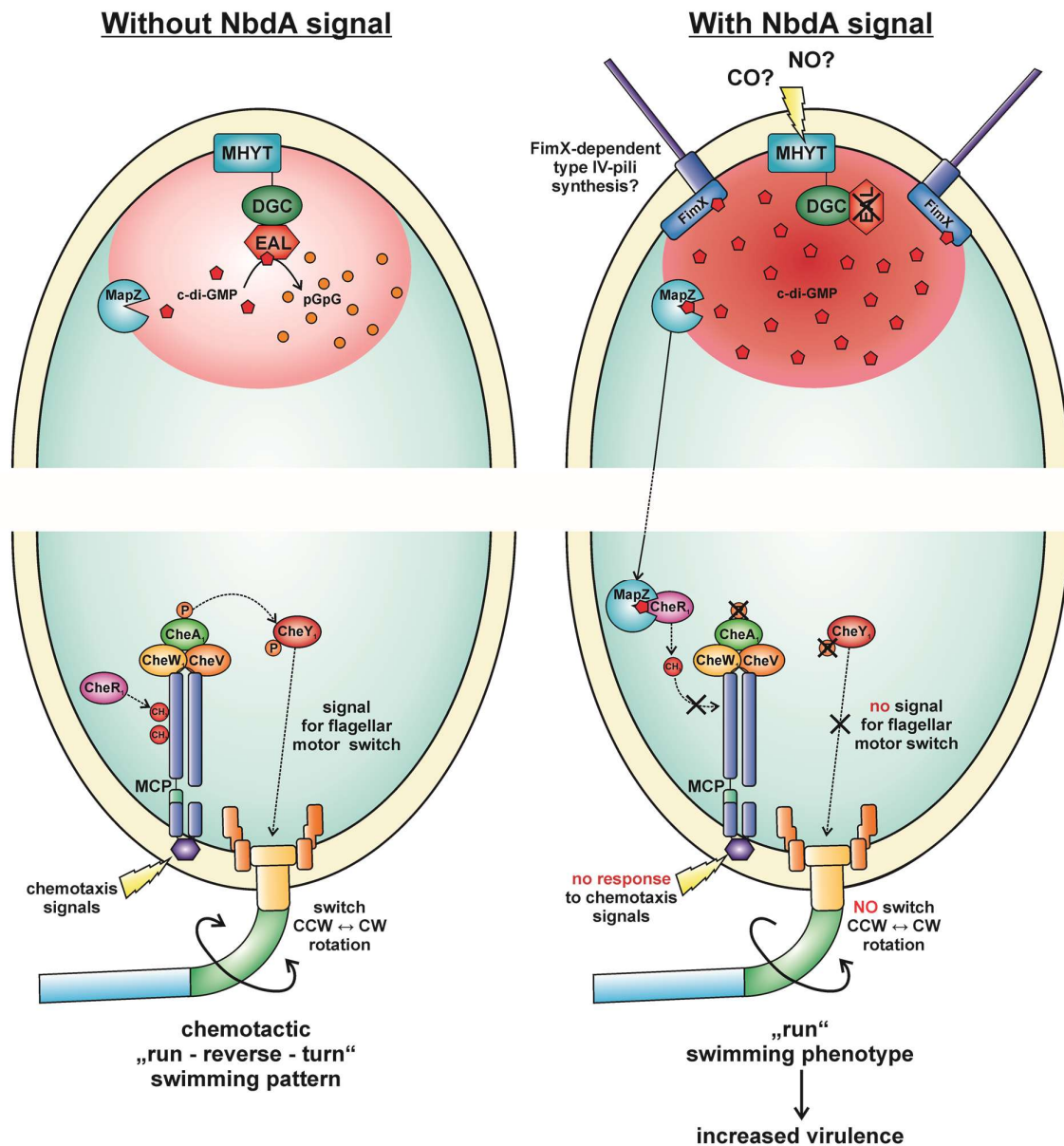


**Fig. 4.1: Putative role of NbdA within chemotaxis-dependent flagellar motor switching**

In its ground state NbdA has PDE activity and degrades c-di-GMP (red polygons) of a local pool into pGpG (orange spheres). Thereby, the c-di-GMP level remains low and MapZ does not bind the second messenger. CheR<sub>1</sub> transfers methyl groups to MCPs of the chemotactic Che pathway. This enables the MCPs to respond to chemotactic signals and eventually leads to phosphorylation of CheY<sub>1</sub> which then induces flagellar motor switching and therefore results in the "run-reverse-turn" swimming pattern of *P. aeruginosa*. Recognition of an unknown signal, putatively NO or CO released by the hosts macrophages, might lead to a conformational change of NbdA and thereby inhibits its PDE activity. Due to increasing levels, MapZ might be able to bind c-di-GMP and interact with CheR<sub>1</sub> which prevents methylation of the MCPs and therefore response to further chemotactic signals. CheY<sub>1</sub> no longer gets phosphorylated and there is no switching in the direction of flagellar rotation. This induces the "run" swimming phenotype of *P. aeruginosa* and might also increase virulence. Regarding the cellular localization of NbdA, an additional increase in FimX-dependent type IV-pili synthesis might be induced by the increasing levels of c-di-GMP.

In future work the steady PDE activity of NbdA within *P. aeruginosa* has to be considered and tested further. As NbdA does not influence the global c-di-GMP concentration in the cell (Kulasakara *et al.*, 2006; Ruger, 2019) but rather regulates a local c-di-GMP pool, indicated by

---

the protein's localization, global measurements of the second messenger should be avoided. Instead, *in vivo* changes of intracellular c-di-GMP pools should be tracked microscopically utilizing a fluorescent c-di-GMP reporter (Christen *et al.*, 2010; Weiss *et al.*, 2019). This method can then be used to investigate the influence of putative signal molecules like NO or CO on the PDE activity of NbdA. Additionally, examination of flagellar motor switching and virulence of PAO1 cells expressing NbdA variants with mutated sensory domain might clarify the role of the MHYT domain of NbdA. Furthermore, FimV dependency of NbdA should be analyzed by deleting either the DGC domain of fluorescently tagged NbdA or deleting *fimV*. If the formation of fluorescent foci is absent in these strains, mutagenesis of the putative FimV interaction motif QK within the DGC domain (personal communication with Kai Thormann, Giessen) could prove whether NbdA localization is directly dependent on FimV or rather mediated by an interaction partner of NbdA. Due to the similar cellular localization pattern of NbdA and the type IV pili (Cowles and Gitai, 2010), co-localization studies using fluorescently labeled pilin antibodies should be considered in order to gain further insights in putative novel functions of NbdA. Additionally, the effect of NbdA interaction with the DGC SadC and the PDE DipA should be characterized further. It might be possible that interaction with a DGC-domain containing protein is able to activate DGC activity of NbdA by dimerization.

## 5 Summary

Like many other bacteria, the opportunistic pathogen *P. aeruginosa* encodes a broad network of enzymes that regulate the intracellular concentration of the second messenger c-di-GMP. One of these enzymes is the phosphodiesterase NbdA that consists of three domains: a membrane anchored, putative sensory MHYT domain, a non-functional diguanylate cyclase domain with degenerated GGDEF motif and an active PDE domain with EAL motif.

Analysis of the *nbdA* open reading frame by 5'-RACE PCR revealed an erroneous annotation of *nbdA* in the Pseudomonas database with the ORF 170 bp shorter than previously predicted. The newly defined promoter region of *nbdA* contains recognition sites for the alternative sigma-factor RpoS as well as the transcription factor AmrZ. Promoter analysis within PAO1 wt as well as *rpoS* and *amrZ* mutant strains utilizing transcriptional fusions of the *nbdA* promoter to the reporter gene *lacZ* revealed transcriptional activation of *nbdA* by RpoS in stationary growth phase and transcriptional repression by AmrZ. Additionally, no influence of nitrite and neither exogenous nor endogenous NO on *nbdA* transcription could be shown in this study. However, deletion of the nitrite reductase gene *nirS* led to a strong increase of *nbdA* promoter activity which needs to be characterized further.

Predicted secondary structures of the 5'-UTR of the *nbdA* mRNA indicated either an RNA thermometer function of the mRNA or post-transcriptional regulation of *nbdA* by the RNA binding proteins RsmA and RsmF. Nevertheless, translational studies using fusions of the 5'-UTR of *nbdA* to the reporter gene *bgaB* did not verify either of these hypotheses. In general, *nbdA* translational levels were very low and neither the production of the reporter BgaB nor genomically encoded NbdA could be detected on a western blot. Overproduction of NbdA variants induced many phenotypic changes in motility and biofilm formation. But strains overproducing variants containing the MHYT domain revealed greatly elongated cells and were impaired in surface growth, indicating a misbalance in the membrane protein homeostasis. Therefore, these phenotypes have to be interpreted very critically.

Microscopic studies with fluorescently tagged NbdA revealed either a diffuse fluorescent signal of NbdA or the formation of fluorescent foci which were located mainly at the cell poles. Co-localization studies with the polar flagellum and the chemotaxis protein CheA showed that NbdA is not generally localizing to the flagellated cell pole. NbdA localization indicates the control of a specific local c-di-GMP pool in the cell which is most likely involved in MapZ mediated chemotactic flagellar motor switching.

## 6 Zusammenfassung

Wie viele andere Bakterien, verfügt auch das opportunistische Pathogen *Pseudomonas aeruginosa* über ein großes Netzwerk an Enzymen die die intrazelluläre Konzentration des sekundären Botenstoffes c-di-GMP regulieren. Eines dieser 40 Enzyme ist die Phosphodiesterase NbdA welche aus drei Domänen besteht: Einer Membran verankerten, putativen MHYT Sensordomäne, einer nicht funktionellen Diguanylatzyklase Domäne mit degeneriertem GGDEF Motiv und einer aktiven PDE Domäne mit EAL Motiv.

Eine 5'-RACE PCR Analyse des offenen Leserahmens von *nbdA* ergab eine fehlerhafte Annotation von *nbdA* in der *Pseudomonas* Datenbank. Der neu bestimmte Promotor des um 170 bp kürzeren Leserahmens enthält Bindestellen für den alternativen Sigmafaktor RpoS sowie den Transkriptionsfaktor AmrZ. Mittels transkriptioneller Fusionen konnte gezeigt werden, dass die Transkription von *nbdA* in der stationären Wachstumsphase durch RpoS aktiviert wird und *nbdA* generell von AmrZ reprimiert wird. Ein Einfluss von Nitrit sowie endogenem oder exogenem NO konnte nicht gezeigt werden, jedoch führte die Deletion der Nitritreduktase NirS zu einem deutlichen Anstieg der *nbdA* Promotoraktivität, welcher noch näher untersucht werden muss.

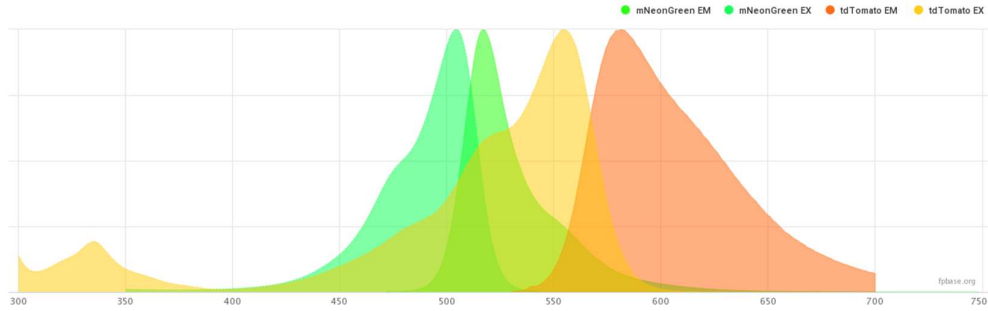
Vorhersagen der Sekundärstruktur der 5'-UTR der *nbdA* mRNA deuten entweder eine Funktion als RNA Thermometer oder eine post-transkriptionelle Regulation von *nbdA* durch die RNA-bindenden Proteine RsmA und RsmF an. Keine der beiden Hypothesen ließ sich in Analysen mit translationalen Fusionen der *nbdA* 5'-UTR an ein Reporter gen bestätigen. Generell war das Translationslevel von *nbdA* sehr niedrig und weder die Bildung des Reporters BgaB noch genomisch codiertes NbdA waren mittels Western Blot nachweisbar. Eine Überproduktion verschiedener NbdA Varianten induzierte phänotypische Veränderungen der Motilität sowie Biofilmbildung. Allerdings zeigten Zellen, welche die MHYT Domäne überproduzieren auch eine stark verlängerte Zellmorphologie und eine Beeinträchtigung im Wachstum auf Oberflächen. Dies deutet auf eine Störung der Membranproteinhomöostase hin und macht deutlich, dass die Ergebnisse der Überexpressionsanalysen nur mit Vorsicht zu interpretieren sind.

Mikroskopische Untersuchungen mit Fluoreszenztag tragendem NbdA zeigten entweder eine diffuse Fluoreszenz von NbdA oder die Bildung fluoreszenter Foki, die überwiegend an den Zellpolen lokalisiert sind. Kolokalisationsstudien mit der polaren Flagelle und dem Chemotaxis Protein CheA zeigten, dass sich NbdA nicht generell am flagellierten Zellpol befindet. Die Lokalisation von NbdA deutet darauf hin, dass die PDE nur einen lokalen c-di-GMP Pool in der Zelle reguliert, welcher wahrscheinlich am MapZ vermittelten Flagellen-Motor Richtungswechsel beteiligt ist.

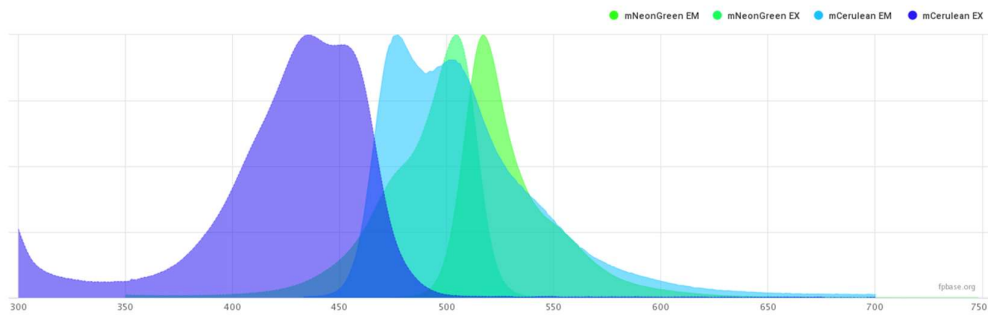


# Appendix

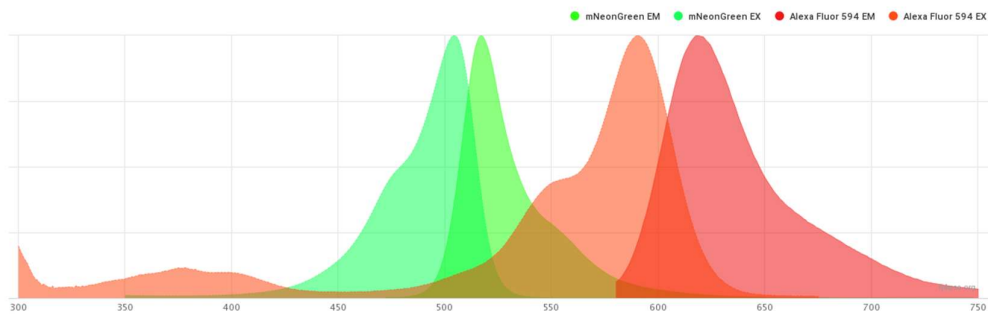
Excitation and emission spectra of mNeonGreen and tdTomato (generated with fpbase.org)



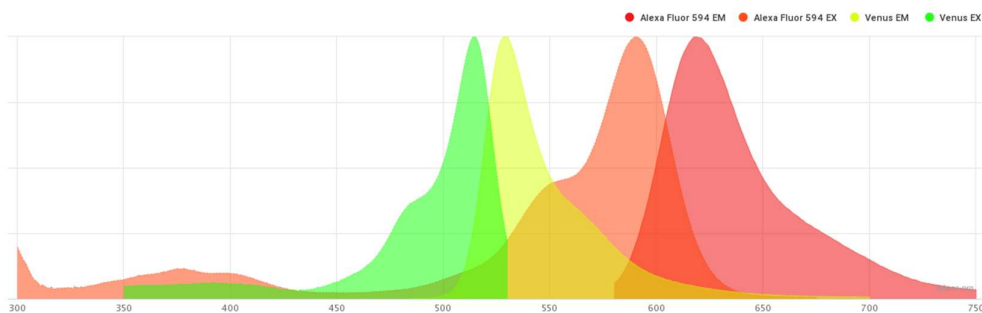
Excitation and emission spectra of mNeonGreen and mCerulean (generated with fpbase.org)



Excitation and emission spectra of mNeonGreen and Alexa Fluor™ 594 (generated with fpbase.org)



Excitation and emission spectra of Venus and Alexa Fluor™ 594 (generated with fpbase.org)



---

## References

- Aaij, C. and Borst, P.** (1972) "The gel electrophoresis of DNA." *Biochimica Biophysica Acta* **269**(2): 192-200. DOI: 10.1016/0005-2787(72)90426-1.
- Achouri, S., Wright, J.A., Evans, L., Macleod, C., Fraser, G., Cicuta, P. and Bryant, C.E.** (2015) "The frequency and duration of *Salmonella*-macrophage adhesion events determines infection efficiency." *Philosophical Transactions of the Royal Society B: Biological Sciences* **370**: 1-8. DOI: 10.1098/rstb.2014.0033.
- Adamczack, J., Hoffmann, M., Papke, U., Haufschildt, K., Nicke, T., Broring, M., Sezer, M., Weimar, R., Kuhlmann, U., Hildebrandt, P. and Layer, G.** (2014) "NirN protein from *Pseudomonas aeruginosa* is a novel electron-bifurcating dehydrogenase catalyzing the last step of heme *d1* biosynthesis." *Journal of Biological Chemistry* **289**(44): 30753-30762. DOI: 10.1074/jbc.M114.603886.
- Adams, J.L. and McLean, R.J.** (1999) "Impact of *rpoS* deletion on *Escherichia coli* biofilms." *Applied and Environmental Microbiology* **65**(9): 4285-4287. DOI: 10.1128/AEM.65.9.4285-4287.1999.
- Adler, J.** (1966) "Chemotaxis in bacteria." *Science* **153**: 708-716. DOI: 10.1126/science.153.3737.708.
- Allsopp, L.P., Wood, T.E., Howard, S.A., Maggiorelli, F., Nolan, L.M., Wettstadt, S. and Filloux, A.** (2017) "RsmA and AmrZ orchestrate the assembly of all three type VI secretion systems in *Pseudomonas aeruginosa*." *Proceedings of the National Academy of Sciences of the United States of America* **114**(29): 7707-7712. DOI: 10.1073/pnas.1700286114.
- Alm, R.A., Boder, A.J., Free, P.D. and Mattick, J.S.** (1996) "Identification of a novel gene, *pilZ*, essential for type 4 fimbrial biogenesis in *Pseudomonas aeruginosa*." *Journal of Bacteriology* **178**(1): 46-53. DOI: 10.1128/jb.178.1.46-53.1996.
- Arai, H., Hayashi, M., Kuroi, A., Ishii, M. and Igarashi, Y.** (2005) "Transcriptional regulation of the flavohemoglobin gene for aerobic nitric oxide detoxification by the second nitric oxide-responsive regulator of *Pseudomonas aeruginosa*." *Journal of Bacteriology* **187**(12): 3960-3968. DOI: 10.1128/JB.187.12.3960-3968.2005.
- Arai, H., Igarashi, Y. and Kodama, T.** (1995) "Expression of the *nir* and *nor* genes for denitrification of *Pseudomonas aeruginosa* requires a novel CRP/FNR-related transcriptional regulator, DNR, in addition to ANR." *FEBS Letters* **371**(1): 73-76. DOI: 10.1016/0014-5793(95)00885-d.
- Baker, A.E., Webster, S.S., Diepold, A., Kuchma, S.L., Bordeleau, E., Armitage, J.P. and O'Toole, G.A.** (2019) "Flagellar stators stimulate c-di-GMP production by *Pseudomonas aeruginosa*." *Journal of Bacteriology* **201**(18): 1-13. DOI: 10.1128/JB.00741-18.

- Balasubramanian, D. and Vanderpool, C.K.** (2013) "New developments in post-transcriptional regulation of operons by small RNAs." *RNA Biology* **10**(3): 337-341. DOI: 10.4161/rna.23696.
- Bali, S., Warren, M.J. and Ferguson, S.J.** (2010) "NirF is a periplasmic protein that binds *d<sub>1</sub>* heme as part of its essential role in *d<sub>1</sub>* heme biogenesis." *FEBS Journal* **277**(23): 4944-4955. DOI: 10.1111/j.1742-4658.2010.07899.x.
- Barraud, N., Hassett, D.J., Hwang, S.H., Rice, S.A., Kjelleberg, S. and Webb, J.S.** (2006) "Involvement of nitric oxide in biofilm dispersal of *Pseudomonas aeruginosa*." *Journal of Bacteriology* **188**(21): 7344-7353. DOI: 10.1128/JB.00779-06.
- Barraud, N., Storey, M.V., Moore, Z.P., Webb, J.S., Rice, S.A. and Kjelleberg, S.** (2009) "Nitric oxide-mediated dispersal in single- and multi-species biofilms of clinically and industrially relevant microorganisms." *Microbial Biotechnology* **2**(3): 370-378. DOI: 10.1111/j.1751-7915.2009.00098.x.
- Battesti, A., Majdalani, N. and Gottesman, S.** (2011) "The RpoS-mediated general stress response in *Escherichia coli*." *Annual Review of Microbiology* **65**: 189-213. DOI: 10.1146/annurev-micro-090110-102946.
- Baynham, P.J., Brown, A.L., Hall, L.L. and Wozniak, D.J.** (1999) "*Pseudomonas aeruginosa* AlgZ, a ribbon-helix-helix DNA-binding protein, is essential for alginate synthesis and *algD* transcriptional activation." *Molecular Microbiology* **33**(5): 1069-1080. DOI: 10.1046/j.1365-2958.1999.01550.x.
- Baynham, P.J., Ramsey, D.M., Gvozdyev, B.V., Cordonnier, E.M. and Wozniak, D.J.** (2006) "The *Pseudomonas aeruginosa* ribbon-helix-helix DNA-binding protein AlgZ (AmrZ) controls twitching motility and biogenesis of type IV pili." *Journal of Bacteriology* **188**(1): 132-140. DOI: 10.1128/JB.188.1.132-140.2006.
- Baynham, P.J. and Wozniak, D.J.** (1996) "Identification and characterization of AlgZ, an AlgT-dependent DNA-binding protein required for *Pseudomonas aeruginosa algD* transcription." *Molecular Microbiology* **22**(1): 97-108. DOI: 10.1111/j.1365-2958.1996.tb02659.x.
- Becher, A. and Schweizer, H.P.** (2000) "Integration-proficient *Pseudomonas aeruginosa* vectors for isolation of single-copy chromosomal *lacZ* and *lux* gene fusions." *Biotechniques* **29**(5): 948-50, 952. DOI: 10.2144/00295bm04.
- Beganovic, S.** (2018) Master thesis: "Investigating the protein interaction network responsible for nitric oxide induced biofilm dispersal in *Pseudomonas aeruginosa*." Department of Microbiology, TU Kaiserslautern.
- Belasco, J.G.** (2010) "All things must pass: contrasts and commonalities in eukaryotic and bacterial mRNA decay." *Nature Reviews Molecular Cell Biology* **11**(7): 467-478. DOI: 10.1038/nrm2917.

- Bellows, L.E., Koestler, B.J., Karaba, S.M., Waters, C.M. and Lathem, W.W.** (2012) "Hfq-dependent, co-ordinate control of cyclic diguanylate synthesis and catabolism in the plague pathogen *Yersinia pestis*." *Molecular Microbiology* **86**(3): 661-674. DOI: 10.1111/mmi.12011.
- Bense, S., Bruchmann, S., Steffen, A., Stradal, T.E.B., Häussler, S. and Duvel, J.** (2019) "Spatiotemporal control of FlgZ activity impacts *Pseudomonas aeruginosa* flagellar motility." *Molecular Microbiology* **111**(6): 1544-1557. DOI: 10.1111/mmi.14236.
- Bi, S. and Sourjik, V.** (2018) "Stimulus sensing and signal processing in bacterial chemotaxis." *Current Opinion in Microbiology* **45**: 22-29. DOI: 10.1016/j.mib.2018.02.002.
- Blattner, F.R., Plunkett, G., 3rd, Bloch, C.A., Perna, N.T., Burland, V., Riley, M., Collado-Vides, J., Glasner, J.D., Rode, C.K., Mayhew, G.F., Gregor, J., Davis, N.W., Kirkpatrick, H.A., Goeden, M.A., Rose, D.J., Mau, B. and Shao, Y.** (1997) "The complete genome sequence of *Escherichia coli* K-12." *Science* **277**(5331): 1453-1462. DOI: 10.1126/science.277.5331.1453.
- Bobrov, A.G., Kirillina, O., Ryjenkov, D.A., Waters, C.M., Price, P.A., Fetherston, J.D., Mack, D., Goldman, W.E., Gomelsky, M. and Perry, R.D.** (2011) "Systematic analysis of cyclic di-GMP signalling enzymes and their role in biofilm formation and virulence in *Yersinia pestis*." *Molecular Microbiology* **79**(2): 533-551. DOI: 10.1111/j.1365-2958.2010.07470.x.
- Boehm, A., Kaiser, M., Li, H., Spangler, C., Kasper, C.A., Ackermann, M., Kaefer, V., Sourjik, V., Roth, V. and Jenal, U.** (2010) "Second messenger-mediated adjustment of bacterial swimming velocity." *Cell* **141**(1): 107-116. DOI: 10.1016/j.cell.2010.01.018.
- Borkovich, K.A., Alex, L.A. and Simon, M.I.** (1992) "Attenuation of sensory receptor signaling by covalent modification." *Proceedings of the National Academy of Sciences of the United States of America* **89**: 6756-6760. DOI: 10.1073/pnas.89.15.6756.
- Borrero-de Acuna, J.M., Molinari, G., Rohde, M., Dammeyer, T., Wissing, J., Jansch, L., Arias, S., Jahn, M., Schobert, M., Timmis, K.N. and Jahn, D.** (2015) "A Periplasmic Complex of the Nitrite Reductase NirS, the Chaperone DnaK, and the Flagellum Protein FliC Is Essential for Flagellum Assembly and Motility in *Pseudomonas aeruginosa*." *Journal of Bacteriology* **197**(19): 3066-3075. DOI: 10.1128/JB.00415-15.
- Borrero-de Acuna, J.M., Timmis, K.N., Jahn, M. and Jahn, D.** (2017) "Protein complex formation during denitrification by *Pseudomonas aeruginosa*." *Microbial Biotechnology* **10**(6): 1523-1534. DOI: 10.1111/1751-7915.12851.
- Botelho, J., Grosso, F. and Peixe, L.** (2019) "Antibiotic resistance in *Pseudomonas aeruginosa* - Mechanisms, epidemiology and evolution." *Drug Resistance Updates* **44**: 26-47. DOI: 10.1016/j.drug.2019.07.002.
- Brencic, A. and Lory, S.** (2009) "Determination of the regulon and identification of novel mRNA targets of *Pseudomonas aeruginosa* RsmA." *Molecular Microbiology* **72**(3): 612-632. DOI: 10.1111/j.1365-2958.2009.06670.x.

- Brencic, A., McFarland, K.A., McManus, H.R., Castang, S., Mogno, I., Dove, S.L. and Lory, S.** (2009) "The GacS/GacA signal transduction system of *Pseudomonas aeruginosa* acts exclusively through its control over the transcription of the RsmY and RsmZ regulatory small RNAs." *Molecular Microbiology* **73**(3): 434-445. DOI: 10.1111/j.1365-2958.2009.06782.x.
- Brown, L., Gentry, D., Elliott, T. and Cashel, M.** (2002) "DksA affects ppGpp induction of RpoS at a translational level." *Journal of Bacteriology* **184**(16): 4455-4465. DOI: 10.1128/jb.184.16.4455-4465.2002.
- Browning, D.F. and Busby, S.J.** (2004) "The regulation of bacterial transcription initiation." *Nature Reviews Microbiology* **2**(1): 57-65. DOI: 10.1038/nrmicro787.
- Bruzaud, J., Tarrade, J., Coudreuse, A., Canette, A., Herry, J.M., Taffin de Givenchy, E., Darmanin, T., Guittard, F., Guilbaud, M. and Bellon-Fontaine, M.N.** (2015) "Flagella but not type IV pili are involved in the initial adhesion of *Pseudomonas aeruginosa* PAO1 to hydrophobic or superhydrophobic surfaces." *Colloids Surf B Biointerfaces* **131**: 59-66. DOI: 10.1016/j.colsurfb.2015.04.036.
- Burrows, L.L.** (2012) "*Pseudomonas aeruginosa* twitching motility: type IV pili in action." *Annual Review of Microbiology* **66**: 493-520. DOI: 10.1146/annurev-micro-092611-150055.
- Cai, Y.M., Hutchin, A., Craddock, J., Walsh, M.A., Webb, J.S. and Tews, I.** (2020) "Differential impact on motility and biofilm dispersal of closely related phosphodiesterases in *Pseudomonas aeruginosa*." *Scientific Reports* **10**(1): 6232. DOI: 10.1038/s41598-020-63008-5.
- Carlson, H.K., Vance, R.E. and Marletta, M.A.** (2010) "H-NOX regulation of c-di-GMP metabolism and biofilm formation in *Legionella pneumophila*." *Molecular Microbiology* **77**(4): 930-942. DOI: 10.1111/j.1365-2958.2010.07259.x.
- Chan, C., Paul, R., Samoray, D., Amiot, N.C., Giese, B., Jenal, U. and Schirmer, T.** (2004) "Structural basis of activity and allosteric control of diguanylate cyclase." *Proceedings of the National Academy of Sciences of the United States of America* **101**(49): 17084-17089. DOI: 10.1073/pnas.0406134101.
- Chiang, P. and Burrows, L.L.** (2003) "Biofilm formation by hyperpiliated mutants of *Pseudomonas aeruginosa*." *Journal of Bacteriology* **185**(7): 2374-2378. DOI: 10.1128/JB.185.7.2374-2378.2003.
- Chihara, K., Barquist, L., Takasugi, K., Noda, N. and Tsuneda, S.** (2021) "Global identification of RsmA/N binding sites in *Pseudomonas aeruginosa* by *in vivo* UV CLIP-seq." *RNA Biology*: 1-16. DOI: 10.1080/15476286.2021.1917184.
- Christen, M., Kulasekara, H.D., Christen, B., Kulasekara, B.R., Hoffman, L.R. and Miller, S.I.** (2010) "Asymmetrical distribution of the second messenger c-di-GMP upon bacterial cell division." *Science* **328**(5983): 1295-1297. DOI: 10.1126/science.1188658.

- Coggan, K.A. and Wolfgang, M.C.** (2012) "Global regulatory pathways and cross-talk control *Pseudomonas aeruginosa* environmental lifestyle and virulence phenotype." *Current Issues in Molecular Biology* **14**(2): 47-70. DOI:
- Cornell, W.C., Morgan, C.J., Koyama, L., Sakhtah, H., Mansfield, J.H. and Dietrich, L.E.P.** (2018) "Paraffin embedding and thin sectioning of microbial colony biofilms for microscopic analysis." *Journal of Visualized Experiments* **133**(e57196): 1-8. DOI: 10.3791/57196.
- Costerton, J.W., Cheng, K.J., Geesey, G.G., Ladd, T.I., Nickel, J.C., Dasgupta, M. and Marrie, T.J.** (1987) "Bacterial biofilms in nature and disease." *Annual Reviews Microbiol* **41**: 435-464. DOI: 10.1146/annurev.mi.41.100187.002251.
- Costerton, J.W., Lewandowski, Z., Caldwell, D.E., Korber, D.R. and Lappin-Scott, H.M.** (1995) "Microbial biofilms." *Annual Reviews Microbiol* **49**: 711-745. DOI: 10.1146/annurev.mi.49.100195.003431.
- Cotter, P.A. and Stibitz, S.** (2007) "c-di-GMP-mediated regulation of virulence and biofilm formation." *Current Opinion in Microbiology* **10**(1): 17-23. DOI: 10.1016/j.mib.2006.12.006.
- Courtney, J.M., Bradley, J., McCaughan, J., O'Connor, T.M., Shortt, C., Bredin, C.P., Bradbury, I. and Elborn, J.S.** (2007) "Predictors of mortality in adults with cystic fibrosis." *Pediatric Pulmonology* **42**(6): 525-532. DOI: 10.1002/ppul.20619.
- Cowles, K.N. and Gitai, Z.** (2010) "Surface association and the MreB cytoskeleton regulate pilus production, localization and function in *Pseudomonas aeruginosa*." *Molecular Microbiology* **76**(6): 1411-1426. DOI: 10.1111/j.1365-2958.2010.07132.x.
- Cutruzzola, F. and Frankenberg-Dinkel, N.** (2016) "Origin and Impact of Nitric Oxide in *Pseudomonas aeruginosa* Biofilms." *Journal of Bacteriology* **198**(1): 55-65. DOI: 10.1128/JB.00371-15.
- Dahlstrom, K.M., Collins, A.J., Doing, G., Taroni, J.N., Gauvin, T.J., Greene, C.S., Hogan, D.A. and O'Toole, G.A.** (2018) "A multimodal strategy used by a large c-di-GMP network." *Journal of Bacteriology* **200**(8): 1-19. DOI: 10.1128/JB.00703-17.
- Darnton, N.C., Turner, L., Rojevsky, S. and Berg, H.C.** (2007) "On torque and tumbling in swimming *Escherichia coli*." *Journal of Bacteriology* **189**(5): 1756-1764. DOI: 10.1128/JB.01501-06.
- Davey, M.E., Caiazza, N.C. and O'Toole, G.A.** (2003) "Rhamnolipid surfactant production affects biofilm architecture in *Pseudomonas aeruginosa* PAO1." *Journal of Bacteriology* **185**(3): 1027-1036. DOI: 10.1128/jb.185.3.1027-1036.2003.
- de Beer, D., Stoodley, P., Roe, F. and Lewandowski, Z.** (1994) "Effects of biofilm structures on oxygen distribution and mass transport." *Biotechnology and Bioengineering* **43**(11): 1131-1138. DOI: 10.1002/bit.260431118.

- de Lorenzo, V. and Timmis, K.N.** (1994) "Analysis and construction of stable phenotypes in gram-negative bacteria with Tn5- and Tn10-derived minitransposons." *Methods in Enzymology* **235**: 386-405. DOI: 10.1016/0076-6879(94)35157-0.
- Deana, A. and Belasco, J.G.** (2005) "Lost in translation: the influence of ribosomes on bacterial mRNA decay." *Genes & Development* **19**(21): 2526-2533. DOI: 10.1101/gad.1348805.
- DeLange, P.A., Collins, T.L., Pierce, G.E. and Robinson, J.B.** (2007) "PilJ localizes to cell poles and is required for type IV pilus extension in *Pseudomonas aeruginosa*." *Current Microbiology* **55**(5): 389-395. DOI: 10.1007/s00284-007-9008-5.
- Denis, M.** (1994) "Human monocytes/macrophages: NO or no NO?" *Journal of Leukocyte Biology* **55**(5): 682-684. DOI: 10.1002/jlb.55.5.682.
- Dong, T. and Schellhorn, H.E.** (2010) "Role of RpoS in virulence of pathogens." *Infection and Immunity* **78**(3): 887-897. DOI: 10.1128/IAI.00882-09.
- Dubey, A.K., Baker, C.S., Romeo, T. and Babitzke, P.** (2005) "RNA sequence and secondary structure participate in high-affinity CsrA-RNA interaction." *RNA* **11**(10): 1579-1587. DOI: 10.1261/rna.2990205.
- Duerig, A., Abel, S., Folcher, M., Nicollier, M., Schwede, T., Amiot, N., Giese, B. and Jenal, U.** (2009) "Second messenger-mediated spatiotemporal control of protein degradation regulates bacterial cell cycle progression." *Genes & Development* **23**(1): 93-104. DOI: 10.1101/gad.502409.
- Dunn, N.W. and Holloway, B.W.** (1971) "Pleiotrophy of p-fluorophenylalanine-resistant and antibiotic hypersensitive mutants of *Pseudomonas aeruginosa*." *Genetics Research* **18**(2): 185-197. DOI: 10.1017/s0016672300012593.
- Duval, M., Simonetti, A., Caldelari, I. and Marzi, S.** (2015) "Multiple ways to regulate translation initiation in bacteria: Mechanisms, regulatory circuits, dynamics." *Biochimie* **114**: 18-29. DOI: 10.1016/j.biochi.2015.03.007.
- Düvel, J., Bertinetti, D., Moller, S., Schwede, F., Morr, M., Wissing, J., Radamm, L., Zimmermann, B., Genieser, H.G., Jansch, L., Herberg, F.W. and Haussler, S.** (2012) "A chemical proteomics approach to identify c-di-GMP binding proteins in *Pseudomonas aeruginosa*." *Journal of Microbiological Methods* **88**(2): 229-236. DOI: 10.1016/j.mimet.2011.11.015.
- Eschbach, M., Schreiber, K., Trunk, K., Buer, J., Jahn, D. and Schobert, M.** (2004) "Long-term anaerobic survival of the opportunistic pathogen *Pseudomonas aeruginosa* via pyruvate fermentation." *Journal of Bacteriology* **186**(14): 4596-4604. DOI: 10.1128/JB.186.14.4596-4604.2004.

- Falcone, M., Ferrara, S., Rossi, E., Johansen, H.K., Molin, S. and Bertoni, G.** (2018) "The small RNA ErsA of *Pseudomonas aeruginosa* contributes to biofilm development and motility through post-transcriptional modulation of AmrZ." *Frontiers in Microbiology* **9**(238): 1-12. DOI: 10.3389/fmicb.2018.00238.
- Fang, X. and Gomelsky, M.** (2010) "A post-translational, c-di-GMP-dependent mechanism regulating flagellar motility." *Molecular Microbiology* **76**(5): 1295-1305. DOI: 10.1111/j.1365-2958.2010.07179.x.
- Fauvart, M., Phillips, P., Bachaspatimayum, D., Verstraeten, N., Fransaer, J., Michiels, J. and Vermant, J.** (2012) "Surface tension gradient control of bacterial swarming in colonies of *Pseudomonas aeruginosa*." *Soft Matter* **8**: 70-76. DOI: 10.1039/c1sm06002c.
- Fleming, D. and Rumbaugh, K.** (2018) "The Consequences of biofilm dispersal on the host." *Scientific Reports* **8**: 1-7. DOI: 10.1038/s41598-018-29121-2.
- Folsom, J.P., Richards, L., Pitts, B., Roe, F., Ehrlich, G.D., Parker, A., Mazurie, A. and Stewart, P.S.** (2010) "Physiology of *Pseudomonas aeruginosa* in biofilms as revealed by transcriptome analysis." *BMC Microbiol* **10**(294): 1-17. DOI: 10.1186/1471-2180-10-294.
- Forrester, M.T. and Foster, M.W.** (2012) "Protection from nitrosative stress: a central role for microbial flavohemoglobin." *Free Radical Biology and Medicine* **52**(9): 1620-1633. DOI: 10.1016/j.freeradbiomed.2012.01.028.
- Friedman, L. and Kolter, R.** (2004) "Genes involved in matrix formation in *Pseudomonas aeruginosa* PA14 biofilms." *Molecular Microbiology* **51**(3): 675-690. DOI: 10.1046/j.1365-2958.2003.03877.x.
- Fujita, M., Tanaka, K., Takahashi, H. and Amemura, A.** (1994) "Transcription of the principal sigma-factor genes, *rpoD* and *rpoS*, in *Pseudomonas aeruginosa* is controlled according to the growth phase." *Molecular Microbiology* **13**(6): 1071-1077. DOI: 10.1111/j.1365-2958.1994.tb00498.x.
- Galperin, M.Y., Gaidenko, T.A., Mulkidjanian, A.Y., Nakano, M. and Price, C.W.** (2001) "MHYT, a new integral membrane sensor domain." *FEMS Microbiology Letters* **205**(1): 17-23. DOI: 10.1111/j.1574-6968.2001.tb10919.x.
- Gaubig, L.C., Waldminghaus, T. and Narberhaus, F.** (2011) "Multiple layers of control govern expression of the *Escherichia coli* *ibpAB* heat-shock operon." *Microbiology* **157**(Pt 1): 66-76. DOI: 10.1099/mic.0.043802-0.
- Gebhardt, M.J., Kambara, T.K., Ramsey, K.M. and Dove, S.L.** (2020) "Widespread targeting of nascent transcripts by RsmA in *Pseudomonas aeruginosa*." *Proceedings of the National Academy of Sciences of the United States of America* **117**(19): 10520-10529. DOI: 10.1073/pnas.1917587117.



- Giardina, G., Rinaldo, S., Castiglione, N., Caruso, M. and Cutruzzolà, F.** (2009) "A dramatic conformational rearrangement is necessary for the activation of DNR from *Pseudomonas aeruginosa*. Crystal structure of wild-type DNR." *Proteins* **77**(1): 174-180. DOI: 10.1002/prot.22428.
- Giardina, G., Rinaldo, S., Johnson, K.A., Di Matteo, A., Brunori, M. and Cutruzzola, F.** (2008) "NO sensing in *Pseudomonas aeruginosa*: structure of the transcriptional regulator DNR." *Journal of Molecular Biology* **378**(5): 1002-1015. DOI: 10.1016/j.jmb.2008.03.013.
- Giuliodori, A.M., Di Pietro, F., Marzi, S., Masquida, B., Wagner, R., Romby, P., Gualerzi, C.O. and Pon, C.L.** (2010) "The *cspA* mRNA is a thermosensor that modulates translation of the cold-shock protein CspA." *Molecular Cell* **37**(1): 21-33. DOI: 10.1016/j.molcel.2009.11.033.
- Goodman, A.L., Kulasekara, B., Rietsch, A., Boyd, D., Smith, R.S. and Lory, S.** (2004) "A signaling network reciprocally regulates genes associated with acute infection and chronic persistence in *Pseudomonas aeruginosa*." *Developmental Cell* **7**(5): 745-754. DOI: 10.1016/j.devcel.2004.08.020.
- Grosso-Becerra, M.V., Croda-Garcia, G., Merino, E., Servin-Gonzalez, L., Mojica-Espinosa, R. and Soberon-Chavez, G.** (2014) "Regulation of *Pseudomonas aeruginosa* virulence factors by two novel RNA thermometers." *Proceedings of the National Academy of Sciences of the United States of America* **111**(43): 15562-15567. DOI: 10.1073/pnas.1402536111.
- Guan, J., Xiao, X., Xu, S., Gao, F., Wang, J., Wang, T., Song, Y., Pan, J., Shen, X. and Wang, Y.** (2015) "Roles of RpoS in *Yersinia pseudotuberculosis* stress survival, motility, biofilm formation and type VI secretion system expression." *Journal of Microbiology* **53**(9): 633-642. DOI: 10.1007/s12275-015-0099-6.
- Gubellini, F., Verdon, G., Karpowich, N.K., Luff, J.D., Boel, G., Gauthier, N., Handelman, S.K., Ades, S.E. and Hunt, J.F.** (2011) "Physiological response to membrane protein overexpression in *E. coli*." *Molecular & Cellular Proteomics* **10**(10): 1-17. DOI: 10.1074/mcp.M111.007930.
- Guilhen, C., Forestier, C. and Balestrino, D.** (2017) "Biofilm dispersal: multiple elaborate strategies for dissemination of bacteria with unique properties." *Molecular Microbiology* **105**(2): 188-210. DOI: 10.1111/mmi.13698.
- Gutierrez, P., Li, Y., Osborne, M.J., Pomerantseva, E., Liu, Q. and Gehring, K.** (2005) "Solution structure of the carbon storage regulator protein CsrA from *Escherichia coli*." *Journal of Bacteriology* **187**(10): 3496-3501. DOI: 10.1128/JB.187.10.3496-3501.2005.
- Ha, D.G., Richman, M.E. and O'Toole, G.A.** (2014) "Deletion mutant library for investigation of functional outputs of cyclic diguanylate metabolism in *Pseudomonas aeruginosa* PA14." *Applied and Environmental Microbiology* **80**(11): 3384-3393. DOI: 10.1128/AEM.00299-14.
- Hahn, H.P.** (1997) "The type-4 pilus is the major virulence-associated adhesin of *Pseudomonas aeruginosa* - a review." *Gene* **192**(1): 99-108. DOI: 10.1016/S0378-1119(97)00116-9.

- Hanahan, D.** (1983) "Studies on transformation of *Escherichia coli* with plasmids." *Journal of Molecular Biology* **166**(4): 557-80. DOI: 10.1016/s0022-2836(83)80284-8.
- Hancock, R.E. and Speert, D.P.** (2000) "Antibiotic resistance in *Pseudomonas aeruginosa*: mechanisms and impact on treatment." *Drug Resistance Updates* **3**(4): 247-255. DOI: 10.1054/drup.2000.0152.
- Harley, C.B. and Reynolds, R.P.** (1987) "Analysis of *E. coli* promoter sequences." *Nucleic Acids Research* **15**(5): 2343-2361. DOI: 10.1093/nar/15.5.2343.
- Hauser, F., Pessi, G., Friberg, M., Weber, C., Rusca, N., Lindemann, A., Fischer, H.M. and Hennecke, H.** (2007) "Dissection of the *Bradyrhizobium japonicum* NifA+sigma54 regulon, and identification of a ferredoxin gene (*fdxN*) for symbiotic nitrogen fixation." *Molecular Genetics and Genomics* **278**(3): 255-271. DOI: 10.1007/s00438-007-0246-9.
- Hay, I.D., Remminghorst, U. and Rehm, B.H.** (2009) "MucR, a novel membrane-associated regulator of alginate biosynthesis in *Pseudomonas aeruginosa*." *Applied and Environmental Microbiology* **75**(4): 1110-1120. DOI: 10.1128/AEM.02416-08.
- He, J., Baldini, R.L., Deziel, E., Saucier, M., Zhang, Q., Liberati, N.T., Lee, D., Urbach, J., Goodman, H.M. and Rahme, L.G.** (2004) "The broad host range pathogen *Pseudomonas aeruginosa* strain PA14 carries two pathogenicity islands harboring plant and animal virulence genes." *Proceedings of the National Academy of Sciences of the United States of America* **101**(8): 2530-2535. DOI: 10.1073/pnas.0304622101.
- Hecht, A., Glasgow, J., Jaschke, P.R., Bawazer, L.A., Munson, M.S., Cochran, J.R., Endy, D. and Salit, M.** (2017) "Measurements of translation initiation from all 64 codons in *E. coli*." *Nucleic Acids Research* **45**(7): 3615-3626. DOI: 10.1093/nar/gkx070.
- Heeb, S., Blumer, C. and Haas, D.** (2002) "Regulatory RNA as mediator in GacA/RsmA-dependent global control of exoproduct formation in *Pseudomonas fluorescens* CHA0." *Journal of Bacteriology* **184**(4): 1046-1056. DOI: 10.1128/jb.184.4.1046-1056.2002.
- Heinrich, T.A., da Silva, R.S., Miranda, K.M., Switzer, C.H., Wink, D.A. and Fukuto, J.M.** (2013) "Biological nitric oxide signalling: chemistry and terminology." *British Journal of Pharmacology* **169**(7): 1417-1429. DOI: 10.1111/bph.12217.
- Hengge, R.** (2009) "Principles of c-di-GMP signalling in bacteria." *Nature Reviews Microbiology* **7**(4): 263-273. DOI: 10.1038/nrmicro2109.
- Hengge, R., Grundling, A., Jenal, U., Ryan, R. and Yildiz, F.** (2016) "Bacterial signal transduction by cyclic di-GMP and other nucleotide second messengers." *Journal of Bacteriology* **198**(1): 15-26. DOI: 10.1128/JB.00331-15.
- Heydorn, A., Ersboll, B., Kato, J., Hentzer, M., Parsek, M.R., Tolker-Nielsen, T., Givskov, M. and Molin, S.** (2002) "Statistical analysis of *Pseudomonas aeruginosa* biofilm development: impact of mutations in genes involved in twitching motility, cell-to-cell signaling, and stationary-phase sigma factor expression." *Applied and Environmental Microbiology* **68**(4): 2008-2017. DOI: 10.1128/aem.68.4.2008-2017.2002.

- Hickman, J.W. and Harwood, C.S.** (2008) "Identification of FleQ from *Pseudomonas aeruginosa* as a c-di-GMP-responsive transcription factor." *Molecular Microbiology* **69**(2): 376-389. DOI: 10.1111/j.1365-2958.2008.06281.x.
- Hickman, J.W., Tifrea, D.F. and Harwood, C.S.** (2005) "A chemosensory system that regulates biofilm formation through modulation of cyclic diguanylate levels." *Proceedings of the National Academy of Sciences of the United States of America* **102**(40): 14422-14427. DOI: 10.1073/pnas.0507170102.
- Hmelo, L.R., Borlee, B.R., Almlad, H., Love, M.E., Randall, T.E., Tseng, B.S., Lin, C., Irie, Y., Storek, K.M., Yang, J.J., Siehnel, R.J., Howell, P.L., Singh, P.K., Tolker-Nielsen, T., Parsek, M.R., Schweizer, H.P. and Harrison, J.J.** (2015) "Precision-engineering the *Pseudomonas aeruginosa* genome with two-step allelic exchange." *Nature Protocols* **10**(11): 1820-1841. DOI: 10.1038/nprot.2015.115.
- Hoang, T.T., Kutchna, A.J., Becher, A. and Schweizer, H.P.** (2000) "Integration-proficient plasmids for *Pseudomonas aeruginosa*: site-specific integration and use for engineering of reporter and expression strains." *Plasmid* **43**(1): 59-72. DOI: 10.1006/plas.1999.1441.
- Hong, C.S., Shitashiro, M., Kuroda, A., Ikeda, T., Takiguchi, N., Ohtake, H. and Kato, J.** (2004) "Chemotaxis proteins and transducers for aerotaxis in *Pseudomonas aeruginosa*." *FEMS Microbiology Letters* **231**(2): 247-252. DOI: 10.1016/S0378-1097(04)00009-6.
- Hossain, S. and Boon, E.M.** (2017) "Discovery of a Novel Nitric Oxide Binding Protein and Nitric-Oxide-Responsive Signaling Pathway in *Pseudomonas aeruginosa*." *ACS Infectious Diseases* **3**(6): 454-461. DOI: 10.1021/acsinfectdis.7b00027.
- Huertas-Rosales, O., Romero, M., Heeb, S., Espinosa-Urgel, M., Cámara, M. and Ramos-González, M.I.** (2017) "The *Pseudomonas putida* CsrA/RsmA homologues negatively affect c-di-GMP pools and biofilm formation through the GGDEF/EAL response regulator CfcR." *Environmental Microbiology* **19**(9): 3551-3566. DOI: 10.1111/1462-2920.13848.
- Inclan, Y.F., Persat, A., Greninger, A., Von Dollen, J., Johnson, J., Krogan, N., Gitai, Z. and Engel, J.N.** (2016) "A scaffold protein connects type IV pili with the Chp chemosensory system to mediate activation of virulence signaling in *Pseudomonas aeruginosa*." *Molecular Microbiology* **101**(4): 590-605. DOI: 10.1111/mmi.13410.
- Irie, Y., La Mensa, A., Murina, V., Hauryliuk, V., Tenson, T. and Shingler, V.** (2020) "Hfq-assisted RsmA regulation is central to *Pseudomonas aeruginosa* biofilm polysaccharide PEL expression." *Frontiers in Microbiology* **11**: 1-15. DOI: 10.3389/fmicb.2020.482585.
- Irie, Y., Starkey, M., Edwards, A.N., Wozniak, D.J., Romeo, T. and Parsek, M.R.** (2010) "*Pseudomonas aeruginosa* biofilm matrix polysaccharide Psl is regulated transcriptionally by RpoS and post-transcriptionally by RsmA." *Molecular Microbiology* **78**(1): 158-172. DOI: 10.1111/j.1365-2958.2010.07320.x.
- Ito, A., May, T., Kawata, K. and Okabe, S.** (2008) "Significance of *rpoS* during maturation of *Escherichia coli* biofilms." *Biotechnology and Bioengineering* **99**(6): 1462-1471. DOI: 10.1002/bit.21695.

- Jain, R., Sliusarenko, O. and Kazmierczak, B.I.** (2017) "Interaction of the cyclic-di-GMP binding protein FimX and the Type 4 pilus assembly ATPase promotes pilus assembly." *PLoS Pathogens* **13**(8): 1-23. DOI: 10.1371/journal.ppat.1006594.
- James, G.A., Ge Zhao, A., Usui, M., Underwood, R.A., Nguyen, H., Beyenal, H., deLancey Pulcini, E., Agostinho Hunt, A., Bernstein, H.C., Fleckman, P., Olerud, J., Williamson, K.S., Franklin, M.J. and Stewart, P.S.** (2016) "Microsensor and transcriptomic signatures of oxygen depletion in biofilms associated with chronic wounds." *Wound Repair and Regeneration* **24**(2): 373-383. DOI: 10.1111/wrr.12401.
- Jampel, H.D., Duff, G.W., Gershon, R.K., Atkins, E. and Durum, S.K.** (1983) "Fever and immunoregulation. III. Hyperthermia augments the primary in vitro humoral immune response." *Journal of Experimental Medicine* **157**(4): 1229-1238. DOI: 10.1084/jem.157.4.1229.
- Janssen, K.H., Diaz, M.R., Gode, C.J., Wolfgang, M.C. and Yahr, T.L.** (2018) "RsmV, a small noncoding regulatory RNA in *Pseudomonas aeruginosa* that sequesters RsmA and RsmF from target mRNAs." *Journal of Bacteriology* **200**(16): 1-13. DOI: 10.1128/JB.00277-18.
- Jensen, P.O., Givskov, M., Bjarnsholt, T. and Moser, C.** (2010) "The immune system vs. *Pseudomonas aeruginosa* biofilms." *FEMS Immunology and Medical Microbiology* **59**(3): 292-305. DOI: 10.1111/j.1574-695X.2010.00706.x.
- Jonas, K., Edwards, A.N., Ahmad, I., Romeo, T., Romling, U. and Melefors, O.** (2010) "Complex regulatory network encompassing the Csr, c-di-GMP and motility systems of *Salmonella typhimurium*." *Environmental Microbiology* **12**(2): 524-540. DOI: 10.1111/j.1462-2920.2009.02097.x.
- Jonas, K., Edwards, A.N., Simm, R., Romeo, T., Romling, U. and Melefors, O.** (2008) "The RNA binding protein CsrA controls cyclic di-GMP metabolism by directly regulating the expression of GGDEF proteins." *Molecular Microbiology* **70**(1): 236-257. DOI: 10.1111/j.1365-2958.2008.06411.x.
- Jones, B.D., Lee, C.A. and Falkow, S.** (1992) "Invasion by *Salmonella typhimurium* is affected by the direction of flagellar rotation." *Infection and Immunity* **60**(6): 2475-2480. DOI: 10.1128/iai.60.6.2475-2480.1992.
- Jones, C.J., Newsom, D., Kelly, B., Irie, Y., Jennings, L.K., Xu, B., Limoli, D.H., Harrison, J.J., Parsek, M.R., White, P. and Wozniak, D.J.** (2014) "ChIP-Seq and RNA-Seq reveal an AmrZ-mediated mechanism for cyclic di-GMP synthesis and biofilm development by *Pseudomonas aeruginosa*." *PLoS Pathogens* **10**(3): 1-17. DOI: 10.1371/journal.ppat.1003984.
- Jones, C.J., Ryder, C.R., Mann, E.E. and Wozniak, D.J.** (2013) "AmrZ modulates *Pseudomonas aeruginosa* biofilm architecture by directly repressing transcription of the *psl* operon." *Journal of Bacteriology* **195**(8): 1637-1644. DOI: 10.1128/JB.02190-12.
- Jorgensen, F., Bally, M., Chapon-Herve, V., Michel, G., Lazdunski, A., Williams, P. and Stewart, G.** (1999) "RpoS-dependent stress tolerance in *Pseudomonas aeruginosa*." *Microbiology (Reading)* **145**: 835-844. DOI: 10.1099/13500872-145-4-835.

- Kakishima, K., Shiratsuchi, A., Taoka, A., Nakanishi, Y. and Fukumori, Y.** (2007) "Participation of nitric oxide reductase in survival of *Pseudomonas aeruginosa* in LPS-activated macrophages." *Biochemical and Biophysical Research Communications* **355**(2): 587-591. DOI: 10.1016/j.bbrc.2007.02.017.
- Kaplan, J.B.** (2010) "Biofilm dispersal: mechanisms, clinical implications, and potential therapeutic uses." *Journal of Dental Research* **89**(3): 205-218. DOI: 10.1177/0022034509359403.
- Kazmierczak, B.I., Lebron, M.B. and Murray, T.S.** (2006) "Analysis of FimX, a phosphodiesterase that governs twitching motility in *Pseudomonas aeruginosa*." *Molecular Microbiology* **60**(4): 1026-1043. DOI: 10.1111/j.1365-2958.2006.05156.x.
- Kim, S., Li, X.H., Hwang, H.J. and Lee, J.H.** (2020) "Thermoregulation of *Pseudomonas aeruginosa* biofilm formation." *Applied and Environmental Microbiology* **86**(22): 1-11. DOI: 10.1128/AEM.01584-20.
- Kirillina, O., Fetherston, J.D., Bobrov, A.G., Abney, J. and Perry, R.D.** (2004) "HmsP, a putative phosphodiesterase, and HmsT, a putative diguanylate cyclase, control Hms-dependent biofilm formation in *Yersinia pestis*." *Molecular Microbiology* **54**(1): 75-88. DOI: 10.1111/j.1365-2958.2004.04253.x.
- Klausen, M., Heydorn, A., Ragas, P., Lambertsen, L., Aaes-Jorgensen, A., Molin, S. and Tolker-Nielsen, T.** (2003) "Biofilm formation by *Pseudomonas aeruginosa* wild type, flagella and type IV pili mutants." *Molecular Microbiology* **48**(6): 1511-1524. DOI: 10.1046/j.1365-2958.2003.03525.x.
- Klinkert, B., Cimdins, A., Gaubig, L.C., Rossmanith, J., Aschke-Sonnenborn, U. and Narberhaus, F.** (2012) "Thermogenetic tools to monitor temperature-dependent gene expression in bacteria." *Journal of Biotechnology* **160**: 55-63. DOI: 10.1016/j.jbiotec.2012.01.007.
- Klockgether, J., Cramer, N., Wiehlmann, L., Davenport, C.F. and Tümmler, B.** (2011) "*Pseudomonas aeruginosa* genomic structure and diversity." *Frontiers in Microbiology* **2**(150): 1-18. DOI: 10.3389/fmicb.2011.00150.
- Klünemann, T., Preuss, A., Adamczack, J., Rosa, L.F.M., Harnisch, F., Layer, G. and Blankenfeldt, W.** (2019) "Crystal structure of dihydro-heme *d<sub>1</sub>* dehydrogenase NirN from *Pseudomonas aeruginosa* reveals amino acid residues essential for catalysis." *Journal of Molecular Biology* **431**(17): 3246-3260. DOI: 10.1016/j.jmb.2019.05.046.
- Köhler, T., Curty, L.K., Barja, F., van Delden, C. and Pechère, J.C.** (2000) "Swarming of *Pseudomonas aeruginosa* is dependent on cell-to-cell signaling and requires flagella and pili." *Journal of Bacteriology* **182**(21): 5990-5996. DOI: 10.1128/JB.182.21.5990-5996.2000.
- Kortmann, J. and Narberhaus, F.** (2012) "Bacterial RNA thermometers: molecular zippers and switches." *Nature Reviews Microbiology* **10**(4): 255-265. DOI: 10.1038/nrmicro2730.

- Koskenkorva-Frank, T.S. and Kallio, P.T.** (2009) "Induction of *Pseudomonas aeruginosa* *fhp* and *fhpR* by reactive oxygen species." *Canadian Journal of Microbiology* **55**(6): 657-663. DOI: 10.1139/w09-024.
- Krajewski, S.S., Nagel, M. and Narberhaus, F.** (2013) "Short ROSE-like RNA thermometers control *lbpA* synthesis in *Pseudomonas* species." *PLoS One* **8**(5): 1-13. DOI: 10.1371/journal.pone.0065168.
- Kulasakara, H., Lee, V., Brencic, A., Liberati, N., Urbach, J., Miyata, S., Lee, D.G., Neely, A.N., Hyodo, M., Hayakawa, Y., Ausubel, F.M. and Lory, S.** (2006) "Analysis of *Pseudomonas aeruginosa* diguanylate cyclases and phosphodiesterases reveals a role for bis-(3'-5')-cyclic-GMP in virulence." *Proceedings of the National Academy of Sciences of the United States of America* **103**(8): 2839-2844. DOI: 10.1073/pnas.0511090103.
- Kulasekara, B.R., Kamischke, C., Kulasekara, H.D., Christen, M., Wiggins, P.A. and Miller, S.I.** (2013) "c-di-GMP heterogeneity is generated by the chemotaxis machinery to regulate flagellar motility." *eLIFE* **2**: 1-19. DOI: 10.7554/eLife.01402.
- Laemmli, U.K.** (1970) "Cleavage of structural proteins during the assembly of the head of bacteriophage T4." *Nature* **227**(5259): 680-685. DOI: 10.1038/227680a0.
- Landini, P., Egli, T., Wolf, J. and Lacour, S.** (2014) "sigmaS, a major player in the response to environmental stresses in *Escherichia coli*: role, regulation and mechanisms of promoter recognition." *Environmental Microbiology Reports* **6**(1): 1-13. DOI: 10.1111/1758-2229.12112.
- Lange, R., Fischer, D. and Hengge-Aronis, R.** (1995) "Identification of transcriptional start sites and the role of ppGpp in the expression of *rpoS*, the structural gene for the sigma S subunit of RNA polymerase in *Escherichia coli*." *Journal of Bacteriology* **177**(16): 4676-4680. DOI: 10.1128/jb.177.16.4676-4680.1995.
- Latifi, A., Foglino, M., Tanaka, K., Williams, P. and Lazdunski, A.** (1996) "A hierarchical quorum-sensing cascade in *Pseudomonas aeruginosa* links the transcriptional activators LasR and RhIR (VsmR) to expression of the stationary-phase sigma factor RpoS." *Molecular Microbiology* **21**(6): 1137-1146. DOI: 10.1046/j.1365-2958.1996.00063.x.
- Lee, V.T., Matewish, J.M., Kessler, J.L., Hyodo, M., Hayakawa, Y. and Lory, S.** (2007) "A cyclic-di-GMP receptor required for bacterial exopolysaccharide production." *Molecular Microbiology* **65**(6): 1474-1484. DOI: 10.1111/j.1365-2958.2007.05879.x.
- Li, Y., Heine, S., Entian, M., Sauer, K. and Frankenberg-Dinkel, N.** (2013) "NO-induced biofilm dispersion in *Pseudomonas aeruginosa* is mediated by an MHYT domain-coupled phosphodiesterase." *Journal of Bacteriology* **195**(16): 3531-3542. DOI: 10.1128/JB.01156-12.
- Li, Z., Chen, J.H., Hao, Y. and Nair, S.K.** (2012) "Structures of the PelD cyclic diguanylate effector involved in pellicle formation in *Pseudomonas aeruginosa* PAO1." *Journal of Biological Chemistry* **287**(36): 30191-30204. DOI: 10.1074/jbc.M112.378273.

- Liu, H., Yan, H., Xiao, Y., Nie, H., Huang, Q. and Chen, W.** (2019) "The exopolysaccharide gene cluster *pea* is transcriptionally controlled by RpoS and repressed by AmrZ in *Pseudomonas putida* KT2440." *Microbiological Research* **218**: 1-11. DOI: 10.1016/j.micres.2018.09.004.
- Luo, Y., Zhao, K., Baker, A.E., Kuchma, S.L., Coggan, K.A., Wolfgang, M.C., Wong, G.C. and O'Toole, G.A.** (2015) "A hierarchical cascade of second messengers regulates *Pseudomonas aeruginosa* surface behaviors." *mBio* **6**(1): 1-11. DOI: 10.1128/mBio.02456-14.
- Lyczak, J.B., Cannon, C.L. and Pier, G.B.** (2000) "Establishment of *Pseudomonas aeruginosa* infection: lessons from a versatile opportunist." *Microbes and Infection* **2**(9): 1051-60. DOI: 10.1016/s1286-4579(00)01259-4.
- MacMicking, J., Xie, Q.W. and Nathan, C.** (1997) "Nitric oxide and macrophage function." *Annual Review of Immunology* **15**: 323-350. DOI: 10.1146/annurev.immunol.15.1.323.
- Marden, J.N., Diaz, M.R., Walton, W.G., Gode, C.J., Betts, L., Urbanowski, M.L., Redinbo, M.R., Yahr, T.L. and Wolfgang, M.C.** (2013) "An unusual CsrA family member operates in series with RsmA to amplify posttranscriptional responses in *Pseudomonas aeruginosa*." *Proceedings of the National Academy of Sciences of the United States of America* **110**(37): 15055-15060. DOI: 10.1073/pnas.1307217110.
- Martínez-Granero, F., Navazo, A., Barahona, E., Redondo-Nieto, M., González de Heredia, E., Baena, I., Martín-Martín, I., Rivilla, R. and Martín, M.** (2014) "Identification of *flgZ* as a flagellar gene encoding a PilZ domain protein that regulates swimming motility and biofilm formation in *Pseudomonas*." *PLoS One* **9**(2): 1-10. DOI: 10.1371/journal.pone.0087608.
- Matilla, M.A., Martín-Mora, D., Gavira, J.A. and Krell, T.** (2021) "*Pseudomonas aeruginosa* as a model to study chemosensory pathway signaling." *Microbiology and Molecular Biology Reviews* **85**(1): 1-32. DOI: 10.1128/MMBR.00151-20.
- Matsuyama, B.Y., Krasteva, P.V., Baraquet, C., Harwood, C.S., Sondermann, H. and Navarro, M.V.** (2016) "Mechanistic insights into c-di-GMP-dependent control of the biofilm regulator FleQ from *Pseudomonas aeruginosa*." *Proceedings of the National Academy of Sciences of the United States of America* **113**(2): 209-218. DOI: 10.1073/pnas.1523148113.
- Mattila-Sandholm, T. and Wirtanen, G.** (1992) "Biofilm formation in the industry - a review." *Food Reviews International* **8**(4): 573-603. DOI:
- McCallum, M., Burrows, L.L. and Howell, P.L.** (2019) "The dynamic structures of the type IV pilus." *Microbiology Spectrum* **7**(2): 1-12. DOI: 10.1128/microbiolspec.PSIB-0006-2018.
- McDougald, D., Rice, S.A., Barraud, N., Steinberg, P.D. and Kjelleberg, S.** (2011) "Should we stay or should we go: mechanisms and ecological consequences for biofilm dispersal." *Nature Reviews Microbiology* **10**(1): 39-50. DOI: 10.1038/nrmicro2695.
- Meliani, A. and Bensoltane, A.** (2015) "Review of *Pseudomonas* attachment and biofilm formation in food industry." *Poultry, Fisheries & Wildlife Sciences* **3**(1): 1-7. DOI:

- Merighi, M., Lee, V.T., Hyodo, M., Hayakawa, Y. and Lory, S.** (2007) "The second messenger bis-(3'-5')-cyclic-GMP and its PilZ domain-containing receptor Alg44 are required for alginate biosynthesis in *Pseudomonas aeruginosa*." *Molecular Microbiology* **65**(4): 876-895. DOI: 10.1111/j.1365-2958.2007.05817.x.
- Merrikh, H., Ferrazzoli, A.E. and Lovett, S.T.** (2009) "Growth phase and (p)ppGpp control of IraD, a regulator of RpoS stability, in *Escherichia coli*." *Journal of Bacteriology* **191**(24): 7436-7446. DOI: 10.1128/JB.00412-09.
- Meyer, M.M.** (2017) "The role of mRNA structure in bacterial translational regulation." *Wiley Interdisciplinary Reviews: RNA* **8**(1): 1-18. DOI: 10.1002/wrna.1370.
- Mika, F. and Hengge, R.** (2014) "Small RNAs in the control of RpoS, CsgD, and biofilm architecture of *Escherichia coli*." *RNA Biology* **11**(5): 494-507. DOI: 10.4161/rna.28867.
- Miller, C.L., Romero, M., Karna, S.L., Chen, T., Heeb, S. and Leung, K.P.** (2016) "RsmW, *Pseudomonas aeruginosa* small non-coding RsmA-binding RNA upregulated in biofilm versus planktonic growth conditions." *BMC Microbiology* **16**(155): 1-16. DOI: 10.1186/s12866-016-0771-y.
- Miller, J.H.** (1972). "Experiments in molecular genetics." *Cold Spring Harbor Laboratory Press*
- Mistry, J., Chuguransky, S., Williams, L., Qureshi, M., Salazar, G.A., Sonnhammer, E.L.L., Tosatto, S.C.E., Paladin, L., Raj, S., Richardson, L.J., Finn, R.D. and Bateman, A.** (2021) "Pfam: The protein families database in 2021." *Nucleic Acids Research* **49**: 412-419. DOI: 10.1093/nar/gkaa913.
- Morgan, R., Kohn, S., Hwang, S.H., Hassett, D.J. and Sauer, K.** (2006) "BdlA, a chemotaxis regulator essential for biofilm dispersion in *Pseudomonas aeruginosa*." *Journal of Bacteriology* **188**(21): 7335-7343. DOI: 10.1128/JB.00599-06.
- Morris, E.R., Hall, G., Li, C., Heeb, S., Kulkarni, R.V., Lovelock, L., Silistre, H., Messina, M., Camara, M., Emsley, J., Williams, P. and Searle, M.S.** (2013) "Structural rearrangement in an RsmA/CsrA ortholog of *Pseudomonas aeruginosa* creates a dimeric RNA-binding protein, RsmN." *Structure* **21**(9): 1659-1671. DOI: 10.1016/j.str.2013.07.007.
- Morris, J.D., Hewitt, J.L., Wolfe, L.G., Kamatkar, N.G., Chapman, S.M., Diener, J.M., Courtney, A.J., Leevy, W.M. and Shrout, J.D.** (2011) "Imaging and analysis of *Pseudomonas aeruginosa* swarming and rhamnolipid production." *Applied and Environmental Microbiology* **77**(23): 8310-8317. DOI: 10.1128/AEM.06644-11.
- Moscoso, J.A., Mikkelsen, H., Heeb, S., Williams, P. and Filloux, A.** (2011) "The *Pseudomonas aeruginosa* sensor RetS switches type III and type VI secretion via c-di-GMP signalling." *Environmental Microbiology* **13**(12): 3128-3138. DOI: 10.1111/j.1462-2920.2011.02595.x.



- Mulcahy, H., O'Callaghan, J., O'Grady, E.P., Maciá, M.D., Borrell, N., Gómez, C., Casey, P.G., Hill, C., Adams, C., Gahan, C.G., Oliver, A. and O'Gara, F.** (2008) "*Pseudomonas aeruginosa* RsmA plays an important role during murine infection by influencing colonization, virulence, persistence, and pulmonary inflammation." *Infection and Immunity* **76**(2): 632-638. DOI: 10.1128/IAI.01132-07.
- Mullis, K.B. and Faloona, F.A.** (1987) "Specific synthesis of DNA *in vitro* via a polymerase-catalyzed chain reaction." *Methods in Enzymology* **155**: 335-350. DOI: 10.1016/0076-6879(87)55023-6.
- Muriel, C., Arrebola, E., Redondo-Nieto, M., Martinez-Granero, F., Jalvo, B., Pfeilmeier, S., Blanco-Romero, E., Baena, I., Malone, J.G., Rivilla, R. and Martin, M.** (2018) "AmrZ is a major determinant of c-di-GMP levels in *Pseudomonas fluorescens* F113." *Scientific Reports* **8**(1979): 1-10. DOI: 10.1038/s41598-018-20419-9.
- Narberhaus, F., Kaser, R., Nocker, A. and Hennecke, H.** (1998) "A novel DNA element that controls bacterial heat shock gene expression." *Molecular Microbiology* **28**(2): 315-323. DOI: 10.1046/j.1365-2958.1998.00794.x.
- Narberhaus, F., Waldminghaus, T. and Chowdhury, S.** (2006) "RNA thermometers." *FEMS Microbiology Reviews* **30**(1): 3-16. DOI: 10.1111/j.1574-6976.2005.004.x.
- Navarro, M.V., De, N., Bae, N., Wang, Q. and Sondermann, H.** (2009) "Structural analysis of the GGDEF-EAL domain-containing c-di-GMP receptor FimX." *Structure* **17**(8): 1104-1116. DOI: 10.1016/j.str.2009.06.010.
- Newman, J.R. and Fuqua, C.** (1999) "Broad-host-range expression vectors that carry the L-arabinose-inducible *Escherichia coli* araBAD promoter and the araC regulator." *Gene* **227**(2): 197-203. DOI: 10.1016/s0378-1119(98)00601-5.
- Nicastro, G.G., Kaihami, G.H., Pulschen, A.A., Hernandez-Montelongo, J., Boechat, A.L., de Oliveira Pereira, T., Rosa, C.G.T., Stefanello, E., Colepicolo, P., Bordi, C. and Baldini, R.L.** (2020) "c-di-GMP-related phenotypes are modulated by the interaction between a diguanylate cyclase and a polar hub protein." *Scientific Reports* **10**(3077): 1-11. DOI: 10.1038/s41598-020-59536-9.
- Nicke, T., Schnitzer, T., Munch, K., Adamczack, J., Haufschildt, K., Buchmeier, S., Kucklick, M., Felgentrager, U., Jansch, L., Riedel, K. and Layer, G.** (2013) "Maturation of the cytochrome cd1 nitrite reductase NirS from *Pseudomonas aeruginosa* requires transient interactions between the three proteins NirS, NirN and NirF." *Bioscience Reports* **33**(3): 529-539. DOI: 10.1042/BSR20130043.
- Nisbett, L.M. and Boon, E.M.** (2016) "Nitric Oxide Regulation of H-NOX Signaling Pathways in Bacteria." *Biochemistry* **55**(35): 4873-4884. DOI: 10.1021/acs.biochem.6b00754.
- Noll, P., Treinen, C., Muller, S., Senkalla, S., Lilge, L., Hausmann, R. and Henkel, M.** (2019) "Evaluating temperature-induced regulation of a ROSE-like RNA-thermometer for heterologous rhamnolipid production in *Pseudomonas putida* KT2440." *AMB Express* **9**(154): 1-10. DOI: 10.1186/s13568-019-0883-5.

- Nudler, E. and Mironov, A.S.** (2004) "The riboswitch control of bacterial metabolism." *Trends in Biochemical Sciences* **29**(1): 11-17. DOI: 10.1016/j.tibs.2003.11.004.
- Nurizzo, D., Silvestrini, M.C., Mathieu, M., Cutruzzola, F., Bourgeois, D., Fulop, V., Hajdu, J., Brunori, M., Tegoni, M. and Cambillau, C.** (1997) "N-terminal arm exchange is observed in the 2.15 Å crystal structure of oxidized nitrite reductase from *Pseudomonas aeruginosa*." *Structure* **5**(9): 1157-1171. DOI: 10.1016/s0969-2126(97)00267-0.
- O'Connor, J.R., Kuwada, N.J., Huangyutitham, V., Wiggins, P.A. and Harwood, C.S.** (2012) "Surface sensing and lateral subcellular localization of WspA, the receptor in a chemosensory-like system leading to c-di-GMP production." *Molecular Microbiology* **86**(3): 720-729. DOI: 10.1111/mmi.12013.
- O'Toole, G.A. and Kolter, R.** (1998) "Flagellar and twitching motility are necessary for *Pseudomonas aeruginosa* biofilm development." *Molecular Microbiology* **30**(2): 295-304. DOI: 10.1046/j.1365-2958.1998.01062.x.
- Orr, M.W., Donaldson, G.P., Severin, G.B., Wang, J., Sintim, H.O., Waters, C.M. and Lee, V.T.** (2015) "Oligoribonuclease is the primary degradative enzyme for pGpG in *Pseudomonas aeruginosa* that is required for cyclic-di-GMP turnover." *Proceedings of the National Academy of Sciences of the United States of America* **112**(36): 5048-5057. DOI: 10.1073/pnas.1507245112.
- Paget, M.S.** (2015) "Bacterial sigma factors and anti-sigma factors: structure, function and distribution." *Biomolecules* **5**(3): 1245-1265. DOI: 10.3390/biom5031245.
- Paiardini, A., Mantoni, F., Giardina, G., Paone, A., Janson, G., Leoni, L., Rampioni, G., Cutruzzola, F. and Rinaldo, S.** (2018) "A novel bacterial L-arginine sensor controlling c-di-GMP levels in *Pseudomonas aeruginosa*." *Proteins* **86**(10): 1088-1096. DOI: 10.1002/prot.25587.
- Paul, D., Kumar, R., Nanduri, B., French, T., Pendarvis, K., Brown, A., Lawrence, M.L. and Burgess, S.C.** (2011) "Proteome and membrane fatty acid analyses on *Oligotropha carboxidovorans* OM5 grown under chemolithoautotrophic and heterotrophic conditions." *PLoS One* **6**(2): 1-9. DOI: 10.1371/journal.pone.0017111.
- Persat, A., Inclan, Y.F., Engel, J.N., Stone, H.A. and Gitai, Z.** (2015) "Type IV pili mechanochemically regulate virulence factors in *Pseudomonas aeruginosa*." *Proceedings of the National Academy of Sciences of the United States of America* **112**(24): 7563-7568. DOI: 10.1073/pnas.1502025112.
- Pesavento, C. and Hengge, R.** (2009) "Bacterial nucleotide-based second messengers." *Current Opinion in Microbiology* **12**(2): 170-176. DOI: 10.1016/j.mib.2009.01.007.
- Pessi, G., Williams, F., Hindle, Z., Heurlier, K., Holden, M.T., Camara, M., Haas, D. and Williams, P.** (2001) "The global posttranscriptional regulator RsmA modulates production of virulence determinants and N-acylhomoserine lactones in *Pseudomonas aeruginosa*." *Journal of Bacteriology* **183**(22): 6676-6683. DOI: 10.1128/JB.183.22.6676-6683.2001.

- Petchiappan, A., Naik, S.Y. and Chatterji, D.** (2020) "Tracking the homeostasis of second messenger cyclic-di-GMP in bacteria." *Biophysical Reviews* **12**(3): 719-730. DOI: 10.1007/s12551-020-00636-1.
- Plate, L. and Marletta, M.A.** (2012) "Nitric oxide modulates bacterial biofilm formation through a multicomponent cyclic-di-GMP signaling network." *Molecular Cell* **46**(4): 449-460. DOI: 10.1016/j.molcel.2012.03.023.
- Plate, L. and Marletta, M.A.** (2013) "Nitric oxide-sensing H-NOX proteins govern bacterial communal behavior." *Trends in Biochemical Sciences* **38**(11): 566-575. DOI: 10.1016/j.tibs.2013.08.008.
- Porter, S.L., Wadhams, G.H. and Armitage, J.P.** (2011) "Signal processing in complex chemotaxis pathways." *Nature Reviews Microbiology* **9**(3): 153-165. DOI: 10.1038/nrmicro2505.
- Potts, A.H., Vakulskas, C.A., Pannuri, A., Yakhnin, H., Babitzke, P. and Romeo, T.** (2017) "Global role of the bacterial post-transcriptional regulator CsrA revealed by integrated transcriptomics." *Nature Communications* **8**(1596): 1-15. DOI: 10.1038/s41467-017-01613-1.
- Potvin, E., Sanschagrín, F. and Levesque, R.C.** (2008) "Sigma factors in *Pseudomonas aeruginosa*." *FEMS Microbiology Reviews* **32**(1): 38-55. DOI: 10.1111/j.1574-6976.2007.00092.x.
- Prakash, B., Veeregowda, B.M. and Krishnappa, G.** (2003) "Biofilms: A survival strategy of bacteria." *Current Science* **85**(9): 1299-1307. DOI:
- Price, M.S., Chao, L.Y. and Marletta, M.A.** (2007) "*Shewanella oneidensis* MR-1 H-NOX regulation of a histidine kinase by nitric oxide." *Biochemistry* **46**(48): 13677-13683. DOI: 10.1021/bi7019035.
- Qi, Y., Chuah, M.L., Dong, X., Xie, K., Luo, Z., Tang, K. and Liang, Z.X.** (2011) "Binding of cyclic diguanylate in the non-catalytic EAL domain of FimX induces a long-range conformational change." *Journal of Biological Chemistry* **286**(4): 2910-2917. DOI: 10.1074/jbc.M110.196220.
- Qian, C., Wong, C.C., Swarup, S. and Chiam, K.H.** (2013) "Bacterial tethering analysis reveals a "run-reverse-turn" mechanism for *Pseudomonas* species motility." *Applied Environmental Microbiology* **79**(15): 4734-4743. DOI: 10.1128/AEM.01027-13.
- Qiu, D., Damron, F.H., Mima, T., Schweizer, H.P. and Yu, H.D.** (2008) "P<sub>BAD</sub>-based shuttle vectors for functional analysis of toxic and highly regulated genes in *Pseudomonas* and *Burkholderia* spp. and other bacteria." *Applied and Environmental Microbiology* **74**(23): 7422-7426. DOI: 10.1128/AEM.01369-08.
- Ramelot, T.A., Yee, A., Cort, J.R., Semesi, A., Arrowsmith, C.H. and Kennedy, M.A.** (2007) "NMR structure and binding studies confirm that PA4608 from *Pseudomonas aeruginosa* is a PilZ domain and a c-di-GMP binding protein." *Proteins* **66**(2): 266-271. DOI: 10.1002/prot.21199.

- Ramsey, D.M., Baynham, P.J. and Wozniak, D.J.** (2005) "Binding of *Pseudomonas aeruginosa* AlgZ to sites upstream of the *algZ* promoter leads to repression of transcription." *Journal of Bacteriology* **187**(13): 4430-4443. DOI: 10.1128/JB.187.13.4430-4443.2005.
- Rao, F., Yang, Y., Qi, Y. and Liang, Z.X.** (2008) "Catalytic mechanism of cyclic di-GMP-specific phosphodiesterase: a study of the EAL domain-containing RocR from *Pseudomonas aeruginosa*." *Journal of Bacteriology* **190**(10): 3622-3631. DOI: 10.1128/JB.00165-08.
- Rehner, J.** (2020) Master thesis: "The role of the MHYT-domain for the function of the phosphodiesterase NbdA in *Pseudomonas aeruginosa* PAO1." Department of Microbiology, TU Kaiserslautern.
- Reznikoff, W.S., Siegele, D.A., Cowing, D.W. and Gross, C.A.** (1985) "The regulation of transcription initiation in bacteria." *Annual Review of Genetics* **19**: 355-387. DOI: 10.1146/annurev.ge.19.120185.002035.
- Rietsch, A., Vallet-Gely, I., Dove, S.L. and Mekalanos, J.J.** (2005) "ExsE, a secreted regulator of type III secretion genes in *Pseudomonas aeruginosa*." *Proceedings of the National Academy of Sciences of the United States of America* **102**(22): 8006-8011. DOI: 10.1073/pnas.0503005102.
- Rinnenthal, J., Klinkert, B., Narberhaus, F. and Schwalbe, H.** (2011) "Modulation of the stability of the *Salmonella* fourU-type RNA thermometer." *Nucleic Acids Research* **39**(18): 8258-8270. DOI: 10.1093/nar/gkr314.
- Rodionov, D.A., Dubchak, I.L., Arkin, A.P., Alm, E.J. and Gelfand, M.S.** (2005) "Dissimilatory metabolism of nitrogen oxides in bacteria: comparative reconstruction of transcriptional networks." *PLoS Computational Biology* **1**(5): 415-431. DOI: 10.1371/journal.pcbi.0010055.
- Romeo, T., Vakulskas, C.A. and Babitzke, P.** (2013) "Post-transcriptional regulation on a global scale: form and function of Csr/Rsm systems." *Environmental Microbiology* **15**(2): 313-324. DOI: 10.1111/j.1462-2920.2012.02794.x.
- Romero, M., Silistre, H., Lovelock, L., Wright, V.J., Chan, K.G., Hong, K.W., Williams, P., Camara, M. and Heeb, S.** (2018) "Genome-wide mapping of the RNA targets of the *Pseudomonas aeruginosa* riboregulatory protein RsmN." *Nucleic Acids Research* **46**(13): 6823-6840. DOI: 10.1093/nar/gky324.
- Römling, U., Galperin, M.Y. and Gomelsky, M.** (2013) "Cyclic di-GMP: the first 25 years of a universal bacterial second messenger." *Microbiology and Molecular Biology Reviews* **77**(1): 1-52. DOI: 10.1128/MMBR.00043-12.
- Römling, U., Liang, Z.X. and Dow, J.M.** (2017) "Progress in understanding the molecular basis underlying functional diversification of cyclic dinucleotide turnover proteins." *Journal of Bacteriology* **199**(5): 1-16. DOI: 10.1128/JB.00790-16.

- Ross, P., Weinhouse, H., Aloni, Y., Michaeli, D., Weinberger-Ohana, P., Mayer, R., Braun, S., de Vroom, E., van der Marel, G.A., van Boom, J.H. and Benziman, M.** (1987) "Regulation of cellulose synthesis in *Acetobacter xylinum* by cyclic diguanylic acid." *Nature* **325**(6101): 279-281. DOI: 10.1038/325279a0.
- Rossmann, F.M., Rick, T., Mrusek, D., Sprankel, L., Dorrich, A.K., Leonhard, T., Bubendorfer, S., Kaefer, V., Bange, G. and Thormann, K.M.** (2019) "The GGDEF domain of the phosphodiesterase PdeB in *Shewanella putrefaciens* mediates recruitment by the polar landmark protein HubP." *Journal of Bacteriology* **201**(7): 1-14. DOI: 10.1128/JB.00534-18.
- Roy, A.B., Petrova, O.E. and Sauer, K.** (2012) "The phosphodiesterase DipA (PA5017) is essential for *Pseudomonas aeruginosa* biofilm dispersion." *Journal of Bacteriology* **194**(11): 2904-2915. DOI: 10.1128/JB.05346-11.
- Rüger, M.** (2019) PhD thesis: "Die Funktion der c-di-GMP modulierenden Membranproteine NbdA und MucR in *Pseudomonas aeruginosa*." Department of Microbiology, TU Kaiserslautern.
- Sambrook, J., Fritsch, E.F. and Maniatis, T.** (1989). "Molecular cloning: a laboratory manual." *Cold Spring Harbor Laboratory*
- Sampedro, I., Parales, R.E., Krell, T. and Hill, J.E.** (2015) "*Pseudomonas* chemotaxis." *FEMS Microbiology Reviews* **39**(1): 17-46. DOI: 10.1111/1574-6976.12081.
- Santiago, B., Schubel, U., Egelseer, C. and Meyer, O.** (1999) "Sequence analysis, characterization and CO-specific transcription of the *cox* gene cluster on the megaplasmid pHCG3 of *Oligotropha carboxidovorans*." *Gene* **236**(1): 115-124. DOI: 10.1016/s0378-1119(99)00245-0.
- Sarenko, O., Klauck, G., Wilke, F.M., Pfiffer, V., Richter, A.M., Herbst, S., Kaefer, V. and Hengge, R.** (2017) "More than Enzymes That Make or Break Cyclic Di-GMP-Local Signaling in the Interactome of GGDEF/EAL Domain Proteins of *Escherichia coli*." *mBio* **8**(5): 1-18. DOI: 10.1128/mBio.01639-17.
- Sauer, K.** (2003) "The genomics and proteomics of biofilm formation." *Genome Biology* **4**(6): 1-5. DOI: 10.1186/gb-2003-4-6-219.
- Sauer, K., Camper, A.K., Ehrlich, G.D., Costerton, J.W. and Davies, D.G.** (2002) "*Pseudomonas aeruginosa* displays multiple phenotypes during development as a biofilm." *Journal of Bacteriology* **184**(4): 1140-1154. DOI: 10.1128/jb.184.4.1140-1154.2002.
- Sauer, K., Cullen, M.C., Rickard, A.H., Zeef, L.A., Davies, D.G. and Gilbert, P.** (2004) "Characterization of nutrient-induced dispersion in *Pseudomonas aeruginosa* PAO1 biofilm." *J Bacteriol* **186**(21): 7312-7326. DOI: 10.1128/JB.186.21.7312-7326.2004.
- Schairer, D.O., Chouake, J.S., Nosanchuk, J.D. and Friedman, A.J.** (2012) "The potential of nitric oxide releasing therapies as antimicrobial agents." *Virulence* **3**(3): 271-279. DOI: 10.4161/viru.20328.

- Schleheck, D., Barraud, N., Klebensberger, J., Webb, J.S., McDougald, D., Rice, S.A. and Kjelleberg, S.** (2009) "*Pseudomonas aeruginosa* PAO1 preferentially grows as aggregates in liquid batch cultures and disperses upon starvation." *PLoS One* **4**(5): 1-15. DOI: 10.1371/journal.pone.0005513.
- Schmidt, J., Musken, M., Becker, T., Magnowska, Z., Bertinetti, D., Moller, S., Zimmermann, B., Herberg, F.W., Jansch, L. and Haussler, S.** (2011) "The *Pseudomonas aeruginosa* chemotaxis methyltransferase CheR1 impacts on bacterial surface sampling." *PLoS One* **6**(3): 1-11. DOI: 10.1371/journal.pone.0018184.
- Schulmeyer, K.H., Diaz, M.R., Bair, T.B., Sanders, W., Gode, C.J., Laederach, A., Wolfgang, M.C. and Yahr, T.L.** (2016) "Primary and secondary sequence structure requirements for recognition and discrimination of target RNAs by *Pseudomonas aeruginosa* RsmA and RsmF." *Journal of Bacteriology* **198**(18): 2458-2469. DOI: 10.1128/JB.00343-16.
- Schultheiß, I.** (2020) Bachelor thesis: "Identifizierung von Interaktionspartnern von NbdA aus *Pseudomonas aeruginosa* mit Hilfe des bakteriellen Two-Hybrid-Systems." Department of Microbiology, TU Kaiserslautern.
- Schulz, S., Eckweiler, D., Bielecka, A., Nicolai, T., Franke, R., Dotsch, A., Hornischer, K., Bruchmann, S., Duvel, J. and Haussler, S.** (2015) "Elucidation of sigma factor-associated networks in *Pseudomonas aeruginosa* reveals a modular architecture with limited and function-specific crosstalk." *PLoS Pathogens* **11**(3): 1-21. DOI: 10.1371/journal.ppat.1004744.
- Schuster, M., Hawkins, A.C., Harwood, C.S. and Greenberg, E.P.** (2004) "The *Pseudomonas aeruginosa* RpoS regulon and its relationship to quorum sensing." *Molecular Microbiology* **51**(4): 973-985. DOI: 10.1046/j.1365-2958.2003.03886.x.
- Schuster, M., Lostroh, C.P., Ogi, T. and Greenberg, E.P.** (2003) "Identification, timing, and signal specificity of *Pseudomonas aeruginosa* quorum-controlled genes: a transcriptome analysis." *Journal of Bacteriology* **185**(7): 2066-2079. DOI: 10.1128/jb.185.7.2066-2079.2003.
- Semmler, A.B.T., Whitchurch, C.B. and Mattick, J.S.** (1999) "A re-examination of twitching motility in *Pseudomonas aeruginosa*." *Microbiology* **145**: 2863-2873. DOI: 10.1099/00221287-145-10-2863.
- Shaner, N.C., Campbell, R.E., Steinbach, P.A., Giepmans, B.N., Palmer, A.E. and Tsien, R.Y.** (2004) "Improved monomeric red, orange and yellow fluorescent proteins derived from *Discosoma* sp. red fluorescent protein." *Nature Biotechnology* **22**(12): 1567-1572. DOI: 10.1038/nbt1037.
- Shaner, N.C., Lambert, G.G., Chammas, A., Ni, Y., Cranfill, P.J., Baird, M.A., Sell, B.R., Allen, J.R., Day, R.N., Israelsson, M., Davidson, M.W. and Wang, J.** (2013) "A bright monomeric green fluorescent protein derived from *Branchiostoma lanceolatum*." *Nature Methods* **10**(5): 407-409. DOI: 10.1038/nmeth.2413.

- 
- Sheng, S., Xin, L., Yam, J.K.H., Salido, M.M., Khong, N.Z.J., Liu, Q., Chea, R.A., Li, H.Y., Yang, L., Liang, Z.X. and Xu, L.** (2019) "The MapZ-mediated methylation of chemoreceptors contributes to pathogenicity of *Pseudomonas aeruginosa*." *Frontiers in Microbiology* **10**: 67. DOI: 10.3389/fmicb.2019.00067.
- Shitashiro, M., Kato, J., Fukumura, T., Kuroda, A., Ikeda, T., Takiguchi, N. and Ohtake, H.** (2003) "Evaluation of bacterial aerotaxis for its potential use in detecting the toxicity of chemicals to microorganisms." *Journal of Biotechnology* **101**(1): 11-18. DOI: 10.1016/s0168-1656(02)00285-7.
- Silversmith, R.E., Guanga, G.P., Betts, L., Chu, C., Zhao, R. and Bourret, R.B.** (2003) "CheZ-mediated dephosphorylation of the *Escherichia coli* chemotaxis response regulator CheY: role for CheY glutamate 89." *Journal of Bacteriology* **185**(5): 1495-1502. DOI: 10.1128/JB.185.5.1495-1502.2003.
- Sommerfeldt, N., Possling, A., Becker, G., Pesavento, C., Tschowri, N. and Hengge, R.** (2009) "Gene expression patterns and differential input into curli fimbriae regulation of all GGDEF/EAL domain proteins in *Escherichia coli*." *Microbiology* **155**: 1318-1331. DOI: 10.1099/mic.0.024257-0.
- Sondermann, H., Shikuma, N.J. and Yildiz, F.H.** (2012) "You've come a long way: c-di-GMP signaling." *Current Opinion in Microbiology* **15**(2): 140-146. DOI: 10.1016/j.mib.2011.12.008.
- Sourjik, V. and Wingreen, N.S.** (2012) "Responding to chemical gradients: bacterial chemotaxis." *Current Opinion in Cell Biology* **24**: 262-268. DOI: 10.1016/j.ceb.2011.11.008.
- St John, R.T. and Hollocher, T.C.** (1977) "Nitrogen 15 tracer studies on the pathway of denitrification in *Pseudomonas aeruginosa*." *Journal of Biological Chemistry* **252**(1): 212-218. DOI:
- Stamler, J.S., Singel, D.J. and Loscalzo, J.** (1992) "Biochemistry of nitric oxide and its redox-activated forms." *Science* **258**(5090): 1898-1902. DOI: 10.1126/science.1281928.
- Stanier, R.Y., Palleroni, N.J. and Doudoroff, M.** (1966) "The aerobic *Pseudomonads*: a taxonomic study." *Journal of General Microbiology* **43**(2): 159-271. DOI: 10.1099/00221287-43-2-159.
- Stelitano, V., Giardina, G., Paiardini, A., Castiglione, N., Cutruzzola, F. and Rinaldo, S.** (2013) "C-di-GMP hydrolysis by *Pseudomonas aeruginosa* HD-GYP phosphodiesterases: analysis of the reaction mechanism and novel roles for pGpG." *PLoS One* **8**(9): 1-13. DOI: 10.1371/journal.pone.0074920.
- Stewart, P.S. and Franklin, M.J.** (2008) "Physiological heterogeneity in biofilms." *Nature Reviews Microbiology* **6**(3): 199-210. DOI: 10.1038/nrmicro1838.

- Stover, C.K., Pham, X.Q., Erwin, A.L., Mizoguchi, S.D., Warren, P., Hickey, M.J., Brinkman, F.S., Hufnagle, W.O., Kowalik, D.J., Lagrou, M., Garber, R.L., Goltry, L., Tolentino, E., Westbrook-Wadman, S., Yuan, Y., Brody, L.L., Coulter, S.N., Folger, K.R., Kas, A., Larbig, K., Lim, R., Smith, K., Spencer, D., Wong, G.K., Wu, Z., Paulsen, I.T., Reizer, J., Saier, M.H., Hancock, R.E., Lory, S. and Olson, M.V.** (2000) "Complete genome sequence of *Pseudomonas aeruginosa* PAO1, an opportunistic pathogen." *Nature* **406**(6799): 959-964. DOI: 10.1038/35023079.
- Suh, S.J., Silo-Suh, L., Woods, D.E., Hassett, D.J., West, S.E. and Ohman, D.E.** (1999) "Effect of *rpoS* mutation on the stress response and expression of virulence factors in *Pseudomonas aeruginosa*." *Journal of Bacteriology* **181**(13): 3890-3897. DOI: 10.1128/JB.181.13.3890-3897.1999.
- Sutherland, I.W.** (2001) "The biofilm matrix - an immobilized but dynamic microbial environment." *Trends in Microbiology* **9**(5): 222-227. DOI: 10.1016/s0966-842x(01)02012-1.
- Taguchi, K., Fukutomi, H., Kuroda, A., Kato, J. and Ohtake, H.** (1997) "Genetic identification of chemotactic transducers for amino acids in *Pseudomonas aeruginosa*." *Microbiology* **143**: 3223-3229. DOI: 10.1099/00221287-143-10-3223.
- Talà, L., Fineberg, A., Kukura, P. and Persat, A.** (2019) "*Pseudomonas aeruginosa* orchestrates twitching motility by sequential control of type IV pili movements." *Nature Microbiology* **4**(5): 774-780. DOI: 10.1038/s41564-019-0378-9.
- Tart, A.H., Blanks, M.J. and Wozniak, D.J.** (2006) "The AlgT-dependent transcriptional regulator AmrZ (AlgZ) inhibits flagellum biosynthesis in mucoid, nonmotile *Pseudomonas aeruginosa* cystic fibrosis isolates." *Journal of Bacteriology* **188**(18): 6483-6489. DOI: 10.1128/JB.00636-06.
- Tart, A.H., Wolfgang, M.C. and Wozniak, D.J.** (2005) "The alternative sigma factor AlgT represses *Pseudomonas aeruginosa* flagellum biosynthesis by inhibiting expression of *fleQ*." *Journal of Bacteriology* **187**(23): 7955-7962. DOI: 10.1128/JB.187.23.7955-7962.2005.
- Tchigvintsev, A., Xu, X., Singer, A., Chang, C., Brown, G., Proudfoot, M., Cui, H., Flick, R., Anderson, W.F., Joachimiak, A., Galperin, M.Y., Savchenko, A. and Yakunin, A.F.** (2010) "Structural insight into the mechanism of c-di-GMP hydrolysis by EAL domain phosphodiesterases." *Journal of Molecular Biology* **402**(3): 524-538. DOI: 10.1016/j.jmb.2010.07.050.
- Thanbichler, M., Iniesta, A.A. and Shapiro, L.** (2007) "A comprehensive set of plasmids for vanillate- and xylose-inducible gene expression in *Caulobacter crescentus*." *Nucleic Acids Research* **35**(20): 1-16. DOI: 10.1093/nar/gkm818.
- Tian, Y., Wang, Q., Liu, Q., Ma, Y., Cao, X. and Zhang, Y.** (2008) "Role of RpoS in stress survival, synthesis of extracellular autoinducer 2, and virulence in *Vibrio alginolyticus*." *Archives of Microbiology* **190**(5): 585-594. DOI: 10.1007/s00203-008-0410-6.



- Toutain, C.M., Caizza, N.C., Zegans, M.E. and O'Toole, G.A.** (2007) "Roles for flagellar stators in biofilm formation by *Pseudomonas aeruginosa*." *Research in Microbiology* **158**: 471-417. DOI: 10.1016/j.resmic.2007.04.001.
- Toutain, C.M., Zegans, M.E. and O'Toole, G.A.** (2005) "Evidence for two flagellar stators and their role in the motility of *Pseudomonas aeruginosa*." *J Bacteriol* **187**(2): 771-777. DOI: 10.1128/JB.187.2.771-777.2005.
- Towbin, H., Staehelin, T. and Gordon, J.** (1979) "Electrophoretic transfer of proteins from polyacrylamide gels to nitrocellulose sheets: procedure and some applications." *Proceedings of the National Academy of Sciences of the United States of America* **76**(9): 4350-4354. DOI: 10.1073/pnas.76.9.4350.
- Townsley, L. and Yildiz, F.H.** (2015) "Temperature affects c-di-GMP signalling and biofilm formation in *Vibrio cholerae*." *Environmental Microbiology* **17**(11): 4290-4305. DOI: 10.1111/1462-2920.12799.
- Travers, A.A.** (1984) "Conserved features of coordinately regulated *E. coli* promoters." *Nucleic Acids Research* **12**(6): 2605-2618. DOI: 10.1093/nar/12.6.2605.
- Trunk, K., Benkert, B., Quack, N., Munch, R., Scheer, M., Garbe, J., Jansch, L., Trost, M., Wehland, J., Buer, J., Jahn, M., Schobert, M. and Jahn, D.** (2010) "Anaerobic adaptation in *Pseudomonas aeruginosa*: definition of the Anr and Dnr regulons." *Environmental Microbiology* **12**(6): 1719-1733. DOI: 10.1111/j.1462-2920.2010.02252.x.
- Tso, W.W. and Adler, J.** (1974) "Negative chemotaxis in *Escherichia coli*." *Journal of Bacteriology* **118**(2): 560-576. DOI: 10.1128/jb.118.2.560-576.1974.
- Tuckerman, J.R., Gonzalez, G., Sousa, E.H., Wan, X., Saito, J.A., Alam, M. and Gilles-Gonzalez, M.A.** (2009) "An oxygen-sensing diguanylate cyclase and phosphodiesterase couple for c-di-GMP control." *Biochemistry* **48**(41): 9764-9774. DOI: 10.1021/bi901409g.
- Valentini, M. and Filloux, A.** (2016) "Biofilms and cyclic di-GMP (c-di-GMP) signaling: Lessons from *Pseudomonas aeruginosa* and other bacteria." *Journal of Biological Chemistry* **291**(24): 12547-12555. DOI: 10.1074/jbc.R115.711507.
- Van Alst, N.E., Wellington, M., Clark, V.L., Haidaris, C.G. and Iglewski, B.H.** (2009) "Nitrite reductase NirS is required for type III secretion system expression and virulence in the human monocyte cell line THP-1 by *Pseudomonas aeruginosa*." *Infection and Immunity* **77**(10): 4446-4454. DOI: 10.1128/IAI.00822-09.
- Van Assche, E., Van Puyvelde, S., Vanderleyden, J. and Steenackers, H.P.** (2015) "RNA-binding proteins involved in post-transcriptional regulation in bacteria." *Frontiers in Microbiology* **6**: 1-16. DOI: 10.3389/fmicb.2015.00141.
- Vassilyev, D.G., Sekine, S., Laptenko, O., Lee, J., Vassilyeva, M.N., Borukhov, S. and Yokoyama, S.** (2002) "Crystal structure of a bacterial RNA polymerase holoenzyme at 2.6 Å resolution." *Nature* **417**(6890): 712-719. DOI: 10.1038/nature752.

- Venturi, V.** (2003) "Control of *rpoS* transcription in *Escherichia coli* and *Pseudomonas*: why so different?" *Molecular Microbiology* **49**(1): 1-9. DOI: 10.1046/j.1365-2958.2003.03547.x.
- Vladimirov, N. and Sourjik, V.** (2009) "Chemotaxis: how bacteria use memory." *Biological Chemistry* **390**: 1097-1104. DOI: 10.1515/BC.2009.130.
- Wadhams, G.H. and Armitage, J.P.** (2004) "Making sense of it all: bacterial chemotaxis." *Nature Reviews Molecular Cell Biology* **5**(12): 1024-1037. DOI: 10.1038/nrm1524.
- Wagner, S., Baars, L., Ytterberg, A.J., Klussmeier, A., Wagner, C.S., Nord, O., Nygren, P.A., van Wijk, K.J. and de Gier, J.W.** (2007) "Consequences of membrane protein overexpression in *Escherichia coli*." *Molecular & Cellular Proteomics* **6**(9): 1527-1550. DOI: 10.1074/mcp.M600431-MCP200.
- Wagner, S., Bader, M.L., Drew, D. and de Gier, J.W.** (2006) "Rationalizing membrane protein overexpression." *Trends in Biotechnology* **24**(8): 364-371. DOI: 10.1016/j.tibtech.2006.06.008.
- Waldminghaus, T., Heidrich, N., Brantl, S. and Narberhaus, F.** (2007) "FourU: a novel type of RNA thermometer in *Salmonella*." *Molecular Microbiology* **65**(2): 413-424. DOI: 10.1111/j.1365-2958.2007.05794.x.
- Wang, W. and Malcolm, B.A.** (1999) "Two-stage PCR protocol allowing introduction of multiple mutations, deletions and insertions using QuikChange™ site-directed mutagenesis." *Biotechniques* **26**(4): 680-682. DOI: 10.2144/99264st03.
- Wang, Y., Hay, I.D., Rehman, Z.U. and Rehm, B.H.** (2015) "Membrane-anchored MucR mediates nitrate-dependent regulation of alginate production in *Pseudomonas aeruginosa*." *Applied Microbiology and Biotechnology* **99**(17): 7253-7265. DOI: 10.1007/s00253-015-6591-4.
- Wassmann, P., Chan, C., Paul, R., Beck, A., Heerklotz, H., Jenal, U. and Schirmer, T.** (2007) "Structure of BeF3<sup>-</sup>-modified response regulator PleD: implications for diguanylate cyclase activation, catalysis, and feedback inhibition." *Structure* **15**(8): 915-927. DOI: 10.1016/j.str.2007.06.016.
- Weber, H., Pesavento, C., Possling, A., Tischendorf, G. and Hengge, R.** (2006) "Cyclic-di-GMP-mediated signalling within the sigma network of *Escherichia coli*." *Molecular Microbiology* **62**(4): 1014-1034. DOI: 10.1111/j.1365-2958.2006.05440.x.
- Wegiel, B., Larsen, R., Gallo, D., Chin, B.Y., Harris, C., Mannam, P., Kaczmarek, E., Lee, P.J., Zuckerbraun, B.S., Flavell, R., Soares, M.P. and Otterbein, L.E.** (2014) "Macrophages sense and kill bacteria through carbon monoxide-dependent inflammasome activation." *The Journal of Clinical Investigation* **124**(11): 4926-4940. DOI: 10.1172/JCI72853.
- Wehbi, H., Portillo, E., Harvey, H., Shimkoff, A.E., Scheurwater, E.M., Howell, P.L. and Burrows, L.L.** (2011) "The peptidoglycan-binding protein FimV promotes assembly of the *Pseudomonas aeruginosa* type IV pilus secretin." *Journal of Bacteriology* **193**(2): 540-550. DOI: 10.1128/JB.01048-10.

- Weiss, C.A., Hoberg, J.A., Liu, K., Tu, B.P. and Winkler, W.C.** (2019) "Single-cell microscopy reveals that levels of cyclic di-GMP vary among *Bacillus subtilis* subpopulations." *Journal of Bacteriology* **201**(16): 1-17. DOI: 10.1128/JB.00247-19.
- Werner, E., Roe, F., Bugnicourt, A., Franklin, M.J., Heydorn, A., Molin, S., Pitts, B. and Stewart, P.S.** (2004) "Stratified growth in *Pseudomonas aeruginosa* biofilms." *Applied Environmental Microbiology* **70**(10): 6188-6196. DOI: 10.1128/AEM.70.10.6188-6196.2004.
- Whitchurch, C.B., Leech, A.J., Young, M.D., Kennedy, D., Sargent, J.L., Bertrand, J.J., Semmler, A.B., Mellick, A.S., Martin, P.R., Alm, R.A., Hobbs, M., Beatson, S.A., Huang, B., Nguyen, L., Commoli, J.C., Engel, J.N., Darzins, A. and Mattick, J.S.** (2004) "Characterization of a complex chemosensory signal transduction system which controls twitching motility in *Pseudomonas aeruginosa*." *Molecular Microbiology* **52**(3): 873-893. DOI: 10.1111/j.1365-2958.2004.04026.x.
- Whiteley, M., Banger, M.G., Bumgarner, R.E., Parsek, M.R., Teitzel, G.M., Lory, S. and Greenberg, E.P.** (2001) "Gene expression in *Pseudomonas aeruginosa* biofilms." *Nature* **413**(6858): 860-864. DOI: 10.1038/35101627.
- Williams, P. and Cámara, M.** (2009) "Quorum sensing and environmental adaptation in *Pseudomonas aeruginosa*: a tale of regulatory networks and multifunctional signal molecules." *Current Opinion in Microbiology* **12**(2): 182-191. DOI: 10.1016/j.mib.2009.01.005.
- Winsor, G.L., Griffiths, E.J., Lo, R., Dhillon, B.K., Shay, J.A. and Brinkman, F.S.** (2016) "Enhanced annotations and features for comparing thousands of *Pseudomonas* genomes in the *Pseudomonas* genome database." *Nucleic Acids Research* **44**: 646-653. DOI: 10.1093/nar/gkv1227.
- Wozniak, D.J., Sprinkle, A.B. and Baynham, P.J.** (2003) "Control of *Pseudomonas aeruginosa* *algZ* expression by the alternative sigma factor AlgT." *Journal of Bacteriology* **185**(24): 7297-7300. DOI: 10.1128/jb.185.24.7297-7300.2003.
- Xin, L., Zeng, Y., Sheng, S., Chea, R.A., Liu, Q., Li, H.Y., Yang, L., Xu, L., Chiam, K.H. and Liang, Z.X.** (2019) "Regulation of flagellar motor switching by c-di-GMP phosphodiesterases in *Pseudomonas aeruginosa*." *Journal of Biological Chemistry* **294**(37): 13789-13799. DOI: 10.1074/jbc.RA119.009009.
- Xu, A., Zhang, M., Du, W., Wang, D. and Ma, L.Z.** (2021) "A molecular mechanism for how sigma factor AlgT and transcriptional regulator AmrZ inhibit twitching motility in *Pseudomonas aeruginosa*." *Environmental Microbiology* **23**(2): 572-587. DOI: 10.1111/1462-2920.14985.
- Xu, B., Ju, Y., Soukup, R.J., Ramsey, D.M., Fishel, R., Wysocki, V.H. and Wozniak, D.J.** (2016a) "The *Pseudomonas aeruginosa* AmrZ C-terminal domain mediates tetramerization and is required for its activator and repressor functions." *Environmental Microbiology Reports* **8**(1): 85-90. DOI: 10.1111/1758-2229.12354.

- 
- Xu, L., Xin, L., Zeng, Y., Yam, J.K., Ding, Y., Venkataramani, P., Cheang, Q.W., Yang, X., Tang, X., Zhang, L.H., Chiam, K.H., Yang, L. and Liang, Z.X.** (2016b) "A cyclic di-GMP-binding adaptor protein interacts with a chemotaxis methyltransferase to control flagellar motor switching." *Science Signaling* **9**: 1-12. DOI: 10.1126/scisignal.aaf7584.
- Ye, R.W., Averill, B.A. and Tiedje, J.M.** (1994) "Denitrification: production and consumption of nitric oxide." *Applied and Environmental Microbiology* **60**(4): 1053-1058. DOI: 10.1128/AEM.60.4.1053-1058.1994.
- Yildiz, F.H. and Schoolnik, G.K.** (1998) "Role of *rpoS* in stress survival and virulence of *Vibrio cholerae*." *Journal of Bacteriology* **180**(4): 773-784. DOI: 10.1128/JB.180.4.773-784.1998.
- Zemke, A.C., D'Amico, E.J., Snell, E.C., Torres, A.M., Kasturiarachi, N. and Bomberger, J.M.** (2020) "Dispersal of Epithelium-Associated *Pseudomonas aeruginosa* Biofilms." *mSphere* **5**(4): 1-15. DOI: 10.1128/mSphere.00630-20.
- Zhao, X., Koestler, B.J., Waters, C.M. and Hammer, B.K.** (2013) "Post-transcriptional activation of a diguanylate cyclase by quorum sensing small RNAs promotes biofilm formation in *Vibrio cholerae*." *Molecular Microbiology* **89**(5): 989-1002. DOI: 10.1111/mmi.12325.
- Zhu, S., Schniederberend, M., Zhitnitsky, D., Jain, R., Galán, J.E., Kazmierczak, B.I. and Liu, J.** (2019) "*In situ* structures of polar and lateral flagella revealed by cryo-electron tomography." *Journal of Bacteriology* **201**(13): 1-13. DOI: 10.1128/JB.00117-19.
- Zuker, M.** (2003) "Mfold web server for nucleic acid folding and hybridization prediction." *Nucleic Acids Research* **31**(13): 3406-3415. DOI: 10.1093/nar/gkg595.

# Curriculum vitae

## PERSÖNLICHE DATEN

---

**Katrin Gerbracht**

## STUDIUM UND SCHULISCHE LAUFBAHN

---

- |         |         |  |
|---------|---------|--|
| 01/2017 | 04/2021 | <b>Wissenschaftliche Mitarbeiterin (TU Kaiserslautern)</b><br>Doktorandin in der Abteilung für Mikrobiologie von Prof. Dr. Nicole Frankenberg-Dinkel |
| 10/2014 | 12/2016 | <b>Studium der Biologie (Ruhr-Universität Bochum)</b><br>Abschluss Master of Science (Note 1,7)  |
| 10/2011 | 07/2014 | <b>Studium der Biologie (Ruhr-Universität Bochum)</b><br>Abschluss Bachelor of Science (Note 2,1)  |
|         | 07/2011 | <b>Abitur Ernst-Barlach-Gymnasium (Castrop-Rauxel)</b>   |

## BERUFSERFAHRUNG

---

- |              |         |  |
|--------------|---------|--|
| seit 06/2021 |         | <b>Analytical Service Manager</b> bei Eurofins INLAB GmbH  |
|              | 06/2019 | <b>Praktikum Columbia University New York (NY   USA)</b><br>Abteilung für Mikrobiologie; Labor von Prof. Dr. Lars Dietrich         |
|              | 09/2017 | <b>Unisense Mikrosensoren Workshop (Aarhus   DK)</b>   |
| 12/2015      | 09/2016 | <b>Wissenschaftliche Hilfskraft (TU Kaiserslautern)</b><br>Abteilung für Mikrobiologie von Prof. Dr. Nicole Frankenberg-Dinkel     |
| 09/2015      | 11/2015 | <b>Praktikum Binghamton University (NY   USA)</b><br>Abteilung Mikrobiologie; Labor von Prof. Dr. Karin Sauer<br>PROMOS Stipendium |

**KONFERENZTEILNAHMEN (Auswahl)**

---

02/2020	Vortrag & Poster	<b>SPP 1879 Progress Meeting</b> (Göttingen) „The role of the c-di-GMP-specific phosphodiesterase NbdA in <i>Pseudomonas aeruginosa</i> PAO1”
03/2019	Vortrag	<b>VAAM Jahrestagung</b> (Mainz) „The role of the c-di-GMP-specific phosphodiesterase NbdA in biofilm dispersal of <i>Pseudomonas aeruginosa</i> ”
01/2019	Poster	<b>SPP 1879 Evaluation Meeting</b> (Bonn)
10/2018	Poster	<b>SPP 1879 International Symposium</b> (Berlin)
04/2018	Poster	<b>VAAM Jahrestagung</b> (Wolfsburg)
09/2017	Poster	<b>International Conference on Pseudomonas</b> (Liverpool)

**PUBLIKATIONEN**

---

04/2021	eingereicht & Vordruck	“The <i>Pseudomonas aeruginosa</i> phosphodiesterase gene <i>nbdA</i> is transcriptionally regulated by RpoS and AmrZ”
---------	------------------------	--

## Eidesstattliche Erklärung

Ich erkläre hiermit an Eides statt, dass ich die vorliegende Dissertation selbstständig und ohne Benutzung anderer als der angegebenen Hilfsmittel angefertigt habe. Die aus fremden Quellen übernommenen Gedanken sind ausnahmslos als solche kenntlich gemacht. Die Promotionsordnung des Fachbereichs Biologie der TU Kaiserslautern ist mir in der derzeit gültigen Fassung bekannt. Die Ergebnisse anderer Mitarbeiter sowie anderer Autoren wurden klar gekennzeichnet. Die Dissertation oder Teile daraus wurden in keinem anderen Fachbereich oder keiner anderen Fakultät als Prüfungsarbeit eingereicht. Ich habe zu keinem früheren Zeitpunkt an einer anderen Universität ein Promotionsverfahren beantragt.

Dortmund, den 03.09.2021

---

Katrin Gerbracht